



# **BINDERLESS FIBERBOARD PRODUCTION FROM *CYNARA CARDUNCULUS* AND *VITIS VINIFERA***

**DISSERTATION PRESENTED BY**

**CAMILO MANCERA ARIAS**

**TO OBTAIN THE DEGREE:**

**DOCTOR BY UNIVERSITAT ROVIRA I VIRGILI**

**DEPARTMENT OF MECHANICAL ENGINEERING**

**UNIVERSITAT ROVIRA I VIRGILI**

**TARRAGONA - SPAIN - SEPTEMBER 2008**

**THESIS DIRECTED BY DR. FRANCESC FERRANDO AND DR. JOAN SALVADÓ**

UNIVERSITAT ROVIRA I VIRGILI  
BINDERLESS FIBERBOARD PRODUCTION FROM CYNARA CARDUNCULUS AND VITIS VINIFERA  
Camilo Mancera Arias  
ISBN:978-84-692-1537-1/DL:T-300-2009

Los doctores Dr. Francesc Ferrando Piera y Dr. Joan Salvadó Rovira, profesores titulares de Universidad Rovira i Virgili, del departamento de ingeniería Mecánica y del departamento de ingeniería química, respectivamente. Directores del trabajo de investigación realizado por Camilo Mancera Arias, titulado:

BINDERLESS FIBERBOARD PRODUCTION FROM *CYNARA CARDUNCULUS*  
AND *VITIS VINIFERA*

Para optar al grado de Doctor en Ingeniería Química por la Universitat Rovira i Virgili

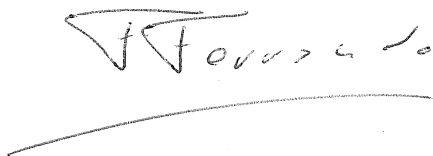
HACEN CONSTAR:

Que el citado trabajo es original y que todos los resultados presentados y los análisis realizados son fruto de su investigación.

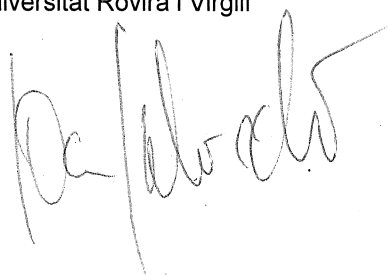
Y para vuestro conocimiento y los efectos que correspondan, firman este documento

Tarragona, 12 de Septiembre de 2008

Dr. Francesc Ferrando Piera  
Dept. Ingeniería Mecánica  
Universitat Rovira i Virgili



Dr. Joan Salvadó Rovira  
Dept. Ingeniería Química  
Universitat Rovira i Virgili



UNIVERSITAT ROVIRA I VIRGILI  
BINDERLESS FIBERBOARD PRODUCTION FROM CYNARA CARDUNCULUS AND VITIS VINIFERA  
Camilo Mancera Arias  
ISBN:978-84-692-1537-1/DL:T-300-2009

Every day I remind myself that my inner and outer life are based on the labors of other men, living and dead, and that I must exert myself in order to give in the same measure as I have received and am still receiving.

**Albert Einstein**

UNIVERSITAT ROVIRA I VIRGILI  
BINDERLESS FIBERBOARD PRODUCTION FROM CYNARA CARDUNCULUS AND VITIS VINIFERA  
Camilo Mancera Arias  
ISBN:978-84-692-1537-1/DL:T-300-2009

## AGRADECIMIENTOS

Estoy profundamente agradecido a muchas personas que han contribuido directa o indirectamente al desarrollo de este trabajo de investigación y que sin su apoyo y ayuda no habría sido posible.

Deseo agradecer a los doctores Francesc Ferrando y Joan Salvadó, por haberme aceptado bajo su tutela para el desarrollo de este proyecto, por su continuo apoyo y paciencia, por su aportación de ideas y por su guía indispensable en cada etapa del proceso.

Gracias especiales a los doctores Jorge Velásquez y Nour-Eddine El Mansouri por su apoyo continuo y la confianza que depositaron en mí, por alentarme en los momentos más difíciles y ayudarme a encontrar soluciones.

Dentro del programa de doctorado, Graduated Studies in Chemical and Process Engineering, quisiera agradecer a todos los compañeros que tuve la oportunidad de conocer y con los cuales compartí tantas inquietudes y expectativas. Compañeros que a lo largo de estos años me han brindado su amistad y ayuda y que me han permitido conocer tantas culturas, costumbres, idiomas y creencias, que me han hecho crecer como persona y sentir menos dura la lejanía del hogar.

Al antiguo grupo de investigación Biopolímeros vegetales y ahora Systemic, por sus continuas aportaciones a nivel técnico en el trabajo, por compartir el material de laboratorio, los espacios de trabajo y los equipos, por hacer más ameno el trabajo, gracias. Dentro del grupo de investigación, deseo agradecerle especialmente a "Pepa", nuestra técnica de laboratorio, por que sin su presencia y ayuda los laboratorios de investigación no son lo mismo.

Gracias especiales a Irama, por su apoyo incondicional, su influencia positiva y su confianza.

Con profunda gratitud, destaco la gran aportación de mi familia, por su profunda influencia en mi vida y pensamiento, por su apoyo incondicional, sus continuos esfuerzos y sacrificios para que mi hermana y yo encontremos nuestro camino.

UNIVERSITAT ROVIRA I VIRGILI  
BINDERLESS FIBERBOARD PRODUCTION FROM CYNARA CARDUNCULUS AND VITIS VINIFERA  
Camilo Mancera Arias  
ISBN:978-84-692-1537-1/DL:T-300-2009



## SUMMARY

Depleting natural resources, regulations on using synthetic materials, growing environmental awareness and economic considerations are the major driving forces to use annually renewable resources such as biomass for industrial applications. Using agricultural residues such as *Cynara cardunculus* stalks and *Vitis vinifera* prunings for the production of binderless fiberboards is an important contribution for solving problems like deforestation. Furthermore, the increasing fuel cost and scarcity of petroleum sources lead to seek for substitutes of petroleum by-products like resins commonly used for the production of fiberboards.

Synthetic resins commonly used on fiberboards production present negative side effects like the health risks caused by the emission of volatile organic compounds such as formaldehyde, or problems concerning issues such as waste disposal or recycling. Binderless boards overcome these difficulties using lignin instead of resin as adherent obtaining in this way a board which does not present formaldehyde emissions and that is completely biodegradable.

The research on non-wood plants in Europe has been focused on species with high biomass productions, which can be growth in available areas as industrial crops for energy, pulp and paper, composites or chemicals. In this context, *Cynara cardunculus* has been considered as fiber source, because it grows in dry and hot regions with high yields and the concept of biorefinery is completely applicable to it, meaning that almost all the parts of the crop can be used for different purposes. *Vitis vinifera* prunings are lignocellulosic agricultural-residues which could also replace wood in the production of fiberboards. Vine is a traditional crop in Spain; it covers large areas of land and is cultivated for wine and fruit production. Large quantities of lignocellulosic materials remain in the fields every year after the pruning season; part of these prunings is used as fuel but large quantities remain unused in the fields, thus increasing the plague and fire risks.

In the present study *Cynara cardunculus* and *Vitis vinifera* were pretreated and used to produce fiberboards without synthetic adhesives. These lignocellulosic materials were steam exploded through a thermo-mechanical vapor process in a batch reactor. After pretreatment the material was dried, ground and hot pressed to produce the boards. The effects of pretreatment factors (reaction temperature and

reaction time) and pressing conditions (pressing pressure, temperature and time) on the chemical and physicochemical properties of the fiberboards were evaluated and the conditions that optimize these properties were found. Physicochemical properties of the fiberboards studied were: Density, modulus of elasticity (MOE), modulus of rupture (MOR), internal bond (IB), water absorption (WA) and thickness swelling (TS) and the chemical properties studied of the raw and pretreated material were: Ash content, Klason lignin content, cellulose and hemicelluloses content. Response surface methodology based on a central composite design and multiple response optimization were used.

Binderless fiberboards produced from *Cynara cardunculus* stalks at the optimum conditions found fulfilled the European standards for boards of internal use. Nevertheless, binderless fiberboards produced from *Vitis vinifera* prunings at the optimum conditions found for this material did not completely met the European standards; modulus of rupture and internal bond values for these boards were lower than required minimums.

Commercial Kraft lignin was reacted in an alkaline medium to enhance its adhesive properties. Chemical changes in reacted Kraft lignins that include ash content, Klason lignin, acid-soluble lignin and sugars were determined, as well as, structural characteristics of these lignins in terms of phenolic hydroxyl, aliphatic hydroxyl, methoxyl, carbonyl, Mw, Mn and polydispersity. The effects of reaction temperature and reaction time on lignin properties were studied using response surface methodology, and optimal reaction conditions were found.

Two different types of Kraft lignin were used, alkali treated Kraft lignin and crude acid-washed Kraft lignin, as additives to enhance the physicochemical properties of binderless fiberboards produced from *Vitis vinifera* to reach and overcome the European standards completely. At the end fiberboards produced with 20% of *Vitis vinifera* fibers replaced by crude acid-washed Kraft lignin were able to meet the European standards completely.

This research work was an effort to reduce our dependency upon petroleum derivatives, to diminish deforestation and to increase the use of renewable and biodegradable materials with the intention of preserving the environment and to encourage a sustainable development of our society.

## RESUMEN

La considerable disminución de los recursos naturales, la cada vez más estricta reglamentación sobre el uso de materiales sintéticos, la creciente conciencia ambiental y las consideraciones económicas son las principales fuerzas impulsoras para utilizar recursos renovables como la biomasa para aplicaciones industriales. El uso de residuos agrícolas tales como tallos de *Cynara cardunculus* y podas de *Vitis vinifera* para la producción de tableros de fibras sin adhesivos sintéticos es una importante contribución para resolver problemas como la deforestación. Por otra parte, el creciente costo de los combustibles y la escasez de fuentes de petróleo conducen a buscar sustitutos para los subproductos del petróleo como las resinas comúnmente utilizadas para la producción de tableros de fibras.

Las resinas sintéticas comúnmente utilizadas en la producción de tableros de fibras presentan efectos secundarios negativos como los riesgos para la salud causados por las emisiones de compuestos orgánicos volátiles, tales como formaldehído, o los problemas relativos a cuestiones como la eliminación de residuos o el reciclaje. Los tableros sin adhesivos sintéticos superan estas dificultades usando lignina en lugar de resina como adherente para la obtención de tableros que no presentan emisiones de formaldehído y que son completamente biodegradables.

La investigación sobre distintos tipos de plantas no maderables en Europa se ha centrado en especies con alta producción de biomasa, que pueden ser cultivadas en las zonas disponibles como cultivos industriales para la obtención de energía, pulpa y papel, materiales compuestos o sustancias químicas. En este contexto, *Cynara cardunculus* ha sido considerada como una fuente de fibra, ya que puede crecer en regiones secas y calientes con altos rendimientos y el concepto de biorefinería es completamente aplicable a ella, lo que significa que casi todas las partes de la cosecha pueden ser utilizada para diferentes fines. Las podas de *Vitis vinifera* son residuos agrícolas lignocelulósicos que también podrían sustituir a la madera en la producción de tableros de fibras. La Viña es un cultivo tradicional en España, abarca grandes extensiones de tierra y se cultiva para la producción de vino y de fruta. Grandes cantidades de material lignocelulósico permanecen en los campos cada año después de la temporada de poda; parte de estas podas se

utiliza como combustible, pero siguen quedando grandes cantidades de este material no utilizado en los campos, aumentando así los riesgos de plaga y de incendio.

En el presente estudio trozos *Cynara cardunculus* y *Vitis vinifera* fueron pretratados, y usados para producir tableros de fibras sin adhesivos sintéticos. Estos materiales lignocelulósicos se explotaron con vapor a través de un proceso termomecánico de vapor en un reactor por lotes. Después del pretratamiento el material fue secado, molido y prensado en caliente para producir los tableros. Se evaluaron los efectos de los factores del pretratamiento (temperatura de reacción y tiempo de reacción) y las condiciones de prensado (presión de prensado, temperatura y tiempo) sobre las propiedades químicas y físico-mecánicas de los tableros de fibras y se establecieron las condiciones que optimizan dichas propiedades. Las propiedades físico-mecánicas de los tableros de fibras que fueron estudiadas son: densidad, módulo de elasticidad (MOE), módulo de ruptura (MOR), enlace interno (IB), absorción de agua (WA) y hinchazón en hinchazón (TS) y las propiedades químicas estudiadas de la materia prima y el material pretratado fueron las siguientes: Cenizas, contenido de lignina Klason, contenido de celulosa y contenido de hemicelulosas. Se uso una metodología de superficie de respuesta basada en un diseño de experimentos del tipo central compuesto y una metodología de optimización de respuesta múltiple.

Los tableros de fibras sin adhesivos sintéticos producidos a partir de tallos de *Cynara cardunculus* a las condiciones óptimas encontradas cumplieron con las normas europeas para los tableros de uso interno. Sin embargo, los tableros de fibras sin adhesivos sintéticos producidos a partir de podas de *Vitis vinifera* a las condiciones óptimas encontradas para este material no cumplieron totalmente las normas europeas; los valores del módulo de ruptura y del enlace interno para estos tableros fueron inferiores a los mínimos requeridos.

Una lignina Kraft comercial fue sometida a reacción en un medio alcalino para mejorar sus propiedades adhesivas. Se determinaron los cambios químicos en las ligninas Kraft tratadas, las propiedades medidas fueron: contenido en cenizas, lignina Klason, lignina soluble en ácido y azúcares, también se determinaron las características estructurales de estas ligninas en términos de hidroxilos fenólicos, hidroxilos alifáticos, metóxilos, carbonilos, Mw, Mn y polidispersidad. Se estudiaron los efectos de la temperatura de reacción y el tiempo de reacción sobre las propiedades de la lignina con una metodología de superficie de respuesta, y se encontraron la condiciones óptimas de reacción.

Se usaron dos tipos diferentes de lignina Kraft, lignina Kraft tratada en medio alcalino y lignina Kraft cruda lavada con ácido, como aditivos para mejorar las propiedades físico-mecánicas de los tableros de fibras sin adhesivos sintéticos producidos a partir de *Vitis vinifera*, para alcanzar y superar las normas europeas completamente. Al final los tableros de fibras producidos con una substitución del 20% de fibras de *Vitis vinifera* por lignina Kraft cruda lavada con ácido fueron capaces de satisfacer las normas europeas por completo.

Este trabajo de investigación fue un esfuerzo para reducir nuestra dependencia de los derivados del petróleo, para disminuir la deforestación y para aumentar el uso de materiales renovables y biodegradables con la intención de preservar el medio ambiente y fomentar un desarrollo sostenible de nuestra sociedad

UNIVERSITAT ROVIRA I VIRGILI  
BINDERLESS FIBERBOARD PRODUCTION FROM CYNARA CARDUNCULUS AND VITIS VINIFERA  
Camilo Mancera Arias  
ISBN:978-84-692-1537-1/DL:T-300-2009

## INDEX

	<b>Page</b>
<b>AGRADECIMIENTOS</b>	I
<b>SUMMARY</b>	III
<b>RESUMEN</b>	V
<b>CHAPTER 1. INTRODUCTION AND OBJECTIVES</b>	
1.1. Introduction	3
1.2. Objectives	5
1.3. Hypothesis	6
1.4. Thesis outline	6
<b>CHAPTER 2. BACKGROUND</b>	
2.1. Introduction	11
2.2. Boards	12
2.2.1. Types of boards and their applications	13
2.2.1.1. Laminated timbers	14
2.2.1.2. Plywood	14
2.2.1.3. Structural composite lumber (SCL)	15
2.2.1.4. Composite beam	15
2.2.1.5. Wafer- and Flakeboard	15
2.2.1.6. Particle boards	15
2.2.1.7. Fiberboards	16
2.2.1.7.1. Low-Density Fiberboard (LDF)	16
2.2.1.7.2. Medium-Density Fiberboard (MDF)	16
2.2.1.7.3. High-Density Fiberboard (HDF)	17
2.2.1.8. Other types of composites	17
2.2.2. Binderless fiberboards	17
2.2.3. Vapor pretreatment of lignocellulosic materials – Steam Explosion	18
2.2.4. Pressing conditions	20
2.2.5. Grinding	22

2.3. Lignin	22
2.3.1. Types and features of lignins	25
2.3.1.1. Kraft lignin	25
2.3.1.2. Lignosulfonate	26
2.3.1.3. Organosolv lignin	27
2.3.2. Potential uses of lignin	28
2.3.2.1. Lignin in adhesives formulation	29
2.3.2.2. Lignin use in other applications	31
2.3.2.3. Advantages and disadvantages in the use of lignin	33
2.3.3. Structural modifications of lignin	33
2.3.3.1. Hydroxymethylation	34
2.3.3.2. Phenolation	35
2.3.3.3. Demethylation	36
2.3.3.4. Fractionation	37
2.3.3.5. Alkaline medium hydrolysis	38
2.3.4. Lignin characterization	39
REFERENCES	41

## **CHAPTER 3. MATERIALS, METHODS AND ANALYTICAL TECHNIQUES**

3.1. Equipment for fiberboard production and characterization	53
3.1.1. Steam explosion reactor	53
3.1.2. Press	54
3.1.3. Mill	55
3.1.4. Mechanical characterization equipment	55
3.2. Equipment for Kraft lignin modification	56
3.2.1. Micro reactor set	56
3.2.2. 10L Batch reactor	57
3.3. Materials	57
3.4. Methods for fiberboard production	59
3.4.1. Chip pretreatment	59
3.4.2. Pulp grinding	59
3.4.3. Fiberboard manufacture	59
3.5. Methods for Kraft lignin modification	60
3.6. Methods for exogenous addition of different types of Kraft lignins	60
3.7. Analytical techniques for fiberboard characterization	61
3.7.1. Physical and mechanical characterization	61



3.7.2. Chemical characterization	61
3.7.3. Scanning Electron microscopy – SEM.	62
3.8. Analytical techniques for Kraft lignin characterization	62
3.9. Experimental design	64
3.9.1. Fiberboard production	64
3.9.2. Kraft lignin modification	65
3.9.3. Exogenous lignin addition	66
3.10. Experimental design analysis	66
3.10.1. ANOVA Table	66
3.10.2. Pareto Chart	66
3.10.3. Main Effects Plot	67
3.10.4. Interaction Plot	67
3.10.5. Response Surface Plot	67
3.10.6. Predicted Value vs. Observed Value	67
3.10.7. Multiple response optimization	67
3.10.8. Overlaid contour plots	67
3.10.9. Scatter plot	67
3.10.10. Means and 95% LSD intervals	68
3.10.11. Box and whisker plot	68
3.10.12. Analysis of means plot	68
REFERENCES	69

#### **CHAPTER 4. BINDERLESS FIBERBOARDS FROM CYNARA CARDUNCULUS**

4.1. Introduction	75
4.2. Results and discussions	77
4.2.1. Physical and mechanical response variables	77
4.2.1.1. Density	80
4.2.1.2. Mechanical properties (MOR, MOE, IB)	85
4.2.1.3. Physical properties (WA, TS)	98
4.2.2. Chemical Response Variables	107
4.2.2.1. Ash content	107
4.2.2.2. Lignin, Cellulose and Hemicelluloses	108
4.2.2.3. Cellulose to Lignin ratio (C/L)	108
4.3. Response variables relationship	115
4.3.1. Density relations with mechanical and physical properties	115

4.3.2. Chemical composition relations with mechanical and physical properties	117
4.4. Multiple response optimization	119
4.5. Conclusions	121
REFERENCES	122

## **CHAPTER 5. BINDERLESS FIBERBOARDS FROM *VITIS VINIFERA***

5.1. Introduction	127
5.2. Results and discussions	129
5.2.1. Physical and mechanical response variables	129
5.2.1.1. Density	131
5.2.1.2. Mechanical properties (MOR, MOE, IB)	135
5.2.1.3. Physical properties (WA, TS)	145
5.2.2. Chemical Response Variables	152
5.2.2.1. Ash content	152
5.2.2.2. Lignin, Cellulose and Hemicelluloses	152
5.2.2.3. Cellulose to Lignin ratio (C/L)	153
5.3. Response variables relationship	160
5.3.1. Density relations with mechanical and physical properties	160
5.3.2. Chemical composition relations with mechanical and physical properties	162
5.4. Multiple response optimization	164
5.5. Conclusions	166
REFERENCES	167

## **CHAPTER 6. KRAFT LIGNIN BEHAVIOR DURING REACTION IN AN ALKALINE MEDIUM**

6.1. Introduction	171
6.2. Results and discussion	173
6.2.1. Alkaline hydrolysis	174
6.2.2. FTIR-spectroscopy	175
6.2.3. Response surface experiment	177
6.2.3.1. Solid yield	178
6.2.3.2. Phenolic hydroxyl content	179
6.2.3.3. Aliphatic hydroxyl content	180
6.2.3.4. Total hydroxyl content	180

6.2.3.5. Active sites increment	181
6.2.3.6. Weight-average molecular weight (Mw)	181
6.2.3.7. Number-average molecular weight (Mn)	182
6.2.3.8. Polydispersity	182
6.3. Conclusions	193
REFERENCES	194

## **CHAPTER 7. EXOGENOUS LIGNIN ADDITION FOR THE PRODUCTION OF BINDERLESS FIBERBOARDS**

7.1. Introduction	199
7.2. Results and discussion	201
7.2.1. Alkali treated Kraft lignin exogenous addition	201
7.2.1.1. Density	202
7.2.1.2. Mechanical properties (MOR, MOE, IB)	204
7.2.1.3. Physical properties (WA, TS)	209
7.2.2. Crude acid washed Kraft lignin exogenous addition	212
7.2.2.1. Density	212
7.2.2.2. Mechanical properties (MOR, MOE, IB)	214
7.2.2.3. Physical properties (WA, TS)	219
7.2.3. Observations by scanning electron microscope (SEM)	222
7.3. Conclusions	224
REFERENCES	225

## **GENERAL CONCLUSIONS, SYNTHESIS AND FUTURE WORK**

Steam explosion pretreatment	229
Hot pressing	230
Exogenous lignin addition	232
Comparison between lignocellulosic materials	233
Future work	234

## **ANNEX**

A. Experimental design	237
B. Detail description of the test equipments and characterization methods	239
C. <sup>1</sup> H-NMR and FTIR spectrums of alkali treated lignin at different reaction conditions	257
REFERENCES	261

UNIVERSITAT ROVIRA I VIRGILI  
BINDERLESS FIBERBOARD PRODUCTION FROM CYNARA CARDUNCULUS AND VITIS VINIFERA  
Camilo Mancera Arias  
ISBN:978-84-692-1537-1/DL:T-300-2009

## LIST OF FIGURES

Figure		Page
2.1	Basic wood elements from largest to smallest	12
2.2	Basic monomers and units of lignin	23
2.3	Lignin structure proposed by Adler	24
2.4	Lignin structure proposed by Forss et al.	24
2.5	PF resin and lignin structures	30
3.1	Steam explosion reactor	54
3.2	Laboratory press Polystat 300 S	54
3.3	Laboratory mill SM 100 Retsch	55
3.4	Mechanical characterization equipment	56
3.5	Micro reactor set	56
3.6	10L batch reactor	57
3.7	Types of phenolic structure determined in different lignin samples.	63
4.1	Statistical Plots for Density Analysis	83
4.2	Statistical Plots for MOR Analysis	88
4.3	Statistical Plots for MOE Analysis	91
4.4	Statistical Plots for IB Analysis	96
4.5	Statistical Plots for WA Analysis	101
4.6	Statistical Plots for TS Analysis	104
4.7	Statistical models	106
4.8	Statistical Plots for Ash Content Analysis	111
4.9	Statistical Plots for Lignin Analysis	112
4.10	Statistical Plots for Cellulose Analysis	113
4.11	Statistical Plots for Hemicelluloses Analysis	114
4.12	Correlation plots between physicomechanical properties and density	116
4.13	Relationship between chemical composition and physicomechanical properties	118
4.14	Statistical plots for multiple response optimization	120
5.1	Statistical Plots for Density Analysis	133
5.2	Statistical Plots for MOR Analysis	137
5.3	Statistical Plots for MOE Analysis	139

5.4	Statistical Plots for IB Analysis	143
5.5	Statistical Plots for WA Analysis	147
5.6	Statistical Plots for TS Analysis	149
5.7	Statistical models	151
5.8	Statistical Plots for Ash Content Analysis	155
5.9	Statistical Plots for Lignin Analysis	156
5.10	Statistical Plots for ASL Analysis	157
5.11	Statistical Plots for Cellulose Analysis	158
5.12	Statistical Plots for Hemicelluloses Analysis	159
5.13	Correlation plots between physicochemical properties and density	161
5.14	Relationship between chemical composition and physicochemical properties	163
5.15	Statistical plots for multiple response optimization	165
6.1	FTIR spectrums for LK4 and LK0	176
6.2	<sup>1</sup> H-NMR spectra of raw Kraft lignin (LK0 sample).	178
6.3	<sup>1</sup> H-NMR spectra of highly reacted Kraft lignin at 170 °C and 90 min (LK4 sample).	178
6.4	Statistical plots for Solid Yield Analysis	185
6.5	Statistical plots for Phenolic OH Analysis	186
6.6	Statistical plots for Aliphatic OH Analysis	187
6.7	Statistical plots for Total OH Analysis	188
6.8	Statistical plots for Active Sites Increment Analysis	189
6.9	Statistical plots for Mw Analysis	190
6.10	Statistical plots for Mn Analysis	191
6.11	Statistical plots for Polydispersity Analysis	192
7.1	Statistical plots for Density Analysis	203
7.2	Statistical plots for MOR Analysis	205
7.3	Statistical plots for MOE Analysis	206
7.4	Statistical plots for IB Analysis	208
7.5	Statistical plots for WA Analysis	210
7.6	Statistical plots for TS Analysis	211
7.7	Statistical plots for Density Analysis	213
7.8	Statistical plots for MOR Analysis	215
7.9	Statistical plots for MOE Analysis	216
7.10	Statistical plots for IB Analysis	218
7.11	Statistical plots for WA Analysis	220

7.12	Statistical plots for TS Analysis	221
7.13	SEM microphotographs of IB tested fiberboards	223
B1	Flexion apparatus description	244
B2	Internal bond testing device	246
B3	Phenolic structures determined in lignin	251
C1	<sup>1</sup> H-NMR spectrums of alkali treated Kraft lignin	257
C2	FTIR spectrums of alkali treated Kraft lignin	259

UNIVERSITAT ROVIRA I VIRGILI  
BINDERLESS FIBERBOARD PRODUCTION FROM CYNARA CARDUNCULUS AND VITIS VINIFERA  
Camilo Mancera Arias  
ISBN:978-84-692-1537-1/DL:T-300-2009



## LIST OF TABLES

Table	Page	
2.1	Classification of wood-based composites	13
2.2	Approximate chemical characteristics of three types of lignin	28
3.1	Average chemical composition of <i>Cynara cardunculus</i> stalks	58
3.2	Average chemical composition of <i>Vitis vinifera</i> prunings	58
4.1	Physicomechanical properties	78
4.2	Variance Analysis for Density	82
4.3	Variance Analysis for MOR	87
4.4	Variance Analysis for MOE	90
4.5	Variance Analysis for IB	95
4.6	Variance Analysis for WA	100
4.7	Variance Analysis for TS	103
4.8	Chemical compositions of <i>Cynara cardunculus</i> with different pretreatment conditions	109
4.9	Variance Analysis for Ash	110
4.10	Variance Analysis for Lignin	110
4.11	Variance Analysis for Cellulose	110
4.12	Variance Analysis for Hemicelluloses	110
5.1	Physicomechanical properties	130
5.2	ANOVA table for Density	133
5.3	ANOVA table for MOR	137
5.4	ANOVA table for MOE	139
5.5	ANOVA table for IB	143
5.6	ANOVA table for WA	147
5.7	ANOVA table for TS	149
5.8	Chemical compositions of <i>Vitis vinifera</i> with different pretreatment conditions	153
5.9	Variance analysis table for Ash	154
5.10	Variance analysis for Lignin	154
5.11	Variance analysis for ASL	154
5.12	Variance analysis for Cellulose	154

5.13	Variance analysis for Hemicelluloses	154
6.1	Chemical composition of Kraft lignins at different reaction conditions	174
6.2	Results of the response surface experiment	175
6.3	Relative absorbance of different group bands of LK0 and LK4 samples	177
6.4	Variance analysis for Solid yield	183
6.5	Variance analysis for Phenolic OH	183
6.6	Variance analysis for Aliphatic OH	183
6.7	Variance analysis for Total OH	183
6.8	Variance analysis for Active sites increment	184
6.9	Variance analysis for Mw	184
6.10	Variance analysis for Mn	184
6.11	Variance analysis for Polydispersity	184
7.1	Alkali treated Kraft lignin exogenous addition	202
7.2	Variance analysis for Density	203
7.3	Variance analysis for MOR	205
7.4	Variance analysis for MOE	206
7.5	Variance analysis for IB	208
7.6	Variance analysis for WA	210
7.7	Variance analysis for TS	211
7.8	Crude acid washed Kraft lignin exogenous addition	212
7.9	Variance analysis for Density	213
7.10	Variance analysis for MOR	215
7.11	Variance analysis for MOE	216
7.12	Variance analysis for IB	218
7.13	Variance analysis for WA	220
7.14	Variance analysis for TS	221
B1	<sup>1</sup> H-NMR spectrum signals assignation	251
B2	Characteristic bands assigned to lignin in FTIR spectra	254

# 1. INTRODUCTION

UNIVERSITAT ROVIRA I VIRGILI  
BINDERLESS FIBERBOARD PRODUCTION FROM CYNARA CARDUNCULUS AND VITIS VINIFERA  
Camilo Mancera Arias  
ISBN:978-84-692-1537-1/DL:T-300-2009

## CHAPTER 1

### Introduction and Objectives

#### 1.1 INTRODUCTION

It is hard to imagine a world without forests. Forests provide a wide range of benefits to people, including clean air and water, productive soils, biological diversity, goods and services, employment, recreation and solely being exposed to nature is beneficial for life. Forests also provide intangible benefits such as beauty, inspiration and wonder. Some of these benefits depend on none or minimal interference with forest. Other benefits can only be realized by harvesting the forest for wood and other products.

The concept of sustainability is central to an adequate forest management and it is the subject of much current debate. Sustainability in all its facets “ecological, economic and social” will continue to become increasingly important for preservation and benefit of world’s forests.

A critical consideration in any discussion about future demand for raw materials is population growth. All projections show a great absolute increase in global population in the future. The greatest growth in population is likely to occur when the standards of living are also expected to show the greatest rise, resulting in a faster economy growth than population. This means that demands for resources, which are already high on a per capita basis, will rise even higher. In numbers, world population doubled from 1850 to 1950 and then doubled again from 1950 to 2000. Over each of the next fourth or five decades, global population is expected to increase by approximately 900 million of people. These figures make it dramatically clear that the world of tomorrow will contain many more people than today’s.

Approximately 3.5 billions m<sup>3</sup> (American system) of wood are harvested worldwide each year; slightly more than half of this is used as fuelwood. Approximately 63 percent of the harvest consists of hardwoods, which are used primarily for fuel in developing countries. Softwood is primarily used for industrial purposes. The global per-capita consumption of wood is around 0.67 m<sup>3</sup>/year, this figure has remained essentially unchanged since 1960. This means that wood demand worldwide is closely following

growth in world population. These tremendous figures make us reflect on how to achieve a sustainable development based on the interdependence of environment and economy and how to use wood technology research and development to make this integration possible.

We can say then that depleting natural resources, regulations on using synthetic materials, growing environmental awareness and economic considerations are the major driving forces to use annually renewable resources such as biomass for industrial applications. Using agricultural residues as *Cynara cardunculus* stalks and *Vitis vinifera* prunings for the production of binderless fiberboards is an important contribution for solving problems like deforestation. Furthermore, the increasing fuel cost and scarcity of petroleum sources led to seek for substitutes of petroleum by-products like common resins used for the production of fiberboards.

Synthetic resins commonly used on fiberboards production present negative side effects like the health risks caused by the emission of volatile organic compounds such as formaldehyde, or problems concerning issues such as waste disposal or recycling. Binderless boards overcome this difficulty using lignin instead of resin as adherent obtaining in this way a board which does not present formaldehyde emissions and that are completely biodegradable.

The research on non-wood plants in Europe has been focused on species with high biomass productions, which can be growth in available areas as industrial crops for energy, pulp and paper, composites or chemicals. In this context, *Cynara cardunculus* has been considered as fiber source, because it grows in dry and hot regions with high yields and the concept of biorefinery is completely applicable to it, meaning that almost all the parts of the crop can be used for different purposes. *Vitis vinifera* prunings are lignocellulosic agricultural-residues which could also replace wood in the production of fiberboards. Vine is a traditional crop in Spain; it covers large areas of land and is cultivated for wine and fruit production. Large quantities of lignocellulosic prunings remain in the fields every year after the pruning season; part of these prunings is used as fuel but large quantities remain unused in the fields, thus increasing the plague and fire risks.

Steam explosion is one of the best ways of pre-treating lignocellulosic materials which are going to be use in chemical fractionation, bioconversion or in the production of boards and composites, because steam explosion allows to preserve the fiber structure and at the same time separate the lignocellulosic material in its main components. It is claimed that steam explosion plasticizes the lignin present in the lignocellulosic material and separates its fibers improving the bonding capacity of the material. Additionally, it is believe that this pretreatment improves the dimensional

stability of fiberboards, hydrolyzing the hemicelluloses present in the material, which are known to be highly hydrophilic.

Raw exogenous lignin addition, grinding the pretreated material and controlling its humidity before being pressed are additional treatments that could improve the board properties. Additionally, structural modification of the Kraft lignin used as additive to improve the fiberboard properties would be implemented to enhance the natural properties of these lignins as adhesives; subsequently, this modified lignin would be tested on the production of fiberboards to assess its performance.

Everything mentioned above, reveals the importance and possibilities of using non-woody materials such as *Cynara cardunculus* and *Vitis vinifera* for the production of binderless fiberboards which are friendlier with the environment and cheaper than conventional boards.

## 1.2 OBJECTIVES

The **main objective** of this research is to produce binderless fiberboards of commercial quality from *Cynara cardunculus* and *Vitis Vinifera* through a process more friendly with the environment.

The **specific aims** related to the main objective of this research are:

- To use steam explosion pretreatment for the production of fiberboards from *Cynara cardunculus* and *Vitis vinifera*.
- To identify and optimize the controllable variables of the steam explosion pretreatment and pressing process affecting the board properties.
- To evaluate the influence of adding raw Kraft lignin on the board properties.
- To achieve structural modification and characterization of Kraft lignin by reaction in alkaline medium and use it as additive to improve fiberboard properties.
- To elucidate the bonding mechanism in binderless fiberboards through the analysis of chemical and morphological changes developed in the steam explosion pretreatment.
- To compare the main results with previous works carried on different raw materials.

### 1.3 HYPOTHESIS

The general hypothesis of the present study is:

“It is possible to produce binderless fiberboards from *Cynara cardunculus* stalks and *Vitis vinifera* prunings that accomplish the European standards, employing friendlier technologies with the environment”.

### 1.4 THESIS OUTLINE

This research project is divided in seven main parts; each part is described in a separated chapter:

#### **Chapter 1 Introduction, objectives and thesis outline**

**Chapter 2 Background** Presents a bibliography review of past studies regarding to binderless fiberboard production and modification of technical lignins to enhance their adhesive properties, and the methodologies and techniques used for achieving them and evaluating their performance.

**Chapter 3 Materials, Equipments and Methodology** Describes in general form the main materials, equipments and methodologies used in the development of the research project going from experimental design to analytical techniques used for the production and characterization of the fiberboards and the modification and characterization of the technical lignins.

**Chapter 4 Binderless fiberboard production from *Cynara cardunculus*** Presents the results obtained from the production of fiberboards from *Cynara cardunculus* without additives. In this chapter is described how the *Cynara cardunculus* stalks undergo the main processes and how their main controllable factors affect the final properties of the fiberboards produced.

**Chapter 5 Binderless fiberboard production from *Vitis Vinifera*** Presents the results obtained from the production of fiberboards from *Vitis vinifera* without additives. In this chapter is described how the *Vitis vinifera* prunings undergo the main processes



and how their main controllable factors affect the final properties of the fiberboards produced.

**Chapter 6 Kraft lignin behavior during reaction in an alkaline medium** Presents the results obtained from the reaction of Kraft lignin in an alkaline medium and how the different process factors affect the lignin structure and properties.

**Chapter 7 Exogenous lignin addition** Based on the best combination of factors found for the production of binderless fiberboards from *Vitis vinifera* and the best conditions found to enhance the adhesive properties of Kraft lignin, fiberboards were produced adding raw and modified Kraft lignin to *Vitis vinifera* fibers before pressing and the results are presented in this chapter.

UNIVERSITAT ROVIRA I VIRGILI  
BINDERLESS FIBERBOARD PRODUCTION FROM CYNARA CARDUNCULUS AND VITIS VINIFERA  
Camilo Mancera Arias  
ISBN:978-84-692-1537-1/DL:T-300-2009

## **2. BACKGROUND**

UNIVERSITAT ROVIRA I VIRGILI  
BINDERLESS FIBERBOARD PRODUCTION FROM CYNARA CARDUNCULUS AND VITIS VINIFERA  
Camilo Mancera Arias  
ISBN:978-84-692-1537-1/DL:T-300-2009

## **CHAPTER 2**

### **Background**

In this chapter it is presented a bibliography review of past studies regarding to binderless fiberboard production and modification of technical lignins to enhance their adhesive properties, and the methodologies and techniques used for achieving them and evaluating their performance.

#### **2.1 INTRODUCTION**

World-wide population is growing up and as consequence the demand of wood and its derived products also increase. Besides, the forest reserves are diminishing in an alarming way and the cost of the raw materials are increasing every day. For all this reasons, the technology is advancing in the sense of being able to produce cheaper materials from residues. In this context, new adhesives systems, that reduce the production costs and which do not damage the environment have been an important aspect of technological development.

Lignocellulosic biomass exploitation, mainly wood, is focused in pulp and paper fabrication, building and carpentry, but there is a part of this lignocellulosic biomass from which no profit is taken (forestry, agricultural, pulp and paper, carpentry and building residues). Lignocellulosic residues offer interesting potential applications as raw material in general, in addition to its possible uses with energetic purposes. They are abundant, renewable and recyclable.

Production of fiberboards without synthetic resins (binderless boards) is valuable in the sense of being completely recyclable and renewable and because resins commonly used in the production of boards come from fossil sources, which are no renewable and increase the price of the product. From the point of view of healthcare and of environmental regulations, the boards produced without synthetic resins are superior because they do not have any formaldehyde emission.

## 2.2 Boards

Wood has played a major role through human history. Since early times humans have used wood to make shelters, cook food, construct tools, and make weapons. Society learned very early the great advantages of using wood, because it was widely distributed, multifunctional, strong, easy to work, aesthetic, sustainable and renewable. People have been using wood for centuries as a building material; accepting its performance limitations such as dimensional instability due to moisture sorption, biodegradability, flammability, and degradability by ultraviolet radiation, acids and bases. These performance limitations that wood presents are caused by how nature had designed wood. Wood has been design by nature to perform in a wet environment and nature has been programmed to recycle wood to carbon dioxide and water using chemical and biological processes like biological decay and thermal, ultraviolet and moisture degradation (Rowell 1990).

Historically, wood was used only in its solid form as large timbers and lumber. As the availability of large-diameter trees decreased, and consequently the price increased, the wood industry looked to replace large-timber products with reconstituted wood products made using smaller-diameter trees, and saw and pulp mill wastes. There has been a trend away from solid wood for some traditional applications toward smaller element sizes. The basic wood elements that can be used in the production of wood-based panels are shown in Figure 2.1. The figure shows the breakdown of solid wood into composite components. The composite can be made in a great variety of sizes and shapes and can be used alone or in combination. The choice is almost unlimited (Berglund and Rowell 2005; Youngquist 1999).

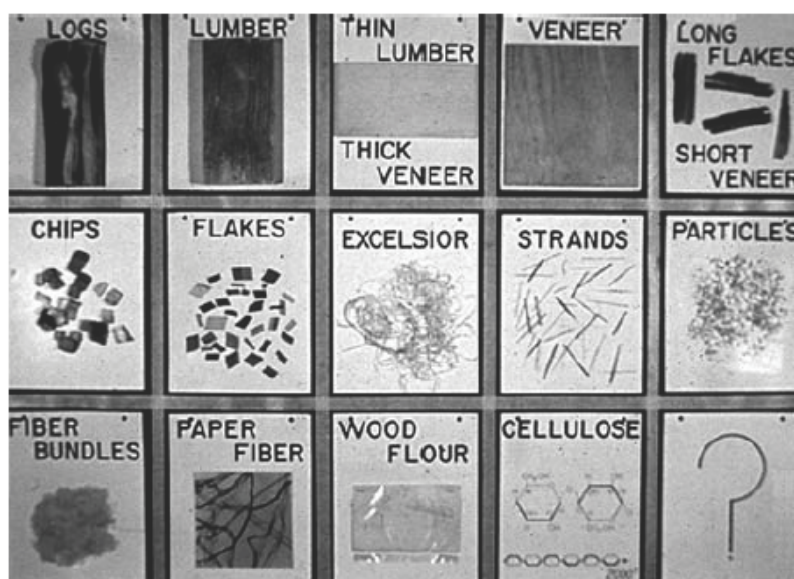


Figure 2.1 Basic wood elements from largest to smallest (Marra 1979)

A composite material can be defined as two or more elements held together by a matrix. Based on this definition solid wood is a composite material. Solid wood is a three dimensional composite made of cellulose, hemicelluloses and lignin (with smaller amounts of inorganic materials and extractives), held together by a lignin matrix (Berglund and Rowell 2005; Rowell 1992).

Wood properties vary among species, between trees of the same species, and between pieces from the same tree. Because of this heterogeneity, solid wood cannot match reconstituted wood in the range of properties that can be controlled during processing. When processing variables are properly selected, the end result can even sometimes surpass nature's best effort. The main advantages of developing wood composites are: to use smaller trees, to use waste wood from other processing, to remove defects, to create more uniform components, to develop composites that are stronger than the original solid wood, and to be able to make composites of different shapes.

### 2.2.1 Types of boards and their applications

Currently, the term composite is being used to describe any wood material adhesive-bonded together. This product mix ranges from fiberboard to laminated beams and components, some composite products found in today's world are panels, molded products, inorganic-bonded products, and lumber or timber products. Table 2.1 shows a logical basis for classifying wood composites proposed by Maloney (Maloney 1996; Youngquist 1999).

**Table 2.1** Classification of wood-based composites (Maloney 1996; Youngquist 1999)

---

<b>Veneer-based material</b>
Plywood
Laminated veneer lumber (LVL)
Parallel-laminated veneer (PLV)
<b>Laminates</b>
Laminated beams
Overlaid materials
Wood–nonwood composites
<b>Composite material</b>
Cellulosic fiberboard
Hardboard
Particleboard

---

---

Waferboard  
Flakeboard  
Oriented strandboard (OSB)  
COM-PLY

**Edge-adhesive-bonded material**

Lumber panels

**Components**

I-beams  
T-beam panels  
Stress-skin panels

**Wood–nonwood composites**

Wood fiber–plastic composites  
Inorganic-bonded composites  
Wood fiber–agricultural fiber composites

---

Composites are used for a number of structural and nonstructural applications in product lines ranging from panels for interior covering purposes to panels for exterior uses and in furniture and support structures in many different types of buildings.

Although this study is centered on fiberboards, a general and brief discussion of the different wood composites will be made.

### **2.2.1.1 Laminated timbers**

Structural glued-laminated beams (glulam) can be made using thick, wide wood members and are used as structural elements in large, open buildings. Glulam is a structural product that consists of two or more layers of lumber glued together with the grain all going parallel to the length. The biggest advantage of using glulam is that large beams can be made using small trees. In addition, lower quality wood can be used, thinner lumber can be dried much faster than large, thick beams, and a variety of curved shapes can be produced (*Youngquist 1999*).

### **2.2.1.2 Plywood**

Thin veneers can be glued together for plywood, a material that is used as a structural underlayment in floors and roofs and in furniture manufacturing. There are two basic types of plywood: construction and decorative. Construction-grade plywood has traditionally been produced using softwoods. Decorative plywood is usually produced using softwoods for the back and inner layers, with a hardwood layer on the outer surface (*Berglund and Rowell 2005; Youngquist 1999*).



### 2.2.1.3 Structural composite lumber (SCL)

Structural composite lumber (SCL) is manufactured by laminating strips of veneers or strands of wood glued parallel to the length. The three main types of SCL products are: Oriented strand lumber (OSL), parallel strand lumber (PSL) and laminated veneer lumber (LVL). Laminated strand lumber (LSL), oriented strand board (OSB) and OSL are produced using different lengths and sizes of strands. LSL uses strands that are about 0.3 m in length while OSB is produced from shorter strands. PSL is made from strands that are 3 mm thick, approximately 19 mm wide, and 0.6 m in length. LVL is produced from veneers that are approximately 2.5 to 3.2 mm thick and varying lengths. All of these SCL products are used as replacements for solid wood and have a specific gravity of 0.5 to 0.8.

### 2.2.1.4 Composite beam

Composite structural beams can be produced by combining several wood elements. I-beam can be made of curved plywood sides and laminated plywood top and bottom. Prefabricated I-beams are used by builders because they are lightweight, uniform, and easy to use; have increased dimensional stability; and meet codes and standards. Com-ply panels are made with veneer and particle/flakes. Three layer panels have veneer faces and particle cores while five-layer panels have a veneer core (laid up with its grain direction at 90 degrees to the face veneer grain direction). Five-layer boards have been successfully used for subfloors, sheathing, combination subfloor/floor and siding. Comply beams can be made also of a flakeboard center with plywood top and bottom (*Maloney 1996; Youngquist 1999*).

### 2.2.1.5 Wafer- and Flakeboard

Large, thin wafers or smaller flakes can be produced by several methods and used to produce a composite board. Wafers are almost as wide as they are long while flakes are much longer than they are wide. Wafers are also thicker than flakes. The wafers and flakes are randomly oriented throughout the panel. Wafer and flakeboard are made with a waterproof adhesive, such as phenol formaldehyde or an isocyanate, and usually have a specific gravity of between 0.6 and 0.8 (*Youngquist 1999*).

### 2.2.1.6 Particle boards

Particle board is a generic term for a panel that is manufactured from lignocellulosic materials (usually wood, primarily in the form of discrete pieces or particles, as distinguishes from fibers, i.e. sawdust, planer shavings and mill residues) combined with a synthetic resin and bonded together under heat and pressure in a hot press.

Particleboards are used as furniture panel and for structural applications as manufactured home floors, roof sheathing, wall panels, stair treads, and house floors.

### **2.2.1.7 Fiberboards**

Several things differentiate fiberboard from particleboard, most notably the physical configuration of the comminuted material. Because wood is fibrous by nature, fiberboard exploits the inherent strength of wood to a greater extent than does particleboard.

Wood can be broken down into fiber bundles and single fibers by grinding or refining. In the grinding process, the wood is mechanically broken down into fibers. In the refining process, wood chips are placed between one or two rotating plates in a wet environment and broken down into fibers. If the refining is done at high temperatures, the fibers tend to slip apart as a result of the softening of the lignin matrix between the fibers, and, consequently, the fibers will have a lignin rich surface. If the refining is done at lower temperatures, the fibers tend to break apart and the surface is rich in carbohydrate polymers. Fiberboards can be formed using a wet-forming or a dry-forming process. In a wet-forming process, water is used to distribute the fibers into a mat, which is then pressed into a board. In many cases an adhesive is not used, and the lignin in the fibers serves as the adhesive. In the dry process, fibers from the refiner go through a dryer and a blowline, where the adhesive is applied, and then formed into a web, which is pressed into a board (*Berglund and Rowell 2005; Youngquist 1999*).

#### **2.2.1.7.1 Low-Density Fiberboard (LDF)**

Low-density fiberboards have a specific gravity of between 0.15 and 0.45, and are used for insulation and for light-weight cores for furniture. They are usually produced by a dry process that uses a ground wood fiber.

Insulation boards are low-density, wet-laid panel products used for insulation, sound deadening, carpet underlayment, and similar applications. In the manufacture of insulation board, the need for refining and screening is a function of the raw material available, the equipment used, and the desired end-product. Insulation boards typically do not use a binder, and they rely on hydrogen bonds to hold the board components together (*Berglund and Rowell 2005; Youngquist 1999*).

#### **2.2.1.7.2 Medium-Density Fiberboard (MDF)**

Medium-density fiberboard has a specific gravity of between 0.6 and 0.8 and is frequently used in place of solid wood, plywood, and particleboard in many furniture

applications. It is also used for interior door skins, moldings, and interior trim components.

### 2.2.1.7.3 High-Density Fiberboard (HDF)

High-density fiberboard has a specific gravity of between 0.85 and 1.2 and is used as an overlay on workbenches and floors, and for siding. It is produced both with and without wax and sizing agents. The wax is added to give the board water resistance. The uses for hardboard can generally be grouped as construction, furniture and furnishings, cabinet and store work, appliances, and automotive and rolling stock (Berglund and Rowell 2005; Youngquist 1999).

### 2.2.1.8 Other types of composites

There are a wide variety of composite products that can be made from wood, as shown above. There are also a lot of wood-based composites that are a combination of wood and non-wood elements. Combinations of wood and inorganics, thermoplastics, fiberglass, metals, and other synthetic polymers have been produced; some are commercial, and some are still in the research phase (Youngquist 1999).

Inorganic-bonded wood composites are molded products or boards that contain between 10% and 70% by weight wood particles or fibers and conversely 90% to 30% inorganic binder. Acceptable properties of an inorganic-bonded wood composite can be obtained only when the wood particles are fully encased with the binder to make a coherent material. Inorganic binders fall into three main categories: gypsum, magnesia cement, and Portland cement (Berglund and Rowell 2005).

The use of lignocellulosics with thermoplastics is a recent innovation. Broadly defined, a thermoplastic softens when heated and hardens when cooled. Thermoplastics selected for use with lignocellulosics must melt or soften at or below the degradation point of the lignocellulosic component, normally 200°C to 220°C. These thermoplastics include polypropylene, polystyrene, vinyls, and low- and high-density polyethylenes. There are two main strategies for processing thermoplastics in lignocellulosic composites. In the first, the lignocellulosic component serves as a reinforcing agent or filler in a continuous thermoplastic matrix. In the second, the thermoplastic serves as a binder to the majority lignocellulosic component (Berglund and Rowell 2005).

## 2.2.2 Binderless fiberboards

There have been many attempts to produced binderless boards, one of which is the production of hardboards from rice straw without using synthetic resins (Fadl, Sefain et

al. 1977); the boards were submitted to a thermal post-treatment at 180 °C improving their water resistance properties but diminishing their bending strength. Hardboards have been also produced from bagasse without pretreatment (*Mobarak, Fahmy et al. 1982*), obtaining bending strengths up to 130 MPa and water absorptions as low as 10%; the boards were molded at 25,5 MPa and 175 °C. Besides, in this study was evaluated the importance of the moisture in the material before molding. Other authors (*Suchsland, Woodson et al. 1983, 1985; Suchsland, Woodson et al. 1987*), have produced hardboards from mansonite pulp without adhesives, they found that the dry forming processes develop higher mechanical properties and lower water absorption in the boards compared with wet forming processes. The hardboards were produced from severely treated pulps, which were refined afterwards. This pretreatment was chosen by the authors to force the separation of the fibers through the lignin-rich part of the material, obtaining fibers covered of lignin; which is very favorable for forming boards using only lignin as adhesive. Binderless boards have been also produced from steam exploded pulps of oil palm fronds (*Laemsak and Okuma 2000; Suzuki, Shintani et al. 1998*), the material was pretreated at temperatures between 210 and 235 °C for 5 or 10 min and subsequently press at pressures between 250 and 400 bars without washing the pulp; in this study, the authors found some evidences for believing that the main bonding strength of the boards is due to a lignin-furfural linkage. Steam exploded fibers from coniferous sawdust (*Angles, Ferrando et al. 2001; Anglès, Reguant et al. 1999*) as well as from *Miscanthus sinensis* (*Velásquez, Ferrando et al. 2003a, b*) have been used for the production of good quality binderless boards following a three steps pressing process, the experimental conditions were mentioned previously.

### **2.2.3 Vapor pretreatment of lignocellulosic materials – Steam Explosion**

In the search for alternative fibers replacing natural wood, different possibilities have been considered, since 1970s, for the production of boards from different residual lignocellulosic-materials (*Blanchet P. 2000; Carvajal, Valdés et al. 1996; Das 2000; Grigoriou 2000a; Grigoriou 2000b; Kumar 1966; Youngquist, English et al. 1994; Youngquist, Krzysik et al. 1996; Zhang, Kawai et al. 1995*). One of the most effective pretreatment techniques used for developing the properties of those lignocellulosic materials is steam explosion. In this process wood or plant chips are treated with high pressure steam followed by a sudden release of the pressure. In the steam explosion process the wood structure is broken by the adiabatic expansion of absorbed water and the autohydrolysis of the cell wall components catalyzed by acetic acid released from the wood (*Kallavus and Gravitis 1995*). The autohydrolysis and explosion system

increase the accessibility and the separation of the lignocellulosic material into its three main components, cellulose, lignin and hemicelluloses (Košíková, Mlynár et al. 1990).

Explosion pulping was developed as an alternative for the utilization of wastes from the agricultural activities by W. H. Mason in the early 1930s. This process reduce the wood structure by exploding chips of wood under high steam pressure instead of grinding them or by chemical means, thus preserving the fiber structure without loss through chemical action.

The sequence of this process is as follows (Boehm 1930):

- The lignocellulosic material is charged to the recipient and then the recipient is closed.
- Low pressure vapor is admitted (24 bar, 220 °C), bringing the chips to a temperature of 190 °C. The chips are left for 30 to 40 s at this temperature.
- High pressure vapor is admitted and the recipient brought up to a pressure of 69, 25 bars, 285 °C in 3 s. The system is left at this pressure for 5 s.
- The hydraulic discharge valve is opened and the chips are exploded immediately due to the difference in pressure. The vapor and fibers are separated in a cyclone.

The result from this pretreatment is a brown pulp, called mansonite pulp that is used for the fabrication of fiberboards through a humid path in a process very similar to the fabrication of paper.

The vapor pretreatment changes the chemical and physical structure of the material. It is believed that the chemical changes produced in the lignocellulosic material account for the hydrolysis, and in more severe treatments for the pyrolysis of the highly hygroscopic hemicelluloses, also for the partial hydrolysis of lignin to smaller molecules which facilitates its flow during the hot pressing process (Hsu 1986). The physical changes in the lignocellulosic material, induced for the adiabatic expansion of the absorbed water inside its pores, account for the rupture of the wood structure, making the material more porous and accessible for lignin redistribution (Kallavus and Gravitis 1995; Košíková, Mlynár et al. 1990).

The effect of steam pressure on binderless boards has been studied, the authors (Suchsland, Woodson et al. 1987) found that increasing the steam pressure to 27,6 bar (229 °C) improved, in general, the mechanical and physical properties of binderless

boards. This improvement in the properties was attributed to the increase in the fines content of the pulp, due to the higher steam pressure at which the pulp was submitted.

Dimensional instability of fiberboards is mainly caused for its high tendency to absorb water under high humidity conditions. Swelling of wood panels consists of reversible and irreversible swelling when they absorb water or moisture. The reversible swelling is caused for the hygroscopic nature of wood. The irreversible swelling is caused in part for the spring back of compressed wood. It is believed that steam pretreatment increases the wood compressibility, reducing the level of internal stresses induced during hot pressing, causing less stress recovery and less thickness recovery of the board when exposed to moisture.

Few modifications of the mansonite pretreatment have been proposed to improve the dimensional stability of the boards. Some authors (*Hsu 1986; Hsu, W. et al. 1988*), have obtained reductions of about one third, compared to the control, on thickness swelling of boards bonded with an urea-formaldehyde resin, treating lignocellulosic material at 200 °C for 1 to 5 minutes and releasing the vapor without explosion. Other authors (*Sekino, Inoue et al. 1997*), have obtained reductions until one-quarter on thickness swelling, increasing the pretreatment temperature to 210 °C and pretreatment time to 10 min.

The irreversible swelling of boards is also caused by the breakage of the adhesive bond network, which would prevent particles or fibers recovery (spring back). Previous studies (*Chow, Bao et al. 1996; Sekino, Inoue et al. 1997; Sekino 1999*), have found that steam pretreatment plays an important role in reducing the breakage of adhesive bonds between particles during wetting/drying cycles, probably because of the decrease of swelling stress imposed on adhesive bonds, the reduction of wood hygroscopicity and the increase of wood compressibility produced for the pretreatment.

#### **2.2.4 Pressing conditions**

The pressing operation is an extremely critical step in fiberboard production. It is during this process that many of the physical properties are developed. The pressing process involves the simultaneous application of both heat and pressure, a combination found necessary to make use of the coarse lignin-rich pulps produced through a defibration process as steam explosion. The heat and pressure applied to the pretreated lignocellulosic material serves the following main purposes (*Back 1987*):

- Pressure overcomes the low auto-contraction forces of the coarse fiber bundles in the hardboard. During the pressure cycle the pressure has to be relieved to permit the evaporation of some extractives and water and thus preventing the

delamination and cracking of the board and to relax internal stresses formed during the pressing.

- The pressing temperature is controlled to keep the mat above the glass transition temperature of lignin to soften the material.
- The pressure-time schedule is manipulated to produce the desired board thickness and density at constant basis weight.

Under conventional pressing conditions, heat from the press plates rapidly converts moisture near the mat surface to steam, establishing temperature, moisture content and vapor pressure gradients from the mat surface to the core. The viscoelastic properties of fibers within the mat depend largely on the combinations of temperature and moisture content found locally, thus influencing the softening and the stress relaxation within the mat during pressing.

Compaction of a fiber mat imparts compressive stresses to the individual wood elements. As a result, densification, fractures and inelastic strain are developed within the fibers, therefore reducing their inherent strength and stiffness. Despite applied stresses are relieved to some extent by the viscoelastic effects mentioned above, a complex state of residual stress exists in the finished board. Releasing these residual stresses induced for moisture uptake as well as microfailures within the wood elements account for the thickness swelling of fiberboards, this effect is also known as spring back.

Some author have evaluated the influence of pressing conditions on the properties of fiber boards (*Anglès, Reguant et al. 1999*). Conifer sawdust was first pretreated thermo-mechanically at 217 °C for 2,8 min. and then press at 7% of moisture content under a three steps pressing cycle. In the first step the material was pressed at 4,2 MPa for 5 min at the desired temperature. In the second step, the pressure was released for 1 min for relieving the steam produced in the first pressing step and in this way preventing blisters or bubbles inside the board. In the third step the material was submitted to a pressure of 4,2 MPa for a time between 5 to 15 min. The pressing cycle was carried out at temperatures between 175 to 230°C. It was found that the pressing temperature should be at least 200 °C to ensure that lignin melts and flows covering the fibers. In general the best mechanical and physical properties were achieved at 230 °C at which the pressure time was not significant. Other authors (*Velásquez, Ferrando et al. 2003a, b*) found the optimal conditions for producing binderless boards from *Miscanthus sinensis* with remarkable properties, the material was first steam exploded at 203 °C for 4 to 14 min then ground and finally press at pressing temperatures between 195 to 245 °C and pressures between 1,9 to 14,6 MPa. It was also used a

three steps pressing cycle with initial and final pressing times constants at 5 and 2 min, respectively and with a breathing time of 1 min. The best mechanical properties obtained were Modulus of ruptures (MOR) of 61 MPa, Modulus of elasticity (MOE) of 7630 MPa, Internal bonds (IB) of 4,1 MPa and thickness swelling (TS) and water absorptions (WA) as low as 2,5 % and 8,9 %, respectively.

### 2.2.5 Grinding

It has been found that changes in particle size caused by changes in the pretreatment severity affect the properties of the boards. The more severe the pretreatment is the smaller the particles of the material obtained. This change in particle size improves the internal bond, water absorption and thickness swelling but it deteriorates the other mechanical properties of the board.

If the particle size is reduced by other means different of increasing the pretreatment severity, probably the strength properties of the boards could be sustained. Some authors (*Velasquez, Ferrando et al. 2002*) have ground the pretreated pulp to achieve this goal. The grinding process considerably improved the internal bond and diminished the density of the board, the other properties MOE, MOR, WA and TS were not significantly affected. Properties improvement was attributed to the segregation of fiber bundles and not to the shortening of the fibers. Segregation increases the inter fiber bonding area.

## 2.3 LIGNIN

Lignin is a phenolic and branched macro-molecule part of lignocellulosic materials, such as wood, annual plants or agricultural residues. As structural component of plants, lignin is one of the most abundant renewable products in nature. In relation to its structure and chemical composition, it is the most complex natural polymer with a great variety of functional groups that provide the active centers available for chemical and biological interactions. Generally, lignin is considered to be a three-dimensional amorphous polymer, randomly arranged, made up of phenyl-propane units, although there is a portion that can be considered to be formed by two-dimensional ordered structures. Lignins from different woody plants exhibit differences to each other, even though their structure and composition respond always to a skeleton of phenyl-propane units. An important problem of studying lignin arises from the practical impossibility, until now, to extract it from the wood without altering its structure; even though the same



procedure is used it is difficult to obtain identical isolated samples (*García, Martín et al. 1984*).

The mass content of lignin in each plant depends on the origin of the vegetable species. In wood its content vary between 19 to 35% (*Dence and Lin 1992*). Available lignin from the market comes from a series of processes, mainly from the paper industry, which could affect the native structure of lignin. The main functional groups of lignin are: phenolic hydroxyls, aliphatic hydroxyls, methoxyls, carbonyls, carboxyls and sulfonates.

Lignin is formed in vegetables through copolymerization of three phenylpropanoid monomers called coniferyl, sinapyl and p-coumaryl alcohols. There are sensible differences between lignin coming from softwood and those coming from hardwood. In softwood lignin, the structural elements are mainly guaiacylpropanoid units derived from coniferyl alcohol. Instead, in hardwood lignins, the structural elements are comprised of syringylpropanoid units together with the guaiacylpropanoid units, in proportions from 4:1 to 2:1, derived from coniferyl and sinapyl alcohols, respectively. The structural elements comprising lignin are linked by carbon-carbon and ether bonds of the type  $\alpha - O - 4$ ,  $\beta - O - 4$ ,  $4 - O - 5$ . Figure 2.2 shows the structural units and monomers of lignin. Lignification process involves many coupling reactions which give rise to the network structure characteristic of lignin.

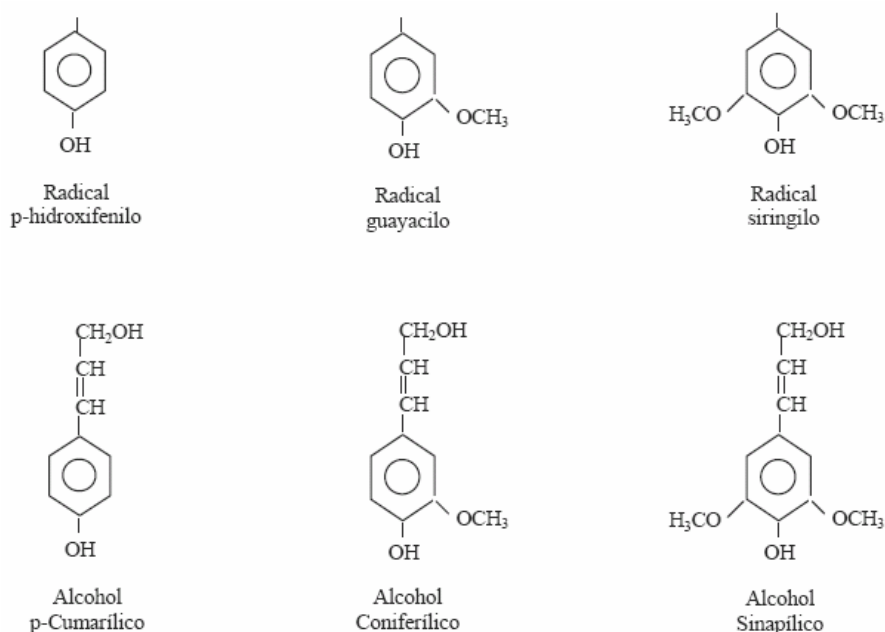


**Figure 2.2** Basic monomers and units of lignin (*García, Martín et al. 1984*)

Arrangement of structural units in the lignin macromolecule is subject to debate between scientists. Most of them think that lignin units are ordered randomly like the

structure proposed by Adler (Adler 1977) (figure 2.3), but others claim that lignin is an ordered polymer comprised by identical structural units which repeat themselves, like the structure proposed by Forss et al. (Forss, Fremer et al. 1966) (figure 2.4).

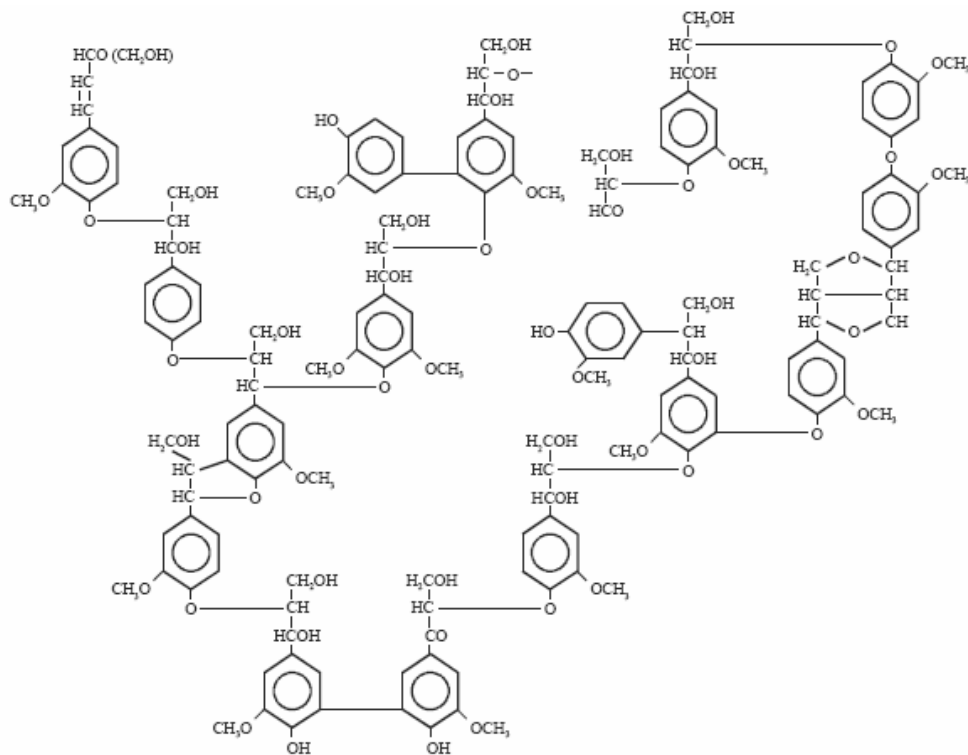


Figure 2.3 Lignin structure proposed by Adler (Adler 1977)

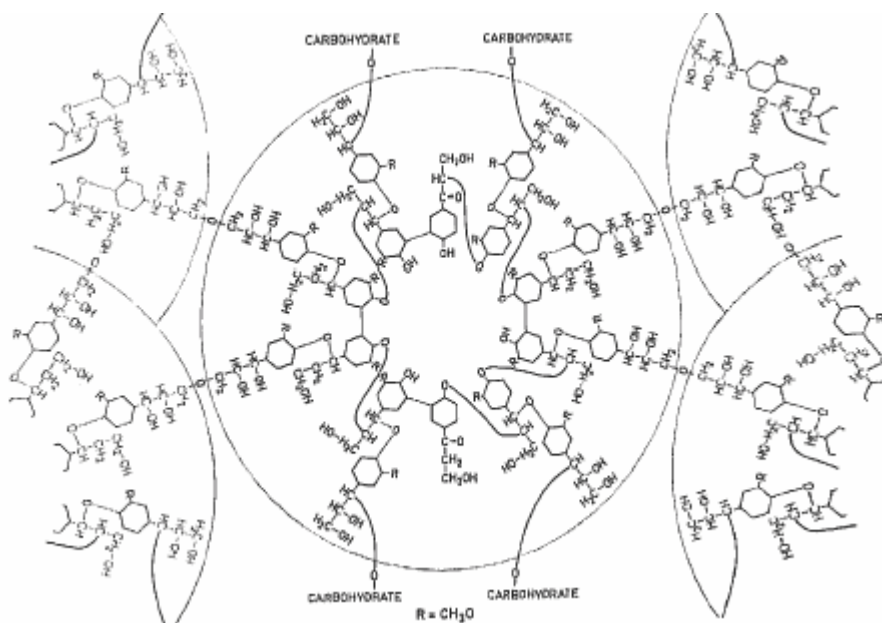


Figure 2.4 Lignin structure proposed by Forss et al. (Forss, Fremer et al. 1966)

### 2.3.1 Types and features of lignins

Pulp and paper industry comprised the main source of lignin byproducts. Wood hydrolysis, to obtain glucose among other fermentable sugars and bioethanol, represents other important source and its importance is expected to rise due to the high availability of forest and vegetable residues. Technical lignins could be classified into two categories depending on its sulfur content: The first category comprised of commercial lignins with sulfur in its chemical structure, between which Kraft lignin and lignosulfonates are found. These types of lignins are the most common type and are mainly produced from softwoods. The second category includes sulfur free lignins obtained from different processes and most of them are not commercially available, between them are found: Lignins from the soda process, organosolv lignins, lignins from the steam explosion process and lignins from biomass hydrolysis process.

#### 2.3.1.1 Kraft lignin

This type of lignin is obtained in the sulfate or Kraft pulping process. This is probably the chemical process most widely used mainly because of its versatility in the use of raw material and the excellent properties of the pulp obtained, particularly its high strength. The main disadvantages of the process are derived mainly from its environmental impact.

The chemical agent used in the Kraft cooking process is an aqueous dissolution of sodium hydroxide and sodium sulfide with a pH between 13 and 14. Pressure and cooking time may vary from 7 to 10 bars and 0.5 to 2 h, respectively, depending on the operation temperature (usually around 180 °C) and the proportion of alkali and sodium sulfide.

After cooking, black alkaline liquor is obtained, containing the non-cellulosic fraction of the wood and non-reacted chemicals. Afterwards, this black liquor is concentrated in multiple effect evaporators and the residue is burned in a furnace to produce energy and to recover part of the chemicals used in the process.

In the Kraft pulping process, the delignification occurs through the action of sodium hydroxide and sodium sulfate on the ether linkages of the lignin macromolecule. The cleavage of these links frees phenolic hydroxyl groups, which favor the dissolution of lignin in the alkaline medium. The delignification is faster in the Kraft than in the sulphite process, which will be addressed further (Lignosulfonates), and with only a small degradation of cellulose. The Kraft lignin is more degraded and therefore has a lower molecular weight than the lignin produced in the sulfite process.

The Kraft black liquor resulting from the stage of cooking contains 15-18% of dissolved solids, mostly lignin, as well as degradation products of carbohydrates, excerpts from wood and inorganic chemicals (García, Martín *et al.* 1984). A two stages acid precipitation can be used to isolate the Kraft lignin (García, Martín *et al.* 1984; Northey 1992), using CO<sub>2</sub> in the first stage, reaching a pH of 8-9 and using H<sub>2</sub>SO<sub>4</sub> in the second stage to a final pH of 2-3.

Kraft lignins present less polydispersity than lignosulfonates and are soluble in aqueous alkaline medium (pH>10.5), dioxane, acetone, dimethyl formamide and 2-Methoxyethanol (Lin and Lin 1990).

### 2.3.1.2 Lignosulfonate

The lignosulfonates are obtained as a byproduct of the sulfite pulp manufacturing process. This process is characterized by its high flexibility, since the pH of the cooking medium can be adjusted throughout the pH range by changing the proportions between reagents. Thus, allows the production of pastes of different types and grades for a wide variety of applications.

Currently, the sulfite process is subdivided based on the different types of cooking mediums and the base employed (acid bisulfite, bisulfite, neutral sulfite, alkaline sulfite, multistage sulfite, sulfite catalyzed with anthraquinone). The use of other bases instead the more soluble calcium, such as magnesium, sodium or ammonium allows to operate in less acidic conditions and to extend the attack to other wood species that are not suitable for the classic calcium bisulfite acid process. Pulp obtained from these more recent processes have higher yields and better properties.

Sulfurous acid and bisulfite ion mixtures are used in the sulfite pulping process to degrade and solubilize lignin. Moreover, the chemical attack mechanism suppresses the lignin as lignosulfonic acid salts, remaining the molecular structure almost intact. The cooking medium is an aqueous solution of sulfur dioxide with varying amounts of one of the bases mentioned above. Temperatures of 120-135 °C and times higher than 4 h are commonly used. This process can be conducted in a wide range of pH determined by the amount of based added.

The delignification in the sulfite process occurs to some extent by the breakage of links, but mostly sulfonation reactions take place solubilizing lignin molecules (Northey 1992). Lignosulfonates are recovered mostly from sulfite process. They are difficult to separate and purificate, being only possible to separate them by precipitation using chemical reagents, such as organic solvents or complexation agents, due to its complete solubility in water at every pH.

Lignosulfonates are considered byproduct of low added value which were sold in the form of not purified black liquor and concentrated to reduce the cost of transportation. Lately, there have been introduced several purification operations to the sulfite process: Fermentation and evaporation of ethanol to remove sugars, membrane filtration for an accurate selection of lignin fractions and salts reduction, spray drying to reduce the water content and to produce lignosulfonates in powder form. The lignosulfonates are distinguished by the nature of their cations such as magnesium, calcium, sodium, etc. Thus, lignosulfonates exist in a wide variety of products at a commercial level.

### 2.3.1.3 Organosolv lignin

Organosolv lignins are derived from the pulping processes known as “organosolv”, which are characterized by the use of organic solvents as a cooking medium, mixed with water and sometimes in presence of acid or basic catalyst. The simplicity of the recovery system is the reason for the lower environmental impact of these processes compared to the conventional ones, because the organic solvents are recovered easily from black liquors by distillation. Other important advantages of these processes are the high pulp yields, the little degradation endures by the lignin and the ease for bleaching the resulting pulps (*Goyal, Lora et al. 1992; Pan, Pla et al. 1992*).

Recently, several projects have been developed with the purpose of replacing conventional processes, which mostly use sulfur, with cleaner pulping technologies based on the use of organic solvents. There have been used as solvents alcohols, organic acids, amines, esters, among others. The designation of such processes is provided by the solvent used, the name of the process, or the company that is developing it: Phenol (Batelle), ethanol (Alcell, Repap), Methanol (Organocell, hyssen), acetic acid (Acetosolv, Veba Oel), formic acid (Milox, Finish pulp and paper research institute) and others. Most of these processes have not had great success, except Organocell (methanol) and Alcell (ethanol) that have taken a significant step towards its industrial implementation. The biggest drawback of these processes is the high pressure of work and its flammability. Ethanol has been used rather than methanol for their lower toxicity and volatility.

The recovery of lignin in the alkaline organosolv processes goes through its precipitation acidulating the black liquor to pH around 2, just like in other conventional alkaline processes, and on the other hand, simultaneously removing the solvent (*Gilarranz, Rodríguez et al. 1998*). In the acid organosolv processes, lignin precipitation is achieved by diluting the black liquor with water. The decrease of the organic solvent

proportion in the liquor reduces the solubility of lignin and causes its precipitation (Ni and Hu 1995; Sarkanen 1990).

Table 2.2 shows a brief summary of the chemical characteristics of the most important lignins afore mentioned.

**Table 2.2** Approximate chemical characteristics of three types of lignin (Glasser 1981)

	<b>Lignosulfonates</b>	<b>Kraft</b>	<b>Organosolv</b>
<b>Elemental Composition</b>	C 53% H 5.4% S 6.5%	C 66% H 5.8% S 1.6%	C 63% H 5.5% S –
<b>Contaminants</b>	Misc. carbohydrate degradation products	None	None
<b>Functionality</b>			
Phenolic OH	1.9%	4.0%	4.8%
Aliphatic OH	7.5%	9.5%	5.0%
SO <sub>3</sub> H	16.0%	–	–
SH	–	3.3%	–
OCH <sub>3</sub>	12.5%	14.0%	19.0%
<b>Solubility</b>	Water	Alkali	Organic solvents
<b>Molecular weight (Da)</b>	400-150,000	2000	700
<b>Predominant interunit bond</b>	Aryl-alkyl Ethers (β-O-4)	C-C (polystyrene type) involving sidechains and aromatic rings and dialkyl ethers	C-C (hydrolysis lignin type) between sidechains and aromatic rings and diaryl ethers

### 2.3.2 Potential uses of lignin

The potential uses of lignin are based on its ability to perform functions such as chemical dispersant, binder, sequestration agent, emulsifier and emulsions stabilizer (Rodríguez, García et al. 1990). Moreover, lignin is used for specific applications and as a copolymer of phenolic resins. The effectiveness of lignic materials in their applications improve by decreasing the presence of impurities such as sugars, acids and extracts (Northey 1992).

The importance of lignin recovering and the development and improvement of new applications that allows the polymeric use of lignin as well as its derivatives is given by economic and environmental reasons. Black liquors from the chemical pulp production processes, from which it is intended to isolate lignin as a byproduct, show a high

environmental burden (Adams 1995; Dong and Frike 1996; González, Riera et al. 1989).

### 2.3.2.1 Lignin in adhesives formulation

The most innovative field for lignin use corresponds to the production of phenolic resins in general. Lignin can act as copolymer in phenol-formaldehyde (PF) and urea-formaldehyde (UF) resins because of its structural similarity to those resins. Figure 2.5 shows the basic structure of lignin and PF resin (Forss and Fuhrmann 1979). The main application of these resins focuses on agglomerated boards industry and plywoods. However, phenolic resins are also used as thermal, electrical and acoustic insulation and as friction materials. Lately, phenol-formaldehyde resins (PF) had displaced urea-formaldehyde resins (UF) as a basis for adhesives used in the manufacture of boards, because basically PF resins have lower emissions of formaldehyde in its application and they offer higher resistance to moisture, which makes them suitable for coatings, even outdoors.

Lignin is more readily available, less toxic and cheaper than phenol. Its use as phenol substitute in phenol-formaldehyde resins or in adhesive mixtures with polymeric methylene diphenyl diisocyanate (pMDI) (Pizzi and Mittal 2003; Stephanou and Pizzi 1993) where prices depend on the fluctuations in oil price, is considered a potentially attractive application from the economical and environmental points of view. Moreover, lignin is obtained from renewable resources and can be used without previous treatments. A complete discussion of the development of lignin-modified phenolic adhesives is given by Pizzi (Pizzi and Mittal 2003) and Sellers et al. (Sellers, McGinnis et al. 2004).

Lignin has also been successfully used as partial substitute of phenol in phenolic resins manufacture and as part of panel products by mixing it with phenol-formaldehyde resins or used directly for fibreboard production as a natural binder (Alonso, Oliet et al. 2004; Velásquez, Ferrando et al. 2003c). The reactivity of industrial lignins is much lower than that of phenolic resins because of their low phenolic hydroxyl content, high ring substitution and steric hindrance (Vázquez, Freire et al. 1999). For these reasons, only a limited amount of industrial lignin can be used as a direct replacement for phenol in the formulation of phenolic adhesives without losing adhesive properties (Nimz 1983). However a higher replacement can be achieved by using modified lignins. The purpose of that modification is to increase the reactivity of lignins, giving them a higher functionality through its demethylation, phenolation and methylation. These techniques of modification have been extensively

studied in the past (Benar, Gonçalves et al. 1999; Gonçalves and Benar 2001; Vázquez, González et al. 1997).

Several studies were focused on the production of lignin with high functionality, meaning high reactivity, in the same pulping process by optimizing the operation conditions to produce good pulp and lignin with high reactivity (Alonso, Oliet et al. 2004; Vázquez, Freire et al. 1999). Unfortunately, these studies confirmed that high severity treatments contribute to the production of lignin with high functionality but accompanied with a loss in pulp quality. These conditions can not be used, since pulp is the main product and essential for the economy of the process.

Hydrolysis of lignin, either in alkaline or acidic medium, degrades lignin molecules and thus new phenolic hydroxyl groups can be generated. Under proper conditions, alkaline hydrolysis of industrial lignins yields reactive degradation products useful for condensation reaction in phenolic resins. Another advantage of using alkaline hydrolysis to modify industrial lignins is that the hydrolyzed products can be directly used in phenolic resins synthesis. Although a substantial amount of simple phenols can be produced by acid hydrolysis of lignin, acid hydrolysis of lignin is usually carried in non-aqueous medium, and the hydrolyzed lignin has to be separated from organic solvent before it can be utilized. In addition, Muller et al. (Muller, Kelley et al. 1984) found that acid-hydrolyzed lignin was incompatible with the normal process of phenolic resins synthesis.

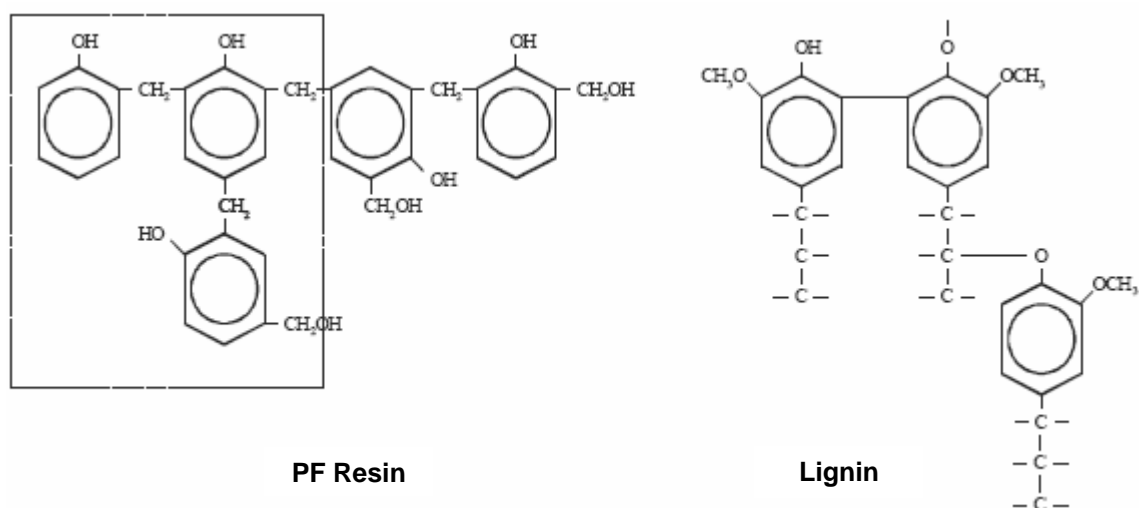


Figure 2.5 PF resin and lignin structures (Forss and Fuhrmann 1979)



### 2.3.2.2 Lignin use in other applications

There are many possible applications for lignin use depending on its physicochemical properties. The more relevant ones are the following (*Anglès Llauradó 1999; García, Martín et al. 1984; Northey 1992*).

#### *Dispersant*

Lignins can act as surface activating agents to avoid the formation of aggregates of insoluble particles in suspension. Lignosulfonates and Kraft lignins contain hydrophobic molecules which in turn contain hydrophilic groups such as sulfonates and carboxyls. Hydrophobic part of lignin is absorbed by the particles staying in contact with water the hydrophilic part, in this way the repulsion between particles increases and consequently the dispersion is more stable and the agglomeration of particles is avoided.

Lignins are found interesting for their dispersant properties in rubber tyres manufacturing, in the ceramic industry, in the preparation of dyes and pesticides and in controlling the accumulation of deposits in water circuits.

In cement industry, lignin use allows reducing significantly the kneading water, which translates into greater and more rapid mechanical strength of the product bound, additionally, it is less permeable. Iron and chromium lignosulfonates are particularly employed as additives for lubricant sludge improving their rheological properties, thus protecting the drill.

#### *Emulsifier*

Lignin can be used as emulsifying agent and as emulsions stabilizer, this property is of particular interest in its application to the stabilization of asphalt emulsions.

It has been also studied the possible uses of lignin linked to its tensoactive character in the manufacture of detergents and flotation agents for the treatment of minerals and water.

#### *Sequestrant*

The large number of functional groups of lignin allows their use in the production of ion exchange resins, in the immobilization of micronutrients in agricultural soils and as flocculant agents.

Elements such as Fe, Cu, Zn, B, Mb, and Mn form chelates with lignosulfonates. This compounds act as micronutrients on the growth of plants on poor soils and they are compatible with most insecticides, fungicides and herbicides.

The water used in cooling towers and boilers is treated with lignosulfonates (1-1000 ppm) to prevent the formation of sediments. In addition, lignosulfonates are added in proportions between 0.05-2.0% in commercial cleaning solutions as dirt dispersant agents.

#### *Fertilizer*

Humic material can be obtained from lignin after a first stage of oxidation, due to the organic nature of lignin. This material can be transformed afterwards, by ammoniation, in a humic fertilizer nitrogenated or combined with a commercial fertilizer, a mixed fertilizer, with a contribution to the soil of humic material and nitrogen.

#### *Reinforcement and antioxidant*

Lignin can replace the carbon black as enhancer in the production of rubber, while exerts an antioxidant action.

#### *Combustible*

Lignin can be used as fuel, either directly, with a calorific value similar to that of coal or following a pyrolysis or hydrogenation, which provide a mixture of hydrocarbons with higher calorific value. Its gasification is in a less developed phase.

#### *Monomers derived from lignin*

The use of lignin as a raw material in the synthesis of chemical monomers is of particular interest in the manufacture of vanillin, dimethyl sulfide and phenolic compounds.

Vanillin is a low molecular weight compound obtained through an alkaline oxidation with air. This commercial derivate of lignin is an aroma and absorbs UV rays. Moreover, it is a precursor of pharmaceutical products such as the ethyl vanillin which is a more stable and aromatic derivative.

Dimethyl sulfide can be obtained treating the Kraft black liquors with sulfur in excess, at temperatures between 200-250 °C. The dimethyl sulfide is used as an agent of methylation in the agrochemical industry to prepare various phenol derivatives. In the other hand, it can oxidize to dimethylsulphoxide using nitrogen tetroxide, this product is primarily used as a solvent in the production of synthetic fibers, also has applications in the pharmaceutical industry and in the manufacture of polymers.

### 2.3.2.3 Advantages and disadvantages in the use of lignin

Lignin, as it was afore mentioned, is an amorphous polymer that has so far been used little in industrial applications because its native structure varies depending on the plant from which it was extracted and also due to its supercondensate structure. For this reason, it has a highly variable formulation from batch to batch. While as we have seen, lignin has a great industrial potential, its market currently is still low. The main reasons for these are:

- The complex chemical structure of lignin and its derivatives
- Heterogeneity and polydispersity of lignin
- High quantity of impurities
- High sulfur content of Kraft lignins and lignosulfonates
- High cost for crude liquor purification and processing
- Lignin is difficult to copolymerize with phenol using formaldehyde in resins formulation. Being necessary to modify the lignin to enhance the quality of lignins obtained.

In the other hand, lignin is obtained from the pulp and paper industry as a residue and in this way lignin came from a renewable resource. Non modified lignin has a much lower cost than synthetic resins and it is easily used. With this in mind and the possibility of reducing the volume of residues generated by the P&P industry make reasonable its valuation.

### 2.3.3 Structural modifications of lignin

In the early research where lignin was used as copolymer in the formulation of phenol-formaldehyde resins its incorporation was direct (*Falkehag 1975*). Posterior investigations found the reasons to the poor results obtained in that case (*Dolenko and Clarke 1978; Forss and Fuhrmann 1979*). Today, almost all the studies using lignin as copolymer for PF resins formulation submit lignin to some kind of modification due to its low reactivity toward formaldehyde. These is explained for the high substitution presented by the lignic aromatic ring compared to phenol and for the consequently steric hindrance (*Jin, Sellers et al. 1990; Kuo, Hse et al. 1991*). There are different ways to modify lignin; the most relevant are the following:

- Hydroxymethylation
- Phenolation
- Demethylation

- Fractionation

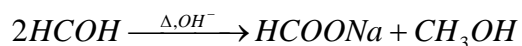
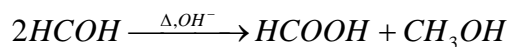
### 2.3.3.1 Hydroxymethylation

The hydroxymethylation consists of introducing hydroxymethyl groups (-CH<sub>2</sub>OH) in the aromatic ring of lignin by its reaction with formaldehyde (*Wooten, Sellers et al. 1988*). These modification increases the reactivity of lignin, since those groups are the precursors of methylene and dimethyl-ether bonds responsible for resin molecules crosslinking.

Hydroxymethylation of lignin with formaldehyde is carried out in basic medium at moderate temperature (40-60 °C). Phenol hydroxymethylation is carried out at 90 °C due to the higher activation energy of this reaction (*Peng and Riedl 1994*). Phenyl propane units react with electrophilic compounds like formaldehyde according to three different reactions (*Wooten, Sellers et al. 1988*):

#### Canizarro Reaction

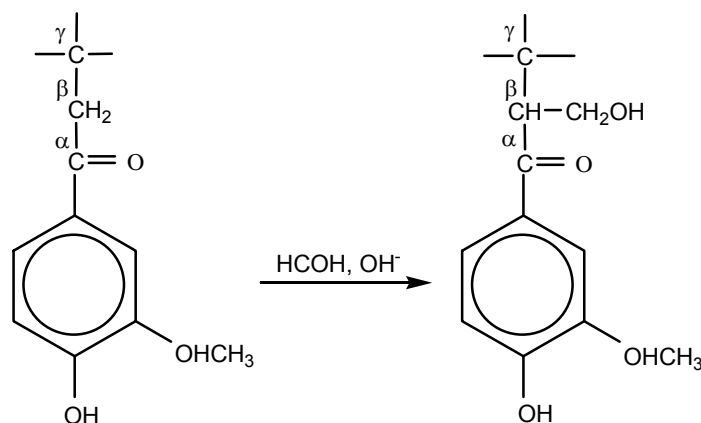
Formaldehyde reacts with itself in basic medium and high temperatures giving as a products formic acid or its corresponding salt and methanol, according to the following reactions:



In severe conditions, this reaction can continue until free formaldehyde and the OH<sup>-</sup> available are exhausted.

#### Tollens Reaction

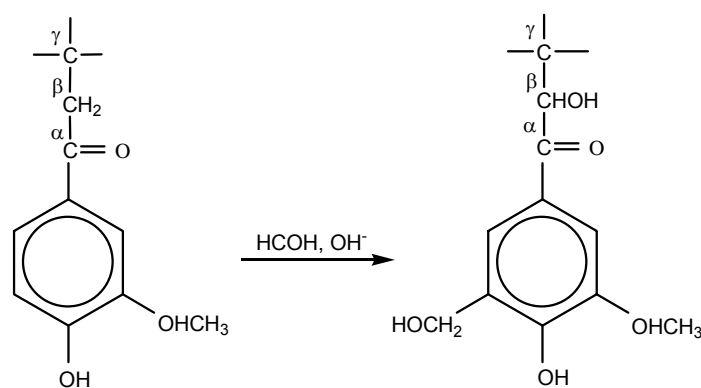
Hydroxymethyl groups are introduced in the side chain by this reaction, in the position next to the carbonyl or double bond groups according to the following reaction:



This Hydroxymethyl group introduced in the side chain is not involved in the resins formation reaction. It was observed (*Marton, Marton et al. 1966*) that when working with Kraft lignin this secondary reaction occurs less than 10% of the times related to the desired one, the Lederer-Manasse reaction.

#### Lederer-Manasse Reaction

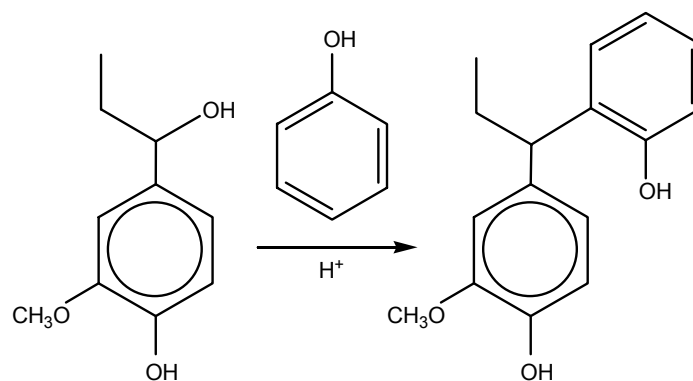
Is through this reaction that formaldehyde joins lignin in the free active positions of the aromatic ring. The active position corresponds to the ortho position related to the hydroxyl group of the aromatic ring. This exothermic reaction follows the next reaction equation:



This reaction allows the incorporation of hydroxymethyl in the aromatic ring of lignin, increasing the reactivity of the molecule. Hydroxymethyl groups in the ring, condensate establishing methylenic bridges. The reaction is endothermic and condensation can occur with active protons or hydroxymethyl groups from other aromatic rings. Hydroxymethylated lignin presents higher reactivity towards condensation reactions and the following methylenic bridge formation that propitiates the crosslinking between resin molecules, due to the faster condensation of two phenolic hydroxymethyl groups than the condensation through active protons (*Peng and Riedl 1994*).

#### 2.3.3.2 Phenolation

Phenolation takes place in acid medium and high temperature. Phenol incorporation is produced through the hydroxyl group on the  $\alpha$  carbon of the propanoid chain of lignin (*Alonso, Oliet et al. 2005; Alonso Rubio 2002; Vázquez, González et al. 1997*), according to the following reaction path:



This reaction produces an increase in active sites and therefore increases its reactivity towards formaldehyde. It can be seen that the presence of a phenolic hydroxyl group in an aromatic ring promotes the creation of two reactive positions (ortho and para related to that group) for the formaldehyde incorporation during phenolic resin formulation. There is a limitation to the phenolation, which is the lignin condensation with itself (*Lindberg, Kuusela et al. 1989*).

It has been shown that lignin phenolation is accompanied with its fractionation (reduction of its molecular weight), which improves the size compatibility between phenolated lignin and the prepolymer or the resin formulation, thus improving the final properties of the resin produced (*Calvé, Shields et al. 1988; Calvé, Shields et al. 1991*).

Besides, carbohydrates with concentrations between 10 to 30% in weight also react with the phenol at the reaction conditions (*Allan, Dalan et al. 1989; Dubois, Gilles et al. 1956*). This means that black liquors with considerable quantities of dissolved carbohydrates can be used. Finally, it was found that demethylation accompanies phenolation of lignin thus generating an increase in phenolic hydroxyl groups available (*Nada, El-Saied et al. 1987*).

### 2.3.3.3 Demethylation

This is a structural modification method where methoxyls groups of lignin are broken under acidic conditions, generating new phenolic hydroxyl groups. An increase in the reactivity of lignin towards formaldehyde is obtained in this way. Formaldehyde is incorporated to the aromatic ring in the positions ortho and para related to the phenolic hydroxyl group.

The feasibility of this method is compromised by the high cost of the reagents used such as potassium dichromate (*Hayashi, Namura et al. 1967*), sodium periodate (*Marton and Alder 1963*), hydrochloric acid (*Gupta and Sehgal 1978*) and ethanolamine (*Wallis 1976*).

#### 2.3.3.4 Fractionation

Lignin cuts of different molecular weight intervals can be obtained using this technique. In this way, the lignin fraction with the most appropriate molecular weight for its use in resin formulation can be selected. In addition, the homogeneity of lignin structure increases at least related to the molecular weight distribution.

There are different techniques available for the preparation of lignin with a defined range of molecular weights, the most relevant ones are: ultrafiltration, selective extraction with a solvent and differential precipitation.

Ultrafiltration scope has increased with the development of membranes capable of withstand relatively high temperatures and extremely acid or alkaline solutions.

Forss and Fuhrmann (*Forss and Fuhrmann 1976*) have attained lignin additions between 40 to 70% in lignin-Phenol-Formaldehyde (LPF) resins for particle board, fiberboard and plywood production using high molecular weight fractions, obtained by ultrafiltration, of Kraft lignin and lignosulfonates; according to the authors, the effectiveness of lignin molecules with high molecular weight lies in its high level of crosslinking, which in turn requires a low pH to form an insoluble copolymer compared to lignin molecules with low molecular weight. Olivares et al. (*Olivares, Guzmán et al. 1988*) obtained good results using a high molecular weight ultrafiltered Kraft lignin fraction ( $MW \geq 10,000$ ) in LPF resin formulation with 20% and 45% of phenol replacement by this lignin, and proposed to use the diluted fraction of the ultrafiltration process for salt recovering and as combustible with a cost reducing purpose.

Pranda et al. (*Pranda, Brezny et al. 1991*) described and studied the behavior of Kraft lignin fractions extracted from softwood using either dichloromethane or ethyl acetate as a solvent. The extracts obtained in this study have less content of methoxyl groups and higher contents of sulfur, phenolic hydroxyl groups and structures reactive towards formaldehyde; but in spite of the higher reactivity of lower molecular weight extracts they showed poorer performance than the high molecular weight fraction. The explanation lies in the interrelation between the molar mass and the reactivity on the adhesive performance. Both effects have a favorable effect on the quality of LPF resins but low molecular weight fractions seems to act like inactive fillers rather than active extenders like high molecular weight fractions of lignin. Lange et al. (*Lange, Faix et al. 1983*) also demonstrated that higher molecular weight fractions obtained by solvent extraction of organosolv lignin form LPF adhesives with a higher degree of crosslinking and shorter gel times. However, there are also studies in which fractions of lower molecular weight were found more suitable for LPF resins (*Calvé, Shields et al. 1991*).

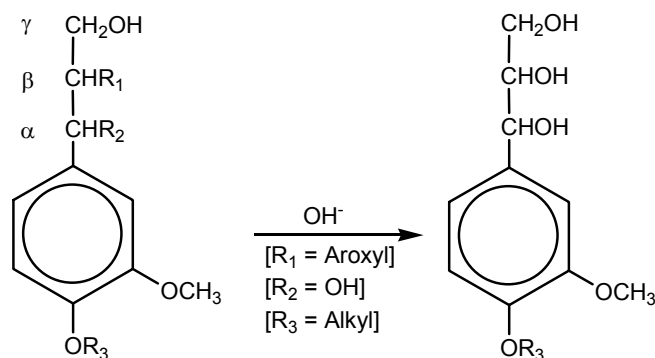
Summarizing, it has been proved that Kraft lignin cuts above determined molecular weight present better results than the ones obtained with non-fractionated lignins (*Olivares,*

Guzmán et al. 1988; Pranda, Brezny et al. 1991). It is also convenient to notice that it is difficult to isolate lignins between a given interval of molecular weights, because the cut is not clean, always will be a portion of lignin with a molecular weight out of the interval (Woerner and McCarthy 1984; Woerner and McCarthy 1986)

### 2.3.3.5 Alkaline medium hydrolysis

Hydrolysis of lignin, either in alkaline or acidic medium, degrades lignin molecules so that new phenolic hydroxyl groups can be generated. Under proper conditions, alkaline hydrolysis of industrial lignins yields reactive degradation products useful for condensation reaction in phenolic resins formulation. Another advantage of using alkaline hydrolysis to modify industrial lignins is that the hydrolyzed products can be directly used in the synthesis of phenolic resins. Although a substantial number of simple phenols can be produced via the acid hydrolysis of lignin, this process is usually performed in a non-aqueous medium, so the hydrolyzed lignin must be separated from an organic solvent before it can be used. Moreover, it was found by Muller et al (Muller, Kelley et al. 1984) that acid hydrolyzed lignin is incompatible with the normal process of phenolic resin synthesis.

Ether linkages at the  $\alpha$ - and  $\beta$ - positions are the most abundant functional groups on the propanoid side chain of lignin. Under alkaline conditions,  $\alpha$ - ether linkages are cleaved when the side chain is attached to a phenolic ring. Nonphenolic  $\alpha$ -ethers are cleaved provided a hydroxyl group is present at the adjacent  $\beta$ -position. Cleavage of  $\beta$ -ether linkages in phenolic and nonphenolic units similarly occurs in strongly alkaline media at elevated temperature when a hydroxyl or carbonyl group is present in the adjacent  $\alpha$ - or  $\gamma$ -position. As well as for acid-promoted cleavage of ether bonds, arylglycerol derivatives are formed as shown in the reaction equation below, which, unlike their behavior in acidic media, are stable in alkali (Gierer 1982; Lin and Dence 1992).





### 2.3.4 Lignin characterization

The absence of well-defined, standard analytical protocols, adopted by both suppliers and end-users of lignins in different markets is an important issue for its broader introduction as raw material in industry. For enhanced utilization of lignin, reliable characterization methods should become available for the identification of chemical and physical properties. Due to the structural complexity of lignin, development of reproducible methods is rather difficult, as described by several researchers (*Dence and Lin 1992; Milne, Chum et al. 1992*). Simple, reliable, quantitative, and widely accepted techniques include elemental analysis, functional group analysis, analytical degradations, various spectroscopic techniques, molecular weight analysis and thermal analysis. These techniques are capable of elucidating the chemical composition of repeating units; the nature of intermonomer bonds; molecular weights and weight distributions and the potential for inter- and intramolecular interactions (*Glasser 2000*).

The major chemical functional groups in lignin include hydroxyl, methoxyl, carbonyl and carboxyl groups in various amounts and proportions, depending on the genetic origin and the extraction processes used.

#### *Phenolic hydroxyl*

The chemical reactivity of lignin in various modification processes is highly influenced by its phenolic hydroxyl content, for instance, the presence of these groups increases the reactivity of the lignin towards formaldehyde in the formulation of phenolic resins or in the preparation of hydroxymethylated lignin. Phenolic hydroxyl group is also one of the most important functional groups of lignin affecting its physical and chemical properties (*Adler 1977*).

#### *Aliphatic hydroxyl*

Generally, the aliphatic hydroxyl content of lignin is determined by subtraction of the phenolic hydroxyl content from the total hydroxyl content of lignin. As aforementioned, lignins are produced by an enzymatic dehydrogenative polymerization of its three monomeric precursors, p-hydroxycinnamyl alcohol, coniferyl alcohol and sinapyl alcohol (see figure 2.2). These compounds, all of them, have a terminal aliphatic hydroxyl group at C- $\gamma$  on the side chain in addition to a phenolic hydroxyl group at C-4 of the aromatic ring. In contrast with phenolic hydroxyl group approximately only 20-25 mol % of the aliphatic hydroxyl groups of the monomeric precursors is involved in the lignification process (*Adler 1977; Chen 1992*). The role of the aliphatic hydroxyl group at

C- $\gamma$  is then considerably less significant than that of the phenolic hydroxyl group in the dehydrogenative polymerization of lignin precursors.

### *Methoxyl*

Methoxyl groups are present in the different lignocellulosic materials although their proportions vary as their content depends not only on the origin of the plant, but also the method of isolation.

### *Carbonyl*

Carbonyl is one of the reactive groups of lignin. Its quantification is of great interest to assess the changes in lignin during pulping, bleaching, or ageing of pulp. However, the determination of these groups is difficult because of its low content in the native lignin. The content of the different carbonyl types (total quinones, ketones, and aldehydes) depends on the method used for its determinations.

### *Carboxyl*

Carboxyl groups are present in small concentrations in native lignin, and in significant concentrations in lignin that has been subjected to a biological or a chemical treatment which breaks the aromatic rings of lignin leading to an increase in the compounds with carboxyl groups. Thus, the quantification of these groups provides information about the degree of degradation and modification of lignin and it also provides additional information about its solubility.

In the next chapter we will review the analytical methods and the equipments used for the quantification of lignin's functional groups, as well as, of other of its properties and for the physicochemical and chemical characterization of the fiberboards.

## REFERENCES

- Adams, T. N. Impact on recovery of pulping and bleaching changes to meet the EPA Cluster Rule. *Tappi Journal* 78(12): 29-36. 1995.
- Adler, E. Lignin Chemistry-Past, Present and Future. *Wood Science and Technology* 11: 169-218. 1977.
- Allan, G. G., J. A. Dalan, *et al.* Modification of lignins for use in phenolic resins. in: Adhesives from renewable resources. R. W. Hemingwaym and A. H. Conner, Ed. ACS symposium series, 385: 55-67. 1989
- Alonso, M. V., M. Oliet, *et al.* Use of methylolated softwood ammonium lignosulfonate as partial substitute of phenol in resol resins manufacture. *Journal of applied polymer science* 94: 643-650. 2004.
- Alonso, M. V., M. Oliet, *et al.* Modification of ammonium lignosulfonate by phenolation for use in phenolic resins. *Bioresource technology* 96(9): 1013-1018. 2005.
- Alonso Rubio, M. V. Formulaci3n y curado de resinas fenol-formaldehido tipo "resol" con sustituci3n parcial del fenol por ligninosulfonatos modificados. Departamento de ingenieria quimica. Madrid, Universidad complutense: 332. 2002
- Anglès Llauredó, M. N. Producci3n de taulers amb material lignocel.lul3sic residual sense addici3n d'adhesius sintetics. Tarragona, Universitat Rovira i Virgili: 237. 1999
- Angles, M. N., F. Ferrando, *et al.* Suitability of steam exploded residual softwood for the production of binderless panels. Effect of the pre-treatment severity and lignin addition. *Biomass and Bioenergy* 21(3): 211-224. 2001.
- Anglès, M. N., J. Reguant, *et al.* Binderless Composites from Pretreated Residual Softwood. *Journal of Applied Polymer Science* 73: 2485-2491. 1999.
- Back, E. L. The Bonding Mechanism in Hard board Manufacture. *Holzforschung* 41(4): 247-258. 1987.

- Benar, P., A. R. Gonçalves, *et al.* Eucalyptus organosolv lignins: study of the hydroxymethylation and use in resols. *Bioresource Technology* 68(1): 11-16. 1999.
- Berglund, L. and R. M. Rowell. Wood Composites. in: Handbook of Wood Chemistry and Wood Composites. R. M. Rowell, Ed. 2005
- Blanchet P., C. A., Riedl B. Particleboard made from hammer milled black spruce bark residues. *Wood Science and Technology*. 2000.
- Boehm, R. M. The Masonite process. *Industrial and Enginnering Chemistry*. 1930.
- Calvé, L. R., J. A. Shields, *et al.* A practical lignin-based adhesive for waferboard/OSB. *Forest Product Journal* 38(5): 15-20. 1988.
- Calvé, L. R., J. A. Shields, *et al.* Commercial trials of a lignin-phenolic waferboard adhesive. *Forest Product Journal* 41(11/12): 36-42. 1991.
- Carvajal, O., J. L. Valdés, *et al.* Bagasse particleboards for building purpose. *Holz als Roh und Werkstoff* 54: 61-63. 1996.
- Chen, C.-L. Determination of total and aliphatic hydroxyl groups. in: Methods in Lignin Chemistry. S. Y. Lin and C. W. Dence, Ed. Berlin: 409-422. 1992
- Chow, P., Z. Bao, *et al.* Effects of two Fiber treatments on properties of Hemlock Hardboard. *Forest Product Journal* 46: 62-66. 1996.
- Das, S., Saha, A.K., Choudhury, P.K., Basak, R.K., Mitra, B.C., Todd, T., Lang, S., Rowell, R.M. Effect of Steam Pretreatment of Jute Fiber on Dimensional Stability of Jute Composite. *Journal of Applied Polymer Science*. 2000.
- Dence, C. W. and S. Y. Lin. General structural features of lignin. in: Methods in Lignin Chemistry. S. Y. Lin and C. W. Dence, Ed. Berlin: 3-6. 1992
- Dolenko, A. J. and M. R. Clarke. Resin binders from Kraft lignin. *Forest Product Journal* 28(8): 41-46. 1978.

Dong, D. and A. L. Frike. Investigation of Pulping Effect on Pulp Yield and the Lignin content of Black Liquor with a central Composite Kraft Pulping Design. *Holzforschung* 50(1): 75-80. 1996.

Dubois, M. D., K. A. Gilles, *et al.* Colorimetric Method for Determination of Sugars and Related Substances. *Analytical chemistry* 28(3): 350-356. 1956.

Fadl, N. A., M. Z. Sefain, *et al.* Effect of Thermal Treatment on Egyptian Rice Straw Hardboard. *Journal of Applied Chemistry and Biotechnology* 27: 93-98. 1977.

Falkehag, S. I. Lignin in materials. *Applied polymer symposia* 28: 247-257. 1975.

Forss, K., K.-e. Fremer, *et al.* Spruce lignin and its reactions in sulfite cooking. *Paperi ja Puu* 48(9): 565-574. 1966.

Forss, K. G. and A. Fuhrmann. Adhesive for the production of laminates and other agglomerated materials. Keskuslaboratorium. DE2601600. 1976

Forss, K. G. and A. Fuhrmann. Finnish plywood, particleboard, and fiberboard made with a lignin-base adhesive. *Forest Product Journal* 29(7): 39-43. 1979.

García, H. F., J. F. Martín, *et al.* Posibilidades de aprovechamiento de la lignina en la industria química. *Ingeniería Química* Octubre: 249-254. 1984.

Gierer, J. The chemistry of delignification - a general concept. Part 1 and Part 2. *Holzforschung* 36: 43-64. 1982.

Gilarranz, M. A., F. Rodríguez, *et al.* Acid Precipitation and Purification of Wheat Straw Lignin. *Separation Science and Technology* 33(9): 1359-1377. 1998.

Glasser, W. G. Potencial role of lignin in tomorrow's wood utilization technologies. *Forest Product Journal* 31(3): 24-29. 1981.

Glasser, W. G. Classification of lignin according to chemical and molecular structure. in: Lignin: Historical, Biological, and Materials Perspectives. American Chemical Society, ACS Symposium series 742: 226-237. 2000.

Gonçalves, A. R. and P. Benar. Hydroxymethylation and oxidation of organosolv lignins and utilization of the products. *Bioresource Technology* 79: 103-111. 2001.

González, C., F. A. Riera, *et al.* Nuevas alternativas para la utilización de lignina. *Ingeniería Química* Septiembre: 237-242. 1989.

Goyal, G. C., J. H. Lora, *et al.* Autocatalized organosolv pulping of hardwoods: Effects of pulping conditions on pulp properties and characteristics of soluble and residual lignin. *Tappi Journal* 75(2): 110-116. 1992.

Grigoriou, A., Passialis, C., Voulgaridis, E. Experimental particleboards from Kenaf plantations grown in Greece. *Holz als Roh- und Werkstoff*. 2000a.

Grigoriou, A. H. Straw-wood composites bonded with various adhesive systems. *Wood Science and Technology*. 2000b.

Gupta, R. C. and V. K. Sehgal. Studies on the effect of methylation and demethylation on resin forming properties of thiolignin from *Picea smithiana*. *Holzforschung und Holzverwertung* 30: 85-87. 1978.

Hayashi, A., Y. Namura, *et al.* Lignonsulfonates. XXVII. Demethylation of lignosulfonates during gelling reaction with dichromates. *Mokuzai Gakkaishi* 13(5): 194-197. 1967.

Hsu, W. E. Method of Making Dimensionally Stable Composite Board and Composite Board Produced by Such Method. 1,215,510. 1986

Hsu, W. E., S. W., *et al.* Chemical and physical changes required for producing dimensionally stable wood-based composites. Part1: Steam pretreatment. *Wood Science and Technology* 22. 1988.

Jin, L., T. J. Sellers, *et al.* Utilization of lignin modified by brown-rot fungi. I. Properties of flakeboard produced with a brown-rotted lignin modified phenolic adhesive. *Holzforschung* 44(3): 207-210. 1990.

Kallavus, U. and J. Gravitis. A Comparative Investigation of the Ultrastructure of Steam Exploded Wood With Light, Scanning and Transmission Electron Microscopy. *Holzsforschung* 49: 182-188. 1995.

Košíková, B., J. Mlynár, *et al.* The Relationship between Ultrastructure and Lignin Extractability of Steamed Hardwoods. *Holzforschung* 44(4): 249-255. 1990.

Kumar, V. B. Suitability of Indian Hardwoods for the Manufacture of Hardboard. *Holzforschung und Holzverwertung* 18(1). 1966.

Kuo, M., C. Y. Hse, *et al.* Alkali treated Kraft lignin as a component in flakeboard resins. *Holzforschung* 45(1): 47-54. 1991.

Laemsak, N. and M. Okuma. Development of boards made from oil palm frond II: properties of binderless boards from steam-exploded fibers of oil palm frond. *Journal of Wood Science* 46(4): 322-326. 2000.

Lange, W., O. Faix, *et al.* Properties and Degradability of Lignins Isolated with Alcohol-Water Mixture. *Holzforschung* 37(2): 63-67. 1983.

Lin, S. Y. and C. W. Dence. Introduction. in: *Methods in Lignin Chemistry*. S. Y. Lin and C. W. Dence, Ed. Berlin: 83-109. 1992

Lin, S. Y. and I. S. Lin. lignin: *Ullmann's encyclopedia of industrial chemistry*, Editorial VCH. 1990.

Lindberg, J. J., T. A. Kuusela, *et al.* Specialty Polymers from Lignin. in: *Lignin: Properties and materials*. W. G. Glasser and S. Sarkanen, Ed. ACS symposium series, 397: 190-200. 1989

Maloney, T. m. The Family of Wood Composites. *Forest Product Journal* 46(2): 19-26. 1996.

Marra, G. Overview of wood as a material. *Journal of Educational Modules for Material Science Engineering* 1(4): 699-710. 1979.

Marton, J. and E. Alder. Oxidative demethylation of lignin. US 3,071,570. 1963

Marton, J., T. Marton, *et al.* Lignin Structure and Reactions. in. *Advances in chemistry Series*, 59: 125-144. 1966

- Milne, T. A., H. L. Chum, *et al.* Standardized analytical methods. *Biomass and Bioenergy* 2(1-6). 1992.
- Mobarak, F., Y. Fahmy, *et al.* Binderless Lignocellulose Composite from Bagasse and Mechanism of Self-Bonding. *Holzforschung* 36: 131-135. 1982.
- Muller, P. C., S. S. Kelley, *et al.* Engineering Plastics from Lignin. IX. Phenolic Resin Synthesis and Characterization. *The Journal of Adhesion* 17(3): 185-206. 1984.
- Nada, A. M. A., H. El-Saied, *et al.* Waste liquors from cellulosic industries. IV. Lignin as component in phenol formaldehyde resol resin. *Journal of Applied Polymer Science* 33: 2915-2924. 1987.
- Ni, Y. and Q. Hu. Alcell® lignin solubility in ethanol-water mixtures. *Journal of Applied Polymer Science* 57(12): 1441-1446. 1995.
- Nimz, H. H. Lignin-based wood adhesives. in: Wood adhesives - Chemistry and technology. A. Pizzi, Ed. New York: 247-288. 1983
- Northey, R. A. Low-cost uses of lignin. in: Materials and chemicals from biomass. ACS Symposium Series, 476: 146-175. 1992
- Olivares, M., J. A. Guzmán, *et al.* Kraft lignin utilization in adhesives. *Wood Science and Technology* 22(2): 157-165. 1988.
- Pan, X., F. Pla, *et al.* Structure and Reactivity of Spruce Mechanical Pulp Lignins Part II. Organosolv Fractionation of Lignins in a Flow-Through Reactor. *Journal of Wood Chemistry and Technology* 12(3): 279-298. 1992.
- Peng, W. and B. Riedl. The chemorheology of phenol-formaldehyde thermoset resin and mixtures of the resin with lignin fillers. *Polymer* 35(6): 1280-1286. 1994.
- Pizzi, A. and K. L. Mittal. Handbook of adhesive technology. New York, Marcel Dekker Inc. 2003.
- Pranda, J., R. Brezny, *et al.* Structure and performance of Kraft lignin fractions as components in resole adhesives. *Tappi Journal* 74(8): 176-182. 1991.



Rodríguez, J. J., F. García, *et al.* Posibilidades de aprovechamiento de los residuos lignocelulósicos. *Ingeniería Química* Mayo(254): 191-197. 1990.

Rowell, R. M. Chemical modification of lignocellulosic fibers to produce high-performance composites. in: *Agricultural and synthetic polymers: Biodegradability and utilization*. J. E. Glass and G. Swift, Ed. ACS symposium series, 433: 242-258. 1990

Rowell, R. M. Opportunities for lignocelluloseic materials and composites. in: *Emerging technologies for materials and chemicals from biomass*. R. M. Rowell, T. P. Schultz and R. Narayan, Ed. ACS symposium series, 476: 12-27. 1992

Sarkanen, K., V. Chemistry of solvent pulping. *Tappi Journal* 73(10): 215-219. 1990.

Sekino, N., M. Inoue, *et al.* Thickness Swelling and Internal Bond Strength of Particleboards Made from Steam-Pretreated Particles. *Mokuzai Gakkaishi* 43(12): 1009-1015. 1997.

Sekino, N., Inoue M., Irle M., Adcock T. The Mechanisms Behind the Improved Dimensional Stability of Particleboards Made from Steam-Pretreated Particles. *Holzforschung*. 1999.

Sellers, T. J., G. D. McGinnis, *et al.* lignin-modified phenol-formaldehyde resin development for fibreboard. *Forest Product Journal* 54(9). 2004.

Stephanou, A. and A. Pizzi. Rapid curing lignins-based exterior wood adhesives. Part 1: Diisocyanates reaction mechanisms and application to panel products. *Holzforschung* 47: 439-445. 1993.

Suchsland, O., G. E. Woodson, *et al.* Effect of hardboard process variables on fiberbonding. *Forest Products Journal* 33(4): 58-64. 1983.

Suchsland, O., G. E. Woodson, *et al.* Binderless fiberboard from two different types of fiber furnishes. *Forest Products Journal* 35(2): 63-68. 1985.

Suchsland, O., G. E. Woodson, *et al.* Effect on cooking conditions on fiber bonding in dry-formed binderless hardboard. *Forest Products Journal* 37: 65-69. 1987.

Suzuki, S., H. Shintani, *et al.* Preparation of Binderless Boards from Steam Exploded Pulps of Oil Palm (*Elaeis guineensis* Jaxq.) Fronds and Structural Characteristics of Lignin and Wall Polysaccharides in Steam Exploded Pulps to be Discussed for Self-Bindings. *Holzforschung* 52(4): 417-426. 1998.

Vázquez, G., S. Freire, *et al.* Structures, and Reactivities with Formaldehyde, of Some Acetosolv Pine Lignins. *Journal of Wood Chemistry and Technology* 19(4): 357-378. 1999.

Vázquez, G., J. González, *et al.* Effect of chemical modification of lignin on the gluebond performance of lignin-phenolic resins. *Bioresource Technology* 60: 191-198. 1997.

Velasquez, J. A., F. Ferrando, *et al.* Binderless fiberboard from steam exploded *Miscanthus sinensis*: The effect of a grinding process. *Holz als Roh- und Werkstoff* 60. 2002.

Velásquez, J. A., F. Ferrando, *et al.* Binderless fiberboard from steam exploded *Miscanthus sinensis*. *wood science and technology* 37: 269-278. 2003a.

Velásquez, J. A., F. Ferrando, *et al.* Binderless fiberboards from steam exploded *Miscanthus sinensis*: optimization of pressing and pretreatment conditions. *wood science and technology* 37: 279-286. 2003b.

Velásquez, J. A., F. Ferrando, *et al.* Effects of Kraft lignin addition in the production of binderless fibreboard from steam exploded *Miscanthus sinensis*. *Industrial crops and Products* 18: 17-23. 2003c.

Wallis, A. F. A. Reaction of lignin model compounds with ethanolamine. *Cellulose chemistry and technology* 10(3): 345-355. 1976.

Woerner, D. L. and J. L. McCarthy. Ultrafiltration of Kraft black liquor. in. AIChE Symposium Series (232), 80: 25-33. 1984

Woerner, D. L. and J. L. McCarthy. The effect of manipulable variables on fractionation by ultrafiltration. in: Industrial membrane processes. R. E. White and P. N. Pintauro, Ed. AIChE Symposium series, 82: 77-86. 1986

Wooten, A. L., T. J. Sellers, *et al.* Reaction of formaldehyde with lignin. *Forest Product Journal* 38(6): 45-46. 1988.

Youngquist, J. A. Wood-based Composites and Panel Products. in: Wood handbook. Wood as an engineering material. F. p. laboratory, Ed. Madison, Wisconsin. 1999

Youngquist, J. A., B. E. English, *et al.* Literature Review on Use of Nonwood Plant Fibers for Building Materials and Panels. Madison, WI, U.S. Department of Agriculture, Forest Service, Forest Products Laboratory. 1994

Youngquist, J. A., A. M. Krzysik, *et al.* Agricultural Fibers for Use in Building Components. in: The use of recycled wood and paper in building applications. Forest Product Society: 123 -134. 1996.

Zhang, M., S. Kawai, *et al.* Manufacture and Properties of Composite Fiberboard II. Fabrication of board manufacturing apparatus and properties of bamboo/wood composite fiberboard. *Mokuzai Gakkaishi* 41(10): 903-910. 1995.

UNIVERSITAT ROVIRA I VIRGILI  
BINDERLESS FIBERBOARD PRODUCTION FROM CYNARA CARDUNCULUS AND VITIS VINIFERA  
Camilo Mancera Arias  
ISBN:978-84-692-1537-1/DL:T-300-2009

### **3. MATERIALS, METHODS AND ANALYTICAL TECHNIQUES**

UNIVERSITAT ROVIRA I VIRGILI  
BINDERLESS FIBERBOARD PRODUCTION FROM CYNARA CARDUNCULUS AND VITIS VINIFERA  
Camilo Mancera Arias  
ISBN:978-84-692-1537-1/DL:T-300-2009

## CHAPTER 3

### Materials, methods and analytical techniques

General descriptions of the main materials, equipments and methodologies used during the development of the research project can be found in this chapter; going from experimental design to analytical techniques used for the production and characterization of the fiberboards and the modification and characterization of technical lignins.

Equipments and methods used for the preparation of fiberboards from *Cynara cardunculus* and *Vitis vinifera* are the same as well as the analytical techniques used to characterize them; but equipments and methods used for the modification of Kraft lignin in alkaline medium and the analytical techniques used to characterize those modifications are completely different.

#### 3.1 EQUIPMENT FOR FIBERBOARD PRODUCTION AND CHARACTERIZATION

##### 3.1.1 Steam explosion reactor

The reactor is a stainless steel, cylindrical batch type reactor with a nominal capacity of 8L, 45 bars of pressure and 250 °C of temperature.

The steam explosion reactor was design by the university staff and built by Justinox (see fig. 3.1). The reactor is communicated with a 100 liters recipient through a pneumatic valve, in this recipient the pretreated material is collected after the flash expansion. The steam is fed to the reactor at the bottom, to facilitate the impregnation of the material.

A more detailed description can be found in the annex B.



**Figure 3.1** Steam explosion reactor.

### 3.1.2 Press

It is a compact laboratory press mainly used for platen samples made of plastic or rubber, its reference is Polystat 300 S build by Schwabenthan in Berlin (see figure 3.2). This press has a working area of 300x300 mm. Press forces can be adjusted by a hydraulic pressure control unit and temperature can be controlled digitally. Working thrust force maximum up to 450kN can be developed. Additionally, we use a mold made of steel with a working area of 50x150 mm and a suited piston.



**Figure 3.2** Laboratory press Polystat 300 S



### 3.1.3 Mill

It was used a cutting mill to reduce fibrous material quickly and gently. The mill reference is SM 100 build by Retsch (see figure 3.3). This particular mill is suitable for grinding dry materials such as plant parts and lignin. Additionally, the mill has the possibility of sieving the samples using different sieve lights.

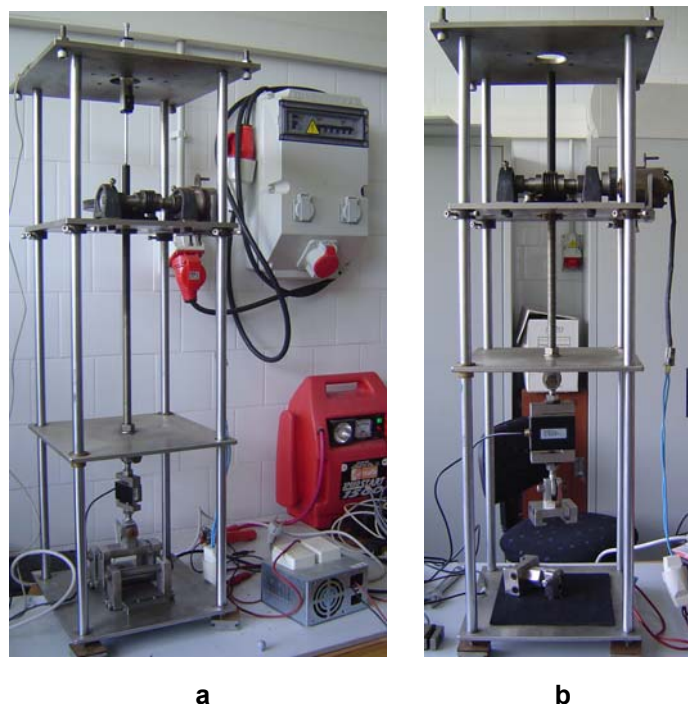


Figure 3.3 Laboratory mill SM 100 Retsch

### 3.1.4 Mechanical characterization equipment

The equipment was design and build by the university staff to accomplish the respective standards. It consists mainly of an engine which by way of a set of gears applies a known force through an axle. Proper devices are coupled to the end of this axle to measure modulus of rupture and modulus of elasticity carrying out a three points bending test or to measure the internal bond. Figure 3.4 shows the equipment with the different devices coupled.

A more detail description can be found in the annex B.



**Figure 3.4** Mechanical characterization equipment **a.** Bending test; **b.** Internal bond test.

## 3.2 EQUIPMENT FOR KRAFT LIGNIN MODIFICATION

### 3.2.1 Micro reactor set

Consist of 4 stainless steel batch tubing-bomb reactors with a capacity of 25 ml each one (see fig. 3.5). The microreactor set was used to study the Kraft lignin behavior during its reaction in alkaline medium at different reaction conditions.



**Figure 3.5** Micro reactor set

### 3.2.2 10L Batch reactor

This is a stainless steel stirred batch reactor with a maximum capacity of 10L (see fig.3.6). It was constructed by EMMSA (Tarragona, Spain). It can stand pressures of up to 40 kg/cm<sup>2</sup> and temperatures of up to 250°C. The agitation system consists of a variable speed Magnedrive II stirrer (Autoclave Engineers, USA). The reactor also has an internal coil for heating and cooling, and a thermocouple for temperature inspection along the experiment.

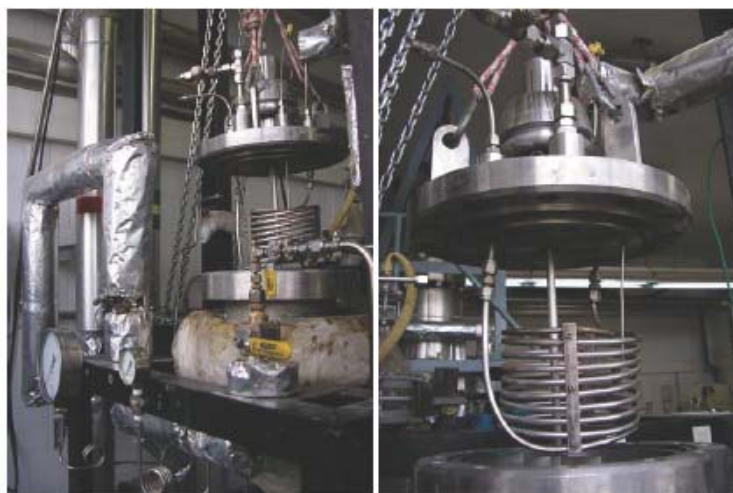


Figure 3.6 10L batch reactor

### 3.3 MATERIALS

*Cynara cardunculus* stalks came from plantations in Madrid, Spain. The material remained in contact with the environment, before being cleaned. After been cleaned, the stalks were broke through, pithed and finally chipped to splinters smaller than 5 cm. For this last operation it was used a GA100 Black & Decker shredder. The average chemical composition of the initial material is shown in table 3.1, as it can be seen from this table the sum of chemicals composition is more than 100% (106.4%), this is a common result due to the overlapping of the testing results(Anglès, Reguant et al. 1997).

**Table 3.1** Average chemical composition of *Cynara cardunculus* stalks

Fraction	%p/p (Dry solid bases)
Ash	5.4
Klason Lignin	17.5
Acid Soluble Lignin	0.8
Cellulose	49.0
Hemicelluloses	24.0
Aqueous Extractives	9.2
Organic Extractives	0.5

*Vitis vinifera* branches came from a plantation in Tarragona, Spain. The material was air dried, stored in jute bags. The branches were chipped to splinters smaller than 5 cm using a GA 100 Black & Decker shredder. The average chemical composition of the initial material is shown in table 3.2, as it can be seen from this table the sum of chemicals composition is more than 100% (103.7%), this is a common result, as mentioned above, due to the overlapping of the testing results (Anglès, Reguant *et al.* 1997).

**Table 3.2** Average chemical composition of *Vitis vinifera* prunings

Fraction	%p/p (Dry solid bases)
Ash	3.7
Klason Lignin	23.3
Acid Soluble Lignin	0.7
Cellulose	43.6
Hemicelluloses	19.1
Aqueous Extractives	1.0
Organic Extractives	12.3

Commercial Kraft lignin, Curan® 27-11 P, supplied by Lignotech Iberica S.A. in powered state, was used for studying its reaction in alkaline medium and also as an additive for the production of boards. This lignin was characterized in a previous work for its chemical composition and functional groups analysis. Its principal characteristics includes the C9 formula ( $C_9H_{7.759}O_{2.479}N_{0.006}S_{0.065}(OCH_3)_{0.597}$ ), lignin content (Klason lignin and acid soluble lignin) 66.1% (w/w), carbohydrate content 3.28%, ash content 27.1% (w/w), methoxyl groups 10.47 (w/w), phenolic hydroxyl groups 4.10 % (w/w) and aliphatic hydroxyl groups 10.09 (w/w) as determined by proton nuclear magnetic

resonance, average-weight molecular weight 1098 g/mol, number-average molecular weight 545 g/mol and polydispersity 2.01 (El Mansouri and Salvadó 2006).

### 3.4 METHODS FOR FIBERBOARD PRODUCTION

#### 3.4.1 Chip pretreatment

*Cynara cardunculus* chips, 150 g dry base, are fed to the steam explosion reactor. The chips are then treated with saturated vapor at the desired conditions of temperature and time. After the set time is reached, the chips are sudden depressurized into a 100 liter recipient. Pulp obtained from this pretreatment is washed and dried until equilibrium with the environment.

#### 3.4.2 Pulp grinding

The pretreated pulps, with a humidity of 7% in equilibrium with atmosphere, were ground to pass through a 4-mm sieve.

#### 3.4.3 Fiberboard manufacture

Test boards are prepared at a laboratory scale following standard techniques and controlled conditions. The ground material is homogenized and its weight and relative humidity recorded. Subsequently, the material is putted into the mold which has been previously heated to the desired temperature together with the press platens. The test boards are made with an objective thickness of 3 mm and an objective density of 1100 kg/m<sup>3</sup>. Once the material is placed into the mold it is hot pressed following a three stages cycle:

1. Pressing at the desired temperature and pressure for a given period of time.
2. Pressure relaxation for 1 or 2 minutes.
3. Pressing at the desired temperature and pressure for a given period of time. Some of the pressing factors (pressure and time) could change in this third stage compared with the first stage values.

### 3.5 METHODS FOR KRAFT LIGNIN MODIFICATION

Kraft lignin was used in its powder form. The relation between lignin and sodium hydroxide solution (2% w/w) was fixed in 1/10 (w/w). Kraft lignin was reacted in a 25ml volume microreactor at the desired conditions. To start a run, the microreactor was immersed in a preheated oil bath according to the experimental conditions. On average, it took between 7-8 minutes to achieve reaction conditions from room temperature at all temperatures studied. After the desired treatment was attained, the reactor was quenched in a cold-water bath. After reaction, the pH of the obtained mixture was measured.

Solid lignin was recovered by precipitation by mixture acidification to pH 2 and filtration. Samples were dried under vacuum and weighted to determine the solid yield and endure posterior analysis.

Finally the reaction conditions that proved to increased the active sites and enhance the adhesive properties of Kraft lignin were used to produce a larger batch of 6 liters using the 10L batch reactor described above. This lignin was used for the study of exogenous lignin addition to the production of fiberboards from *Vitis vinifera* described in chapter 7.

### 3.6 METHODS FOR EXOGENOUS ADDITION OF DIFFERENT TYPES OF KRAFT LIGNINS

*Vitis vinifera* prunings were used in this part of the research, as well as, alkali treated Kraft lignin based on the procedure described above. The conditions of the treatment were the best conditions found during the research and reported on chapter 6. Acid washed crude Kraft lignin was also used in this part of the research, the procedure employed for washing the commercial lignin is described below.

Vapor pretreatment conditions of *Vitis vinifera* prunings, as well as, the conditions for hot pressing the fiberboards produced with additions of exogenous Kraft lignin were the best conditions found during the research for the production of binderless fiberboards from *Vitis vinifera* without any additive, these conditions are reported in chapter 5.

### Acid washing of Kraft lignin

The main objective of this treatment is to eliminate minerals and other organic contaminants from the commercial Kraft lignins.

Around 100g of raw Kraft lignin were mixed with 0.5L of H<sub>2</sub>SO<sub>4</sub> 1N and stirred over a stirring plate for 30 minutes at 60°C. After this, the mixture is left to decant and cool down. Once the mixture is at atmospheric temperature it is filtrated and the remaining solid, acid washed Kraft lignin, is rinsed with Milli Q water until the filtrate reach neutral pH. Finally, solid acid-washed Kraft lignin is dried until equilibrium with the atmosphere at atmospheric temperature or at a temperature up to 40°C maximum to speed up the process.

## 3.7 ANALYTICAL TECHNIQUES FOR FIBERBOARD CHARACTERIZATION

### 3.7.1 Physical and mechanical characterization

The boards were characterized using European standards. The mechanical properties measured were: modulus of elasticity (MOE) and modulus of rupture (MOR)(*AENOR 1993a*), internal bond (IB)(*AENOR 1993c*). Dimensional stability was characterized by measuring: thickness swelling (TS) and water absorption (WA)(*AENOR 1993b*). Additionally, the density was determined (*AENOR 1993d*). Boards were conditioned at 20 °C and 65% RH before any physical or mechanical test was conducted and the dimensions of test pieces were determined based on EN 325 standard(*AENOR 1993e*). Calculations and a more detail description of physico-mechanical characterizations can be found in the annex B.

European standards for these properties are as follows: Density >800 Kg/m<sup>3</sup>, MOR ≥ 40 MPa, MOE ≥ 3000 MPa, IB ≥ 0.7 MPa, WA ≤ 30% and TS ≤ 20%.

### 3.7.2 Chemical characterization

Original raw material and pretreated pulps were analyzed chemically to evaluate the pretreatment process. Standard ASTM methods were used for this aim, the chemical properties analyzed were: Humidity(*ASTM 2006*), ash content(*ASTM 2001*), aqueous extractives(*ASTM 2007c*), organic extractives(*ASTM 2007b*) and Klason lignin(*ASTM 2007a*), Carbohydrates from Klason lignin hydrolysis were analyzed by HPLC(*Yuan JP. and Chen 1999*) to determine Cellulose and Hemicelluloses content. Acid-soluble lignin was also analyzed for the original material by UV absorption(*Kaar*

and Brink 1991). Calculations and a more detail description of chemical characterizations can be found in the annex B.

### 3.7.3 Scanning Electron microscopy – SEM.

SEM was used to visualize structural changes caused for the steam explosion pretreatment to the lignocellulosic material, as well as, for visualizing IB tested board's rupture surfaces when exogenous lignin addition was assessed. . For magnification purposes, a JEOL JSM6400 scanning electron microscope was used. Samples were mounted on a stub and sputter coated with gold. The metallization conditions were 0:05 mbar and 30 mA, and the observation conditions were at acceleration voltages of 10 kV and a distance of 20 mm.

## 3.8 ANALYTICAL TECHNIQUES FOR KRAFT LIGNIN CHARACTERIZATION

### Ash content

The ash contents of all the reacted Kraft lignins were obtained gravimetrically after in-furnace calcinations for 3 h at 600 °C.

### Lignins and elemental sugar contents

For all the Kraft lignin the Klason lignin was determined by the conventional method as the fraction left insoluble after two-step acid hydrolysis (Tappi 2005), acid-soluble lignin was determined by applying the spectrophotometric method used by Maekawa et al. (Maekawa, Ichizawa et al. 1989) to the filtrate produced by this hydrolysis, and elemental sugars were determined using HPLC to the same filtrate (William, Lawrence et al. 1991).

### Phenolic hydroxyl groups by UV-spectroscopy method. ( $\Delta\epsilon$ method).

The content of various phenolic units in lignin samples was determined by a method based on the difference in absorption at 300 and 360 nm between phenolic units in neutral and alkaline solutions (Zakis 1994). The content of ionizing phenol hydroxyl groups can be quantitatively evaluated by comparing the  $\Delta\epsilon$  values of substances studied at certain wavelengths to the values of  $\Delta\epsilon$  of the respective model compounds (I, II, III, IV types) (see Fig. 3.7)



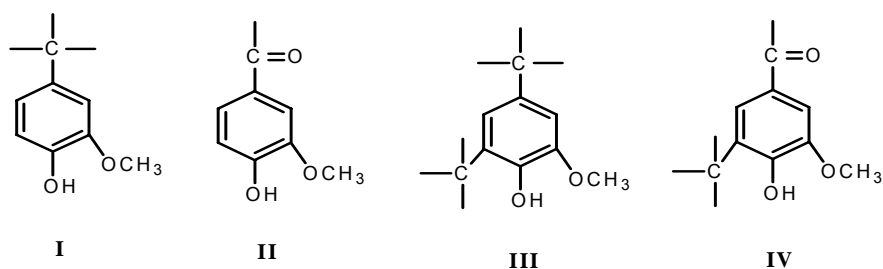


**Figure 3.7** Types of phenolic structure determined in different lignin samples.

### FTIR spectroscopy

The FTIR spectra of the unacetylated lignin samples were obtained, by pressing their finely powder on the diamond surface of an ATR probe, with a JASCO FTIR-680 plus spectrometer using a resolution of  $2\text{cm}^{-1}$  and 32 co-addition scans in a frequency range of  $400$  to  $4600\text{cm}^{-1}$ . The spectra were analyzed by MestRec software to compare the absorbance corresponding to each functional group. The absorption bands were assigned as suggested by Faix (Faix 1992) and Nada et al. (Nada, Yousef et al. 1998)

### Acetylation for $^1\text{H-NMR}$ and GPC analysis

A weighted amount of each reacted Kraft lignin was acetylated for 48 hours with a mixture of purified pyridine-acetic anhydride (1:1, v/v). Methanol was used to quench the remaining acetic anhydride. Finally, a flow of nitrogen was applied to evaporate the solvents and the samples were dried under vacuum (Chum, Johnson et al. 1985).

### Molecular weight distribution

The molecular weight of acetylated lignins was studied by gel permeation chromatography (GPC) equipped with three styrene-divinylbenzene copolymer gel columns of 50, 500, and  $10^4$  Å from Polymer Laboratories. The effluent was monitored at 254 nm with a BECKMAN UV-detector. The columns were calibrated using polystyrene standards in the 92–66,000 g/mol range. The flux of THF was 1 ml/min and the samples were dissolved in THF at a concentration of 1 mg/ml and stored for 24 h at  $5^\circ\text{C}$  to avoid variations in molecular weight (Glasser, Davé et al. 1993). The signal detected was digitized at a frequency of 2 Hz and the MWD was calculated from the recorded signal using normal GPC calculation procedures (Yau, Kirkland et al. 1979).

### Proton Nuclear magnetic resonance (<sup>1</sup>H-NMR-spectroscopy)

Acetylated lignins were analyzed with <sup>1</sup>H-NMR using a Varian Gemini 300 MHz. This technique quantitatively determined the relative amount of methoxyl, aromatic and aliphatic acetoxyl groups with reference to the internal standard, p-nitrobenzaldehyde, as suggested by Kubo et al. (Kubo, Uraki et al. 1996). The conditions for measurements were as follows: Pulse width 5μs, pulse angle 45°, acquisition time 2s, pulse delay time 2s, accumulations 256. The procedures consist to dissolve 30mg of sample in 0.70ml of CDCl<sub>3</sub> and about 1.5mg of p-nitrobenzaldehyde added as internal standard.

The signals appearing around 1.70-2.17, 2.17-2.50 and 3.10-4.10 were assigned to aliphatic acetoxyl, aromatic acetoxyl and methoxyl protons, respectively according to information in previous reports (Lundquist 1992). The amount of each functional group in hydrolyzed Kraft lignins was estimated from the integral intensity of corresponding signals by application of the following equation:

$$Relative\ amount = (I_a / W_{ta}) / (I_{is} / W_{tis})$$

Where I<sub>a</sub> is the integral of functional group in Kraft lignins, I<sub>is</sub> is the integral of the internal standard, W<sub>ta</sub> is the weight of sample and W<sub>tis</sub> is the weight of the internal standard.

## 3.9 EXPERIMENTAL DESIGN

### 3.9.1 Fiberboard production

We use experimental design to develop a model that interrelate the response variables, in this case mechanical, physical or chemical properties of the fiberboards, with the controllable factors that will be investigated; and use this model to optimize the responses.

The experimental design methodology chosen for the production of *Cynara cardunculus* fiberboards is a second order, response surface methodology; which is an approach to process optimization. The design is a Draper-Lin orthogonal and rotatable, which is a central composite design that runs a fraction rather than a full factorial, composed by 48 runs with 10 center repetitions in a single block.

For the study of the chemical properties it will be used part of the design explained above reducing it to a  $2^2$  central composite design, orthogonal and rotatable, composed by 16 runs with 8 center repetitions.

Factors that from previous investigations are known to have relevant influence on the quality of the boards will be analyzed. These factors are: Pretreatment temperature and time, pressing temperature, pressure and time for the first and third pressing steps.

The experimental design methodology used for the production of fiberboards from *Vitis vinifera* differs with the one used for the production of fiberboards from *Cynara cardunculus* only in that it was reduced in two experimental factors: pressure and time for the third pressing stage. Thus, the complete experimental design for the study of *Vitis vinifera* as a raw material for the production of fiberboards is a Draper-Lin orthogonal and rotatable, composed by 30 instead of 48 runs with 8 center repetitions ran in a single block.

The physical and mechanical properties commonly analyzed in fiber boards production are: Density, MOR (Modulus of Rupture), MOE (Modulus of Elasticity), IB (Internal Bond), TS (Thickness Swelling) and WA (Water Absorption); all these properties will be analyzed.

For studying the chemical properties, only two factors will be taken in consideration: Pretreatment temperature and time. Chemical response variables to be analyzed are: Cellulose, lignin, hemicelluloses, ashes and cellulose to lignin ratio.

### 3.9.2 Kraft lignin modification

To study and quantify the effect of process factor on the response variables defining the efficiency of the lignin properties, we used a response surface methodology based in a central composite design. A central composite design is basically a three-level design that starts with a two-level factorial and some centerpoints. Typically used for quantitative factors and designed to estimate the main effects plus the desired quadratics and two-way interactions. The design has two parts: A factorial and a star. The star portion of the design consists of an additional set of points arranged at equal distances from the center of the cube on radii that pass through the centerpoint in the face of the cube.

The experimental design was used to study the effects of two factors in 11 experiments and was run in a single block. The two variables were the reaction time ( $t_r$ ) and the temperature of the reaction ( $Tr$ ) and the response variables were: Solid yield percentage, methoxyl, phenolic hydroxyl, aliphatic hydroxyl, Mw, Mn and polydispersity. The order of the experiments was fully randomized to protect against the effect of lurking variables.

### 3.9.3 Exogenous lignin addition

For the study and quantification of the effect of exogenous lignin addition on the final properties of fiberboards, we chose a single factor categorical experimental design consisting of 12 runs. The design is to be run in 1 block, which consists of 12 runs with 4 levels and 2 repetitions of the single factor. This design was employed two times, the first one, corresponds to alkali treated Kraft lignin and the second one, corresponds to washed Kraft lignin. The order of the experiments was fully randomized to protect against the effects of lurking variables.

Single factor categorical designs compare levels of a single non-quantitative variable, with or without blocking factors. This type of experiment is the simplest type of experiment because it contains only a single factor of interest.

## 3.10 EXPERIMENTAL DESIGN ANALYSIS

Statistical methods were used to analyze the experimental data to guarantee that the results and conclusions were objective rather than judgmental in nature. Mainly the statistical analysis was based on variance analysis and different graphical methods which facilitated data analysis, interpretation and presentation; these tools are explained in more detail subsequently and in the annex A.

### 3.10.1 ANOVA Table

Each response variable will be analyzed based on the variability of the data obtained. It will be used an ANOVA table for this purpose. The ANOVA table shows which of the factors are statistically significant and if there are relevant interactions between them.

### 3.10.2 Pareto Chart

The Pareto Chart is a graphical tool, which displays a frequency histogram where the length of each bar on the chart is proportional to the absolute value of its associated estimated effect or the standardized effect. The standardized effect is the ratio between the estimated effect and its error. Each of the estimated effects is shown in decreasing order, with the largest and most important effect on top. In this chart there is also a vertical line which is used to assess which of the factors are statistically important. Any bar that exceeds this vertical line corresponds to an effect statistically important at a confidence level of 95%.

### 3.10.3 Main Effects Plot

This plot estimates the influence of a single experimental factor on the response variable when the factor is changed from its low to its high level while the other experimental factors are held constant in their central values.

### 3.10.4 Interaction Plot

This plot estimates the influence of two-factor interactions on the response variable. The first factor varies from its low to its high level while the second factor is held in its low level in one line and in its high level in the other line, meanwhile the other factors are held in their central values. Nonparallel trends between those lines in the plot indicate interaction.

### 3.10.5 Response Surface Plot

This plot shows the pattern of a predicted response variable vs. two experimental factors based on the assumed model derived from the experimental observations. The other factors are held constant in their central values.

### 3.10.6 Predicted Value vs. Observed Value

This is a diagnostic plot which shows the experimental values against the predicted values by the model. This plot also shows the variability of the experimental values.

### 3.10.7 Multiple response optimization

This kind of optimization determines the combination of levels for the experimental factors that simultaneously optimize several response variables. The procedure consists on building a desirability function based on the fitted models of each factor to be optimized.

### 3.10.8 Overlaid contour plots

The overlaid contour plots show the contour functions for each of the response variables as a function of the process parameters. This type of analysis was used in conjunction with multiple response optimization methodology to present the optimum operational values found for each of the process factors.

### 3.10.9 Scatter plot

The Scatter plot displays the values for the single variable along a single axis as point symbols with no connecting lines. The pattern of the points indicates the strength

and direction of the correlation among the values. The plot allow us to easily identify the range of the data, however, it may be difficult to identify individual points if they overlap.

#### **3.10.10 Means and 95% LSD intervals**

It is a plot of the mean for each factor level and the intervals for the means. The bars that do not overlap indicate a significant difference between the two means. Bars that overlap indicate no significant difference between the means.

The least significant difference (LSD) intervals is a method for testing the statistically significant differences between means when the F-ratio is significant and comparisons are planned.

#### **3.10.11 Box and whisker plot**

This plot, which is particularly useful for comparing parallel batches of data, divides the data into four equal areas of frequency. A box encloses the middle 50 percent, where the median is represented as a vertical line inside the box. The mean may be plotted as a point.

Horizontal lines, called whiskers, extend from each end of the box. The lower (left) whisker is drawn from the lower quartile to the smallest point within 1.5 interquartile ranges from the lower quartile. The other whisker is drawn from the upper quartile to the largest point within 1.5 interquartile ranges from the upper quartile.

Values that fall beyond the whiskers, but within 3 interquartile ranges (suspect outliers), are plotted as individual points. Far outside points (outliers) are distinguished by a special character (a point with a + through it). Outliers are points more than 3 interquartile ranges below the lower quartile or above the upper quartile.

#### **3.10.12 Analysis of means plot**

It is a plot that shows each group mean, the centerline at the grand mean, and the decision limits, which determine the groups that differ significantly at the grand mean. If any points are outside the decision limits, it can be concluded that there is a statistically significant difference between the counts.

## REFERENCES

- AENOR. EN 310. Wood-based panels. Determination of modulus of elasticity in bending and of bending strength. 1993a.
- AENOR. EN 317. Particleboards and fiberboards. Determination of swelling in thickness after immersion in water. 1993b.
- AENOR. EN 319. Particleboards and fiberboards. Determination of tensile strength perpendicular to the plane of the board. 1993c.
- AENOR. EN 323. Wood-based panels. Determination of density . 1993d.
- AENOR. EN 325. Wood-based panels. Determination of dimensions of test pieces. 1993e.
- Anglès, M. N., J. Reguant, *et al.* Influence of the ash fraction on the mass balance during the summative analysis of high-ash content lignocellulosics. *Bioresource Technology* 59(2-3): 185-193. 1997.
- ASTM. D1102-84. Standard Test Method for Ash in Wood. 2001.
- ASTM. E871-82. Standard Test Method for Moisture Analysis of Particulate Wood Fuels. 2006.
- ASTM. D1106-96. Standard Test Method for Acid-Insoluble Lignin in Wood. 2007a.
- ASTM. D1107-96. Standard Test Method for Ethanol-Toluene Solubility of Wood. 2007b.
- ASTM. D1110-84. Standard Test Methods for Water Solubility of Wood. 2007c.
- Chum, H. L., D. K. Johnson, *et al.* Lignin characterization research: a process report. *Biochemical Conversion Program Semi-annual Review Meeting*: 25-50. 1985.

El Mansouri, N. E. and J. Salvadó. Structural Characterization of technical lignins for the production of adhesives: Application to liginosulfonate, Kraft, soda-anthraquinone, organosolv and ethanol process lignins. *Industrial crops and products* 24: 8-16. 2006.

Faix, O. Fourier transform infrared spectroscopy. in: *Methods in lignin chemistry*. S. Y. Lin and C. W. Dence, Ed. Berlin: 83-109. 1992

Glasser, W. G., V. Davé, *et al.* Molecular weight distribution of semi-commercial lignin derivatives. *Journal of wood chemistry and Technology* 13(4): 545-559. 1993.

Kaar, W. E. and D. L. Brink. Simplified Analysis of Acid Soluble Lignin. *Journal of Wood Chemistry and Technology* 11(4): 465 - 477. 1991.

Kubo, S., Y. Uraki, *et al.* Thermomechanical Analysis of Isolated Lignins. *Holzforschung* 50: 144-150. 1996.

Lundquist, K. Proton (1H) NMR spectroscopy. in: *Methods in Lignin Chemistry*. S. Y. Lin and C. W. Dence, Ed. Berlin. Springer series in wood science: 242-247. 1992

Maekawa, E., T. Ichizawa, *et al.* An evaluation of acid soluble lignin determination in analyses of lignin by the sulphuric acid method. *Journal of Wood Chemistry and Technology* 9(4): 549-567. 1989.

Nada, A. M. A., M. A. Yousef, *et al.* Infrared spectroscopy of some treated lignins. *Polymer degradarion and stability* 62: 157-163. 1998.

Tappi. TAPPI standard T-13. 2005.

William, E. K., G. C. Lawrence, *et al.* The complete analysis of wood polysaccharides using HPLC. *Journal of Wood Chemistry and Technology* 11(4): 447-463. 1991.

Yau, W. W., J. J. Kirkland, *et al.* *Modern Size-exclusion liquid chromatography*. Canada. 1979.

Yuan JP. and F. Chen. Simultaneous separation and determination of sugars, ascorbic acid and furanic compounds by HPLC-dual detection. *Food Chemistry* 64: 423 - 427. 1999.



Zakis, G. F. Functional analysis of lignins and their derivatives. Atlanta, GA, Tappi press. 1994.

UNIVERSITAT ROVIRA I VIRGILI  
BINDERLESS FIBERBOARD PRODUCTION FROM CYNARA CARDUNCULUS AND VITIS VINIFERA  
Camilo Mancera Arias  
ISBN:978-84-692-1537-1/DL:T-300-2009

## **4. BINDERLESS FIBERBOARDS FROM CYNARA CARDUNCULUS**

UNIVERSITAT ROVIRA I VIRGILI  
BINDERLESS FIBERBOARD PRODUCTION FROM CYNARA CARDUNCULUS AND VITIS VINIFERA  
Camilo Mancera Arias  
ISBN:978-84-692-1537-1/DL:T-300-2009

## CHAPTER 4

### Binderless fiberboard production from *Cynara cardunculus* Stalks

In this chapter the results obtained from the production of fiberboards from *Cynara cardunculus* without additives are presented. I also described how the *Cynara cardunculus* stalks undergo the main processes and how their main controllable factors affect the final properties of the fiberboards produced.

#### 4.1 INTRODUCTION

*Cynara cardunculus*, is a perennial plant of the thistle-like type (Venendaal, Jorgensen et al. 1997), it has been adapted to the dry Mediterranean conditions. In its natural cycle, *Cynara* sprouts in autumn and passes the winter as a rosette. In spring, a floral scape is developed which dries during the summer and the whole crop can be harvested dry (10-15% water) in the late summer. Winter rains are used for the energy crop production and no irrigation during the summer is necessary.

In Spain, about 50 ha of experimental fields have been established. The crop is sown either in spring or autumn, depending of the climatic conditions of the location. The harvest material consists of about 33% leaves, 22% stems and 45% capitula. There have been reported productions of about 20 odt/ha (odt: oven dry ton). The productive life of a plantation of *C. cardunculus* grown for biomass production is more than 10 years for the rain fed conditions of central Spain (Curt, Sanchez et al. 2002).

*Cynara* crop has also been tested in other EU countries as: Greece, Portugal and Italy, proving to be suitable for biomass production in the southern regions of Europe. *Cynara cardunculus* is considered to be of interest due to its low cost of establishment by seeding.

This crop is well adapted to the dry Mediterranean conditions where must precipitations occurs in winter season (Venendaal, Jorgensen et al. 1997). It can therefore produce high yields without irrigation in contrast to crops like *Miscanthus* and sorghum. *Cynara* has also the possibility of been harvested for fodder, this increase its value at farm level.

Some authors (Curt, Sanchez et al. 2002) have suggest the possibility of using the different parts of the plant for different purposes, for instance using the lignocellulosic biomass for energy or/and pulp production and the seeds for oil production. Thus, exploiting integrally the crop harvested.

*Cynara cardunculus* is the most promising species for lignocellulosic biomass production in Spanish rain fed lands (Venendaal, Jorgensen et al. 1997). The economic calculations from Spain indicate costs of *Cynara* biomass of about 24 Euros/odt. This is very competitive compared with other energy crops and due to the oil content of the seeds the energy value per odt is high. This emphasizes the need for studies dealing with the harvest and uses of this crop. The low cost of the crop is due to low establishment cost, low input of fertilizer and irrigation and its high yield.

### **Using *Cynara cardunculus* as raw material**

The fibers in the stalk are the most important cells for pulping. In *Cynara*, the fibers are medium long, narrow and with medium thickness, with a length:width ratio of 69. *Cynara* belong to a group of annual plants including straw, bagasse, esparto and reeds, that are comparable to pulp hardwoods (Gominho, Fernandez et al. 2001).

Some authors (Antunes, Amaral et al. 2000; Benjelloun-Mlayah, de Lopez et al. 1997; Gominho, Fernandez et al. 2001) have investigated the possibility of producing pulp from *Cynara cardunculus*, finding that the stalks of *Cynara* have a good potential for pulping and that the pulps obtained were comparable to hardwood pulps with low rejects, higher tensile strength and less energy requirements for refining. *Cynara* Stalks were cook under standard Kraft pulping conditions (Gominho, Fernandez et al. 2001) to produce pulps with initial tensile strength values of 77 N/m per g for unbeaten pulps. These tensile strength values were developed with beating, attaining 104 N/m per g. Tensile strength values for unbleached eucalypt pulps are about 70 N/m per g. Pulp yields obtained from *Cynara* lay between 44 – 47%.

Other authors (Antunes, Amaral et al. 2000) studied the exploitation of *C. cardunculus* fibers through sosa-antraquinone cooking process, obtaining yields of pulps around 36%, despite this value is lower than wood species, it can be considered very promising, taking into account that the original material contained up to 15% of water extractives and ashes.

Currently there are some ongoing studies related to the use of *Cynara* fibers in the boards area (Antunes, Amaral et al. 2000), but the authors have not published any results devoted to this.

## 4.2 RESULTS AND DISCUSSIONS

The experimental factors and their levels were chosen based on the literature review and previous experiences on production of binderless boards inside the investigation group, they are:

- A: Vapor pretreatment temperature ( $T_r$ ): 180 – 220 °C.
- B: Vapor pretreatment time ( $t_r$ ): 5 – 10 min.
- C: Pressing temperature ( $T_p$ ): 200 – 220 °C.
- D: Initial press pressure ( $P_{p_i}$ ): 8 – 16 MPa.
- E: Final press pressure ( $P_{p_f}$ ): 8 – 16 MPa.
- F: Initial press time ( $t_{p_i}$ ): 3 – 7 min.
- G: Final press time ( $t_{p_f}$ ): 3 – 7 min.

### 4.2.1 Physical and mechanical response variables

In this section, I will discuss the physical and mechanical properties. Each of the response variables will be analyzed separately using the tools of the experimental design and afterwards the interactions between the experimental factors will be analyzed, if there is any.

The results obtained are shown in table 4.1. There is an extra factor included in this table, the severity factor (*Overend and Chornet 1987*) ( $\log(R_o)$ ) which group the vapor pretreatment temperature and time in a single variable giving a weight for the severity of the global pretreatment. For each response variable a variance analysis was performed at a confidence level of 95%.

Table 4.1. Physicomechanical properties

Run	Process Factors								Response Variables					
	Tr [°C]	t <sub>r</sub> [min.]	Log (Ro)	Tp [°C]	Pp <sub>i</sub> [MPa]	Pp <sub>f</sub> [MPa]	tp <sub>i</sub> [min.]	tp <sub>f</sub> [min.]	Density [kg/m <sup>3</sup> ]	MOR [MPa]	MOE [MPa]	IB [Mpa]	WA [%]	TS [%]
1	200	7.5	3.82	210	12	12	5	5	1337	41	5400	0.6	21.4	17.7
2	220	10	4.53	200	16	8	3	7	1342	41	5200	0.6	20.0	14.5
3	180	5	3.05	200	16	8	7	7	1289	27	4029	0.1	37.2	22.6
4	200	7.5	3.82	210	12	12	5	5	1344	39	4688	0.8	24.2	16.5
5	220	5	4.23	200	8	8	7	3	1324	39	5165	0.8	19.8	12.5
6	220	10	4.53	200	8	16	7	7	1349	34	7123	1.3	17.0	13.0
7	180	10	3.36	220	8	8	7	7	1291	25	4315	1.0	27.1	20.2
8	180	5	3.05	200	16	16	7	7	1276	36	5016	0.2	46.4	38.8
9	200	7.5	3.82	210	12	12	5	5	1357	40	4484	0.6	23.2	16.3
10	180	10	3.36	220	16	8	3	7	1253	33	4491	0.4	28.2	14.0
11	200	7.5	3.82	210	12	12	5	5	1333	45	5393	0.7	19.0	22.1
12	180	10	3.36	200	8	16	7	3	1330	20	2527	0.4	36.5	26.5
13	220	5	4.23	200	8	8	3	7	1326	55	4915	0.8	24.5	14.2
14	220	5	4.23	220	16	8	3	3	1344	38	4762	0.4	17.3	15.0
15	200	7.5	3.82	210	12	12	5	5	1346	41	5861	1.0	23.8	16.6
16	180	5	3.05	220	8	8	7	3	1272	30	2871	0.5	33.0	28.6
17	200	7.5	3.82	210	12	12	5	5	1350	49	5280	0.5	20.8	15.4
18	180	10	3.36	200	8	16	3	3	1334	48	5340	0.0	53.4	28.4
19	180	5	3.05	200	8	8	3	3	1237	25	2821	0.0	105.8	54.6
20	200	7.5	3.82	210	12	12	5	5	1348	40	4811	0.7	20.6	18.2
21	180	10	3.36	200	16	16	3	3	1336	34	4482	0.2	67.7	49.2
22	180	5	3.05	220	16	16	3	3	1336	36	4882	0.4	62.6	50.4
23	180	10	3.36	220	8	8	3	7	1346	26	2751	0.8	29.9	23.6
24	220	10	4.53	220	16	8	7	3	1362	27	5444	0.5	13.1	9.5



**Table 4.1.** Physicomechanical properties (continuation)

Run	Process Factors								Response Variables					
	Tr [°C]	t <sub>r</sub> [min.]		Tp [°C]	Pp <sub>i</sub> [MPa]	Pp <sub>f</sub> [MPa]	tp <sub>i</sub> [min.]	tp <sub>f</sub> [min.]	Density [kg/m <sup>3</sup> ]	MOR [MPa]	MOE [MPa]	IB [Mpa]	WA [%]	TS [%]
25	200	7.5	3.82	210	12	12	5	5	1330	45	4274	0.7	21.0	15.7
26	220	5	4.23	200	16	16	3	7	1343	42	3992	0.4	22.5	22.3
27	220	10	4.53	200	16	8	7	3	1369	43	6097	0.6	16.1	12.4
28	180	5	3.05	220	16	16	7	7	1275	52	4923	0.3	32.3	25.8
29	220	10	4.53	220	8	16	3	7	1414	35	6234	0.6	13.0	10.6
30	220	5	4.23	220	8	16	3	3	1363	42	6164	1.3	15.8	15.1
31	220	10	4.53	220	16	16	7	3	1349	28	5400	0.5	13.6	10.9
32	200	7.5	3.82	210	12	12	5	5	1353	35	4946	0.6	23.9	16.7
33	220	5	4.23	220	8	16	7	7	1370	36	5405	0.3	15.1	13.4
34	200	7.5	3.82	210	12	12	5	5	1337	36	4516	0.5	20.4	21.1
35	200	7.5	3.82	210	12	12	1	5	1338	45	4749	0.1	27.9	31.3
36	200	7.5	3.82	210	12	12	5	9	1359	43	5949	0.5	19.7	16.4
37	160	7.5	2.64	210	12	12	5	5	1292	28	4619	0.2	70.3	56.4
38	200	7.5	3.82	210	12	12	5	1	1371	45	5812	0.3	24.8	20.6
39	200	7.5	3.82	210	4	12	5	5	1281	38	3627	0.8	29.1	23.9
40	200	2.5	3.34	210	12	12	5	5	1297	21	2859	0.3	37.2	37.9
41	200	7.5	3.82	190	12	12	5	5	1376	40	5017	0.6	36.7	26.1
42	200	12.5	4.04	210	12	12	5	5	1389	50	6601	0.6	22.2	16.6
43	200	7.5	3.82	210	12	20	5	5	1326	44	5683	0.7	19.3	21.1
44	200	7.5	3.82	210	12	12	9	5	1311	43	6607	0.7	21.7	14.3
45	200	7.5	3.82	210	20	12	5	5	1392	49	5384	0.3	21.4	20.5
46	240	7.5	5.00	210	12	12	5	5	1371	15	4822	1.0	8.2	4.3
47	200	7.5	3.82	230	12	12	5	5	1277	30	5811	1.1	15.8	12.2
48	200	7.5	3.82	210	12	4	5	5	1355	43	5737	0.6	26.4	18.3

#### 4.2.1.1 Density

ANOVA table for density is shown in table 4.2 and the statistical plots for density are shown in figure 4.1. The model as fitted presents an R-square of 0.925 and a standard deviation of the residuals (SDR) of 20.3 kg/m<sup>3</sup>. Only four factors (pretreatment temperature, pretreatment time, pressing temperature and initial pressing pressure) were found to be statistically important at a confidence level of 95%. The modeled response surface (figure 4.1d) shows that increasing the severity of the pretreatment, either by increasing the temperature or increasing the time, increases the density due to a reduction in the compression resistance of the *C. cardunculus*. The same results have been obtained with other materials (Hsu, W. et al. 1988; Sekino 1999; Velásquez, Ferrando et al. 2003). Figure 4.1d also shows that the pretreatment time has a bigger influence at low temperatures than at high temperatures.

From the response surfaces shown in figures 4.1f and 4.1h, it can be seen that low pressing temperatures or high initial press pressures and long pressing times favor an increase in density. To allow a good distribution of lignin between the fibers during the pressing process, it is necessary to apply enough heat and pressure to melt the lignin through the whole board.

Interaction plot (figure 4.1c), Pareto chart (figure 4.1a) and the ANOVA table (table 4.2) show that the relevant interactions are: BC, AC and AB; this last interaction can be expected, because the factors involve in it are those that control the pretreatment process. The other two interactions are quite different, the first one (BC) shows that at low pressing temperatures (C) the increase of the pretreatment time (B) favors largely a density increase, but at high pressing temperatures the influence of the pretreatment time is in the other direction and less relevant. The second interaction (AC) shows that at high pressing temperatures the increase of the pretreatment temperature (A) favors largely a density increase but at low pressing temperatures the influence of the pretreatment temperature is in the other direction and smaller in magnitude. In this last interaction analyzed, it is important to notice that even if the influence of the pretreatment temperature at low pressing temperatures is smaller in magnitude than at high ones, the interaction is located at the maximum values of the density obtained. Interactions between factors which are not statistically significant were not analyzed.

There is a very good correlation between the observed values and the values predicted by the model as shown in figure 4.1e. The equation of the fitted model is shown in figure 4.7a.

The following table shows the combination of the factors levels which maximizes density into the studied region:

<b>Tr</b>	<b>t_r</b>	<b>Tp</b>	<b>Pp_i</b>	<b>Pp_f</b>	<b>tp_i</b>	<b>tp_f</b>
<b>[°C]</b>	<b>[min.]</b>	<b>[°C]</b>	<b>[MPa]</b>	<b>[MPa]</b>	<b>[min.]</b>	<b>[min.]</b>
186	12.5	190	14.7	4	9	4.34

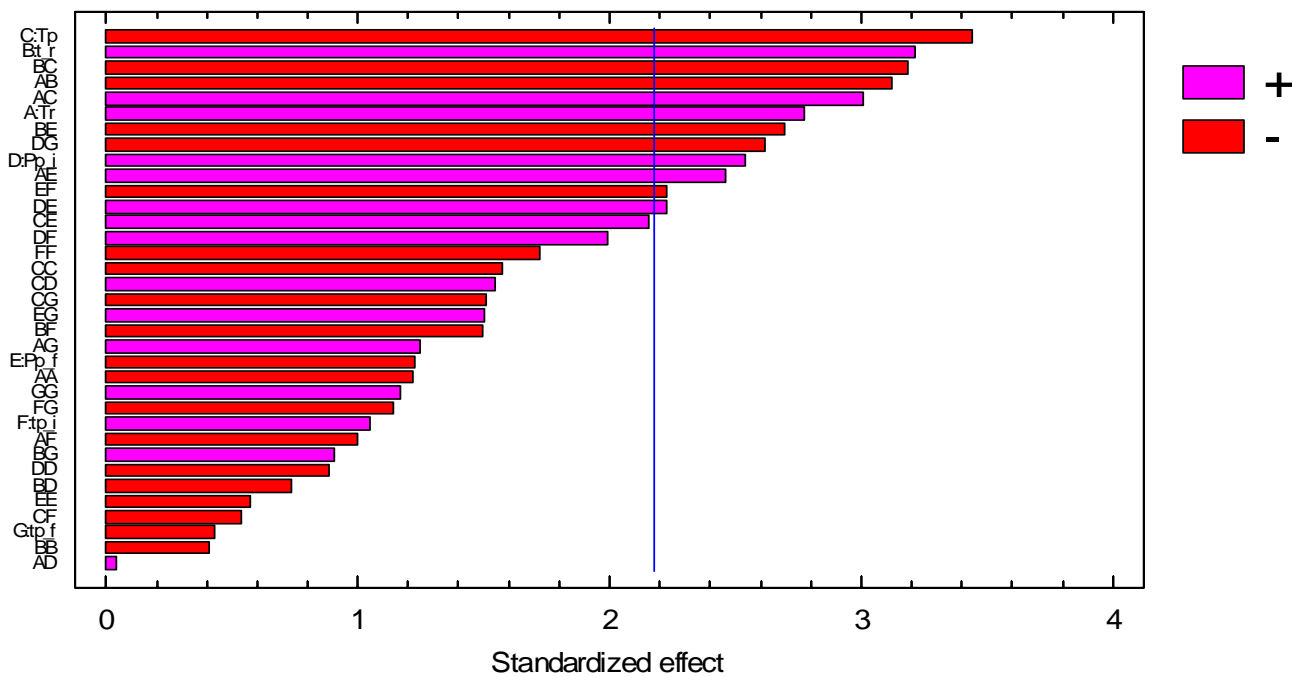
Shadow values correspond to no statistically significant factors; this means that those factors can be set with the most convenient values without affecting considerably the maximum value of density.

Previous studies (Suchsland, Woodson *et al.* 1983) have shown that, the higher the density better the mechanical properties will be. It seems that there is a correlation between the density and some of the properties that will be subsequently analyzed. If that correlation exists, the important factors, the shapes of the response surfaces, the interactions, etc. should be similar.

**Table 4.2.** Variance Analysis for Density

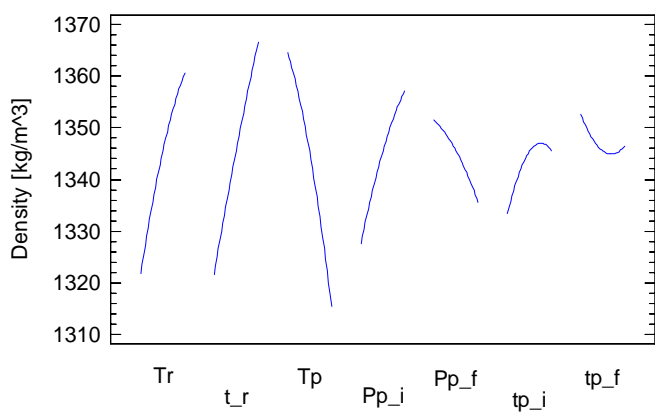
Variation source	Sum of Squares	Degrees of Freedom	Mean Square	F-Ratio	P-Value
A:Tr	3.16E+03	1	3.16E+03	7.70	0.0168
B:t_r	4.23E+03	1	4.23E+03	10.31	0.0075
C:Tp	4.86E+03	1	4.86E+03	11.85	0.0049
D:Pp_i	2.65E+03	1	2.65E+03	6.46	0.0258
E:Pp_f	6.18E+02	1	6.18E+02	1.51	0.2433
F:tp_i	4.50E+02	1	4.50E+02	1.10	0.3159
G:tp_f	7.54E+01	1	7.54E+01	0.18	0.6759
AA	6.09E+02	1	6.09E+02	1.48	0.2468
AB	4.00E+03	1	4.00E+03	9.73	0.0089
AC	3.72E+03	1	3.72E+03	9.06	0.0109
AD	6.17E-01	1	6.17E-01	0.00	0.9697
AE	2.49E+03	1	2.49E+03	6.07	0.0298
AF	4.12E+02	1	4.12E+02	1.00	0.3360
AG	6.41E+02	1	6.41E+02	1.56	0.2354
BB	6.86E+01	1	6.86E+01	0.17	0.6900
BC	4.17E+03	1	4.17E+03	10.15	0.0078
BD	2.23E+02	1	2.23E+02	0.54	0.4752
BE	2.99E+03	1	2.99E+03	7.27	0.0194
BF	9.22E+02	1	9.22E+02	2.25	0.1598
BG	3.36E+02	1	3.36E+02	0.82	0.3837
CC	1.01E+03	1	1.01E+03	2.47	0.1421
CD	9.78E+02	1	9.78E+02	2.38	0.1487
CE	1.90E+03	1	1.90E+03	4.64	0.0523
CF	1.20E+02	1	1.20E+02	0.29	0.5992
CG	9.37E+02	1	9.37E+02	2.28	0.1568
DD	3.24E+02	1	3.24E+02	0.79	0.3918
DE	2.04E+03	1	2.04E+03	4.97	0.0457
DF	1.63E+03	1	1.63E+03	3.98	0.0693
DG	2.82E+03	1	2.82E+03	6.87	0.0224
EE	1.35E+02	1	1.35E+02	0.33	0.5771
EF	2.04E+03	1	2.04E+03	4.97	0.0457
EG	9.23E+02	1	9.23E+02	2.25	0.1596
FF	1.22E+03	1	1.22E+03	2.96	0.1109
FG	5.33E+02	1	5.33E+02	1.30	0.2769
GG	5.61E+02	1	5.61E+02	1.37	0.2650
Total error	4.93E+03	12	4.11E+02		
Total (corr.)	6.54E+04	47			

Standardized Pareto Chart for Density



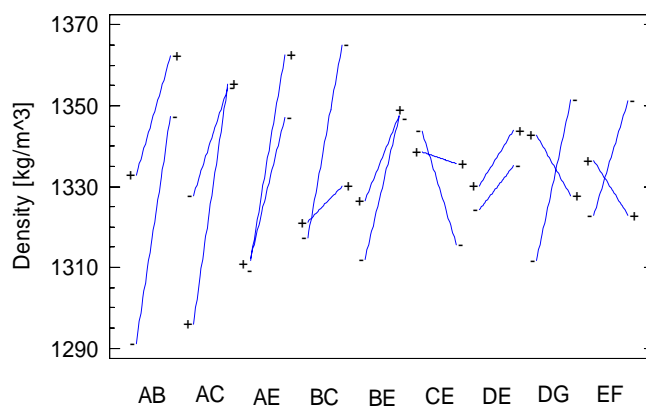
a

Main Effects Plot for Density



b

Interaction Plot for Density



c

**Figure 4.1.** Statistical Plots for Density Analysis  
 a. Pareto chart, b. Main effects plot, c. Interaction plot

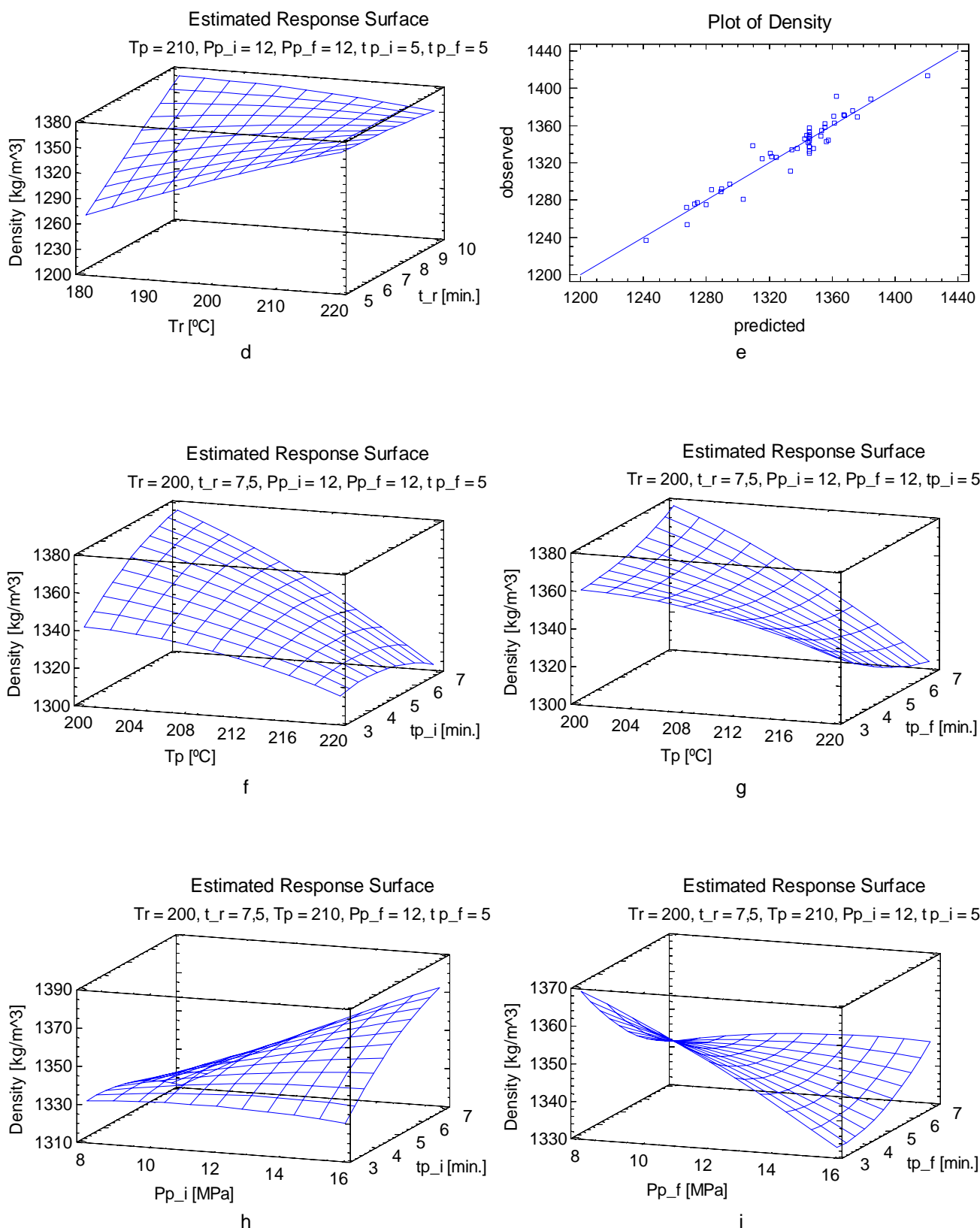


**Figure 4.1.** Statistical Plots for Density Analysis (continuation)  
 d, f, g, h, i. Estimated responses sufeces, e. Diagnostic plot

#### 4.2.1.2 Mechanical properties (MOR, MOE, IB)

The modulus of rupture (MOR) and modulus of elasticity (MOE) were analyzed together because they came from the same bending assay. ANOVA tables for MOR and MOE are shown in tables 4.3 and 4.4, respectively. The statistical plots for MOR and MOE are shown in figures 4.2 and 4.3, respectively. The fitted model for MOR gave an R-squared of 0.941 and an SDR of 4.2 MPa. The fitted model for MOE gave an R-squared of 0.884 and an SDR of 696 MPa. Only two factor (pretreatment time and initial pressing pressure) were statistically significant for MOR, while for MOE three factors were statistically significant (pretreatment time, initial pressing pressure and initial pressing time). The modeled surface in figure 4.2d shows that the best MOR values are obtained at low pretreatment temperatures and long pretreatment times. The same is true for MOE. These results also agree with density behavior. Vapor pretreatments at low temperatures preserve the fibrillar structure, but long times are needed to achieve the chemical and physical modifications that enhance the adhesive behavior of the lignin. This is confirmed by the behavior of pretreatment time, which has a bigger influence at low pretreatment temperatures than at high pretreatment temperatures (see figure 4.2d).

The modeled surface in figure 4.2f shows that low pressing temperatures and long pressing times enhance MOR, which agrees with density behavior. However, in figure 4.3f it can be seen that the trend for MOE is different: it increases when the pressing time rises at high pressing temperatures while the MOR decreases with the same combination of factors.

Figures 4.2h and 4.3h show that initial press pressure influence MOR and MOE in the same way, and very similar to the density behavior.

Interaction plots (figures 4.2c and 4.3c), Pareto charts (figure 4.2a and 4.3a) and ANOVA tables (tables 4.3 and 4.4) for MOR and MOE show that the relevant interactions are: AB, EG, CG, CE and DF, the first one was already explained for the density analysis. The interactions EG and DF correspond to interactions in the first and last pressing cycle steps, between the press pressure and the press time; this interactions can be expected because these factors control the pressing cycle; they were explained above. The really interesting interactions are CG and CE; these interactions have effects of the same magnitude but opposite direction. Figures 4.2g and 4.3g show that at short final pressing times (G), the pressing temperature (C) has a positive influence over the MOR and MOE but at long final pressing times, this influence becomes negative. However, long final pressing times enhance both MOR and MOE at low pressing temperatures. This behavior is due to difficulties in the heat

transfer from the press platens to and through the board at short pressing times; this difficulty is greatly overcome increasing the pressing temperature.

There is a very good correlation between the observed values and the values predicted by the models as is shown in figures 4.2e and 4.3e. The equations of the fitted models are shown in figures 4.7b and 4.7c.

The following table shows the combination of factor levels which maximizes MOR and MOE into the studied region:

	<b>Tr</b> [°C]	<b>t<sub>r</sub></b> [min.]	<b>Tp</b> [°C]	<b>Pp<sub>i</sub></b> [MPa]	<b>Pp<sub>f</sub></b> [MPa]	<b>tp<sub>i</sub></b> [min.]	<b>tp<sub>f</sub></b> [min.]
MOR	160	12.5	222.1	17.7	12.2	1	1
MOE	160	11.3	229.9	11.6	9.1	3.8	1

We can see that high severity pretreatments are preferred for developing the mechanical properties of the fiberboards, but this high severity should be based on long times rather than on high temperatures. There are clear differences between the materials treated at the same severity but at different temperatures. Low pretreatment temperatures preserve fibers strength but long pretreatment times are necessary to release lignin, making easier the pressing process.

With regard to pressing process, we can see that short pressing times are preferred; this is profitable from the economical point of view. High pressing temperatures and mid-high press pressures are necessary to melt and redistribute lignin and to form chemical bonds between the fibers, at those short pressing times.



**Table 4.3.** Variance Analysis for MOR

Variation source	Sum of Squares	Degrees of Freedom	Mean Square	F-Ratio	P-Value
A:Tr	6.01E+01	1	6.01E+01	3.33	0.0930
B:t_r	5.14E+02	1	5.14E+02	28.46	0.0002
C:Tp	5.76E+01	1	5.76E+01	3.19	0.0995
D:Pp_i	1.00E+02	1	1.00E+02	5.56	0.0361
E:Pp_f	2.08E+01	1	2.08E+01	1.15	0.3038
F:tp_i	1.84E+00	1	1.84E+00	0.10	0.7553
G:tp_f	1.45E+00	1	1.45E+00	0.08	0.7821
AA	8.53E+02	1	8.53E+02	47.24	0.0000
AB	6.47E+02	1	6.47E+02	35.83	0.0001
AC	1.50E+02	1	1.50E+02	8.33	0.0137
AD	2.14E+01	1	2.14E+01	1.18	0.2979
AE	2.08E+01	1	2.08E+01	1.15	0.3042
AF	8.83E+01	1	8.83E+01	4.89	0.0472
AG	6.10E+01	1	6.10E+01	3.38	0.0910
BB	8.18E+01	1	8.18E+01	4.53	0.0547
BC	6.61E+00	1	6.61E+00	0.37	0.5563
BD	4.66E+01	1	4.66E+01	2.58	0.1342
BE	4.10E+01	1	4.10E+01	2.27	0.1579
BF	9.77E+01	1	9.77E+01	5.41	0.0384
BG	1.23E+01	1	1.23E+01	0.68	0.4254
CC	8.63E+01	1	8.63E+01	4.78	0.0493
CD	7.87E+01	1	7.87E+01	4.35	0.0589
CE	3.76E+02	1	3.76E+02	20.81	0.0007
CF	2.45E+01	1	2.45E+01	1.36	0.2668
CG	3.79E+02	1	3.79E+02	20.96	0.0006
DD	1.17E+01	1	1.17E+01	0.65	0.4373
DE	1.37E+01	1	1.37E+01	0.76	0.4014
DF	2.62E+02	1	2.62E+02	14.53	0.0025
DG	4.26E+01	1	4.26E+01	2.36	0.1505
EE	1.12E+01	1	1.12E+01	0.62	0.4459
EF	5.03E+01	1	5.03E+01	2.79	0.1209
EG	6.15E+02	1	6.15E+02	34.02	0.0001
FF	1.42E+01	1	1.42E+01	0.79	0.3923
FG	7.01E+01	1	7.01E+01	3.88	0.0724
GG	1.59E+01	1	1.59E+01	0.88	0.3673
Total error	2.17E+02	12	1.81E+01		
Total (corr.)	3.67E+03	47			

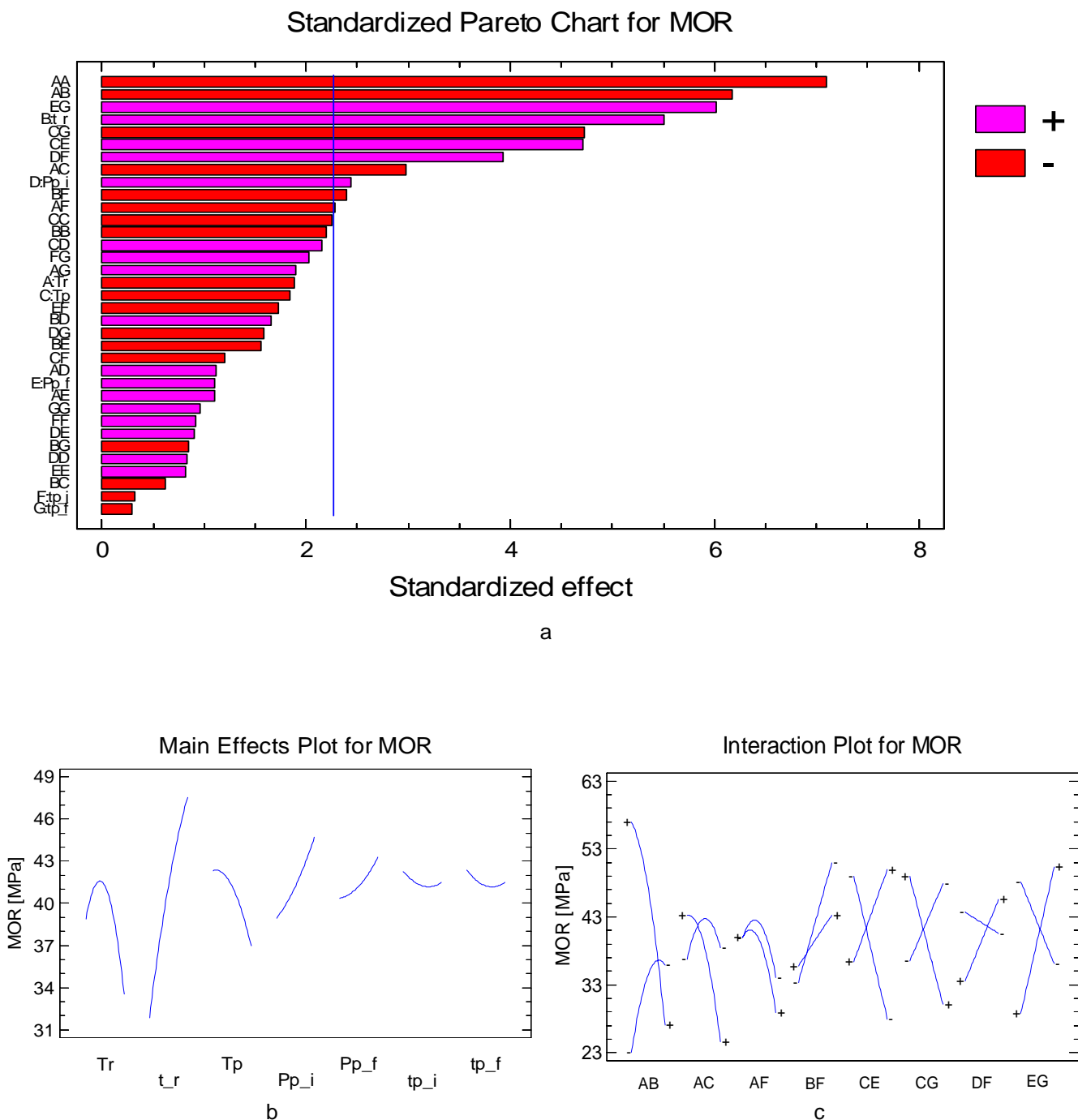


**Figure 4.2.** Statistical Plots for MOR Analysis  
 a. Pareto chart, b. Main effects plot, c. Interaction plot

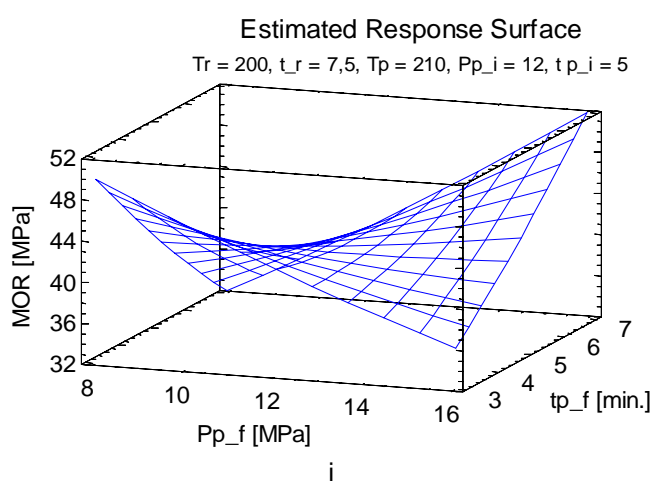
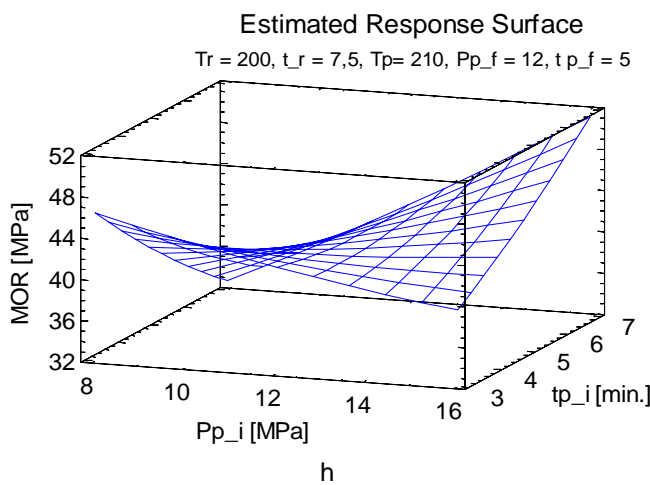
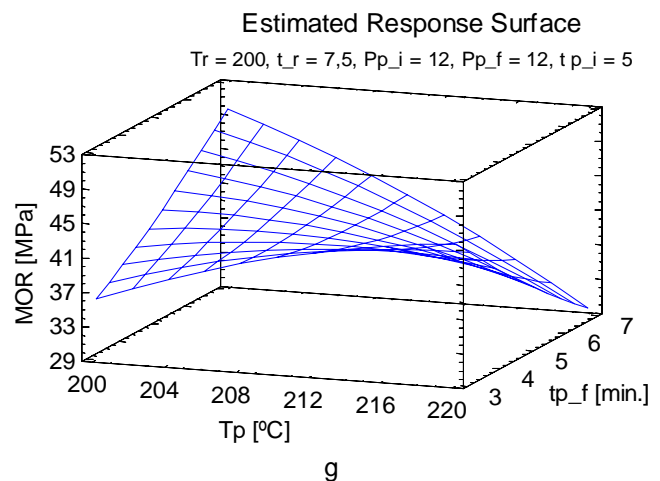
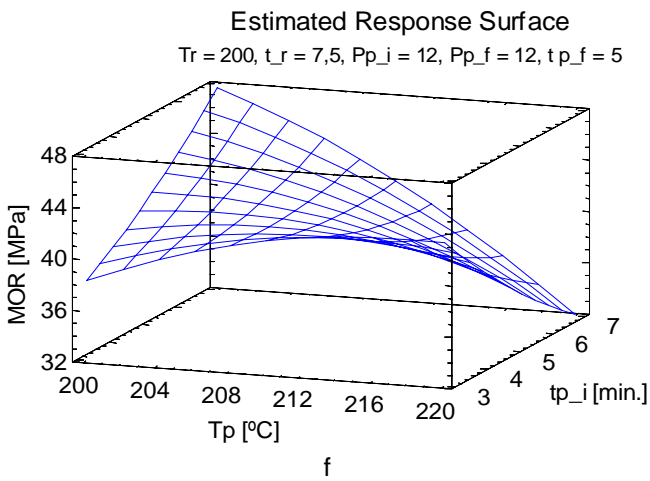
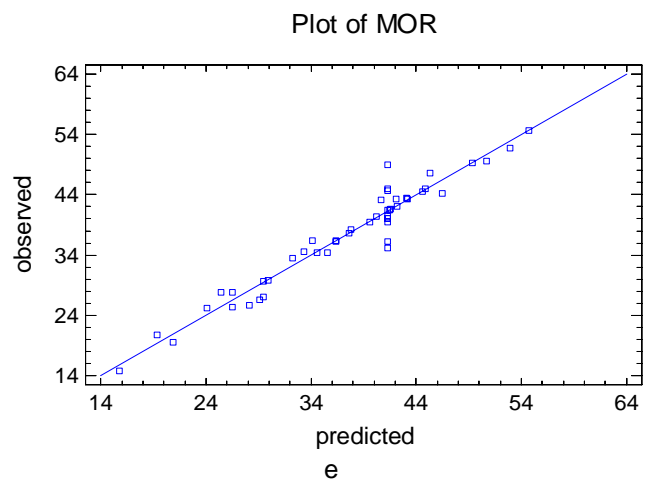
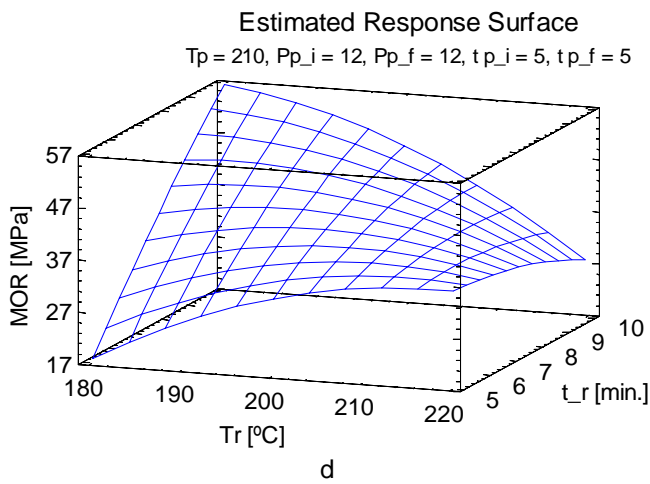
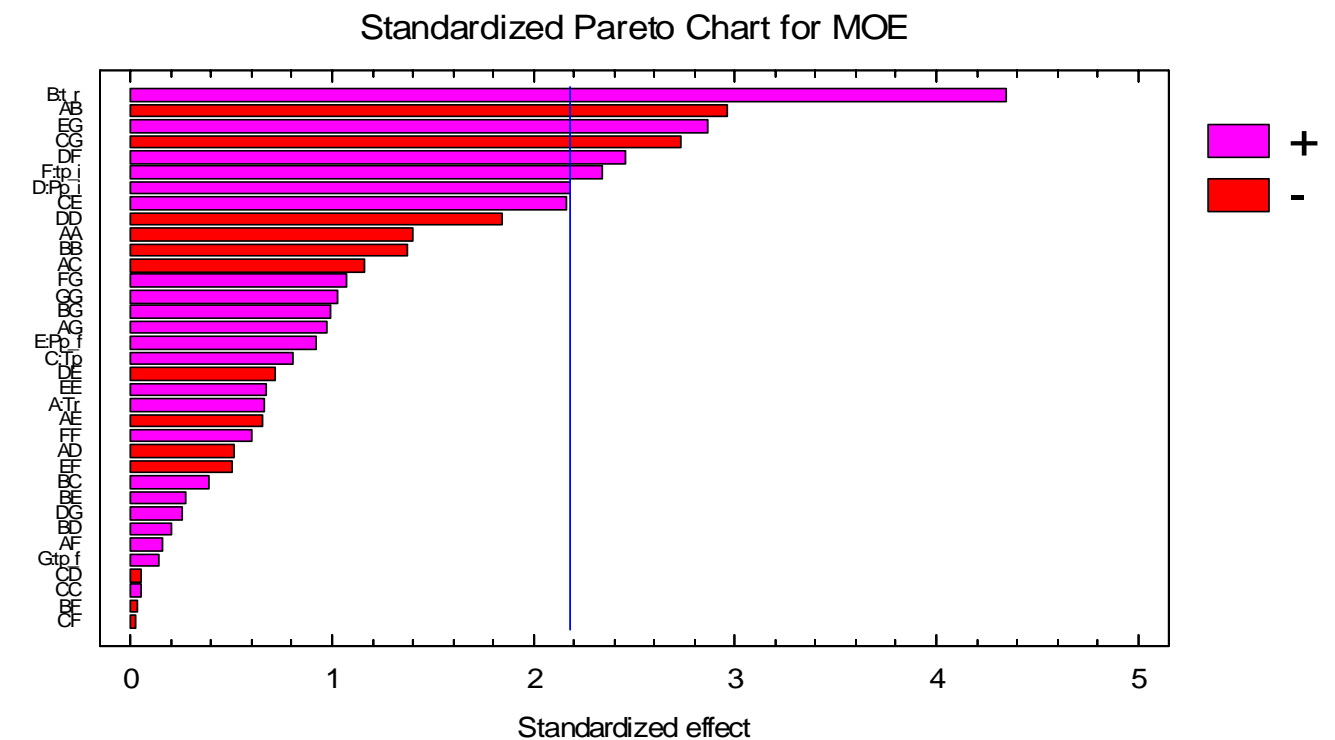


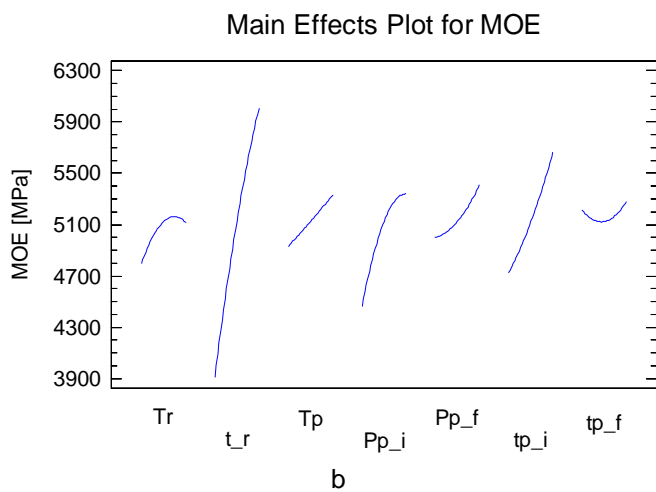
**Figure 4.2.** Statistical Plots for MOR Analysis (continuation)  
 d, f, g, h, i. Estimated responses surfaces, e. Diagnostic plot

**Table 4.4.** Variance Analysis for MOE

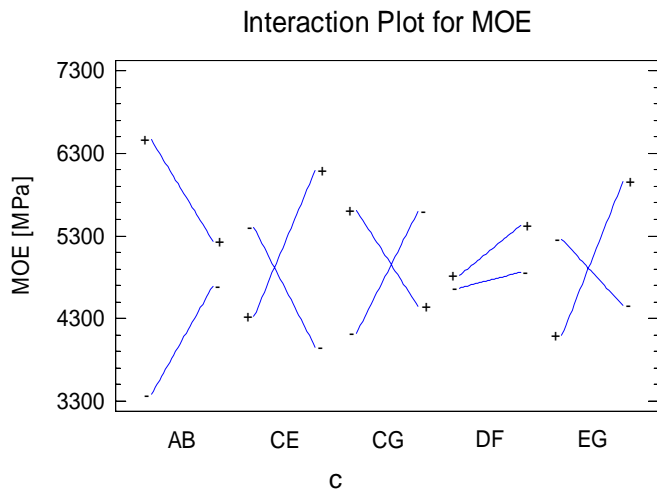
Variation source	Sum of Squares	Degrees of Freedom	Mean Square	F-Ratio	P-Value
A:Tr	2.14E+05	1	2.14E+05	0.44	0.5184
B:t_r	9.15E+06	1	9.15E+06	18.91	0.0009
C:Tp	3.15E+05	1	3.15E+05	0.65	0.4354
D:Pp_i	2.30E+06	1	2.30E+06	4.76	0.0497
E:Pp_f	4.10E+05	1	4.10E+05	0.85	0.3753
F:tp_i	2.64E+06	1	2.64E+06	5.46	0.0376
G:tp_f	9.32E+03	1	9.32E+03	0.02	0.8919
AA	9.43E+05	1	9.43E+05	1.95	0.1879
AB	4.26E+06	1	4.26E+06	8.79	0.0118
AC	6.54E+05	1	6.54E+05	1.35	0.2676
AD	1.26E+05	1	1.26E+05	0.26	0.6194
AE	2.08E+05	1	2.08E+05	0.43	0.5249
AF	1.21E+04	1	1.21E+04	0.02	0.8771
AG	4.57E+05	1	4.57E+05	0.95	0.3501
BB	9.17E+05	1	9.17E+05	1.89	0.1939
BC	7.32E+04	1	7.32E+04	0.15	0.7041
BD	1.95E+04	1	1.95E+04	0.04	0.8444
BE	3.68E+04	1	3.68E+04	0.08	0.7874
BF	5.43E+02	1	5.43E+02	0.00	0.9738
BG	4.78E+05	1	4.78E+05	0.99	0.3399
CC	1.29E+03	1	1.29E+03	0.00	0.9596
CD	1.36E+03	1	1.36E+03	0.00	0.9586
CE	2.26E+06	1	2.26E+06	4.68	0.0514
CF	3.38E+02	1	3.38E+02	0.00	0.9794
CG	3.61E+06	1	3.61E+06	7.47	0.0182
DD	1.65E+06	1	1.65E+06	3.41	0.0897
DE	2.49E+05	1	2.49E+05	0.52	0.4866
DF	2.92E+06	1	2.92E+06	6.04	0.0302
DG	3.15E+04	1	3.15E+04	0.07	0.8029
EE	2.17E+05	1	2.17E+05	0.45	0.5158
EF	1.21E+05	1	1.21E+05	0.25	0.6258
EG	3.97E+06	1	3.97E+06	8.20	0.0143
FF	1.77E+05	1	1.77E+05	0.36	0.5571
FG	5.52E+05	1	5.52E+05	1.14	0.3067
GG	5.10E+05	1	5.10E+05	1.05	0.3251
Total error	5.81E+06	12	4.84E+05		
Total (corr.)	5.02E+07	47			



a



b



c

**Figure 4.3.** Statistical Plots for MOE Analysis  
 a. Pareto chart, b. Main effects plot, c. Interaction plot

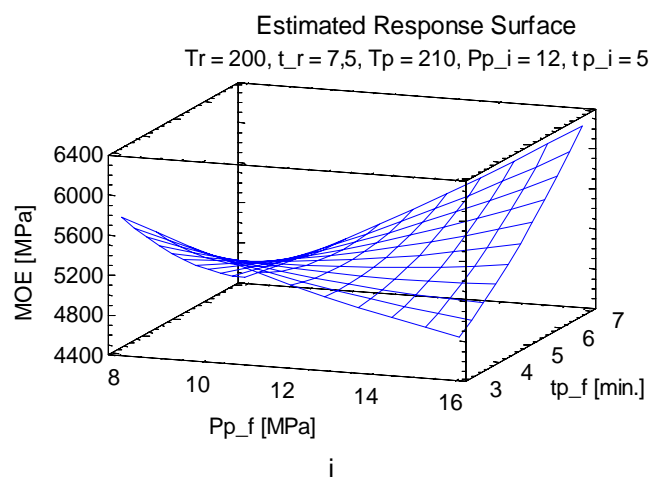
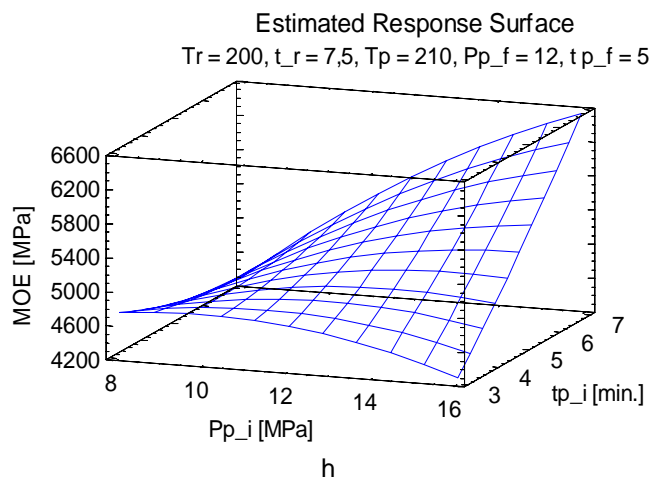
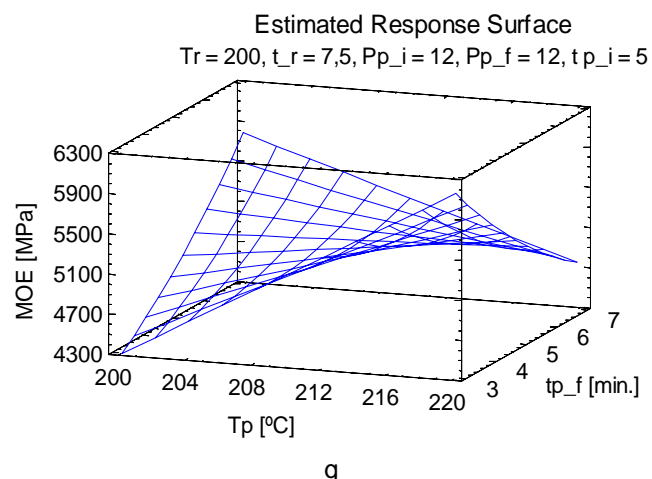
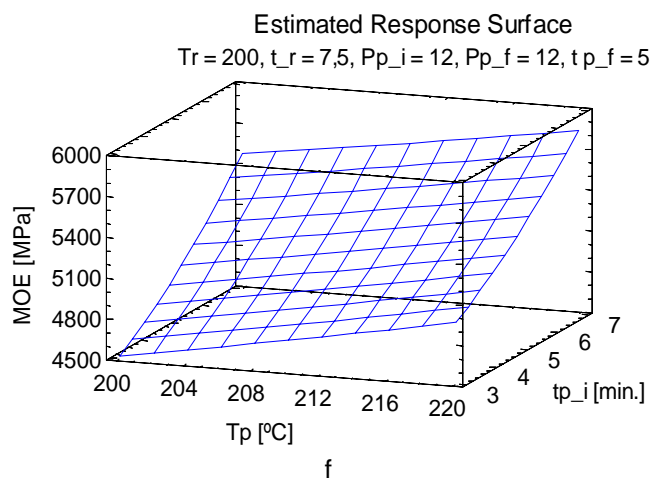
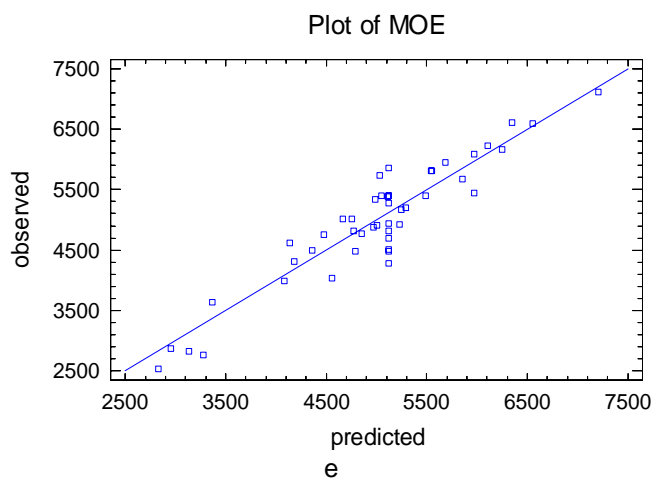
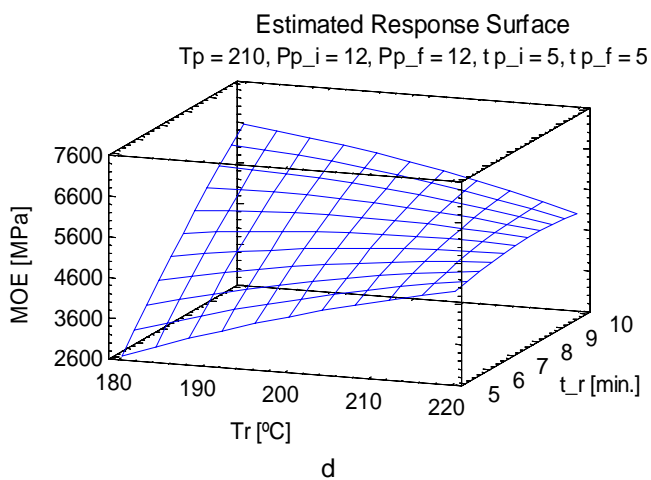


**Figure 4.3.** Statistical Plots for MOE Analysis (continuation)  
 d, f, g, h, i. Estimated responses surfaces, e. Diagnostic plot

Internal Bond (IB) is the mechanical property that accounts for the strength of the bonds between the fibers; because the fibers are mainly oriented in the board plane the IB measures the tension perpendicular to the faces of the board. ANOVA table for IB is shown in table 4.5 and the statistical plots for IB are shown in figure 4.4. The fitted model gave an R-squared of 0.945 and an SDR of 0.14 MPa. Four factors (pretreatment temperature, pressing temperature, initial pressing time and initial press pressure) were statistically significant. The modeled surface on figure 4.4d shows that the best IB values were obtained at high pretreatment temperatures. This can be explained by the rising quantity of particles that appeared when the pretreatment temperature increased (Suchsland, Woodson *et al.* 1987), which increased the area available for bonding. Also, high pretreatment temperatures promote a higher extraction of hemicelluloses and extractives and partially depolymerize the lignin, which helps the bonding action.

The modeled surface in figure 4.4f shows that high pressing temperatures are preferred. This behavior is common to other non woody materials (Anglès, Reguant *et al.* 1999) and is in accordance with the behavior of the other mechanical properties (MOR and MOE).

Figure 4.4h shows that low pressing pressures and intermediate pressing times are preferred. As we have seen before, a suitable combination of process factors is the key to obtaining the desired properties. For the IB, due to the upward trend of the pretreatment and pressing temperatures, the pressing pressure should be low to avoid spoiling the fibers and enable the proper distribution of lignin between them.

Interaction plot (figure 4.4c), Pareto chart (figure 4.4a) and ANOVA table (Table 4.5) show that the most important interactions are presented between BF and BG. The interactions between the pretreatment time (B) and the initial (F) and final (G) pressing times are to be expected. For the material pretreated at high severities, based on long pretreatment times, long pressing times favor the development of the chemical bonds. Thus improving the IB, but if the pretreatment is not enough for releasing the lignin and separating the fibers, long pressing times deteriorate the fibers instead of promoting the chemical bonds.

There is a very good correlation between the observed values and the values predicted by the models as shown in figure 4.4e. The equation of the fitted model is shown in figure 4.7d.

The following table shows the combination of the factor levels which maximizes IB into the studied region:

	<b>Tr</b>	<b>t_r</b>	<b>Tp</b>	<b>Pp_i</b>	<b>Pp_f</b>	<b>tp_i</b>	<b>tp_f</b>
	<b>[°C]</b>	<b>[min.]</b>	<b>[°C]</b>	<b>[MPa]</b>	<b>[MPa]</b>	<b>[min.]</b>	<b>[min.]</b>
IB	238	7.4	230	4	4	6	3.9

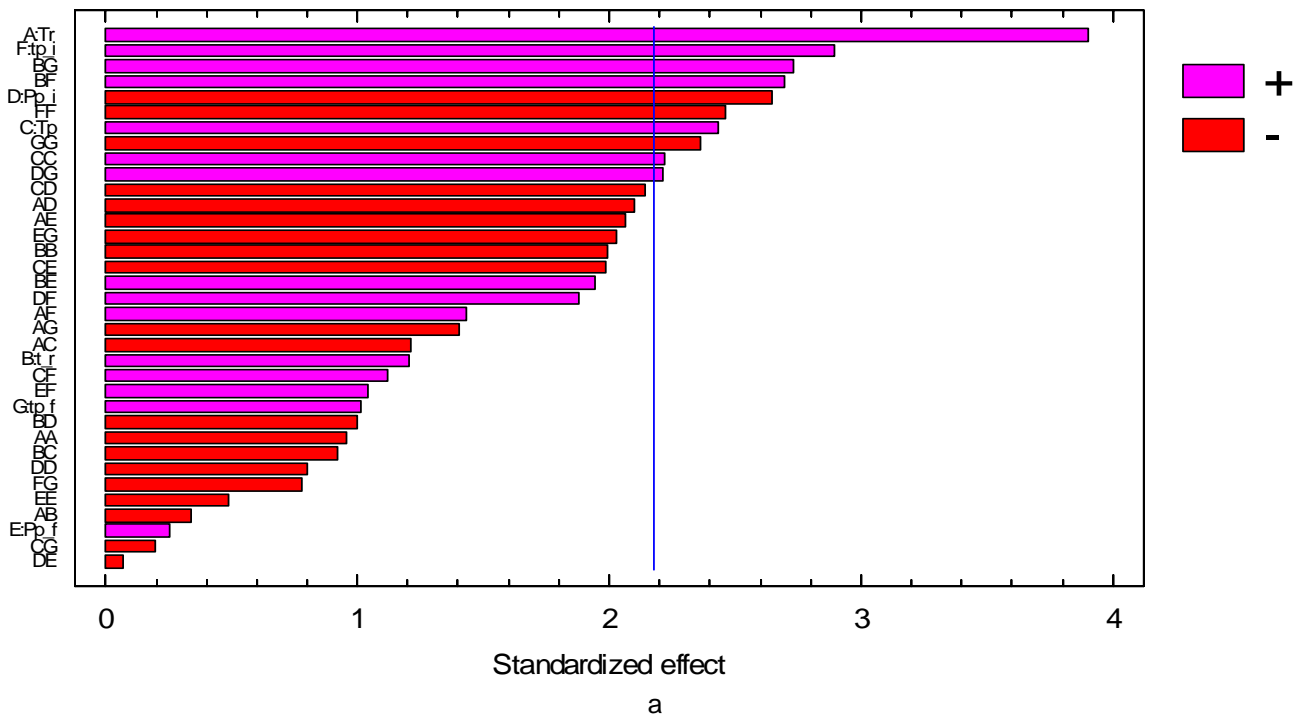
High severity pretreatments favor the internal bond but this high severity based on temperature rather than time deteriorates the MOR and MOE. With regard to the pressing process, the optimum press temperature is the highest studied and the optimum press pressure is the lowest. Clearly, the optimum values for maximizing the IB are in a different direction to those for maximizing the MOE and MOR. Based on these observations it is advisable to optimize all variables at the same time and to study other possibilities for increasing the mechanical properties, such as the addition of exogenous lignin for improving the bonding capability of the material or finding the optimum sieve size in the milling process for separating the fibers instead of cutting them.



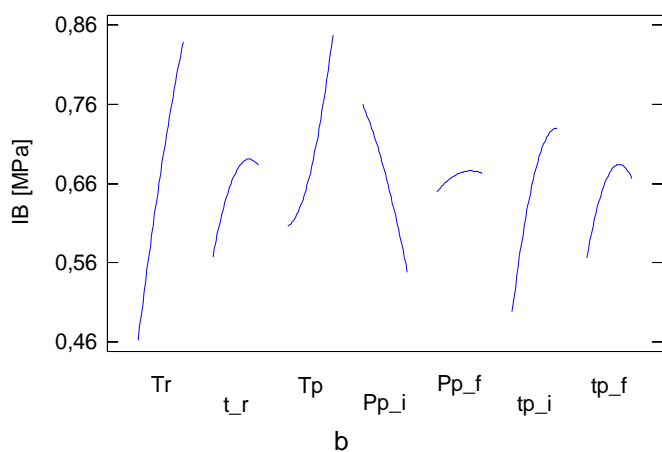
Table 4.5. Variance Analysis for IB

Variation source	Sum of Squares	Degrees of Freedom	Mean Square	F-Ratio	P-Value
A:Tr	2.97E-01	1	2.97E-01	15.25	0.0021
B:t_r	2.84E-02	1	2.84E-02	1.46	0.2505
C:Tp	1.15E-01	1	1.15E-01	5.92	0.0316
D:Pp_i	1.36E-01	1	1.36E-01	7.00	0.0214
E:Pp_f	1.26E-03	1	1.26E-03	0.06	0.8033
F:tp_i	1.63E-01	1	1.63E-01	8.38	0.0135
G:tp_f	2.00E-02	1	2.00E-02	1.03	0.3307
AA	1.77E-02	1	1.77E-02	0.91	0.3590
AB	2.23E-03	1	2.23E-03	0.11	0.7408
AC	2.84E-02	1	2.84E-02	1.46	0.2499
AD	8.56E-02	1	8.56E-02	4.40	0.0579
AE	8.28E-02	1	8.28E-02	4.25	0.0615
AF	4.00E-02	1	4.00E-02	2.06	0.1770
AG	3.84E-02	1	3.84E-02	1.97	0.1856
BB	7.75E-02	1	7.75E-02	3.98	0.0692
BC	1.64E-02	1	1.64E-02	0.84	0.3764
BD	1.95E-02	1	1.95E-02	1.00	0.3366
BE	7.35E-02	1	7.35E-02	3.77	0.0759
BF	1.41E-01	1	1.41E-01	7.25	0.0196
BG	1.45E-01	1	1.45E-01	7.45	0.0183
CC	9.62E-02	1	9.62E-02	4.94	0.0462
CD	8.94E-02	1	8.94E-02	4.59	0.0533
CE	7.65E-02	1	7.65E-02	3.93	0.0708
CF	2.43E-02	1	2.43E-02	1.25	0.2856
CG	7.36E-04	1	7.36E-04	0.04	0.8490
DD	1.24E-02	1	1.24E-02	0.64	0.4406
DE	1.01E-04	1	1.01E-04	0.01	0.9437
DF	6.90E-02	1	6.90E-02	3.54	0.0842
DG	9.53E-02	1	9.53E-02	4.90	0.0471
EE	4.58E-03	1	4.58E-03	0.24	0.6363
EF	2.12E-02	1	2.12E-02	1.09	0.3172
EG	8.02E-02	1	8.02E-02	4.12	0.0652
FF	1.18E-01	1	1.18E-01	6.07	0.0298
FG	1.17E-02	1	1.17E-02	0.60	0.4524
GG	1.08E-01	1	1.08E-01	5.57	0.0361
Total error	2.34E-01	12	1.95E-02		
Total (corr.)	4.22E+00	47			

Standardized Pareto Chart for IB



Main Effects Plot for IB



Interaction Plot for IB

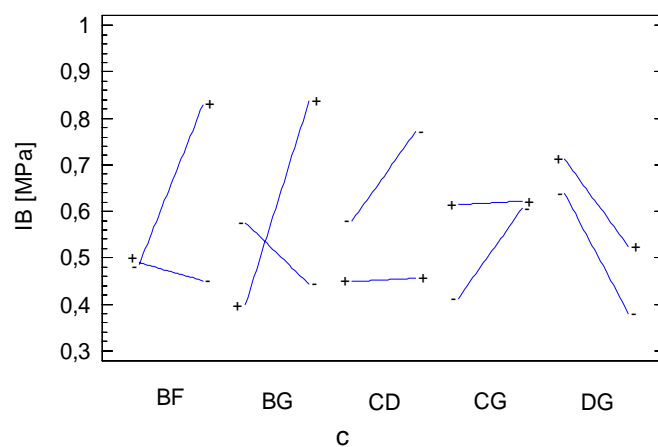


**Figure 4.4.** Statistical Plots for IB Analysis  
 a. Pareto chart, b. Main effects plot, c. Interaction plot

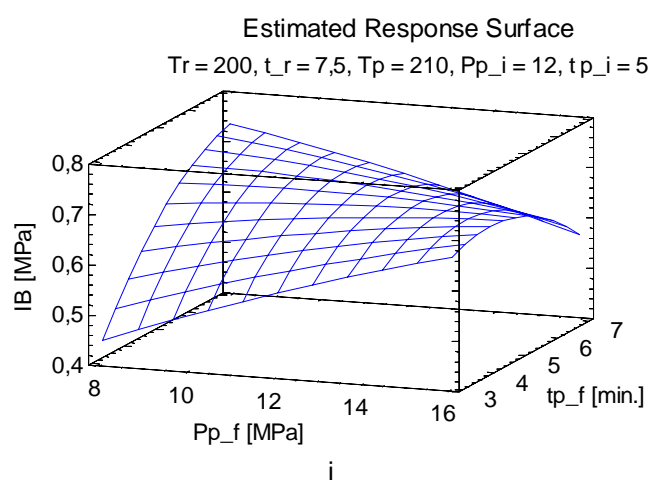
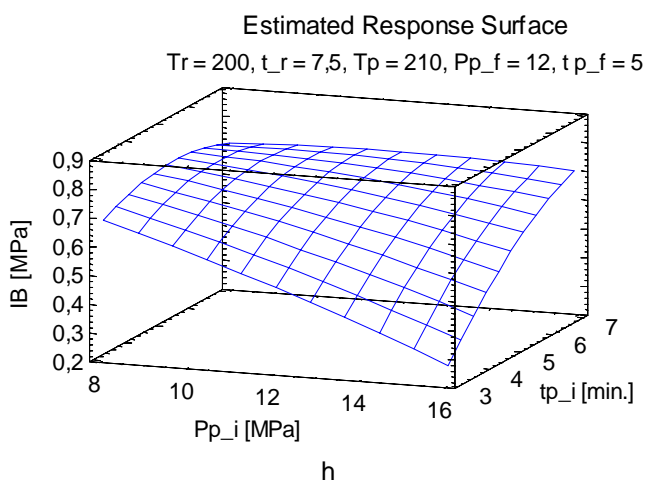
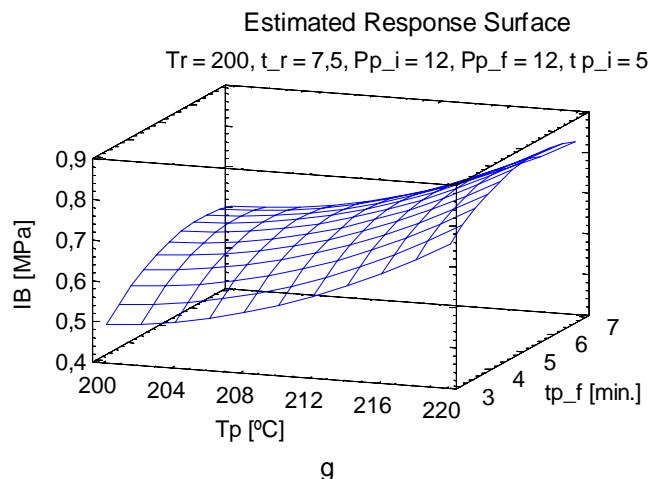
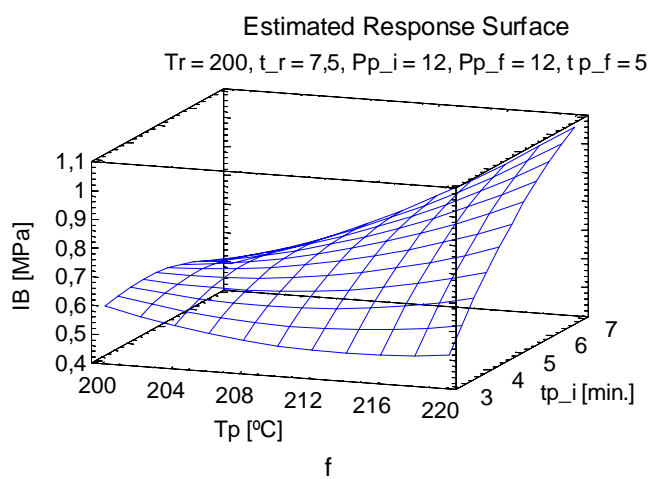
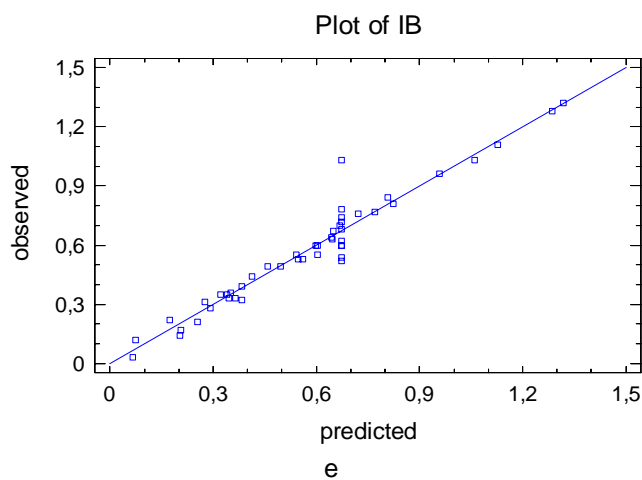
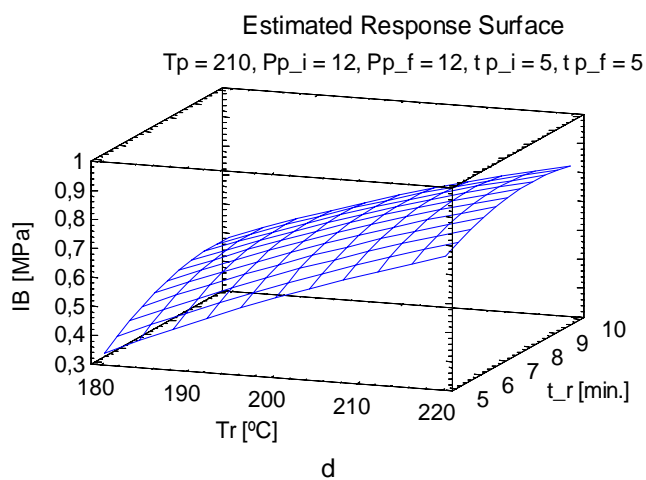


**Figure 4.4.** Statistical Plots for IB Analysis (continuation)  
 d, f, g, h, i. Estimated responses surfaces, e. Diagnostic plot

#### 4.2.1.3 Physical properties (WA, TS)

Water absorption (WA) and Thickness swelling (TS) are the physical properties related with the dimensional stability of the boards. These properties give us an idea of how the boards will behave when used under conditions of severe humidity, they are especially important to boards for external use. WA and TS were analyzed together because came from the same assay. ANOVA tables for WA and TS are shown in tables 4.6 and 4.7, respectively. The statistical plots for WA and TS are shown in figures 4.5 and 4.6, respectively. The fitted models gave R's-squared of 0.988 for WA and 0.984 for TS and SDRs of 3.8% and 2.9%, respectively. Four factors (pretreatment temperature, pretreatment time, pressing temperature and initial pressing time) were significant for both response variables. The modeled surface (figure 4.5d) shows that the lower values of WA were obtained at high pretreatment temperatures and intermediate-to-long pretreatment times. The same was true for TS (figure 4.6d). This is because high-severity pretreatments enhance the hydrolysis of the hemicelluloses, which are largely responsible for board instability (Jianying, Ragil et al. 2006).

The general trend for the pressing process (figures 4.5f and 4.6f) is to get lower WA and TS at high pressing temperatures and short times, possibly to overcome the heat and mass transfer limitations in the pressing process.

Interaction plots (figures 4.5c and 4.6c), Pareto charts (figures 4.5a and 4.6a) and ANOVA tables (tables 4.6 and 4.7) for WA and TS show that the relevant interactions common to both properties are: AC, AF and BF. Figures 4.5c and 4.6c show that, in the first interaction, at low pressing temperatures (C), the pretreatment temperature (A) has a stronger effect over the WA and TS than at high ones; which makes easier to achieve low WA values with high pressing temperatures than with low ones. However, even with low pressing temperatures we can get low WA but only at high pretreatment temperatures. This is because the materials pretreated at low severities need higher pressing temperatures to melt the lignin and to develop stable bonds. The other two interactions AF and BF are regarding to the pretreatment variables and the initial pressing time. The interaction plots show that high severity pretreatments are needed to obtain low values of WA and TS, and that pretreatment temperature has a bigger influence over these variables than pretreatment time.

There is a very good correlation between the observed values and the values predicted for the models as is shown in figures 4.5e and 4.6e. The equations of the fitted models are shown in figures 4.7e and 4.7f.

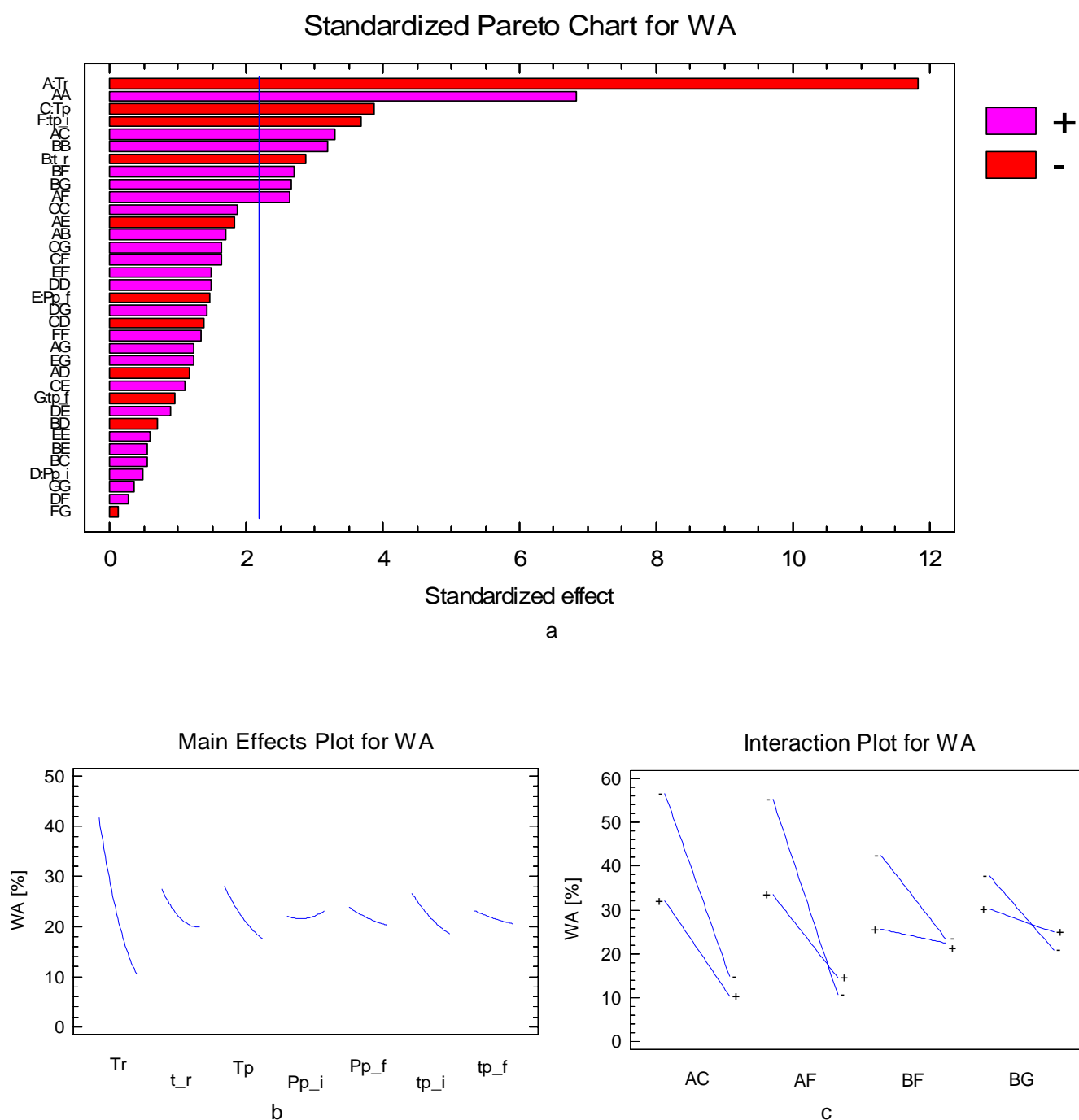
The following table shows the combination of factor levels which approach WA and TS to zero into the studied region:

	<b>Tr</b> [°C]	<b>t<sub>r</sub></b> [min.]	<b>Tp</b> [°C]	<b>Pp<sub>i</sub></b> [MPa]	<b>Pp<sub>f</sub></b> [MPa]	<b>tp<sub>i</sub></b> [min.]	<b>tp<sub>f</sub></b> [min.]
WA	229	7.4	215	9.7	13.5	2.8	4.5
TS	232	11	214	11.7	6.7	3.7	4

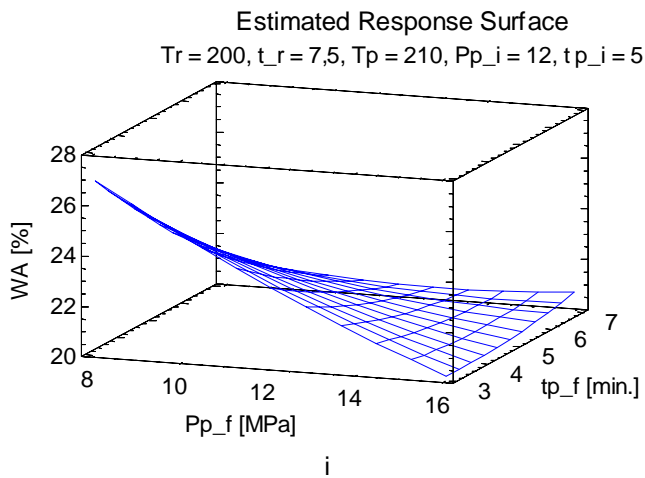
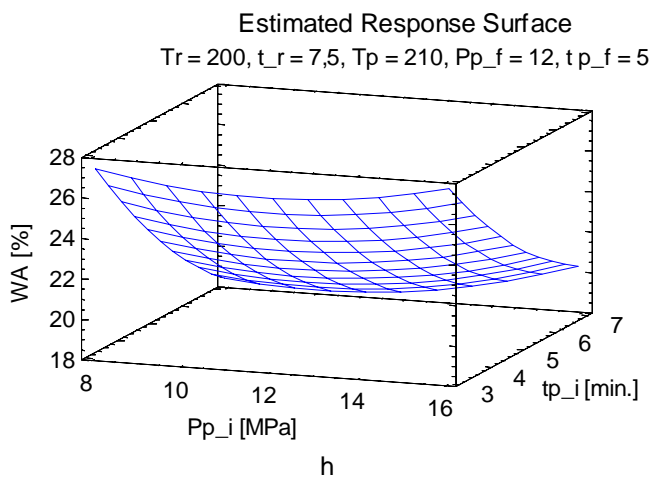
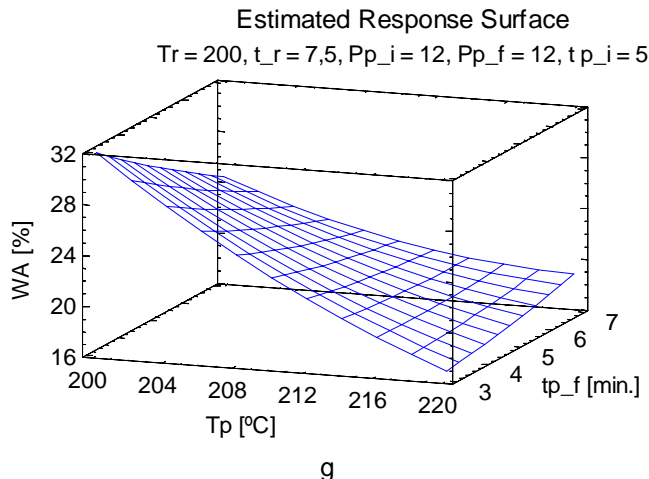
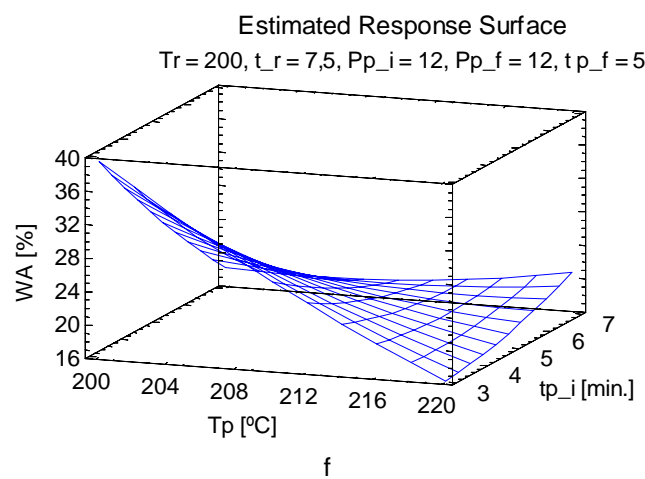
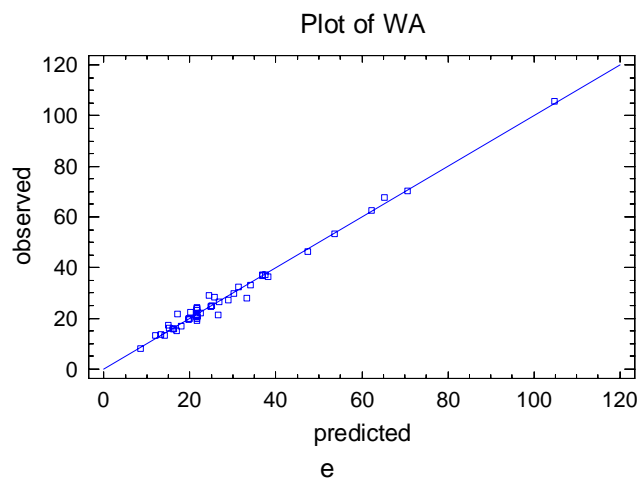
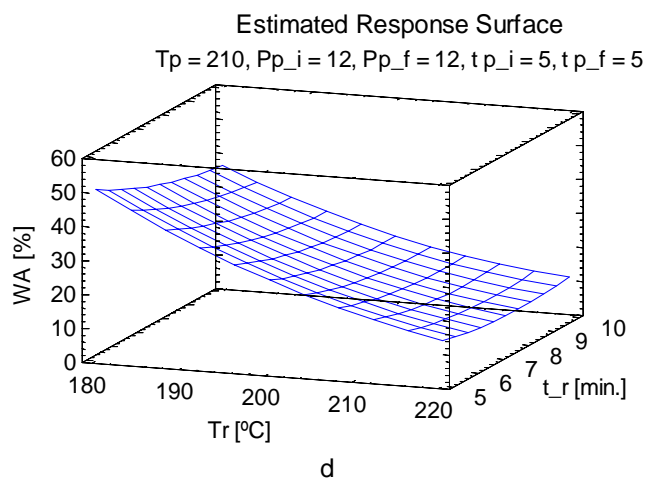
The main differences between the optimums for the mechanical and physical properties were in the pretreatment temperatures and times: very high temperatures improved WA and TS whereas very low temperatures maximized MOR and MOE. These different tendencies suggest that there must be an agreement between the operational factors that result in the production of boards that fully satisfy the European standards.

**Table 4.6.** Variance Analysis for WA

Variation source	Sum of Squares	Degrees of Freedom	Mean Square	F-Ratio	P-Value
A:Tr	2.03E+03	1	2.03E+03	139.99	0.0000
B:t_r	1.19E+02	1	1.19E+02	8.23	0.0141
C:Tp	2.17E+02	1	2.17E+02	14.96	0.0022
D:Pp_i	3.35E+00	1	3.35E+00	0.23	0.6390
E:Pp_f	3.09E+01	1	3.09E+01	2.14	0.1697
F:tp_i	1.95E+02	1	1.95E+02	13.45	0.0032
G:tp_f	1.33E+01	1	1.33E+01	0.92	0.3573
AA	6.77E+02	1	6.77E+02	46.78	0.0000
AB	4.17E+01	1	4.17E+01	2.88	0.1155
AC	1.58E+02	1	1.58E+02	10.89	0.0063
AD	1.99E+01	1	1.99E+01	1.38	0.2635
AE	4.87E+01	1	4.87E+01	3.36	0.0915
AF	1.01E+02	1	1.01E+02	6.98	0.0215
AG	2.17E+01	1	2.17E+01	1.50	0.2440
BB	1.48E+02	1	1.48E+02	10.22	0.0077
BC	4.22E+00	1	4.22E+00	0.29	0.5989
BD	7.20E+00	1	7.20E+00	0.50	0.4941
BE	4.25E+00	1	4.25E+00	0.29	0.5980
BF	1.05E+02	1	1.05E+02	7.28	0.0194
BG	1.02E+02	1	1.02E+02	7.08	0.0208
CC	5.08E+01	1	5.08E+01	3.51	0.0855
CD	2.77E+01	1	2.77E+01	1.92	0.1915
CE	1.74E+01	1	1.74E+01	1.21	0.2938
CF	3.83E+01	1	3.83E+01	2.65	0.1298
CG	3.90E+01	1	3.90E+01	2.70	0.1264
DD	3.21E+01	1	3.21E+01	2.22	0.1621
DE	1.15E+01	1	1.15E+01	0.80	0.3900
DF	1.08E+00	1	1.08E+00	0.07	0.7896
DG	2.88E+01	1	2.88E+01	1.99	0.1836
EE	4.94E+00	1	4.94E+00	0.34	0.5697
EF	3.21E+01	1	3.21E+01	2.22	0.1621
EG	2.15E+01	1	2.15E+01	1.49	0.2464
FF	2.54E+01	1	2.54E+01	1.76	0.2097
FG	2.28E-01	1	2.28E-01	0.02	0.9021
GG	1.73E+00	1	1.73E+00	0.12	0.7355
Total error	1.74E+02	12	1.45E+01		
Total (corr.)	1.47E+04	47			



**Figure 4.5.** Statistical Plots for WA Analysis  
 a. Pareto chart, b. Main effects plot, c. Interaction plot



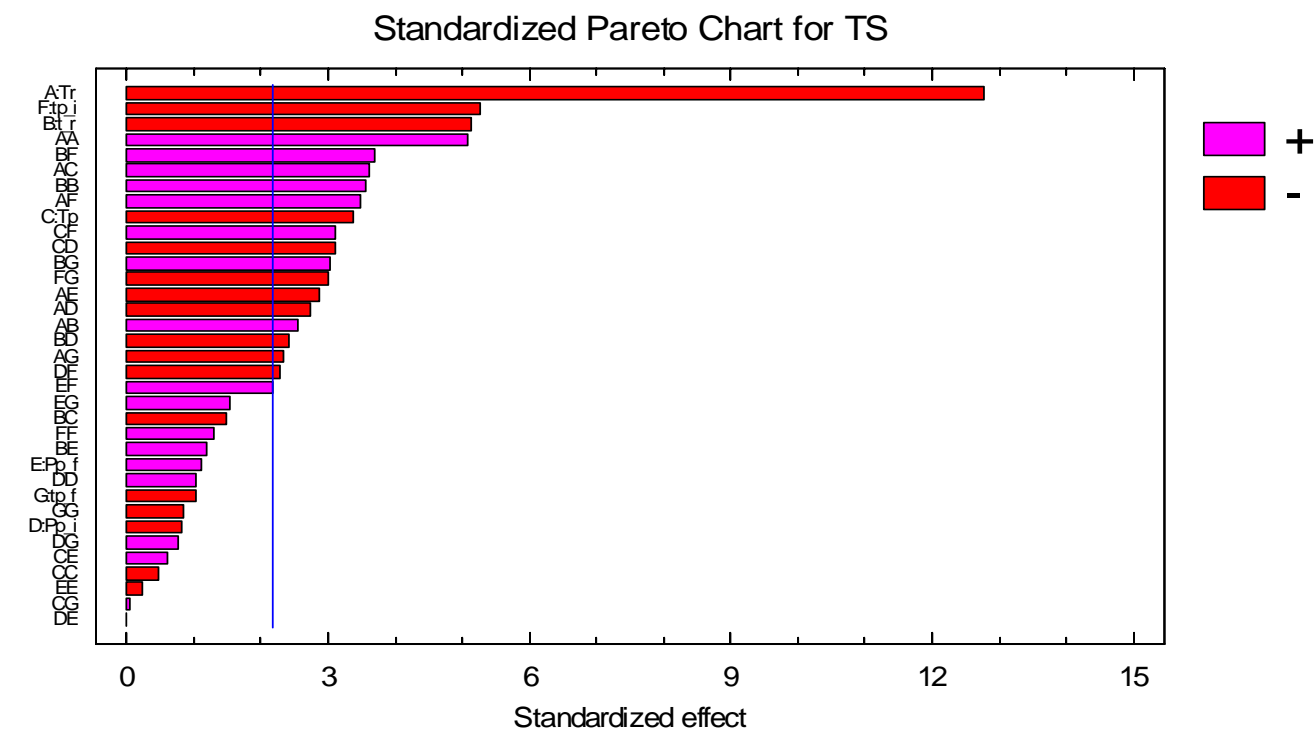
**Figure 4.5.** Statistical Plots for WA Analysis (continuation)  
 d, f, g, h, i. Estimated responses surfaces, e. Diagnostic plot



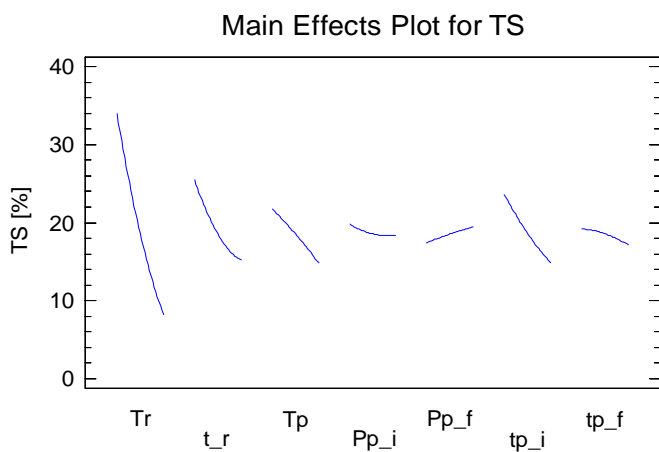
Table 4.7. Variance Analysis for TS

Variation source	Sum of Squares	Degrees of Freedom	Mean Square	F-Ratio	P-Value
A:Tr	1.39E+03	1	1.39E+03	163.31	0.0000
B:t_r	2.25E+02	1	2.25E+02	26.46	0.0002
C:Tp	9.66E+01	1	9.66E+01	11.38	0.0055
D:Pp_i	5.71E+00	1	5.71E+00	0.67	0.4282
E:Pp_f	1.04E+01	1	1.04E+01	1.23	0.2898
F:tp_i	2.34E+02	1	2.34E+02	27.57	0.0002
G:tp_f	8.82E+00	1	8.82E+00	1.04	0.3282
AA	2.19E+02	1	2.19E+02	25.74	0.0003
AB	5.54E+01	1	5.54E+01	6.52	0.0253
AC	1.11E+02	1	1.11E+02	13.03	0.0036
AD	6.31E+01	1	6.31E+01	7.44	0.0184
AE	7.02E+01	1	7.02E+01	8.27	0.0139
AF	1.02E+02	1	1.02E+02	12.02	0.0047
AG	4.59E+01	1	4.59E+01	5.40	0.0384
BB	1.07E+02	1	1.07E+02	12.59	0.0040
BC	1.84E+01	1	1.84E+01	2.17	0.1662
BD	4.97E+01	1	4.97E+01	5.86	0.0323
BE	1.19E+01	1	1.19E+01	1.40	0.2599
BF	1.15E+02	1	1.15E+02	13.58	0.0031
BG	7.78E+01	1	7.78E+01	9.17	0.0105
CC	1.95E+00	1	1.95E+00	0.23	0.6406
CD	8.13E+01	1	8.13E+01	9.58	0.0093
CE	3.11E+00	1	3.11E+00	0.37	0.5561
CF	8.17E+01	1	8.17E+01	9.62	0.0092
CG	1.40E+05	1	1.40E-02	0.00	0.9682
DD	8.95E+00	1	8.95E+00	1.05	0.3247
DE	7.60E+04	1	7.60E-05	0.00	0.9977
DF	4.39E+01	1	4.39E+01	5.17	0.0422
DG	5.03E+00	1	5.03E+00	0.59	0.4563
EE	4.29E-01	1	4.29E-01	0.05	0.8260
EF	4.02E+01	1	4.02E+01	4.74	0.0501
EG	1.99E+01	1	1.99E+01	2.34	0.1519
FF	1.45E+01	1	1.45E+01	1.71	0.2159
FG	7.60E+01	1	7.60E+01	8.96	0.0112
GG	5.89E+00	1	5.89E+00	0.69	0.4211
Total error	1.02E+02	12	8.49E+00		
Total (corr.)	6.37E+03	47			

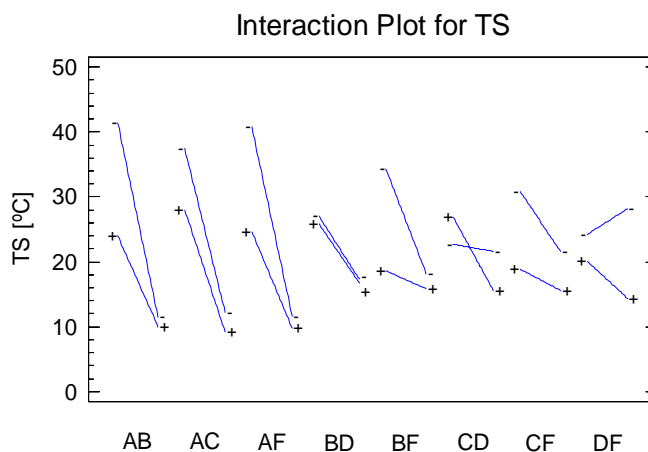
Binderless Fiberboard Production from *Cynara cardunculus* and *Vitis vinifera*



a



b



c

**Figure 4.6.** Statistical Plots for TS Analysis  
 a. Pareto chart, b. Main effects plot, c. Interaction plot

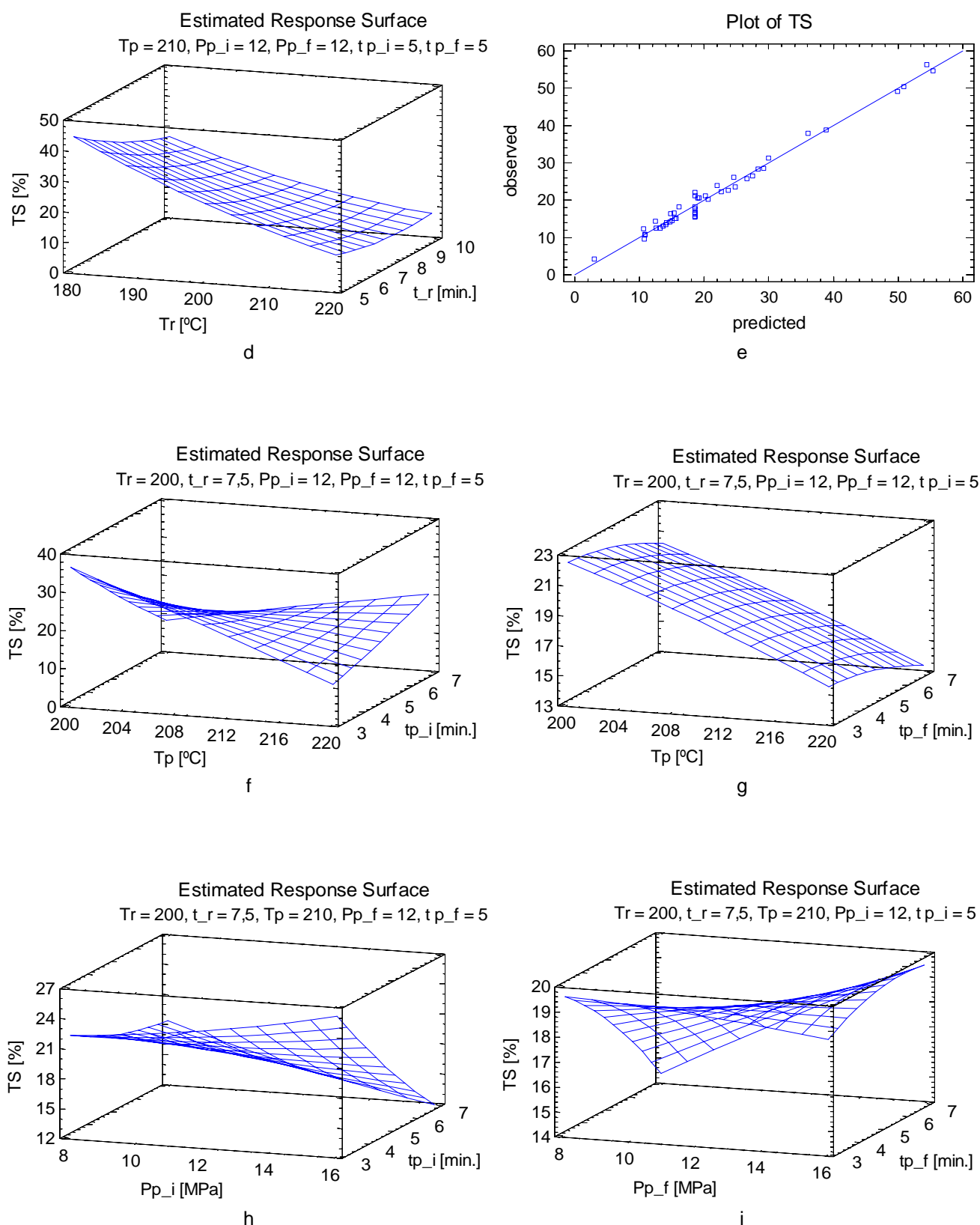


**Figure 4.6.** Statistical Plots for TS Analysis (continuation)  
 d, f, g, h, i. Estimated responses sufeces, e. Diagnostic plot

$$\begin{aligned}
 \text{Density} = & 4590.76 - 28.8963 \times Tr + 486.355 \times t_r - 10.6907 \times Tp - 161.683 \times Pp_i - 147.206 \times Pp_f + \\
 & 293.629 \times tp_i + 70.5335 \times tp_f - 0.0106 \times Tr^2 - 0.577 \times Tr \times t_r + 0.1625 \times Tr \times Tp + 0.009 \times Tr \times Pp_i + \\
 & 0.3677 \times Tr \times Pp_f - 0.4355 \times Tr \times tp_i + 0.3954 \times Tr \times tp_f - 0.2279 \times t_r^2 - 1.3757 \times t_r \times Tp - \\
 & 1.3654 \times t_r \times Pp_i - 3.2209 \times t_r \times Pp_f - 5.21 \times t_r \times tp_i + 2.2892 \times t_r \times tp_f - 0.0549 \times Tp^2 + \\
 & 0.8155 \times Tp \times Pp_i + 0.4165 \times Tp \times Pp_f - 0.566 \times Tp \times tp_i - 0.5796 \times Tp \times tp_f - 0.1936 \times Pp_i^2 + \\
 & 1.4356 \times Pp_i \times Pp_f + 1.9684 \times Pp_i \times tp_i - 3.9713 \times Pp_i \times tp_f - 0.1249 \times Pp_f^2 - 2.4637 \times Pp_f \times \\
 & tp_i + 1.2891 \times Pp_f \times tp_f - 1.5002 \times tp_i^2 - 4.9213 \times tp_i \times tp_f + 1.0191 \times tp_f^2
 \end{aligned}$$

a

$$\begin{aligned}
 \text{MOR} = & -2336.65 + 12.8542 \times Tr + 72.5203 \times t_r + 11.5179 \times Tp - 66.8905 \times Pp_i + 47.9819 \times Pp_f + \\
 & 91.2298 \times tp_i + 38.6458 \times tp_f - 0.0126 \times Tr^2 - 0.2322 \times Tr \times t_r - 0.0327 \times Tr \times Tp + 0.0528 \times Tr \times Pp_i + \\
 & 0.0336 \times Tr \times Pp_f - 0.2015 \times Tr \times tp_i + 0.122 \times Tr \times tp_f - 0.249 \times t_r^2 - 0.0548 \times t_r \times Tp + \\
 & 0.6239 \times t_r \times Pp_i - 0.3773 \times t_r \times Pp_f - 1.6956 \times t_r \times tp_i - 0.4382 \times t_r \times tp_f - 0.016 \times Tp^2 + \\
 & 0.2313 \times Tp \times Pp_i + 0.185 \times Tp \times Pp_f - 0.2561 \times Tp \times tp_i - 0.3684 \times Tp \times tp_f + 0.0367 \times Pp_i^2 + \\
 & 0.1175 \times Pp_i \times Pp_f + 0.7889 \times Pp_i \times tp_i - 0.4881 \times Pp_i \times tp_f + 0.036 \times Pp_f^2 - 0.3869 \times Pp_f \times \\
 & tp_i + 1.0518 \times Pp_f \times tp_f + 0.1622 \times tp_i^2 + 1.7847 \times tp_i \times tp_f + 0.1713 \times tp_f^2
 \end{aligned}$$

b

$$\begin{aligned}
 \text{MOE} = & -125347 + 793.044 \times Tr + 2667.22 \times t_r + 405.435 \times Tp + 1065.13 \times Pp_i - 2635.99 \times Pp_f - \\
 & 1751.88 \times tp_i + 2543.93 \times tp_f - 0.4178 \times Tr^2 - 18.8279 \times Tr \times t_r - 2.1544 \times Tr \times Tp - 4.0545 \times Tr \times \\
 & Pp_i - 3.3566 \times Tr \times Pp_f + 2.3576 \times Tr \times tp_i + 10.5641 \times Tr \times tp_f - 26.3578 \times t_r^2 + 5.7665 \times t_r \times Tp + \\
 & 12.7571 \times t_r \times Pp_i + 11.3051 \times t_r \times Pp_f - 3.9967 \times t_r \times tp_i + 86.3907 \times t_r \times tp_f + 0.0618 \times \\
 & Tp^2 - 0.9619 \times Tp \times Pp_i + 14.3632 \times Tp \times Pp_f - 0.9508 \times Tp \times tp_i - 36 \times Tp \times tp_f - 13.8086 \times Pp_i^2 - \\
 & 15.8692 \times Pp_i \times Pp_f + 83.2503 \times Pp_i \times tp_i + 13.2743 \times Pp_i \times tp_f + 5.0096 \times Pp_f^2 - 18.9871 \times \\
 & Pp_f \times tp_i + 84.5205 \times Pp_f \times tp_f + 18.0731 \times tp_i^2 + 158.349 \times tp_i \times tp_f + 30.7059 \times tp_f^2
 \end{aligned}$$

c

$$\begin{aligned}
 \text{IB} = & -32.5098 + 0.1893 \times Tr + 0.1993 \times t_r - 0.0143 \times Tp + 2.2279 \times Pp_i + 0.903 \times Pp_f - 2.9633 \times \\
 & tp_i + 0.5123 \times tp_f - 0.0001 \times Tr^2 - 0.0004 \times Tr \times t_r - 0.0004 \times Tr \times Tp - 0.0033 \times Tr \times Pp_i - 0.0021 \times \\
 & Tr \times Pp_f + 0.0043 \times Tr \times tp_i - 0.0031 \times Tr \times tp_f - 0.0077 \times t_r^2 - 0.0027 \times t_r \times Tp - 0.0128 \times t_r \times \\
 & Pp_i + 0.016 \times t_r \times Pp_f + 0.0644 \times t_r \times tp_i + 0.0476 \times t_r \times tp_f + 0.0005 \times Tp^2 - 0.0078 \times Tp \times \\
 & Pp_i - 0.0026 \times Tp \times Pp_f + 0.008 \times Tp \times tp_i - 0.0005 \times Tp \times tp_f - 0.0012 \times Pp_i^2 - 0.0003 \times Pp_i \times \\
 & Pp_f + 0.0128 \times Pp_i \times tp_i + 0.0231 \times Pp_i \times tp_f - 0.0007 \times Pp_f^2 + 0.0079 \times Pp_f \times tp_i - 0.012 \times \\
 & Pp_f \times tp_f - 0.0148 \times tp_i^2 - 0.0231 \times tp_i \times tp_f - 0.0142 \times tp_f^2
 \end{aligned}$$

d

**Figure 4.7.** Statistical models  
 a. Density, b. MOR, c. MOR, d. IB

$$\begin{aligned}
 WA = & 3333.13 - 12.9315 \times Tr - 41.147 \times t_r - 13.7109 \times Tp + 35.988 \times Pp_i - 3.8419 \times Pp_f - \\
 & 131.532 \times tp_i - 56.7682 \times tp_f + 0.0112 \times Tr^2 + 0.0589 \times Tr \times t_r + 0.0334 \times Tr \times Tp - 0.051 \times Tr \times Pp_i - \\
 & 0.0514 \times Tr \times Pp_f + 0.2155 \times Tr \times tp_i + 0.0728 \times Tr \times tp_f + 0.3438 \times t_r^2 + 0.0438 \times t_r \times Tp - \\
 & 0.2452 \times t_r \times Pp_i + 0.1214 \times t_r \times Pp_f + 1.7604 \times t_r \times tp_i + 1.2644 \times t_r \times tp_f + 0.0123 \times Tp^2 - \\
 & 0.1373 \times Tp \times Pp_i + 0.0399 \times Tp \times Pp_f + 0.3202 \times Tp \times tp_i + 0.1183 \times Tp \times tp_f + 0.0609 \times Pp_i^2 + \\
 & 0.1078 \times Pp_i \times Pp_f + 0.0506 \times Pp_i \times tp_i + 0.4014 \times Pp_i \times tp_f + 0.0239 \times Pp_f^2 + 0.3091 \times Pp_f \times \\
 & tp_i + 0.1967 \times Pp_f \times tp_f + 0.2169 \times tp_i^2 - 0.1019 \times tp_i \times tp_f + 0.0566 \times tp_f^2
 \end{aligned}$$

e

$$\begin{aligned}
 TS = & 1287.56 - 8.3043 \times Tr - 10.1272 \times t_r - 3.9867 \times Tp + 72.1975 \times Pp_i + 5.0354 \times Pp_f - \\
 & 150.167 \times tp_i + 17.9532 \times tp_f + 0.0064 \times Tr^2 + 0.0679 \times Tr \times t_r + 0.028 \times Tr \times Tp - 0.0908 \times Tr \times Pp_i - \\
 & 0.0617 \times Tr \times Pp_f + 0.2166 \times Tr \times tp_i - 0.1058 \times Tr \times tp_f + 0.2846 \times t_r^2 - 0.0915 \times t_r \times Tp - \\
 & 0.6447 \times t_r \times Pp_i + 0.203 \times t_r \times Pp_f + 1.842 \times t_r \times tp_i + 1.1023 \times t_r \times tp_f - 0.0024 \times Tp^2 - \\
 & 0.2351 \times Tp \times Pp_i + 0.0168 \times Tp \times Pp_f + 0.4676 \times Tp \times tp_i + 0.0022 \times Tp \times tp_f + 0.0322 \times Pp_i^2 + \\
 & 0.0003 \times Pp_i \times Pp_f - 0.3226 \times Pp_i \times tp_i + 0.1678 \times Pp_i \times tp_f + 0.007 \times Pp_f^2 + 0.346 \times Pp_f \times \\
 & tp_i + 0.1891 \times Pp_f \times tp_f + 0.1637 \times tp_i^2 - 1.8589 \times tp_i \times tp_f - 0.1044 \times tp_f^2
 \end{aligned}$$

f

**Figure 4.7.** Statistical models  
 e. WA, f. TS

## 4.2.2 Chemical Response Variables

The results obtained for the chemical properties are shown in table 4.8. Material composition is expressed on an oven dry basis. Severity factor and composition of the initial material are also included. Variance analysis was performed for each response variable at a confidence level of 95%. Because we were interested in evaluating the pretreatment process and the quality of the material to be used in the board preparation, all the response variables were referred to dry pretreated-material rather than to initial material.

### 4.2.2.1 Ash content

ANOVA table for ash content is shown in table 4.9 and the statistical plots for ash content are shown in figure 4.8. The fitted model gave an R-squared of 0.848 and an SDR of 0.31%. For this variable, only pretreatment temperature was statistically significant. Ash accounts for mineral salts that are undesirable for the manufacture of fiberboards. Table 4.8 shows that the original material has a considerable amount of ash that could negatively influence the conformation of the boards. Ash content is

greatly reduced by pretreatment; this reduction is due to solubilization of the mineral salts contained in the material, during the pretreatment. The minimum values for this response variable are found at intermediate reaction temperatures and long pretreatment times.

#### 4.2.2.2 Lignin, Cellulose and Hemicelluloses

The lignin, cellulose and hemicelluloses were analyzed together because they came from the same hydrolysis assay. ANOVA tables for lignin, cellulose and hemicelluloses are shown in tables 4.10, 4.11, and 4.12, respectively. The statistical plots for lignin, cellulose and hemicelluloses are shown in figures 4.9, 4.10 and 4.11, respectively. Fitted models gave an R-squared of 0.651 and an SDR of 3.59% for cellulose, an R-squared of 0.97 and an SDR of 1.94% for hemicelluloses and an R-squared of 0.44 and an SDR of 1.40% for Lignin. Both pretreatment temperature and time were statistically significant for hemicelluloses content and only pretreatment temperature was statistically significant for cellulose content, but neither of them was significant for lignin content. The response surfaces for the three variables (figures 4.9d, 4.10d and 4.11d) show that the cellulose content increased but the hemicelluloses content decreased as the severity increased. The quantity of lignin slightly diminished as the severity increased. Similar results for cellulose and hemicelluloses behavior have been obtained for other materials (Hsu, W. et al. 1988; Jianying, Ragil et al. 2006; Velásquez, Ferrando et al. 2003). However, the lignin content appears not to be very affected by pretreatment. This is understandable because lignin is much more stable than cellulose and hemicelluloses.

Hemicelluloses have been almost completely eliminated from the material at high pretreatment temperatures and intermediate to long pretreatment times.

Interaction between pretreatment time and temperature is not important for any of the response variables. However, pretreatment temperature has larger impact over all the variables than time.

#### 4.2.2.3 Cellulose to Lignin ratio (C/L)

Even though cellulose and lignin have different tendencies, the C to L ratio increases when the severity increases (see table 4.8). This behavior is explained for the great amount of hemicelluloses hydrolyzed during the pretreatment, which leads to a net increase in the amount of cellulose available for bonding. Lignin, as said before, is pretty stable with the pretreatment, causing in this way the increase in C/L ratio. Increasing the lignin content to reach all the cellulose available could improve the

board properties. Addition of different kinds and quantities of exogenous lignin were studied to explore this possibility, see chapter 7.

**Table 4.8.** Chemical compositions of *Cynara cardunculus* with different pretreatment conditions

Run	Process Factors			Response Variables				
	Tr [°C]	t <sub>r</sub> [min.]	Log (Ro)	Ash [%]	Lignin [%]	Cellulose [%]	Hemicelluloses [%]	C to L Ratio
Original	-	-	-	7.2	12.9	55.8	19.3	4.3
4	200	7.5	3.8	0.5	18.7	59.3	15.1	3.2
5	220	5	4.2	0.4	13.6	65.5	9.4	4.8
9	200	7.5	3.8	0.5	18.7	60.1	15.9	3.2
10	180	10	3.4	1.0	19.9	53.9	23.2	2.7
11	200	7.5	3.8	0.5	17.8	60.8	14.4	3.4
16	180	5	3.1	1.3	17.8	53.8	29.3	3.0
17	200	7.5	3.8	0.5	17.9	63.0	13.2	3.5
20	200	7.5	3.8	0.6	18.2	64.6	17.8	3.5
24	220	10	4.5	0.6	14.9	68.1	0.2	4.6
25	200	7.5	3.8	0.5	17.8	62.4	14.3	3.5
32	200	7.5	3.8	0.6	17.9	62.7	15.0	3.5
34	200	7.5	3.8	0.7	18.3	58.5	16.9	3.2
37	160	7.5	2.6	1.9	16.5	50.5	35.2	3.1
40	200	2.5	3.3	0.9	17.4	58.0	21.8	3.3
42	200	12.5	4.0	0.5	16.7	62.8	13.6	3.8
46	240	7.5	5.0	2.8	16.3	53.2	0.2	3.3

**Table 4.9.** Variance Analysis for Ash

Variation source	Sum of Squares	Degrees of Freedom	Mean Square	F-Ratio	P-Value
A:Tr	3.63E-02	1	3.63E-02	0.38	0.5496
B:t_r	6.75E-02	1	6.75E-02	0.71	0.4181
AA	5.05E+00	1	5.05E+00	53.34	0.0000
AB	6.76E-02	1	6.76E-02	0.71	0.4178
BB	2.75E-02	1	2.75E-02	0.29	0.6014
Total error	9.46E-01	10	9.46E-02		
Total (corr.)	6.23E+00	15			

**Table 4.10.** Variance Analysis for Lignin

Variation source	Sum of Squares	Degrees of Freedom	Mean Square	F-Ratio	P-Value
A:Tr	7.78E+00	1	7.78E+00	3.96	0.0746
B:t_r	3.14E-01	1	3.14E-01	0.16	0.6978
AA	5.89E+00	1	5.89E+00	3.00	0.1140
AB	2.03E-01	1	2.03E-01	0.10	0.7547
BB	2.67E+00	1	2.67E+00	1.36	0.2703
Total error	1.96E+01	10	1.96E+00		
Total (corr.)	3.53E+01	15			

**Table 4.11.** Variance Analysis for Cellulose

Variation source	Sum of Squares	Degrees of Freedom	Mean Square	F-Ratio	P-Value
A:Tr	8.26E+01	1	8.26E+01	6.42	0.0296
B:t_r	1.29E+01	1	1.29E+01	1.00	0.3409
AA	1.41E+02	1	1.41E+02	10.95	0.0079
AB	1.46E+00	1	1.46E+00	0.11	0.7427
BB	8.34E-01	1	8.34E-01	0.06	0.8041
Total error	6.60E+01	10	6.60E+00		
Total (corr.)	7.80E+02	15			

**Table 4.12.** Variance Analysis for Hemicelluloses

Variation source	Sum of Squares	Degrees of Freedom	Mean Square	F-Ratio	P-Value
A:Tr	1.07E+03	1	1.07E+03	282.74	0.0000
B:t_r	8.36E+01	1	8.36E+01	22.18	0.0008
AA	7.98E+00	1	7.98E+00	2.12	0.1765
AB	2.31E+00	1	2.31E+00	0.61	0.4519
BB	7.87E+00	1	7.87E+00	2.09	0.1792
Total error	3.77E+01	10	3.77E+00		
Total (corr.)	1.20E+03	15			



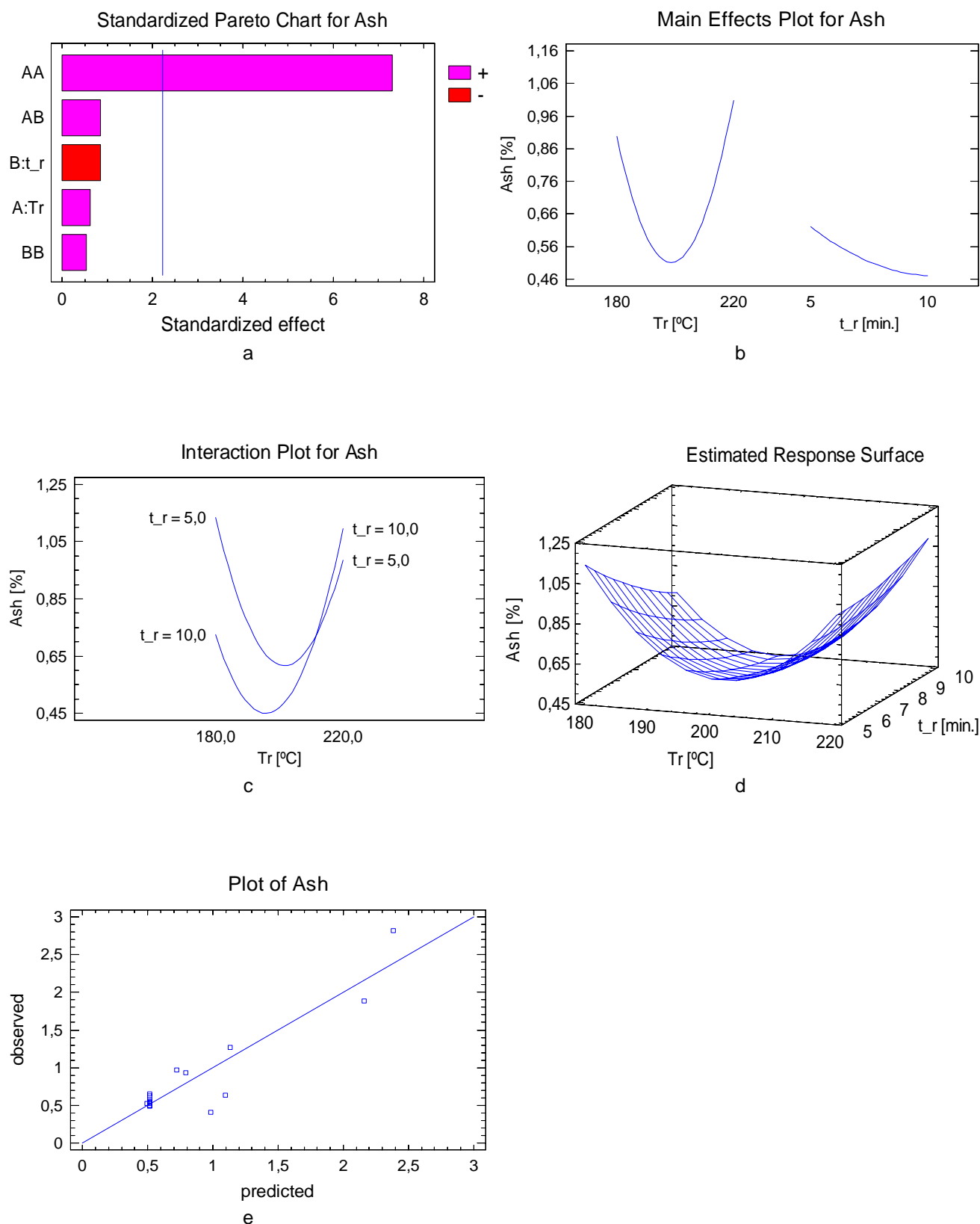


**Figure 4.8.** Statistical Plots for Ash Content Analysis  
 a. Pareto chart, b. Main effects plot, c. Interaction plot, d. Response surface, e. Diagnostic plot

Binderless Fiberboard Production from *Cynara cardunculus* and *Vitis vinifera*

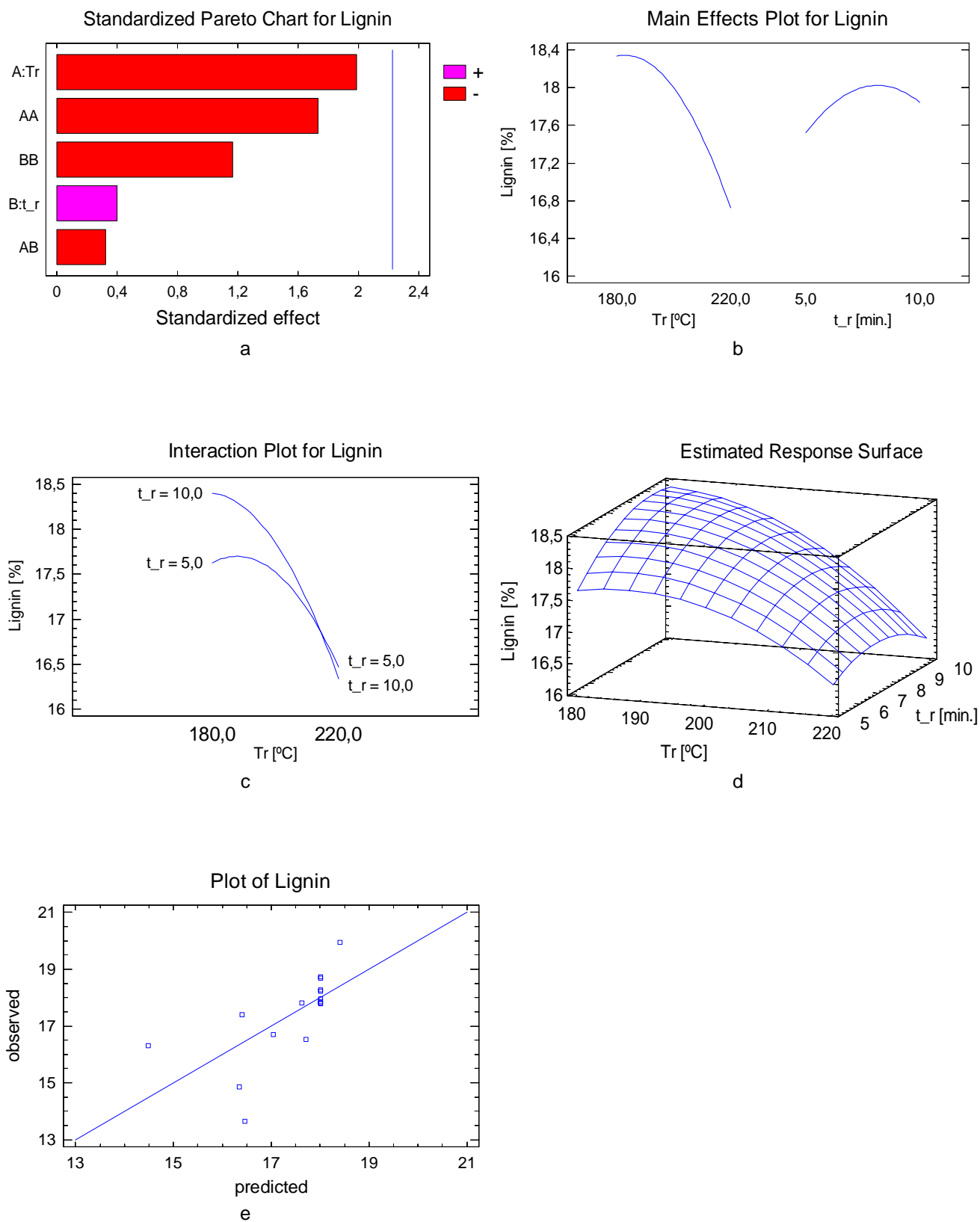


**Figure 4.9.** Statistical Plots for Lignin Analysis  
 a. Pareto chart, b. Main effects plot, c. Interaction plot, d. Response surface, e. Diagnostic plot

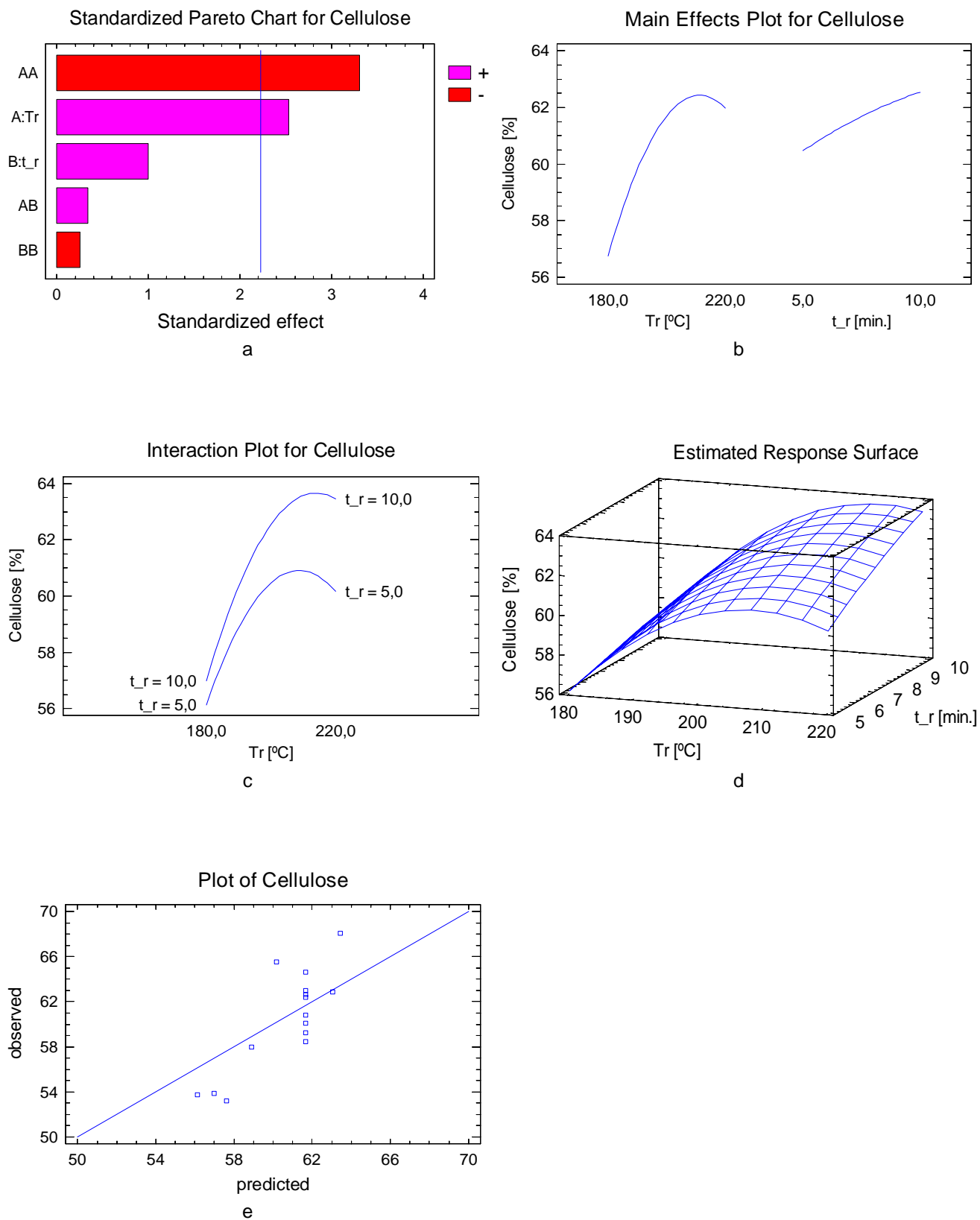


**Figure 4.10.** Statistical Plots for Cellulose Analysis  
 a. Pareto chart, b. Main effects plot, c. Interaction plot, d. Response surface, e. Diagnostic plot

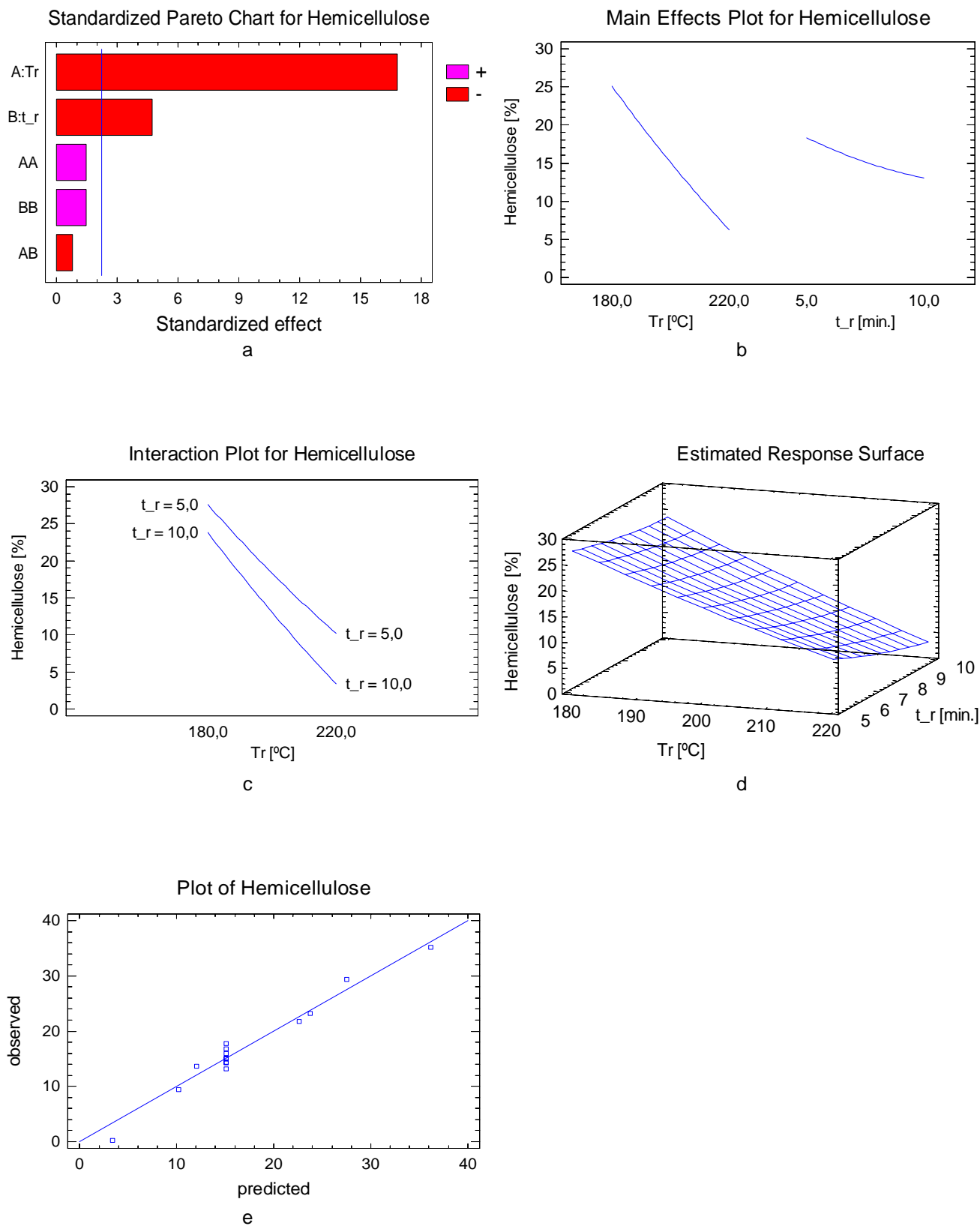


**Figure 4.11.** Statistical Plots for Hemicelluloses Analysis  
 a. Pareto chart, b. Main effects plot, c. Interaction plot, d. Response surface, e. Diagnostic plot

### 4.3 RESPONSE VARIABLES RELATIONSHIP

In this section some relations between response variables are investigated. We should be very careful analyzing these relations because the pressing conditions were changed and this evidently affects in a different way the physical and mechanical properties of boards.

#### 4.3.1 Density relations with mechanical and physical properties

Several authors (Sekino 1999; Suchsland, Woodson et al. 1983; Wilcox 1953) have stated the relationship between density and physicomechanical properties of the fiberboards. In this study, the fiberboards were produced using the same quantity of pretreated material, dry basis, so the variations in density are produced by changes in the pretreatment and pressing conditions rather than intentional changes to study the density impact over the physicomechanical properties of the fiberboards. Because of this, density does not vary a lot among the fiberboards produced, from 1237 to 1362 kg/m<sup>3</sup>, and the relationship between density and the physicomechanical properties can not be established properly from this data.

Figure 4.12 shows the correlation plots between density and physicomechanical properties. The results of fitting a linear model to describe the relationship between the variables and density are the following:

Variables	R-Squared	SDR	P-Value
MOR	0.077	8.6	0.0569
MOE	0.255	901.0	0.0002
IB	0.045	0.3	0.1478
WA	0.267	15.3	0.0002
TS	0.212	10.4	0.0010

P-values for MOE, WA and TS show that there is a statistically significant relationship between these variables and density at a confidence level higher than 95%, for MOR the P-value shows a statistically significant relationship with density at a confidence level of 90%, and for IB the P-value shows that there is not a statistically significant relationship between this variable and density. Although, the P-values suggest the existence of a relationship between density and most of the physicomechanical variables, the R-squared statistics show that these relations are relatively weak.

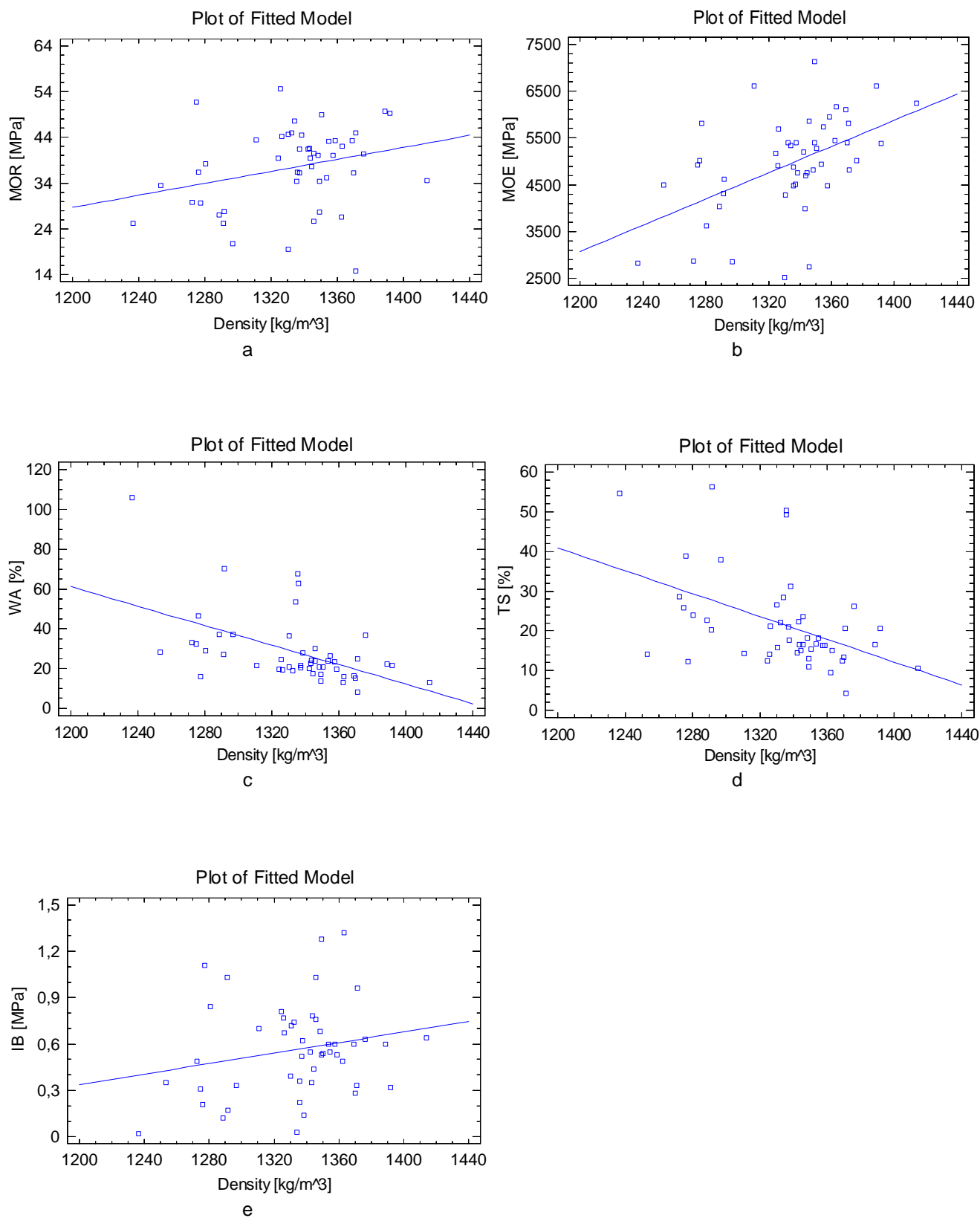


**Figure 4.12.** Correlation Plots between Physico-mechanical properties and Density  
a. MOR, b. MOE, c. WA, d. TS, e. IB

#### 4.3.2 Chemical composition relations with mechanical and physical properties

It is well known that the dimensional stability of the fiberboards is related to partial hemicelluloses hydrolysis because hemicelluloses are very hydrophilic. In figure 4.13a we can see that, as expected, WA decreased as the hemicelluloses content decreased. The same was true for TS (figure 4.13b). Some authors (*Hsu, W. et al. 1988; Jianying, Ragil et al. 2006; Suchsland, Woodson et al. 1987; Velásquez, Ferrando et al. 2003*) have obtained similar results with other materials. The relationship between WA and TS with hemicelluloses is supported by the good R-squared statistics: 0.734 for WA and 0.689 for TS. The SDR were 7.36% for WA and 7.10% for TS.

It has been said also that the mechanical properties of the boards are related to cellulose and lignin content of the material. From figures 4.13c and d we can see that an increment of cellulose content enhances both IB and MOE, thus confirming the structural function of cellulose in the boards. The R-squared statistics obtained were: 0.123 for IB and 0.239 for MOE. The SDR were: 0.194 for IB and 818.83 for MOE. As we can see the relationship between MOE and cellulose is clearer than between IB and cellulose, this is because MOE is more susceptible to the cellulose changes than IB.

The relationships between IB and MOE with lignin are not very clear because the lignin from *Cynara cardunculus* seems to be very stable with the pretreatment used. In addition to this fact, the changing pressing conditions also affect negatively every analysis that we could do regarding the interaction between lignin and any other variable. The relations between lignin and the physicomechanical properties will be analyzed in more detail in the section of addition of exogenous lignin, chapter 7.

Binderless Fiberboard Production from *Cynara cardunculus* and *Vitis vinifera*

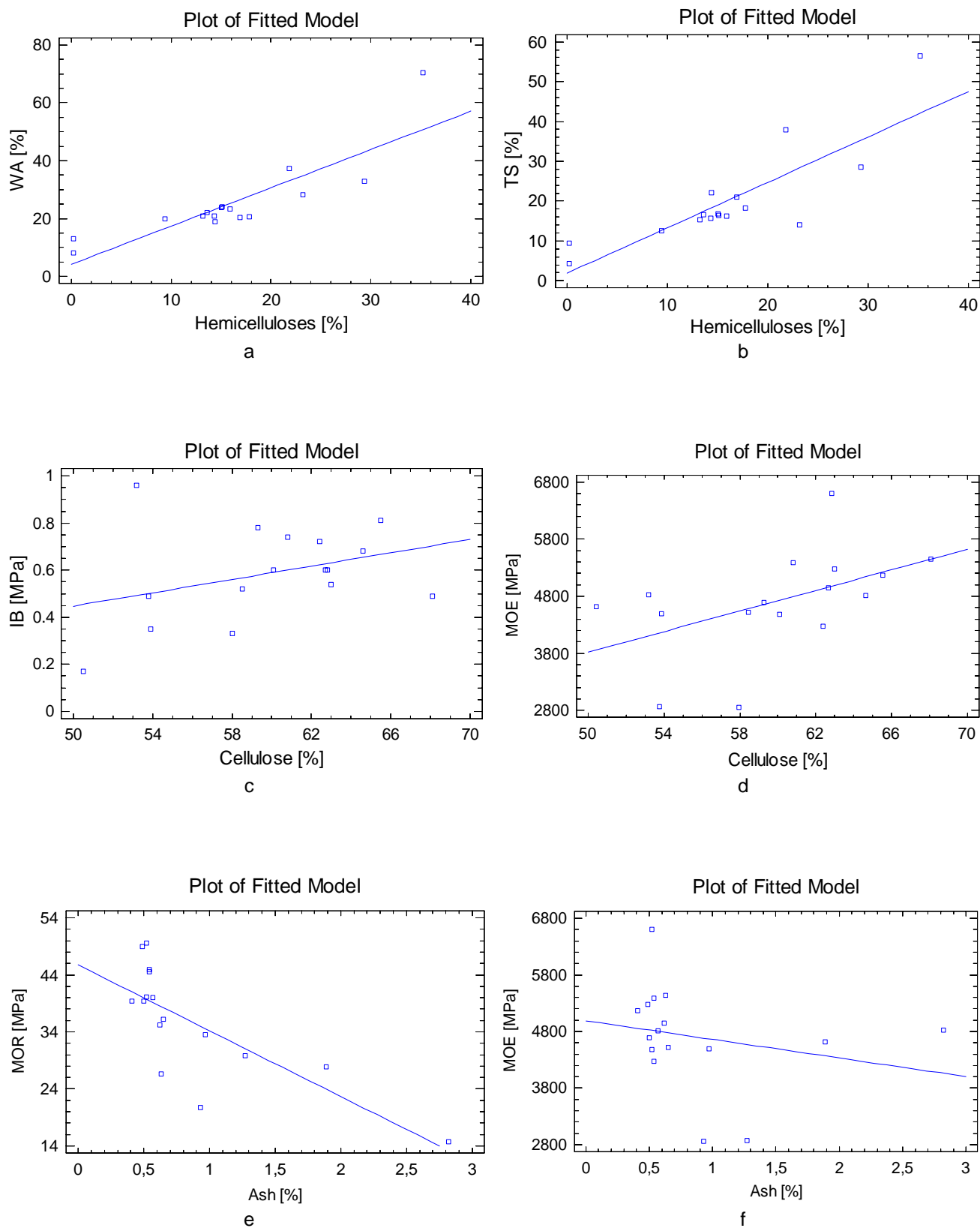


**Figure 4.13.** Relationships between chemical composition and physicochemical properties  
 a., b. WA, TS vs Hemicelluloses, c., d. IB, MOE vs Cellulose, e., f. MOR, MOE vs Ash



#### 4.4 MULTIPLE RESPONSE OPTIMIZATION

Multiple response optimization determines the combination of levels for the experimental factors that simultaneously optimize several response variables. The procedure consists of building a desirability function based on the fitted models of each factor to be optimized. Figure 4.14 shows the statistical plots for multiple response optimization. The optimum value of desirability was 0.995 over 1 for the following factor levels:

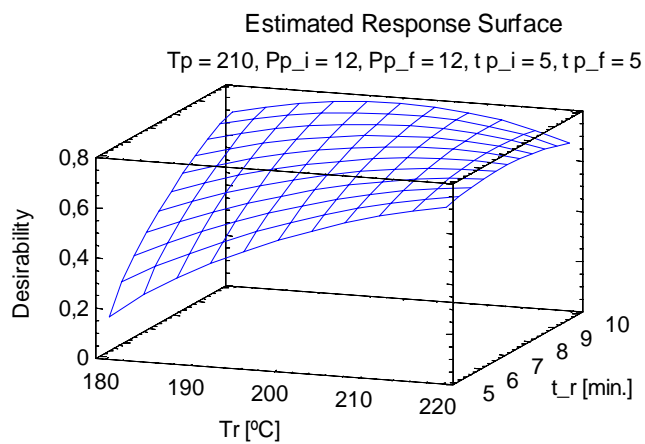
Tr	t_r	Tp	Pp_i	Pp_f	tp_i	tp_f
[°C]	[min.]	[°C]	[MPa]	[MPa]	[min.]	[min.]
218	5.4	220	7.2	19	2.5	2.8

Figure 4.14a shows that mid-high pretreatment temperatures and short times are the best choice for simultaneously preserving the fiber structure and encouraging hemicelluloses hydrolysis and lignin release.

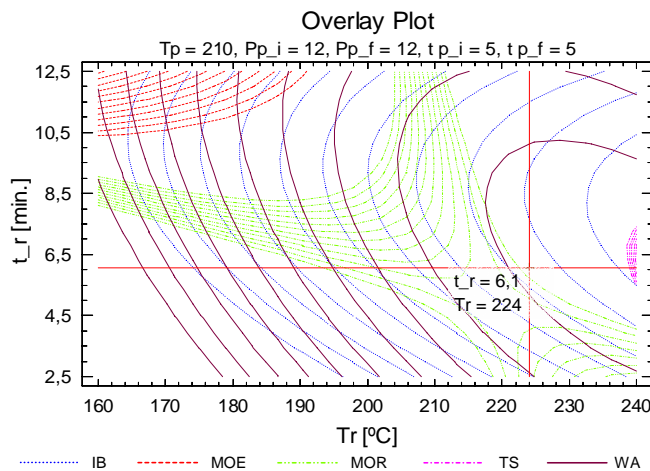
A set of fiberboards were prepared using the combination of factors provided by the multiple response optimization. These fiberboards fully satisfy the European standards. The mean values for the board properties were:

Density	MOR	MOE	IB	WA	TS
[kg/m <sup>3</sup> ]	[MPa]	[MPa]	[MPa]	[%]	[%]
1320	52	5970	0.8	18.5	13.5

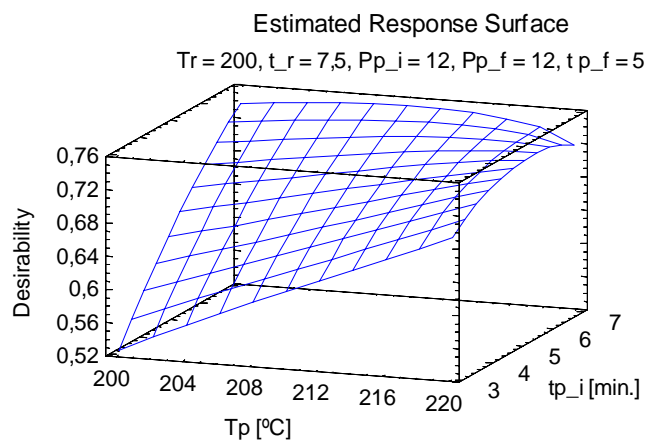
The multiple response optimization model studied suggests that the best physicomechanical properties for the boards are found at high pretreatment temperatures and low pretreatment times. The model also suggests using high pressing temperatures in combination with short pressing times and low pressing pressures in the first stage but high pressures in the third pressing stage. This suggests that in the third pressing stage, the internal defects generated in the relaxation stage are corrected and that, in the first stage, the humidity is vaporized and the lignin is redistributed over the fibers where the chemical bonds are developed.



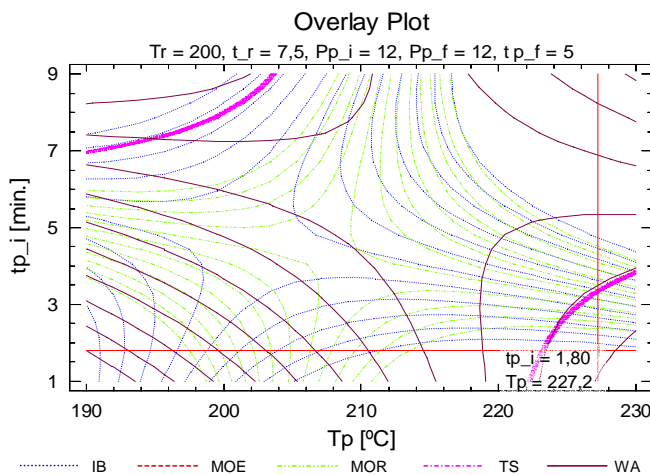
a



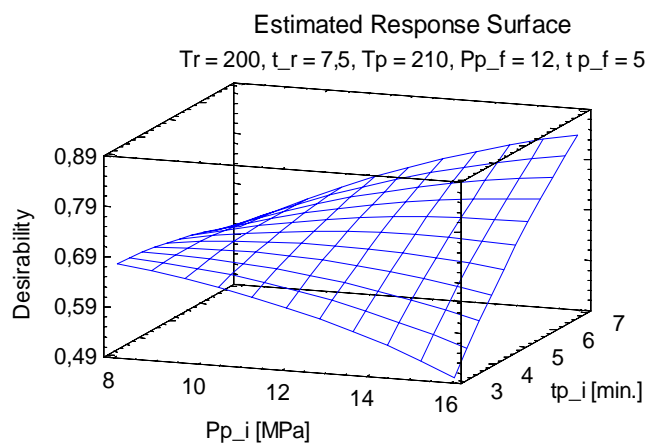
b



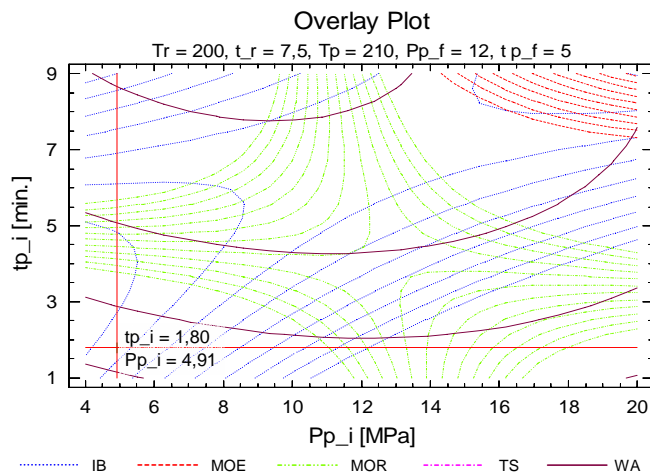
c



d



e



f

**Figure 4.14.** Statistical Plots for Multiple Response Optimization  
 a., c., e. Estimated response surfaces, b., d., f. Overlay plots

## 4.5 CONCLUSIONS

It was possible to produce binderless fiberboards from *Cynara cardunculus* that meet the European standards for fiberboards of internal use, thus giving an aggregated value to this energetic crop and contributing to its full exploitation. *Cynara cardunculus* is not the best material to produce binderless fiberboards compared with other materials studied previously such as *Miscanthus sinensis* (Velásquez, Ferrando et al. 2003) and residual softwood (Angles, Ferrando et al. 2001; Anglès, Reguant et al. 1999), this is probably due to its lower lignin content and its higher ash content (see table 1), but still it can be used to obtain fiberboards of good quality without adhesives of fossil origin.

Both, steam explosion pretreatment and hot pressing, had great influence on the final physicommechanical properties of the fiberboards obtained. First pressing stage has shown to be statistically significant for almost all the mechanical properties analyzed (Density, MOE and IB), but the last stage of the pressing was not statistically significant, in the range studied. It can be concluded that the values of the analyzed parameters in the last stage of pressing can be adjusted to lower pressing times and lower pressing pressures than the studied according to the convenience of an industrial application.

Increasing the severity of the pretreatment improves the physical properties (WA and TS) of the boards. Similarly, hemicelluloses and ash contents of the pretreated fibers clearly decrease as the severity increases, which lead to lower hygroscopicity and to avoid the presence of abrasive materials that is undesirable for the fabrication of fiberboards. Pretreated *Cynara* generally has higher cellulose and lignin contents than original material due to diminishing of the hemicelluloses content.

The multiple response optimization model has been useful for finding the best levels of the process factors for producing the best fiberboards, particularly for the difference found between the optimization trends for physical and mechanical properties.

## REFERENCES

- Angles, M. N., F. Ferrando, *et al.* Suitability of steam exploded residual softwood for the production of binderless panels. Effect of the pre-treatment severity and lignin addition. *Biomass and Bioenergy* 21(3): 211-224. 2001.
- Anglès, M. N., J. Reguant, *et al.* Binderless Composites from Pretreated Residual Softwood. *Journal of Applied Polymer Science* 73: 2485-2491. 1999.
- Antunes, A., E. Amaral, *et al.* *Cynara cardunculus* L.: chemical composition and soda-anthraquinone cooking. *Industrial Crops and Products* 12(2): 85-91. 2000.
- Benjelloun-Mlayah, B., S. de Lopez, *et al.* Oil and paper pulp from *Cynara cardunculus*: preliminary results. *Industrial Crops and Products* 6: 233-236. 1997.
- Curt, M. D., G. Sanchez, *et al.* The potential of *Cynara cardunculus* L. for seed oil production in a perennial cultivation system. *Biomass & Bioenergy* 23(1): 33-46. 2002.
- Gominho, J., J. Fernandez, *et al.* *Cynara cardunculus* L. - a new fibre crop for pulp and paper production. *Industrial Crops and Products* 13(1): 1-10. 2001.
- Hsu, W. E., S. W., *et al.* Chemical and physical changes required for producing dimensionally stable wood-based composites. Part1: Steam pretreatment. *Wood Science and Technology* 22. 1988.
- Jiaying, X., W. Ragil, *et al.* Development of binderless fiberboard from kenaf core. *Journal of Wood Science* 52(3): 236-243. 2006.
- Overend, R. P. and E. Chornet. Fractionation of lignocellulosics by steam-aqueous pretreatments. *Phil. Trans. R. Soc. Lond. A* 321: 523-536. 1987.
- Sekino, N., Inoue M., Irle M., Adcock T. The Mechanisms Behind the Improved Dimensional Stability of Particleboards Made from Steam-Pretreated Particles. *Holzforschung* 53: 435-440. 1999.

Suchsland, O., G. E. Woodson, *et al.* Effect of hardboard process variables on fiberbonding. *Forest Products Journal* 33(4): 58-64. 1983.

Suchsland, O., G. E. Woodson, *et al.* Effect on cooking conditions on fiber bonding in dry-formed binderless hardboard. *Forest Products Journal* 37: 65-69. 1987.

Velásquez, J. A., F. Ferrando, *et al.* Binderless fiberboard from steam exploded *Miscanthus sinensis*. *wood science and technology* 37: 269-278. 2003.

Venendaal, R., U. Jorgensen, *et al.* European Energy Crops: A Synthesis. *Biomass & Bioenergy* 13(3): 147 - 185. 1997.

Wilcox, h. Interrelationships of Temperature, Pressure, and Pressing Time in the Production of Hardboard from Douglas-Fir Fiber. *Tappi Journal* 36(2): 89-94. 1953.

UNIVERSITAT ROVIRA I VIRGILI  
BINDERLESS FIBERBOARD PRODUCTION FROM CYNARA CARDUNCULUS AND VITIS VINIFERA  
Camilo Mancera Arias  
ISBN:978-84-692-1537-1/DL:T-300-2009

## **5. BINDERLESS FIBERBOARDS FROM VITIS VINIFERA**

UNIVERSITAT ROVIRA I VIRGILI  
BINDERLESS FIBERBOARD PRODUCTION FROM CYNARA CARDUNCULUS AND VITIS VINIFERA  
Camilo Mancera Arias  
ISBN:978-84-692-1537-1/DL:T-300-2009



## CHAPTER 5

### Binderless fiberboard production from *Vitis vinifera* prunings

In this chapter the results obtained from the production of fiberboards from *Vitis vinifera* without additives are presented. I also described how the *Vitis vinifera* prunings undergo the main processes and how their main controllable factors affect the final properties of the fiberboards produced.

#### 5.1 INTRODUCTION

Among the chemical-energetic renewable resources, biomass derivatives are distinguishable, and amid them, lignocellulosic residues acquire a particular significance due to its constitution and availability. Lignocellulosic residues offer interesting potential applications as raw material in general, in addition to its possible uses with energetic purposes. Forestal residues coming from pruning and cleaning operations of arboreal species together with woody agricultural residues are important resources in determined zones of Spain.

Potential uses of lignocellulosic materials coming from agricultural residues to replace wood as raw materials for panel products have had considerable attention (Hague, McLauchlin et al. 1998; Roffael 1997; Seber and Lloyd 1996).

Vine (*Vitis vinifera*) is one of the lignocellulosic agricultural-residues which could replace wood in the production of fiberboards. It is a perennial, woody climbing plant that, when left to grow freely can reach more than 30 m long, but in cultivation usually reduced by annual pruning to 1 to 3 m bush. Vine is a traditional crop in Spain; it covers large areas of land and is cultivated for wine and fruit production. Large quantities of lignocellulosic prunings remain in the fields every year after the pruning season. The average pruning yield per hectare is about 5 tons and currently in Spain there are about 1,200,000 hectares of grape crops harvested. After pruning, part of the prunings is used as fuel but large quantities remain unused in the fields, thus increasing the plague and fire risks.

Moreover, the growing global population demanding for various wood products and especially wood panels leads to a continuous effort to find new wood resources as an

alternative to forest wood. Over each of the next four to five decades, global population is expected to increase by approximately 900 million and the global consumption per-capita of wood is approximately 0.67 m<sup>3</sup>/year (Schultz 1993; Youngquist and Hamilton 1999). This means that growth in wood demand worldwide is closely following growth in world population. Particularly, there has been an increase in worldwide fiberboard-production from 20,215,627 m<sup>3</sup> produced in 1990 to 61,861,241 m<sup>3</sup> produced in 2005 (FAOSTAT 2008).

This study pretends to assess the suitability of *Vitis vinifera* as raw material for the production of binderless fiberboards based on a manufacturing process comprised by a steam-explosion pretreatment of the vine prunings and a hot pressing of the material pretreated without using any kind of synthetic adhesive. All the process was conceived to be friendlier with the environment and to produce a completely biodegradable panel.

### Using *Vitis vinifera* as raw material

Vine shoots have been investigated to produce pulp for paper making. The authors (Jiménez, Angulo et al. 2006) characterized four different vine varieties grown employing two different methods and did not find any significant difference in their compositions irrespective of their variety or growing method. The holocellulose contents were similar to those in pine, but lower than those in other non-wood raw materials such as wheat straw and sun flower stalks. However, lignin content was similar to those of eucalyptus and non-woody raw materials. The different pulping processes studied – soda, Kraft, ethanol and ethylene-glycol – showed low yields (29-47%) compared to other materials. Kraft pulp showed the best properties, including higher  $\alpha$ -cellulose content than pulp from wheat straw, but higher lignin content. Finally, the authors found that the properties of the paper obtained with Kraft pulp from vine shoots were at the intermediate values of the paper properties obtained from wheat straw and sunflower, but they believe that those values could be substantially improved by refining the pulp properly.

Other authors (Ntalos and Grigoriou 2002) have investigated the suitability of vine prunings as a raw material for particleboards production using a commercial urea-formaldehyde resin as binder. Vine pruning particles appeared to be shorter and wider than industrial wood particles and their length to thickness ratio was found to be lower than industrial wood particles in this study. Authors managed to substitute industrial wood particles by vine pruning particles up to 50% in the core of experimental 3-layer boards without substantially affecting the board properties, but they found that vine pruning particles should not be used as surface material because it deteriorates all board properties, except for internal bond.

## 5.2 RESULTS AND DISCUSSIONS

The experimental factors and their levels were chosen based on the literature review and previous experiences on production of binderless boards inside the investigation group, they are:

- A: Vapor pretreatment temperature ( $T_r$ ): 190 – 210 °C.
- B: Vapor pretreatment time ( $t_r$ ): 5 – 10 min.
- C: Pressing temperature ( $T_p$ ): 190 – 210 °C.
- D: Initial press pressure ( $P_p$ ): 8 – 16 MPa.
- F: Initial press time ( $t_p$ ): 3 – 7 min.

Pressure and time for the third pressing step were kept in the central levels of their corresponding factors in the first step, 12 MPa and 5 min., respectively.

### 5.2.1 Physical and mechanical response variables

In this section, I will discuss the physical and mechanical properties. Each of the response variables will be analyzed separately using the tools of the experimental design and afterwards the interactions between the experimental factors will be analyzed, if there is any.

The results obtained are shown in table 5.1. There is an extra factor included in this table, the severity factor (*Overend and Chornet 1987*) ( $\log(R_o)$ ) which group the vapor pretreatment temperature and time in a single variable giving a weight for the severity of the global pretreatment. For each response variable a variance analysis was performed at a confidence level of 95%.

Table 5.1. Physicomechanical properties

Run	Process Factors						Response Variables					
	Tr [°C]	t_r [min.]	Log (Ro)	Tp [°C]	Pp [MPa]	t_p [min.]	Density [kg/m <sup>3</sup> ]	MOE [MPa]	MOR [MPa]	IB [Mpa]	WA [%]	TS [%]
1	190	10	3.65	210	16	3	1336	3439	19	0.1	22.2	19.0
2	200	7.5	3.82	200	12	5	1346	3670	25	0.2	20.2	15.6
3	200	2.8	3.40	200	12	5	1337	3410	22	0.3	34.7	18.2
4	210	5	3.94	210	16	3	1288	3843	24	0.2	19.4	11.6
5	200	7.5	3.82	200	12	5	1329	3615	24	0.3	20.8	16.5
6	200	7.5	3.82	200	12	8.7	1360	3654	20	0.2	16.2	14.4
7	210	10	4.24	190	16	7	1353	4334	25	0.2	16.1	14.9
8	181.4	7.5	3.27	200	12	5	1342	2468	15	0.2	37.8	28.9
9	200	7.5	3.82	200	12	5	1325	3426	27	0.3	20.2	13.4
10	200	7.5	3.82	218.6	12	5	1259	3283	22	0.2	19.1	8.6
11	210	5	3.94	210	16	7	1290	3778	23	0.2	20.2	10.1
12	200	7.5	3.82	181.4	12	5	1334	3508	24	0.2	29.8	22.2
13	200	7.5	3.82	200	12	5	1349	3733	23	0.3	19.2	15.0
14	200	7.5	3.82	200	12	5	1355	3402	23	0.3	18.4	13.1
15	190	10	3.65	190	16	7	1363	3176	19	0.2	27.6	18.9
16	200	7.5	3.82	200	12	5	1355	3987	24	0.3	19.8	15.0
17	200	7.5	3.82	200	12	5	1320	3897	25	0.3	18.5	16.6
18	210	10	4.24	210	8	3	1333	3443	24	0.1	15.1	11.4
19	210	5	3.94	190	8	7	1336	4487	26	0.3	24.9	8.5
20	200	7.5	3.82	200	4.6	5	1302	3152	24	0.2	25.4	17.5
21	190	5	3.35	190	16	3	1300	2771	15	0.2	47.6	29.2
22	218.6	7.5	4.37	200	12	5	1359	4607	28	0.2	12.2	8.0
23	190	5	3.35	190	8	3	1311	2859	17	0.2	48.1	28.3
24	190	10	3.65	210	8	7	1317	3430	20	0.2	20.0	10.2
25	200	12.2	4.03	200	12	5	1353	3040	20	0.1	18.9	10.9
26	200	7.5	3.82	200	12	1.3	1315	3665	23	0.2	25.1	21.7
27	190	5	3.35	210	8	7	1291	2614	15	0.2	24.1	14.6
28	200	7.5	3.82	200	19.4	5	1347	3852	27	0.2	17.5	16.4
29	210	10	4.24	190	8	3	1321	3245	27	0.1	20.4	16.5
30	200	7.5	3.82	200	12	5	1320	3643	24	0.3	19.7	16.0

### 5.2.1.1 Density

ANOVA table for density is shown in table 5.2 and the statistical plots for density are shown in figure 5.1. The model as fitted presents an R-square of 0.884 and a standard deviation of the residuals (SDR) of 15.6 kg/m<sup>3</sup>. Only two factors (pressing temperature and initial pressing pressure) were found to be statistically significant at a confidence level of 95%. The modeled response surface (figure 5.1d) shows that increasing the severity of the pretreatment, either by increasing the temperature or increasing the time, increases the density due to a reduction in the compression resistance of the *V. vinifera* and the presence of more fine material. The same results have been obtained with other materials (Hsu, W. et al. 1988; Sekino 1999; Velásquez, Ferrando et al. 2003).

From the response surfaces shown in figures 5.1f and 5.1h, it can be seen that low pressing temperatures or high initial press pressures and long pressing times favor an increase in density. To allow a good distribution of lignin between the fibers during the pressing process, it is necessary to apply enough heat and pressure to melt the lignin through the whole board.

Interaction plot (figure 5.1c), Pareto chart (figure 5.1a) and the ANOVA table (table 5.2) show that the relevant interaction is only BC; this interaction shows that at high pressing temperatures (C) the increase of the pretreatment time (B) favors largely a density increase, but at low pressing temperatures the influence of the pretreatment time is in the other direction and less relevant. Interactions between factors which are not statistically significant were not analyzed.

There is a very good correlation between the observed values and the values predicted by the model as shown in figure 5.1e. The equation of the fitted model is shown in figure 5.7a.

The following table shows the combination of the factors levels which maximizes density into the studied region:

Tr	t_r	Tp	Pp	t_p
[°C]	[min.]	[°C]	[MPa]	[min.]
181.4	2.9	181.5	18	8.2

Shadow values correspond to no statistically significant factors; this means that those factors can be set with the most convenient values without affecting considerably the maximum value of density.

Previous studies (Suchsland, Woodson et al. 1983) have shown that, the higher the density better the mechanical properties will be. It seems that there is a correlation between the density and some of the properties that will be subsequently analyzed. If that correlation exists, the important factors, the shapes of the response surfaces, the interactions, etc. should be similar.

Table 5.2 ANOVA table for Density

Source	Sum of Squares	Degrees of Freedom	Mean Square	F-Ratio	P_Value
A:Tr	3.65E+01	1	3.65E+01	0.15	0.7081
B:t_r	3.54E+02	1	3.54E+02	1.45	0.2595
C:Tp	2.47E+03	1	2.47E+03	10.11	0.0112
D:Pp	1.65E+03	1	1.65E+03	6.76	0.0287
E:t_p	7.36E+02	1	7.36E+02	3.01	0.1167
AA	1.31E+02	1	1.31E+02	0.54	0.4819
AB	4.06E+00	1	4.06E+00	0.02	0.9002
AC	3.65E+01	1	3.65E+01	0.15	0.7082
AD	1.23E+02	1	1.23E+02	0.5	0.4957
AE	1.12E+03	1	1.12E+03	4.57	0.0613
BB	1.35E+01	1	1.35E+01	0.06	0.8195
BC	1.74E+03	1	1.74E+03	7.12	0.0257
BD	1.16E+02	1	1.16E+02	0.47	0.5083
BE	2.69E+02	1	2.69E+02	1.1	0.3211
CC	4.22E+03	1	4.22E+03	17.29	0.0025
CD	1.12E+01	1	1.12E+01	0.05	0.8354
CE	2.24E+02	1	2.24E+02	0.92	0.3629
DD	6.43E+02	1	6.43E+02	2.63	0.1392
DE	2.15E+02	1	2.15E+02	0.88	0.3723
EE	4.83E+01	1	4.83E+01	0.2	0.6672
Total error	2.20E+03	9	2.44E+02		
Total (corr.)	1.89E+04	29			

Standardized Pareto Chart for Density

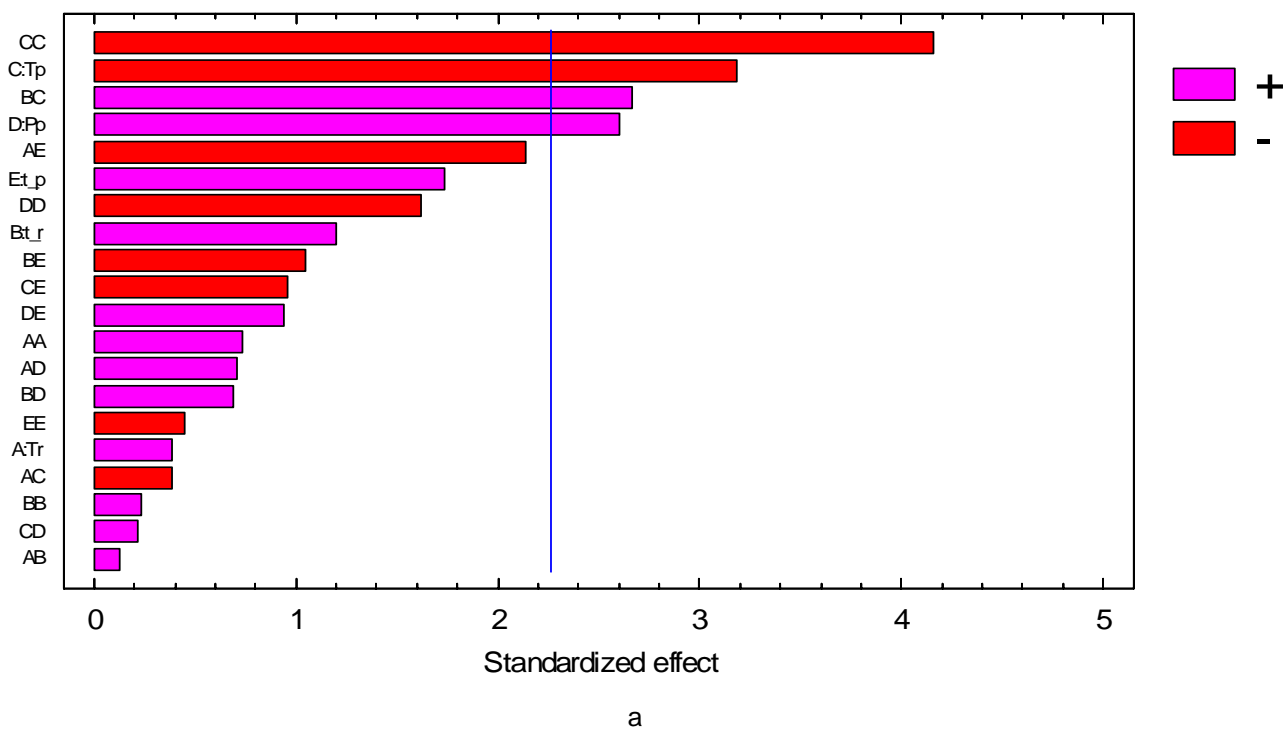
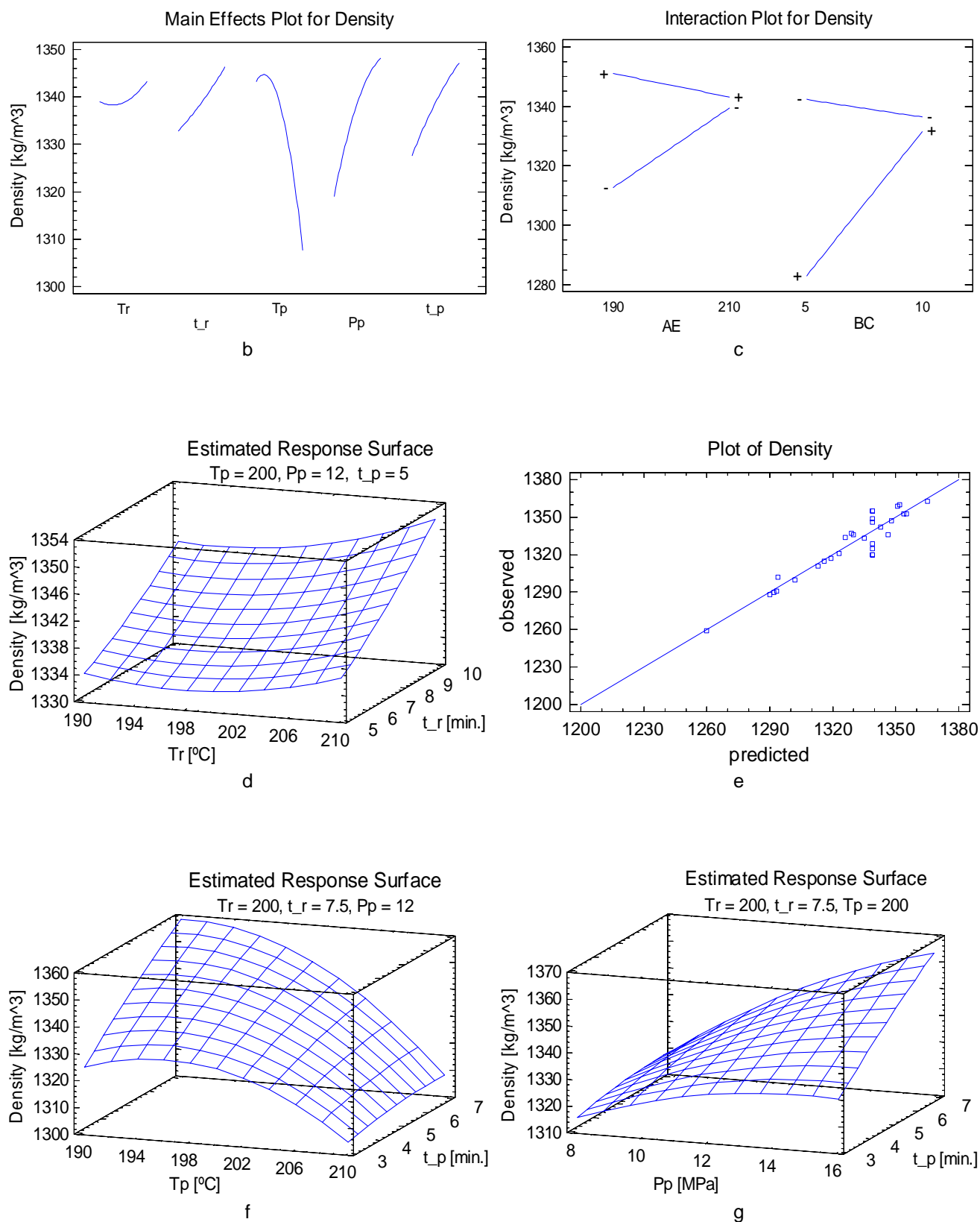


Figure 5.1. Statistical Plots for Density Analysis  
 a. Pareto chart.



**Figure 5.1.** Statistical Plots for Density Analysis (continuation)  
 b. Main effects plot, c. Interaction plot, d, f, g. Estimated responses surfaces, e. Diagnostic plot



### 5.2.1.2 Mechanical properties (MOR, MOE, IB)

The modulus of rupture (MOR) and modulus of elasticity (MOE) were analyzed together because they came from the same bending assay. ANOVA tables for MOR and MOE are shown in tables 5.3 and 5.4, respectively. The statistical plots for MOR and MOE are shown in figures 5.2 and 5.3, respectively. The fitted model for MOR gave an R-squared of 0.966 and an SDR of 1.2 MPa. The fitted model for MOE gave an R-squared of 0.956 and an SDR of 186 MPa. Only one factor (pretreatment temperature) was statistically significant for MOR, while for MOE two factors were statistically significant (pretreatment temperature and initial pressing pressure). The modeled surface in figure 5.2d shows that the best MOR values are obtained at high pretreatment temperatures and short pretreatment times. The same is true for MOE. These results also agree with density behavior. It seems that *Vitis vinifera* prunings need vapor pretreatments at high severities, based on high temperatures and short times, to segregate the fibers and release the lignin over the fibers. This combination of levels of the pretreatment factors, high temperature and short time, are complementary; thus, allowing to preserve the fibrillar structure and to achieve the chemical and physical modifications that enhance the adhesive behavior of the lignin. This is confirmed by the behavior of pretreatment time, which has a bigger influence at high pretreatment temperatures than at low pretreatment temperatures (see figure 5.2d).

The modeled surface in figure 5.2f shows low pressing temperatures and mid to short pressing times enhance MOR, the same is true for MOE (see figure 5.3f). This behavior is similar to density behavior except for the long pressing times that enhance density but seem to deteriorate MOR and MOE.

Figures 4.2g and 4.3g show that initial press pressure influence MOR and MOE in the same way, and very similar to the density behavior.

Interaction plots (figures 5.2c and 5.3c), Pareto charts (figure 5.2a and 5.3a) and ANOVA tables (tables 5.3 and 5.4) for MOR and MOE show that the relevant interactions common to both variables are: AB, and AC. The first interaction can be anticipated because the interacting factors are those that control the pretreatment process. However, AC interaction shows that at low pressing temperatures (C), an increase of pretreatment temperature (A) favors largely both MOR and MOE; but that at high pressing temperatures the effect is smaller in magnitude though in the same direction. DE interaction was statistically significant for MOR but not for MOE; while for MOE, BC interaction was statistically significant but not for MOR. DE interaction can be expected because the interaction factors are those that control the initial pressing step

and its interaction was explained above. However, BC interaction shows that short pretreatment times are preferred if low pressing temperatures are going to be used, but long pretreatment times will do better if high pressing temperatures are going to be used.

There is a very good correlation between the observed values and the values predicted by the models as is shown in figures 5.2e and 5.3e. The equations of the fitted models are shown in figures 5.7b and 5.7c.

The following table shows the combination of factor levels which maximizes MOR and MOE into the studied region:

	Tr	t <sub>r</sub>	Tp	Pp	t <sub>p</sub>
	[°C]	[min.]	[°C]	[MPa]	[min.]
MOR	218.6	5.4	181.4	19.2	2.3
MOE	218.6	2.8	181.4	19.4	5.9

We can see that high severity pretreatments are preferred for developing the mechanical properties of the fiberboards, but this high severity should be based on high temperatures rather than on long times. There are clear differences between the materials treated at the same severity but at different temperatures. High pretreatment temperatures develop materials with higher fines content but short pretreatment times are necessary to preserve fiber structure while segregation is produced.

With regard to pressing process, we can see that short pressing times are preferred; this is profitable from the economical point of view. The short pressing times predicted for the model as optimums for both factors were due to the high predicted values for pressing pressures. Pressing temperature and pressure affect the progressive temperature rise at the midthickness of the fiberboard, and consequently the fiberboard properties finally obtained. Elevated pressing temperature and pressures decrease drying time, but a practical limit is set by the danger of blowouts and the resultant decrease in fiber strength caused by superheated vapor inside the boards. The selection of proper pressing conditions is evident to produce fiberboards of good quality and uniform properties.

Table 5.3. ANOVA Table for MOR

Source	Sum of Squares	Degrees of Freedom	Mean Square	F-Ratio	P_Value
A:Tr	9.94E+01	1	9.94E+01	69.3	0
B:t_r	2.84E+00	1	2.84E+00	1.98	0.1926
C:Tp	2.84E+00	1	2.84E+00	1.98	0.1927
D:Pp	4.32E+00	1	4.32E+00	3.01	0.1166
E:t_p	4.32E+00	1	4.32E+00	3.01	0.1166
AA	2.04E+01	1	2.04E+01	14.23	0.0044
AB	9.17E+00	1	9.17E+00	6.4	0.0323
AC	2.00E+01	1	2.00E+01	13.91	0.0047
AD	2.19E-02	1	2.19E-02	0.02	0.9045
AE	7.27E+00	1	7.27E+00	5.07	0.0509
BB	2.73E+01	1	2.73E+01	19.05	0.0018
BC	6.40E+00	1	6.40E+00	4.46	0.0638
BD	1.15E-02	1	1.15E-02	0.01	0.9306
BE	2.67E-01	1	2.67E-01	0.19	0.6763
CC	5.73E+00	1	5.73E+00	4	0.0767
CD	4.21E-02	1	4.21E-02	0.03	0.8678
CE	3.47E-03	1	3.47E-03	0	0.9618
DD	1.31E+00	1	1.31E+00	0.92	0.3636
DE	1.32E+01	1	1.32E+01	9.22	0.0141
EE	2.04E+01	1	2.04E+01	14.24	0.0044
Total error	1.29E+01	9	1.43E+00		
Total (corr.)	3.81E+02	29			

Standardized Pareto Chart for MOR

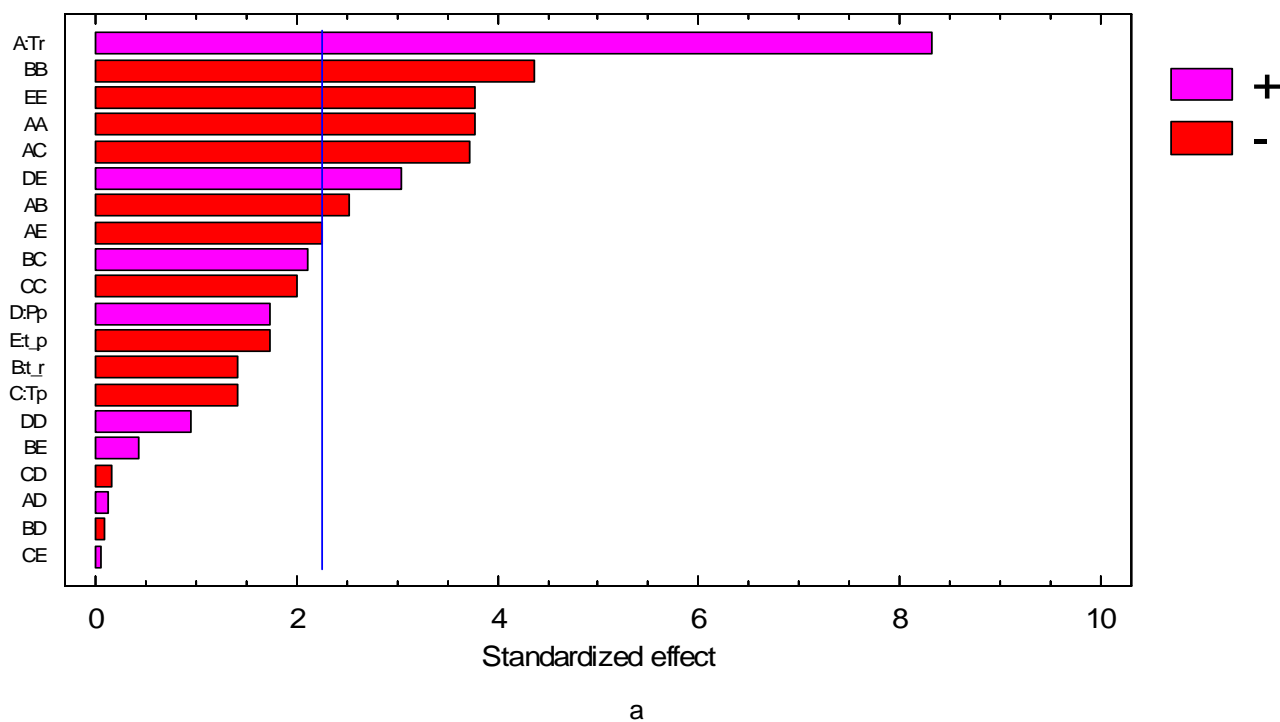
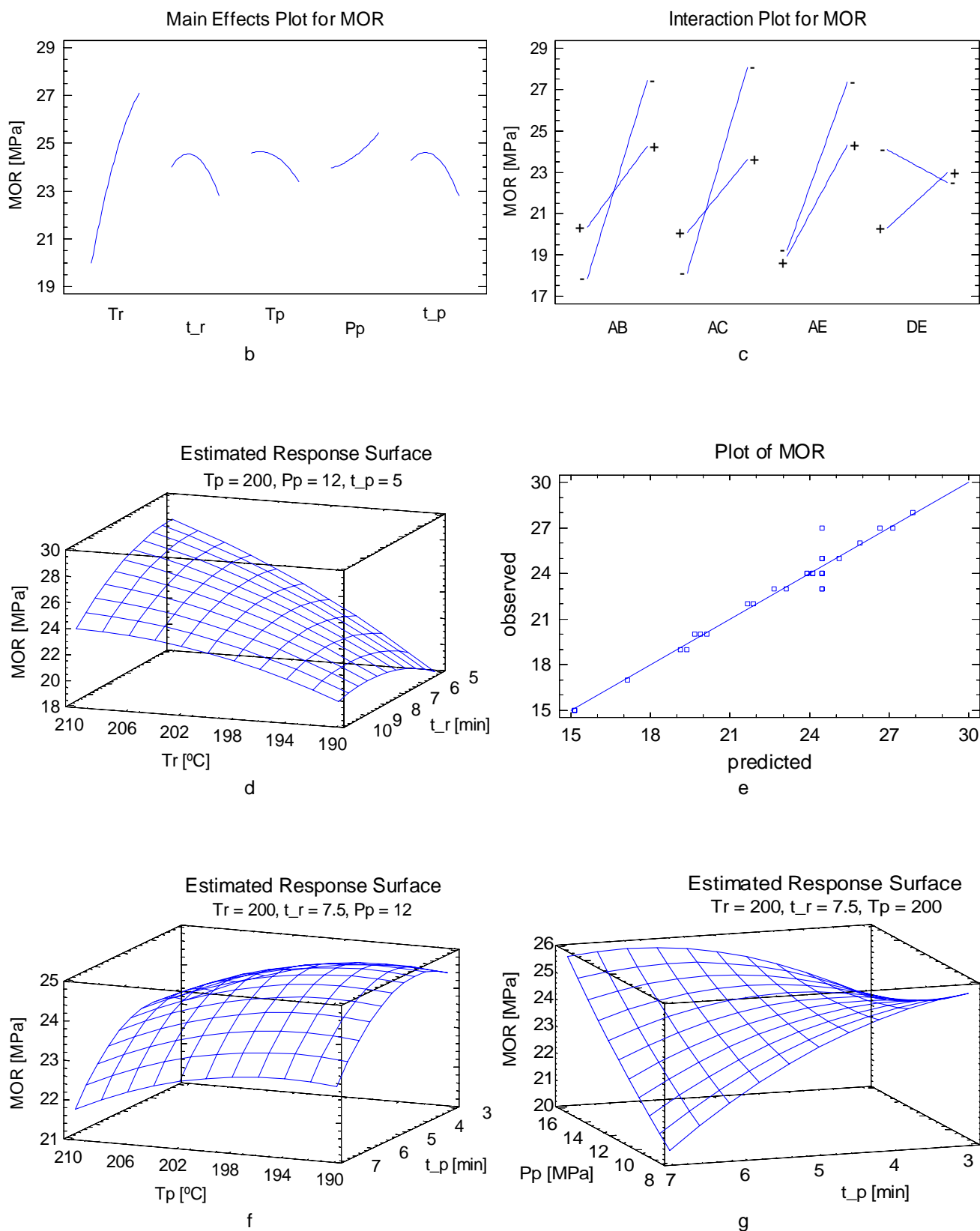


Figure 5.2. Statistical Plots for MOR Analysis  
 a. Pareto chart.



**Figure 5.2.** Statistical Plots for MOR Analysis (continuation)  
 b. Main effects plot, c. Interaction plot, d, f, g. Estimated responses surfaces, e. Diagnostic plot

Table 5.4. ANOVA Table for MOE

Source	Sum of Squares	Degrees of Freedom	Mean Square	F-Ratio	P_Value
A:Tr	2.57E+06	1	2.57E+06	74.32	0
B:t_r	7.41E+04	1	7.41E+04	2.14	0.1776
C:Tp	2.66E+04	1	2.66E+04	0.77	0.4039
D:Pp	2.85E+05	1	2.85E+05	8.22	0.0186
E:t_p	2.17E+02	1	2.17E+02	0.01	0.9386
AA	1.40E+04	1	1.40E+04	0.4	0.5405
AB	2.97E+05	1	2.97E+05	8.58	0.0168
AC	2.59E+05	1	2.59E+05	7.49	0.0229
AD	3.08E+04	1	3.08E+04	0.89	0.3705
AE	1.60E+04	1	1.60E+04	0.46	0.5132
BB	3.15E+05	1	3.15E+05	9.09	0.0146
BC	3.47E+05	1	3.47E+05	10.03	0.0114
BD	7.88E+04	1	7.88E+04	2.28	0.1657
BE	2.35E+04	1	2.35E+04	0.68	0.4312
CC	1.02E+05	1	1.02E+05	2.95	0.1202
CD	5.01E+04	1	5.01E+04	1.45	0.2596
CE	9.03E+01	1	9.03E+01	0	0.9604
DD	2.84E+04	1	2.84E+04	0.82	0.3885
DE	5.53E+04	1	5.53E+04	1.6	0.238
EE	2.96E+03	1	2.96E+03	0.09	0.7765
Total error	3.12E+05	9	3.46E+04		
Total (Corr.)	7.15E+06	29			

Standardized Pareto Chart for MOE

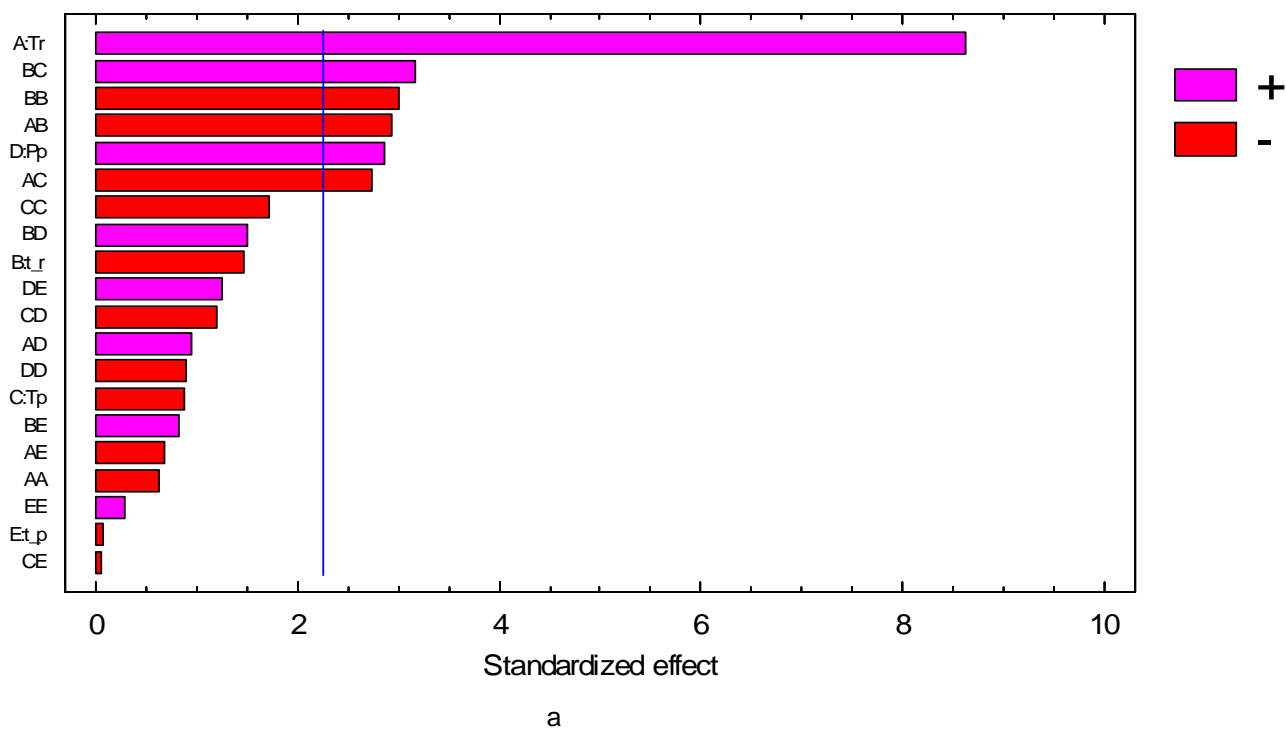
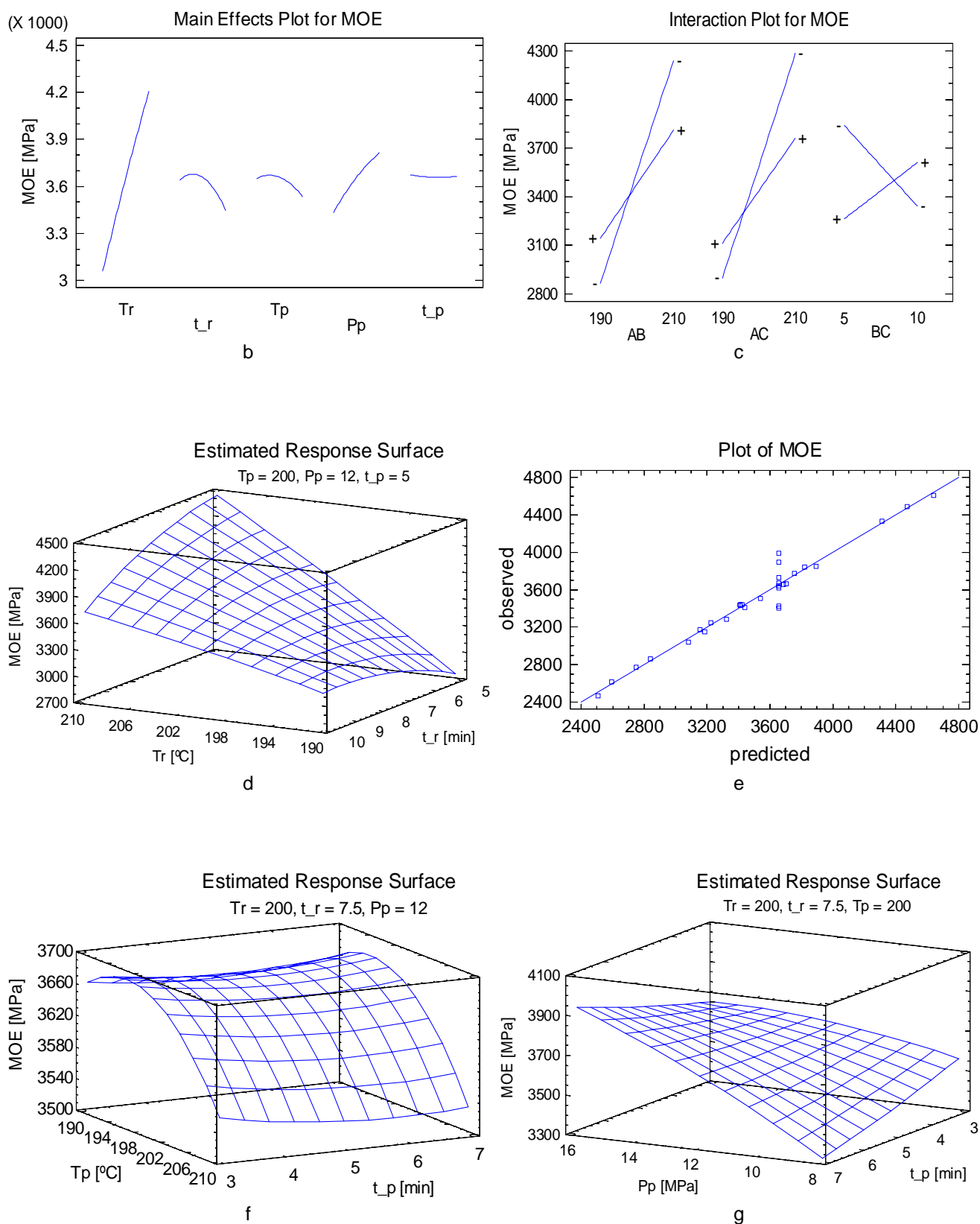


Figure 5.3. Statistical Plots for MOE Analysis  
 a. Pareto chart



**Figure 5.3.** Statistical Plots for MOE Analysis (continuation)  
 b. Main effects plot, c. Interaction plot, d, f, g. Estimated responses surfaces, e. Diagnostic plot

Internal Bond (IB) is the mechanical property that accounts for the strength of the bonds between the fibers; because the fibers are mainly oriented in the board plane the IB measures the tension perpendicular to the faces of the board. ANOVA table for IB is shown in table 5.5 and the statistical plots for IB are shown in figure 5.4. The fitted model gave an R-squared of 0.936 and an SDR of 0.02 MPa. Only one factor (pretreatment time) was statistically significant. The modeled surface on figure 5.4d shows that the best IB values were obtained at high pretreatment temperatures and short pretreatment times. This can be explained by the rising quantity of particles that appeared when the pretreatment temperature increased (Suchsland, Woodson *et al.* 1987), which increased the area available for bonding. Also, high pretreatment temperatures promote a higher extraction of hemicelluloses and extractives and partially depolymerize the lignin, which helps the bonding action.

The modeled surface in figure 5.4f shows that high pressing temperatures are preferred. This behavior is common to other non woody materials (Anglès, Reguant *et al.* 1999), but is in discordance with the behavior of the other mechanical properties (MOR and MOE).

The modeled surface in figure 5.4g shows that low pressing pressures and intermediate pressing times are preferred. As we have seen before, a suitable combination of process factors is the key to obtaining the desired properties. For the IB, due to the upward trend of the pretreatment and pressing temperatures, the pressing pressure should be low to avoid spoiling the fibers and enable the proper distribution of lignin between them.

Interaction plot (figure 5.4c), Pareto chart (figure 5.4a) and ANOVA table (Table 5.5) show that there are not statistically significant interactions at a confidence level of 95%. The interaction between the pretreatment temperature (A) and pretreatment time (B) is expected and is significant at a confidence level of 90%. A combination of high pretreatment temperatures and short pretreatment times are preferred to increase IB, as shown in figure 5.4c. Long pretreatment times affect considerably the IB. Furthermore, the effect of pretreatment temperature over IB is substantially reduced at long pretreatment times. *Vitis vinifera* prunings were submerged in water overnight before steam pretreatment to facilitate fibers segregation, lignin release and hemicelluloses hydrolysis. The water absorbed by vine-prunings becomes steam during the steam pretreatment, causing a more intense pretreatment even at short pretreatment times.

There is a very good correlation between the observed values and the values predicted by the models as shown in figure 5.4e. The equation of the fitted model is shown in figure 5.7d.

The following table shows the combination of the factor levels which maximizes IB into the studied region:

	<b>Tr</b>	<b>t_r</b>	<b>Tp</b>	<b>Pp</b>	<b>t_p</b>
	<b>[°C]</b>	<b>[min.]</b>	<b>[°C]</b>	<b>[MPa]</b>	<b>[min.]</b>
IB	218.4	2.8	218	4.6	3.9

High severity pretreatments based on high temperatures and short times, favor the internal bond; this behavior is in accordance to the behaviors of the other mechanical properties (MOR and MOE). With regard to the pressing process, the optimum press temperature is the highest studied and the optimum press pressure is the lowest. Clearly, the optimum values for maximizing the IB are in a different direction to those for maximizing the MOE and MOR. Based on these observations it is advisable to optimize all variables at the same time and to study other possibilities for increasing the mechanical properties, such as the addition of exogenous lignin for improving the bonding capability of the material or finding the optimum sieve size in the milling process for separating the fibers instead of cutting them.



Table 5.5. ANOVA Table for IB

Source	Sum of Squares	Degrees of Freedom	Mean Square	F-Ratio	P_Value
A:Tr	5.87E-04	1	5.87E-04	1.03	0.336
B:t_r	1.15E-02	1	1.15E-02	20.18	0.002
C:Tp	4.39E-04	1	4.39E-04	0.77	0.402
D:Pp	2.19E-03	1	2.19E-03	3.86	0.081
E:t_p	8.41E-05	1	8.41E-05	0.15	0.709
AA	1.94E-03	1	1.94E-03	3.42	0.098
AB	1.99E-03	1	1.99E-03	3.51	0.094
AC	2.73E-04	1	2.73E-04	0.48	0.506
AD	1.70E-06	1	1.70E-06	0	0.958
AE	6.41E-04	1	6.41E-04	1.13	0.316
BB	6.32E-03	1	6.32E-03	11.12	0.009
BC	4.84E-04	1	4.84E-04	0.85	0.380
BD	5.85E-04	1	5.85E-04	1.03	0.337
BE	1.43E-03	1	1.43E-03	2.52	0.147
CC	3.39E-03	1	3.39E-03	5.97	0.037
CD	6.96E-04	1	6.96E-04	1.23	0.297
CE	3.49E-05	1	3.49E-05	0.06	0.810
DD	6.32E-03	1	6.32E-03	11.12	0.009
DE	7.51E-09	1	7.51E-09	0	0.997
EE	1.32E-02	1	1.32E-02	23.24	0.001
Total error	5.11E-03	9	5.68E-04		
Total (corr.)	7.97E-02	29			

Standardized Pareto Chart for IB

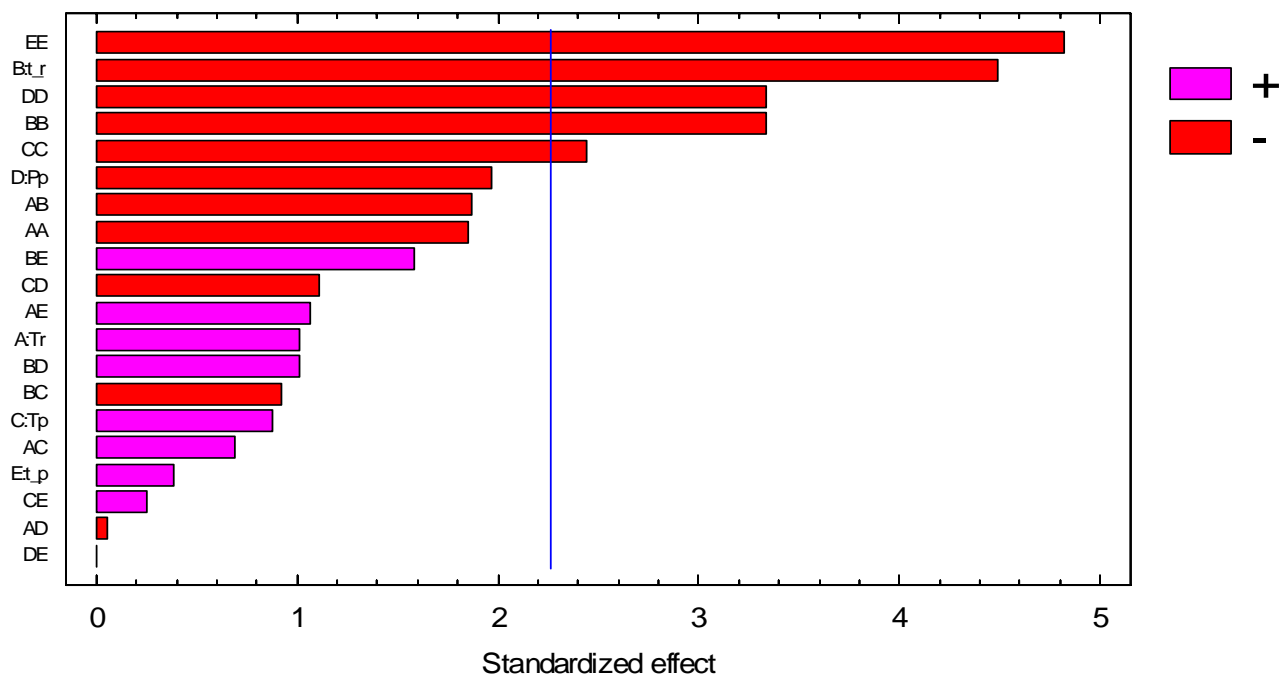
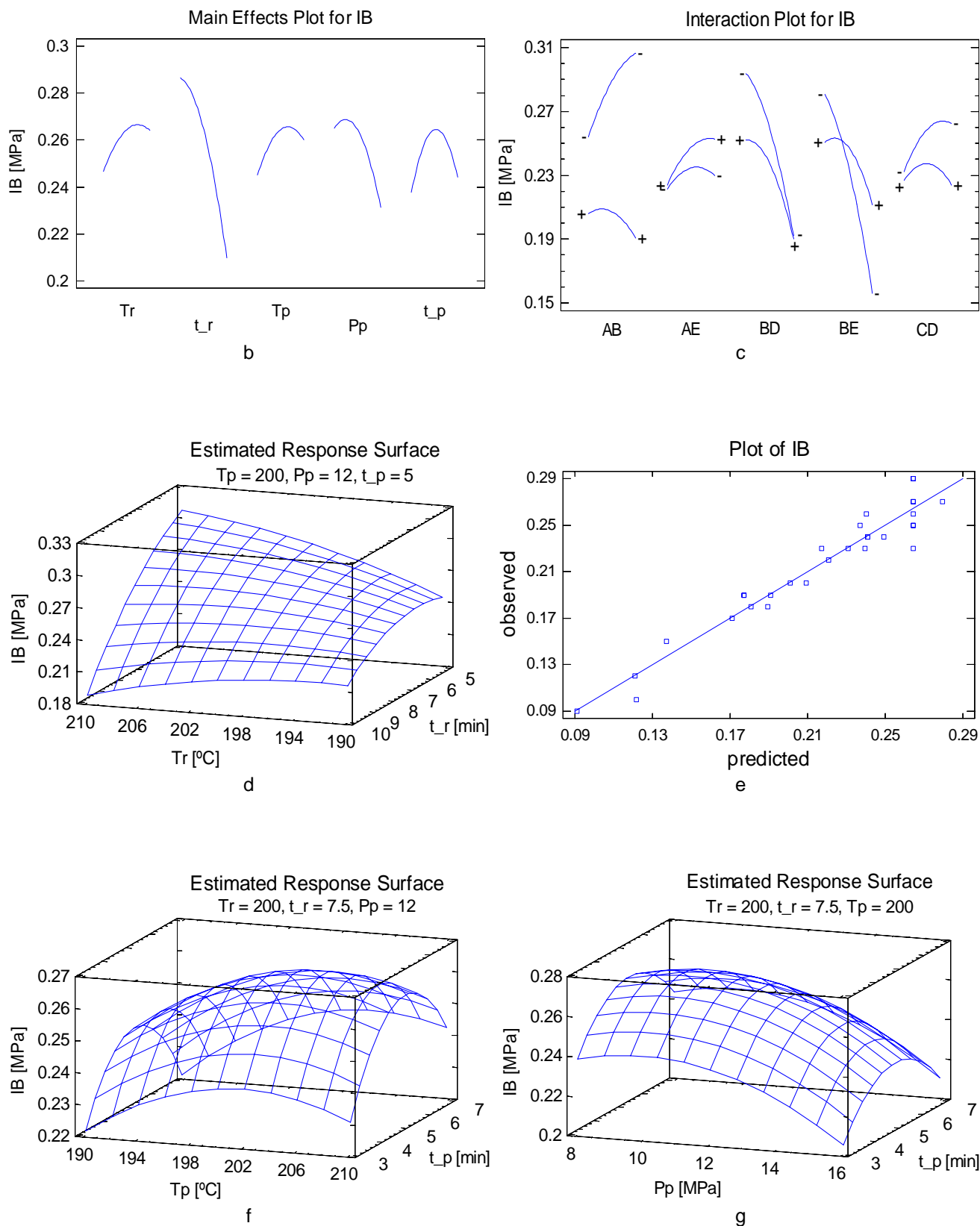


Figure 5.4. Statistical Plots for IB Analysis  
 a. Pareto chart.



**Figure 5.4.** Statistical Plots for IB Analysis (continuation)  
 b. Main effects plot, c. Interaction plot, d, f, g. Estimated responses surfaces, e. Diagnostic plot

### 5.2.1.3 Physical properties (WA, TS)

Water absorption (WA) and Thickness swelling (TS) are the physical properties related with the dimensional stability of the boards. These properties give us an idea of how the boards will behave when used under conditions of severe humidity, they are especially important to boards for external use. WA and TS were analyzed together because came from the same assay. ANOVA tables for WA and TS are shown in tables 5.6 and 5.7, respectively. The statistical plots for WA and TS are shown in figures 5.5 and 5.6, respectively. The fitted models gave R's-squared of 0.997 for WA and 0.971 for TS and SDRs of 0.84% and 1.73%, respectively. All the five factors (pretreatment temperature, pretreatment time, pressing temperature, initial pressing pressure and initial pressing time) were significant for WA; while for TS four factors were statistically significant (pretreatment temperature, pretreatment time, pressing temperature, and initial pressing time). The modeled surface (figure 5.5d) shows that the lower values of WA were obtained at high pretreatment temperatures and intermediate-to-long pretreatment times. The same was true for TS (see figure 5.6d). This is because high-severity pretreatments enhance the hydrolysis of the hemicelluloses, which are largely responsible for board instability (Jianying, Ragil et al. 2006).

The general trend for the pressing process (figures 5.5f, g and 5.6f, g) is to get lower WA and TS at high pressing temperatures, high pressing pressures and long pressing times, possibly to overcome the heat and mass transfer limitations in the pressing process.

Interaction plots (figures 5.5C and 5.6c), Pareto charts (figures 5.5a and 5.6a) and ANOVA tables (tables 5.6 and 5.7) for WA and TS show that the relevant interactions common to both properties are: AE and BD. Figures 5.5c and 5.6c show that, in the first interaction, at short pressing times (E), the pretreatment temperature (A) has a stronger effect over the WA and TS than at long ones; which makes necessary to use high pretreatment temperatures to achieve low WA and TS values when short pretreatment times are employed. However, the best values of TS appear when long pressing times and high pretreatment temperatures are used, because hemicelluloses hydrolysis is favored in both pretreatment and pressing process with this combination of factors. The other interaction BD is regarding to the pretreatment time and the initial pressing pressure. The interaction plots show that at high pressing pressures (D) the pretreatment time (B) has a bigger influence over WA and TS than at low pressing pressures and in accordance with the AE interaction, the lower values of WA and TS are obtained at long pretreatment times and high press pressures, combination of

factors that favors hemicelluloses hydrolysis in both pretreatment process and pressing process.

Other interactions CE for TS and AC, AD, BE and DE for WA are less relevant or simply support the above mentioned.

There is a very good correlation between the observed values and the values predicted for the models as is shown in figures 5.5e and 5.6e. The equations of the fitted models are shown in figures 5.7e and 5.7f.

The following table shows the combination of factor levels which approach WA and TS to zero into the studied region:

	Tr [°C]	t_r [min.]	Tp [°C]	Pp [MPa]	t_p [min.]
WA	210.7	12	200.7	18	3.6
TS	215.8	6.2	214.3	8.7	5.4

High severity pretreatments improved both WA and TS as well as MOR and MOE, but the optimum values for the mechanical and physical properties differ slightly: Very high pretreatment temperatures improved MOR and MOE with mid to short pretreatment times whereas mid to high pretreatment temperatures combined with mid to long pretreatment times improved WA and TS. Another significant difference between the optimums for the mechanical and physical properties was found in the pressing temperature: Very low pressing temperatures favored MOR and MOE whereas mid to high pressing temperatures favored WA and TS. These different tendencies suggest that there must be an agreement between the operational factors that result in the production of boards of good quality.

Table 5.6. ANOVA table for WA

Source	Sum of Squares	Degrees of Freedom	Mean Square	F-Ratio	P_Value
A:Tr	3.54E+02	1	3.54E+02	498.26	0.000
B:t_r	1.53E+02	1	1.53E+02	215.19	0.000
C:Tp	7.25E+01	1	7.25E+01	102.06	0.000
D:Pp	4.10E+01	1	4.10E+01	57.78	0.000
E:t_p	3.91E+01	1	3.91E+01	55.04	0.000
AA	5.86E+01	1	5.86E+01	82.47	0.000
AB	1.80E-01	1	1.80E-01	0.25	0.627
AC	6.27E+00	1	6.27E+00	8.82	0.016
AD	8.58E+00	1	8.58E+00	12.09	0.007
AE	4.78E+01	1	4.78E+01	67.35	0.000
BB	1.04E+02	1	1.04E+02	147.02	0.000
BC	2.97E+00	1	2.97E+00	4.18	0.071
BD	9.32E+00	1	9.32E+00	13.12	0.006
BE	1.45E+01	1	1.45E+01	20.39	0.002
CC	4.70E+01	1	4.70E+01	66.13	0.000
CD	5.21E-03	1	5.21E-03	0.01	0.934
CE	4.90E-03	1	4.90E-03	0.01	0.936
DD	6.94E+00	1	6.94E+00	9.77	0.012
DE	3.94E+00	1	3.94E+00	5.54	0.043
EE	2.19E+00	1	2.19E+00	3.08	0.113
Total error	6.39E+00	9	7.10E-01		
Total (corr.)	2.15E+03	29			

Standardized Pareto Chart for WA

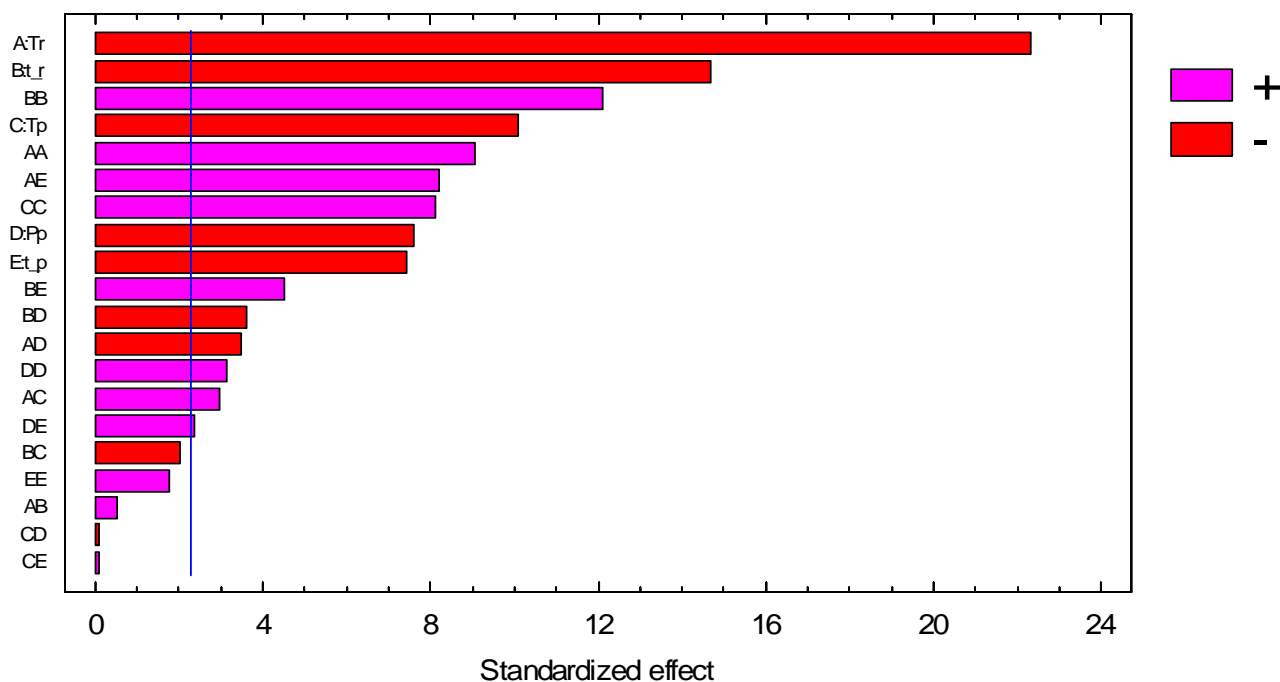
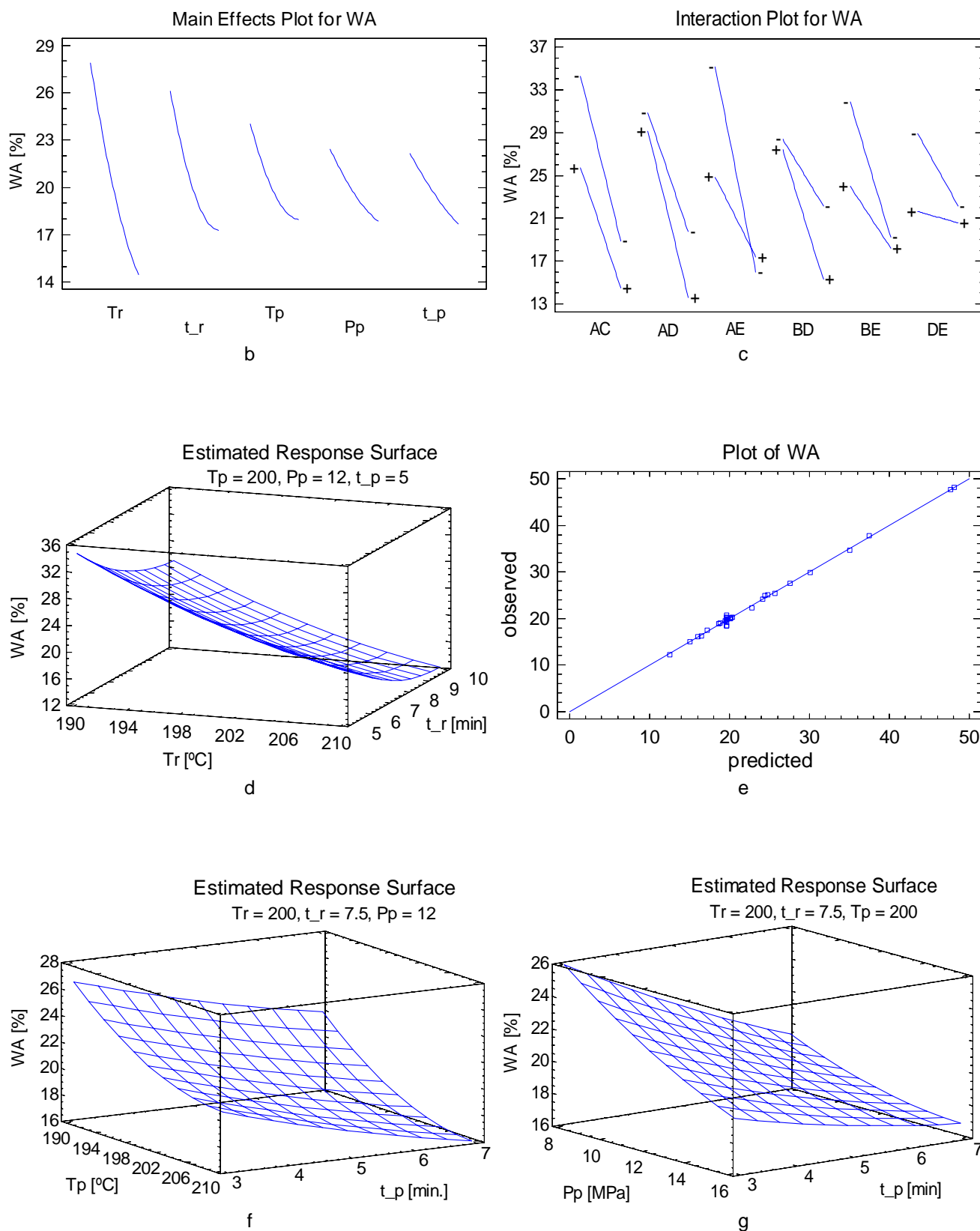


Figure 5.5. Statistical Plots for WA Analysis  
 a. Pareto chart.



**Figure 5.5.** Statistical Plots for WA Analysis (continuation)  
 b. Main effects plot, c. Interaction plot, d, f, g. Estimated responses surfaces, e. Diagnostic plot

Table 5.7. ANOVA table for TS

Source	Sum of Squares	Degrees of Freedom	Mean Square	F-Ratio	P_Value
A:Tr	2.87E+02	1	2.87E+02	95.3	0
B:t_r	1.87E+01	1	1.87E+01	6.22	0.0342
C:Tp	8.20E+01	1	8.20E+01	27.25	0.0005
D:Pp	1.38E-01	1	1.38E-01	0.05	0.8354
E:t_p	4.47E+01	1	4.47E+01	14.87	0.0039
AA	1.27E+01	1	1.27E+01	4.22	0.0702
AB	7.90E+00	1	7.90E+00	2.63	0.1396
AC	1.97E-01	1	1.97E-01	0.07	0.804
AD	1.89E+00	1	1.89E+00	0.63	0.4483
AE	1.16E+01	1	1.16E+01	3.86	0.0811
BB	3.96E+00	1	3.96E+00	1.32	0.281
BC	3.76E+00	1	3.76E+00	1.25	0.2924
BD	2.12E+01	1	2.12E+01	7.03	0.0264
BE	1.18E+00	1	1.18E+00	0.39	0.5474
CC	5.10E-01	1	5.10E-01	0.17	0.6903
CD	4.24E-04	1	4.24E-04	0	0.9908
CE	1.42E+01	1	1.42E+01	4.73	0.0577
DD	1.99E+00	1	1.99E+00	0.66	0.4376
DE	6.82E+00	1	6.82E+00	2.27	0.1664
EE	9.10E+00	1	9.10E+00	3.02	0.1161
Total error	2.71E+01	9	3.01E+00		
Total (corr.)	9.24E+02	29			

Standardized Pareto Chart for TS

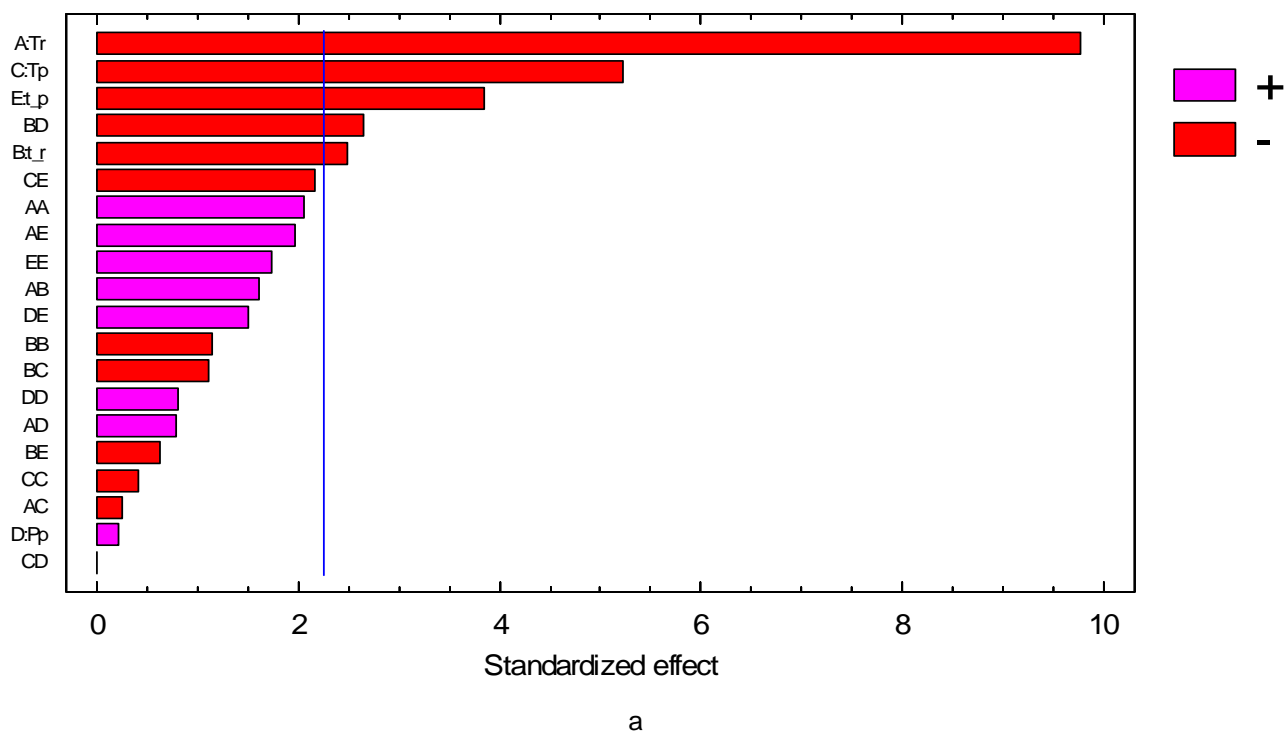
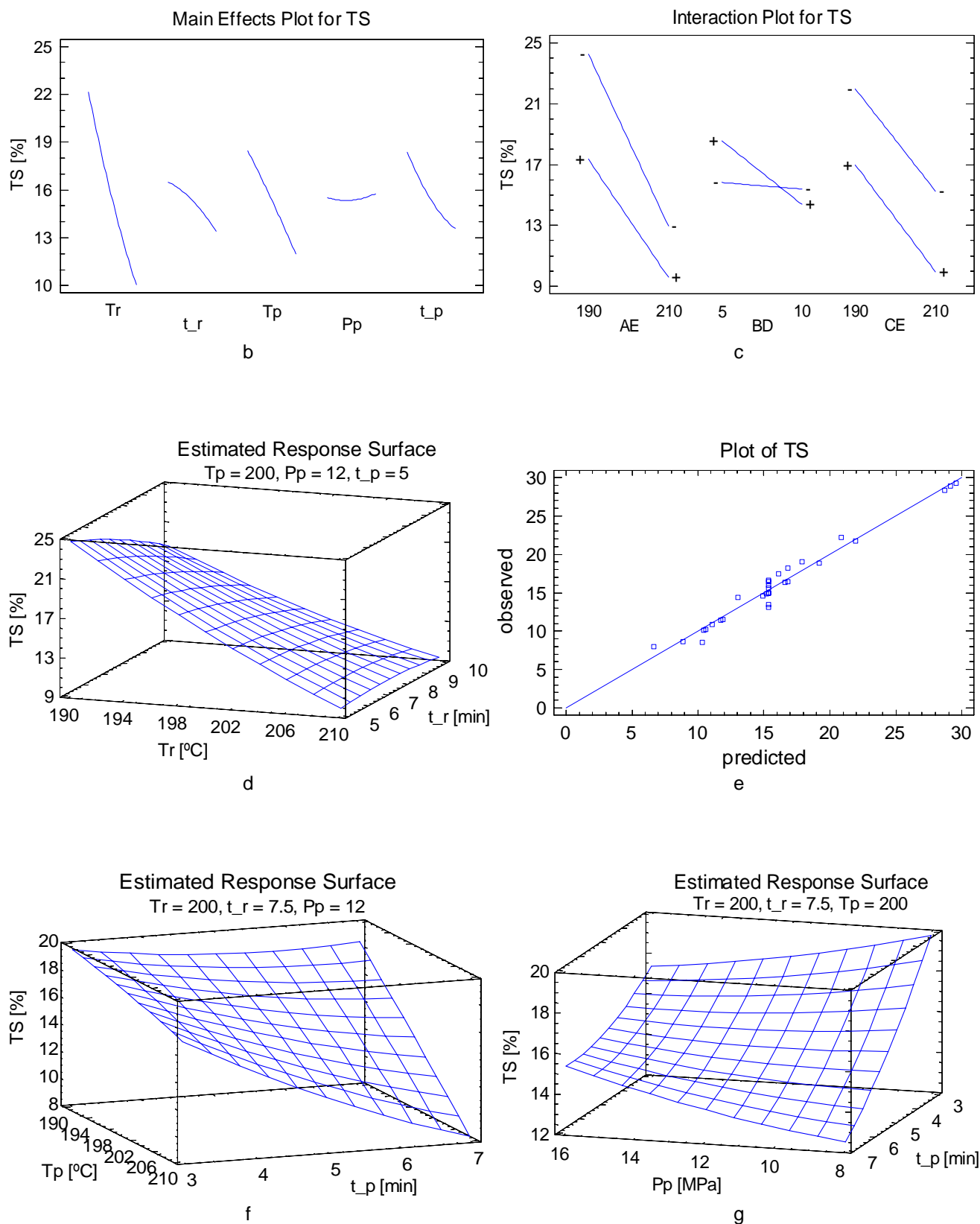


Figure 5.6. Statistical Plots for TS Analysis  
 a. Pareto chart.



**Figure 5.6.** Statistical Plots for TS Analysis (continuation)  
 b. Main effects plot, c. Interaction plot, d, f, g. Estimated responses surfaces, e. Diagnostic plot



$$\begin{aligned} \text{Density} = & -3485.22 - 0.8584 \times Tr - 172.909 \times t_r + 52.3982 \times Tp - 33.491 \times Pp + \\ & 252.5 \times t_p + 0.0234 \times Tr^2 + 0.0405 \times Tr \times t_r - 0.0303 \times Tr \times Tp + \\ & 0.1392 \times Tr \times Pp - 0.8383 \times Tr \times t_p + 0.1994 \times t_r^2 + 0.8373 \times t_r \times Tp + \\ & 0.5401 \times t_r \times Pp - 1.6469 \times t_r \times t_p - 0.1325 \times Tp^2 + 0.042 \times Tp \times Pp - \\ & 0.3758 \times Tp \times t_p - 0.3235 \times Pp^2 + 0.9204 \times Pp \times t_p - 0.3546 \times t_p^2 \end{aligned}$$

a

$$\begin{aligned} \text{MOE} = & -1574.43 + 9.2948 \times Tr + 4.1249 \times t_r + 6.0173 \times Tp - 1.1216 \times Pp + \\ & 12.0427 \times t_p - 0.0092 \times Tr^2 - 0.0609 \times Tr \times t_r - 0.0224 \times Tr \times Tp + \\ & 0.0018 \times Tr \times Pp - 0.0676 \times Tr \times t_p - 0.1707 \times t_r^2 + 0.0508 \times t_r \times Tp \\ & - 0.0054 \times t_r \times Pp + 0.0518 \times t_r \times t_p - 0.0049 \times Tp^2 - 0.0026 \times Tp \times Pp + \\ & 0.001478 \times Tp \times t_p + 0.0147 \times Pp^2 + 0.2281 \times Pp \times t_p - 0.2306 \times t_p^2 \end{aligned}$$

b

$$\begin{aligned} \text{MOR} = & -146923 + 736.471 \times Tr - 187.735 \times t_r + 712.109 \times Tp + 41.5861 \times Pp + \\ & 360.376 \times t_p - 0.2414 \times Tr^2 - 10.9367 \times Tr \times t_r - 2.5558 \times Tr \times Tp + 2.1998 \times \\ & Tr \times Pp - 3.1775 \times Tr \times t_p - 18.3168 \times t_r^2 + 11.8253 \times t_r \times Tp + 14.0816 \times t_r \times \\ & Pp + 15.3848 \times t_r \times t_p - 0.6514 \times Tp^2 - 2.8084 \times Tp \times Pp - 0.2384 \times Tp \times t_p - \\ & 2.1508 \times Pp^2 + 14.7502 \times Pp \times t_p + 2.7781 \times t_p^2 \end{aligned}$$

c

$$\begin{aligned} \text{IB} = & -7.1724 + 0.024 \times Tr + 0.2576 \times t_r + 0.0382 \times Tp + 0.0805 \times Pp - \\ & 0.125 \times t_p - 0.0001 \times Tr^2 - 0.0009 \times Tr \times t_r + 0.0001 \times Tr \times Tp - \\ & 0.00002 \times Tr \times Pp + 0.0006 \times Tr \times t_p - 0.0026 \times t_r^2 - 0.0004 \times t_r \times Tp + \\ & 0.0012 \times t_r \times Pp + 0.0038 \times t_r \times t_p - 0.0001 \times Tp^2 - 0.000330902 \times Tp \times \\ & Pp + 0.0001 \times Tp \times t_p - 0.0010 \times Pp^2 - 0.0059 \times t_p^2 \end{aligned}$$

d

$$\begin{aligned} \text{WA} = & 2005.33 - 9.9166 \times Tr - 1.6311 \times t_r - 8.1447 \times Tp + 6.678 \times Pp - \\ & 41.2802 \times t_p + 0.0156 \times Tr^2 + 0.0085 \times Tr \times t_r + 0.0126 \times Tr \times Tp - \\ & 0.0367 \times Tr \times Pp + 0.1735 \times Tr \times t_p + 0.3337 \times t_r^2 - 0.0346 \times t_r \times Tp - \\ & 0.1532 \times t_r \times Pp + 0.3818 \times t_r \times t_p + 0.014 \times Tp^2 - 0.0009 \times Tp \times Pp + \\ & 0.0018 \times Tp \times t_p + 0.0336 \times Pp^2 + 0.1244 \times Pp \times t_p + 0.0755 \times t_p^2 \end{aligned}$$

e

$$\begin{aligned} \text{TS} = & 400.038 - 4.1225 \times Tr + 0.1733 \times t_r + 1.4724 \times Tp - 2.8847 \times Pp - \\ & 2.0623 \times t_p + 0.0073 \times Tr^2 + 0.0564 \times Tr \times t_r - 0.0022 \times Tr \times Tp + \\ & 0.0172 \times Tr \times Pp + 0.0855 \times Tr \times t_p - 0.065 \times t_r^2 - 0.0389 \times t_r \times Tp - \\ & 0.2308 \times t_r \times Pp - 0.1088 \times t_r \times t_p - 0.0015 \times Tp^2 - 0.0003 \times Tp \times Pp - \\ & 0.0946 \times Tp \times t_p + 0.018 \times Pp^2 + 0.1638 \times Pp \times t_p + 0.1539 \times t_p^2 \end{aligned}$$

f

**Figure 5.7.** Statistical models  
 a. Density, b. MOR, c. MOE, d. IB, e. WA, f. TS

## 5.2.2 Chemical Response Variables

The results obtained for the chemical properties are shown in table 5.8. Material composition is expressed on an oven dry basis. Severity factor and composition of the initial material are also included. Variance analysis was performed for each response variable at a confidence level of 95%. Because we were interested in evaluating the pretreatment process and the quality of the material to be used in the board preparation, all the response variables were referred to dry pretreated-material rather than to initial material.

### 5.2.2.1 Ash content

ANOVA table for ash content is shown in table 5.9 and the statistical plots for ash content are shown in figure 5.8. The fitted model gave an R-squared of 0.846 and an SDR of 0.12%. For this variable, only pretreatment temperature was statistically significant. Ash accounts for mineral salts that are undesirable for the manufacture of fiberboards. Table 5.8 shows that the original material has a considerable amount of ash that could negatively influence the conformation of the boards. Ash content is greatly reduced by pretreatment; this reduction is due to solubilization of the mineral salts contained in the material, during the pretreatment. The minimum values for this response variable are found at high reaction temperatures and intermediate pretreatment times.

### 5.2.2.2 Lignin, Cellulose and Hemicelluloses

The lignin, cellulose and hemicelluloses were analyzed together because they came from the same hydrolysis assay. ANOVA tables for Klason lignin, Acid soluble lignin (ASL), cellulose and hemicelluloses are shown in tables 5.10, 5.11, 5.12 and 5.13, respectively. The statistical plots for Klason lignin, ASL, cellulose and hemicelluloses are shown in figures 5.9, 5.10, 5.11 and 5.12, respectively. Fitted models gave an R-squared of 0.935 and an SDR of 1.51% for cellulose, an R-squared of 0.99 and an SDR of 0.40% for hemicelluloses, an R-squared of 0.824 and an SDR of 1.26% for Klason lignin and R-squared of 0.726 and an SDR of 0.04% for ASL. Both pretreatment temperature and time were statistically significant for cellulose, hemicelluloses, Klason lignin and ASL content. The response surfaces for the three main variables (figures 5.9, 5.11 and 5.12) show that the cellulose content increased but the hemicelluloses content decreased as the severity increased. The quantity of lignin increased as the severity increased. Similar results for cellulose, hemicelluloses

and lignin behavior have been obtained for other materials (Hsu, W. et al. 1988; Jianying, Ragil et al. 2006; Velásquez, Ferrando et al. 2003).

Hemicelluloses have been almost completely eliminated from the material at high pretreatment temperatures and intermediate to long pretreatment times.

Interaction between pretreatment time and temperature was statistically significant only for ASL and cellulose contents. However, pretreatment temperature has larger impact over all the variables than pretreatment time for all the chemical properties; this is understandable because temperature affects exponentially the severity of the pretreatment while time affects severity linearly.

### 5.2.2.3 Cellulose to Klason Lignin ratio (C/L)

Cellulose and Klason lignin presented the same trend, both variables increased when pretreatment severity was increased. However, the C to L ratio remained almost constant with the severity increase (see table 5.8). This behavior is explained for the great amount of hemicelluloses hydrolyzed during the pretreatment, which leads to a net increase in the amount of cellulose and Klason lignin available for bonding but the ratio between these variables does not change much because cellulose and Klason lignin are much more stable with the pretreatment than hemicelluloses.

**Table 5.8.** Chemical compositions of *Vitis vinifera* with different pretreatment conditions

Run	Process Factors			Response Variables					
	Tr [°C]	t_r [min.]	Log (Ro)	Ash [%]	KLignin [%]	ASL [%]	Cellulose [%]	Hemicelluloses [%]	C to L Ratio
Original	-	-	-	3.7	23.3	0.7	43.6	19.1	1.9
1	190	10	3.65	2.3	30.9	0.7	49.9	8.3	1.6
2	200	7.5	3.82	1.9	32.1	0.7	51.1	4.8	1.6
3	200	2.8	3.40	2.4	29.9	0.7	45.0	10.7	1.5
4	210	5	3.94	2.1	29.4	0.7	53.7	5.5	1.8
5	200	7.5	3.82	1.8	32.1	0.7	50.7	5.9	1.6
6	200	7.5	3.82	1.7	31.7	0.7	51.6	5.1	1.6
7	210	10	4.24	2.0	34.9	0.5	53.8	2.3	1.5
8	181.4	7.5	3.27	2.4	29.0	0.7	41.6	13.1	1.4
9	200	7.5	3.82	1.8	30.3	0.7	52.0	5.1	1.7
10	200	7.5	3.82	1.8	32.3	0.7	50.4	5.3	1.6
12	200	7.5	3.82	1.8	30.8	0.7	51.6	5.3	1.7
13	200	7.5	3.82	1.8	30.6	0.7	50.9	5.3	1.7
14	200	7.5	3.82	1.8	31.0	0.7	52.1	5.2	1.7
21	190	5	3.35	2.3	28.0	0.7	43.4	11.7	1.5
22	218.6	7.5	4.37	1.8	38.3	0.6	63.2	1.7	1.7
25	200	12.2	4.03	2.1	33.4	0.7	50.8	3.7	1.5

**Table 5.9.** Variance Analysis for Ash

Variation source	Sum of Squares	Degrees of Freedom	Mean Square	F-Ratio	P-Value
A:Tr	2.21E-01	1	2.21E-01	15.13	0.0030
B:t_r	2.43E-02	1	2.43E-02	1.67	0.2258
AA	2.33E-01	1	2.33E-01	15.95	0.0025
AB	6.25E-04	1	6.25E-04	0.04	0.8402
BB	4.11E-01	1	4.11E-01	28.14	0.0003
Total error	1.46E-01	10	1.46E-02		
Total (corr.)	9.46E-01	15			

**Table 5.10.** Variance Analysis for KLignin

Variation source	Sum of Squares	Degrees of Freedom	Mean Square	F-Ratio	P-Value
A:Tr	4.62E+01	1	4.62E+01	28.99	0.0003
B:t_r	2.00E+01	1	2.00E+01	12.51	0.0054
AA	6.36E+00	1	6.36E+00	3.99	0.0738
AB	1.64E+00	1	1.64E+00	1.03	0.3347
BB	4.70E-03	1	4.70E-03	0.00	0.9578
Total error	1.59E+01	10	1.59E+00		
Total (corr.)	9.04E+01	15			

**Table 5.11.** Variance Analysis for ASL

Variation source	Sum of Squares	Degrees of Freedom	Mean Square	F-Ratio	P-Value
A:Tr	1.46E-02	1	1.46E-02	10.90	0.0080
B:t_r	1.20E-02	1	1.20E-02	8.96	0.0135
AA	1.07E-03	1	1.07E-03	0.80	0.3929
AB	1.32E-02	1	1.32E-02	9.90	0.0104
BB	1.72E-04	1	1.72E-04	0.13	0.7274
Total error	1.34E-02	10	1.34E-03		
Total (corr.)	5.42E-02	15			

**Table 5.12.** Variance Analysis for Cellulose

Variation source	Sum of Squares	Degrees of Freedom	Mean Square	F-Ratio	P-Value
A:Tr	2.70E+02	1	2.70E+02	167.63	0.0000
B:t_r	2.75E+01	1	2.75E+01	17.09	0.0020
AA	1.52E+00	1	1.52E+00	0.94	0.3547
AB	1.04E+01	1	1.04E+01	6.48	0.0291
BB	2.07E+01	1	2.07E+01	12.84	0.0050
Total error	1.61E+01	10	1.61E+00		
Total (corr.)	3.49E+02	15			

**Table 5.13** Variance Analysis for Hemicelluloses

Variation source	Sum of Squares	Degrees of Freedom	Mean Square	F-Ratio	P-Value
A:Tr	1.02E+02	1	1.02E+02	646.31	0.0000
B:t_r	3.58E+01	1	3.58E+01	227.46	0.0000
AA	8.46E+00	1	8.46E+00	53.83	0.0000
AB	2.89E-02	1	2.89E-02	0.18	0.6772
BB	7.15E+00	1	7.15E+00	45.49	0.0001
Total error	1.57E+00	10	1.57E-01		
Total (corr.)	1.52E+02	15			

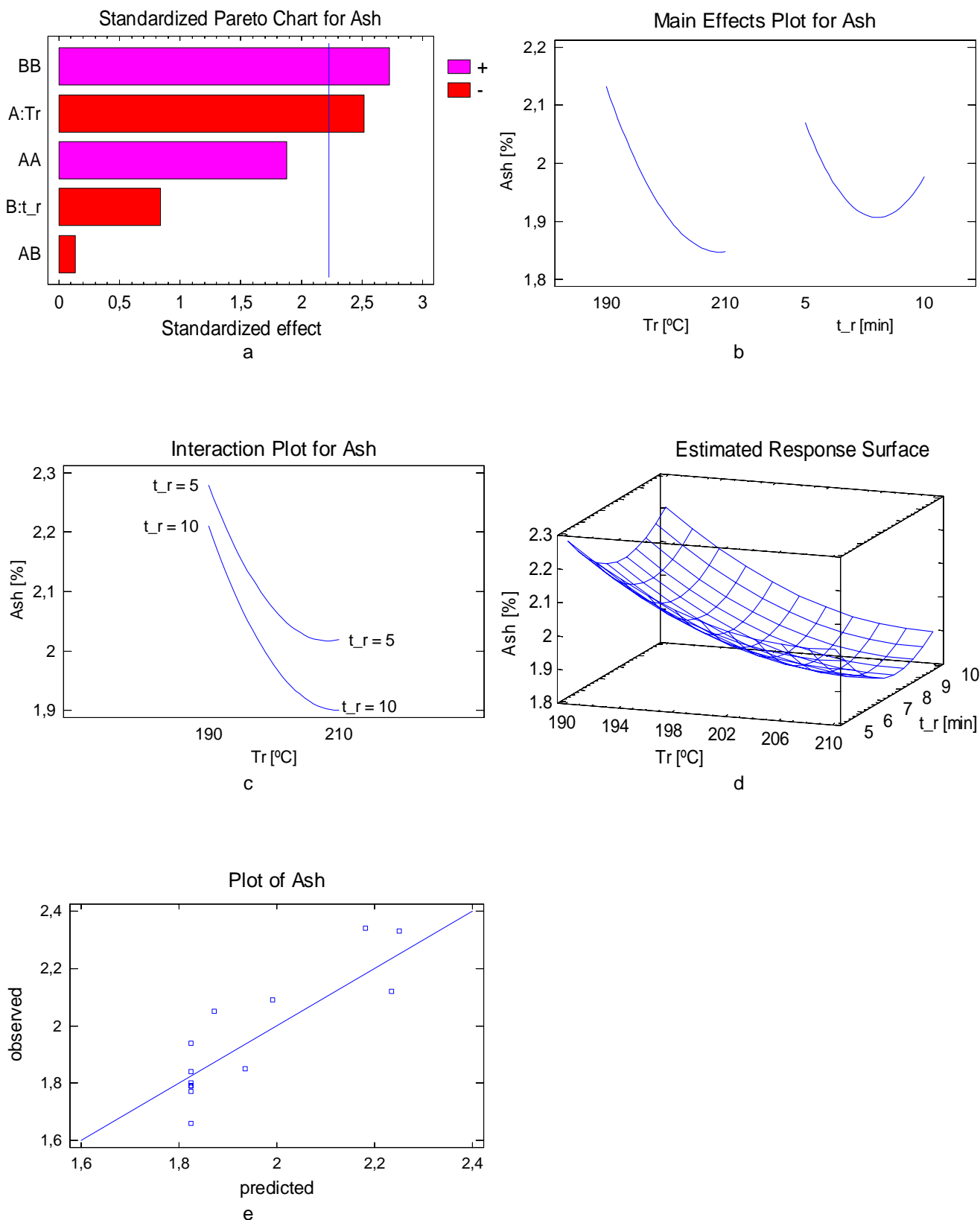


**Figure 5.8.** Statistical Plots for Ash Content Analysis  
 a. Pareto chart, b. Main effects plot, c. Interaction plot, d. Response surface, e. Diagnostic plot

Binderless Fiberboard Production from *Cynara cardunculus* and *Vitis vinifera*

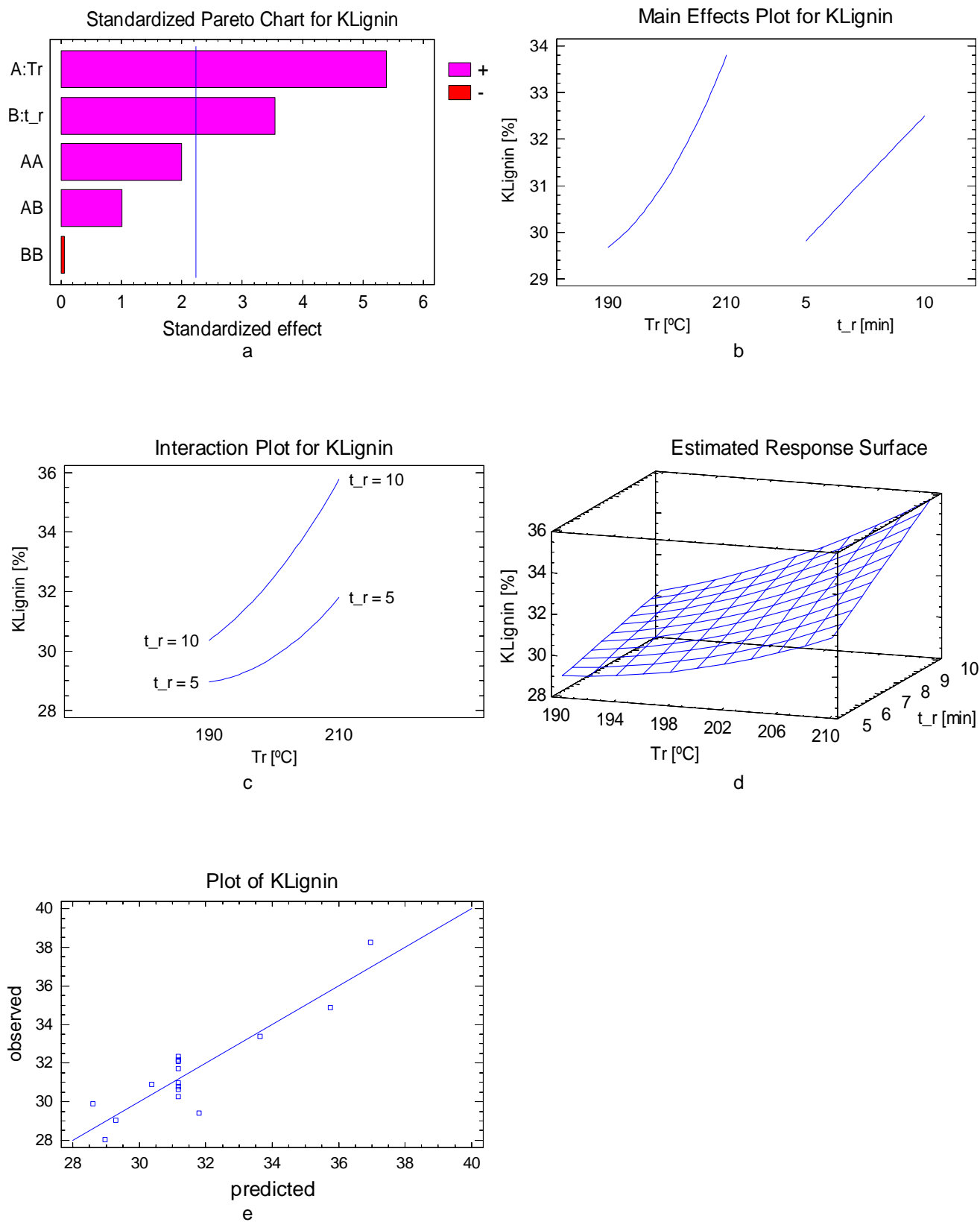


**Figure 5.9.** Statistical Plots for Klason Lignin Analysis  
 a. Pareto chart, b. Main effects plot, c. Interaction plot, d. Response surface, e. Diagnostic plot

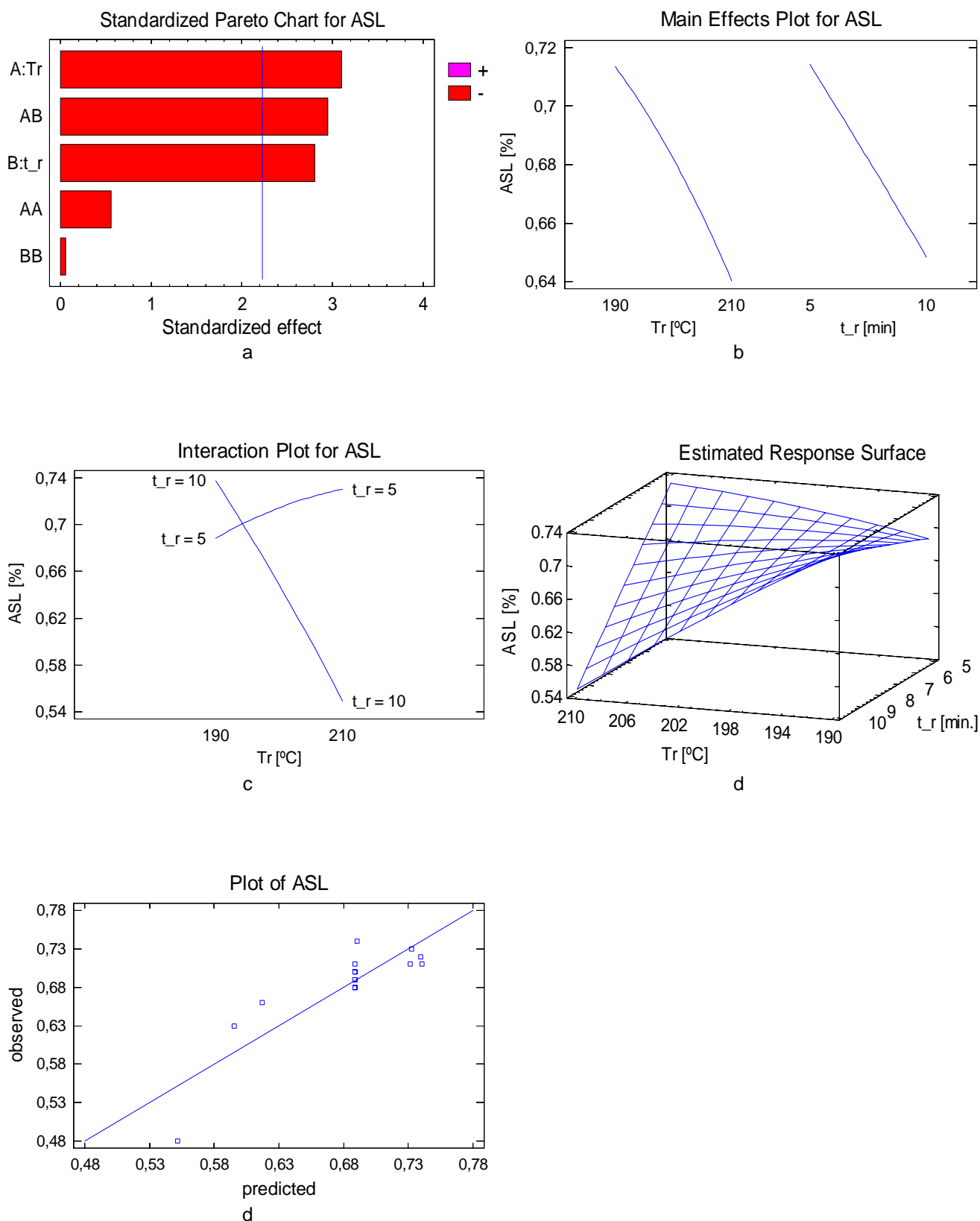


**Figure 5.10.** Statistical Plots for ASL Analysis  
 a. Pareto chart, b. Main effects plot, c. Interaction plot, d. Response surface, e. Diagnostic plot

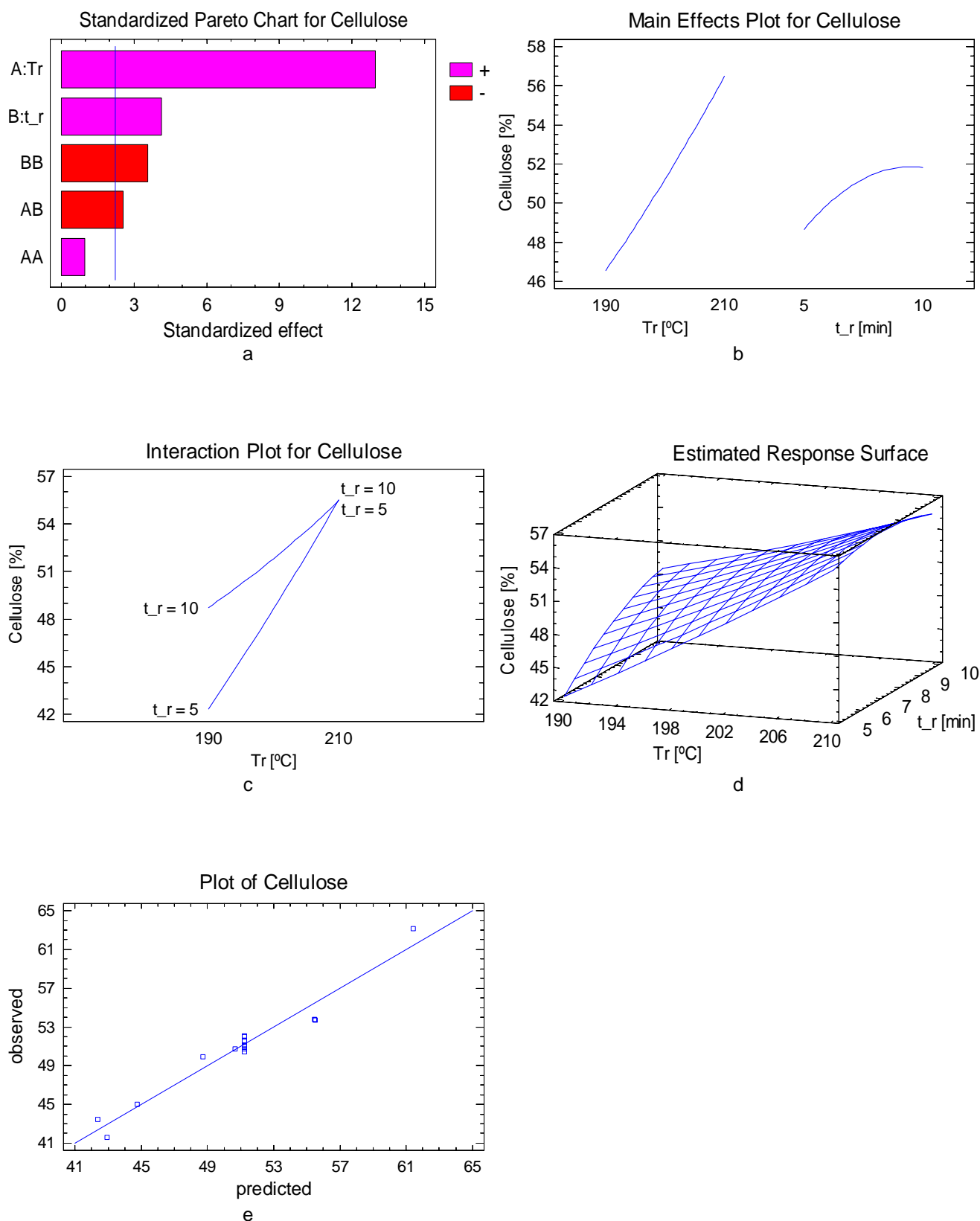


**Figure 5.11.** Statistical Plots for Cellulose Analysis  
 a. Pareto chart, b. Main effects plot, c. Interaction plot, d. Response surface, e. Diagnostic plot



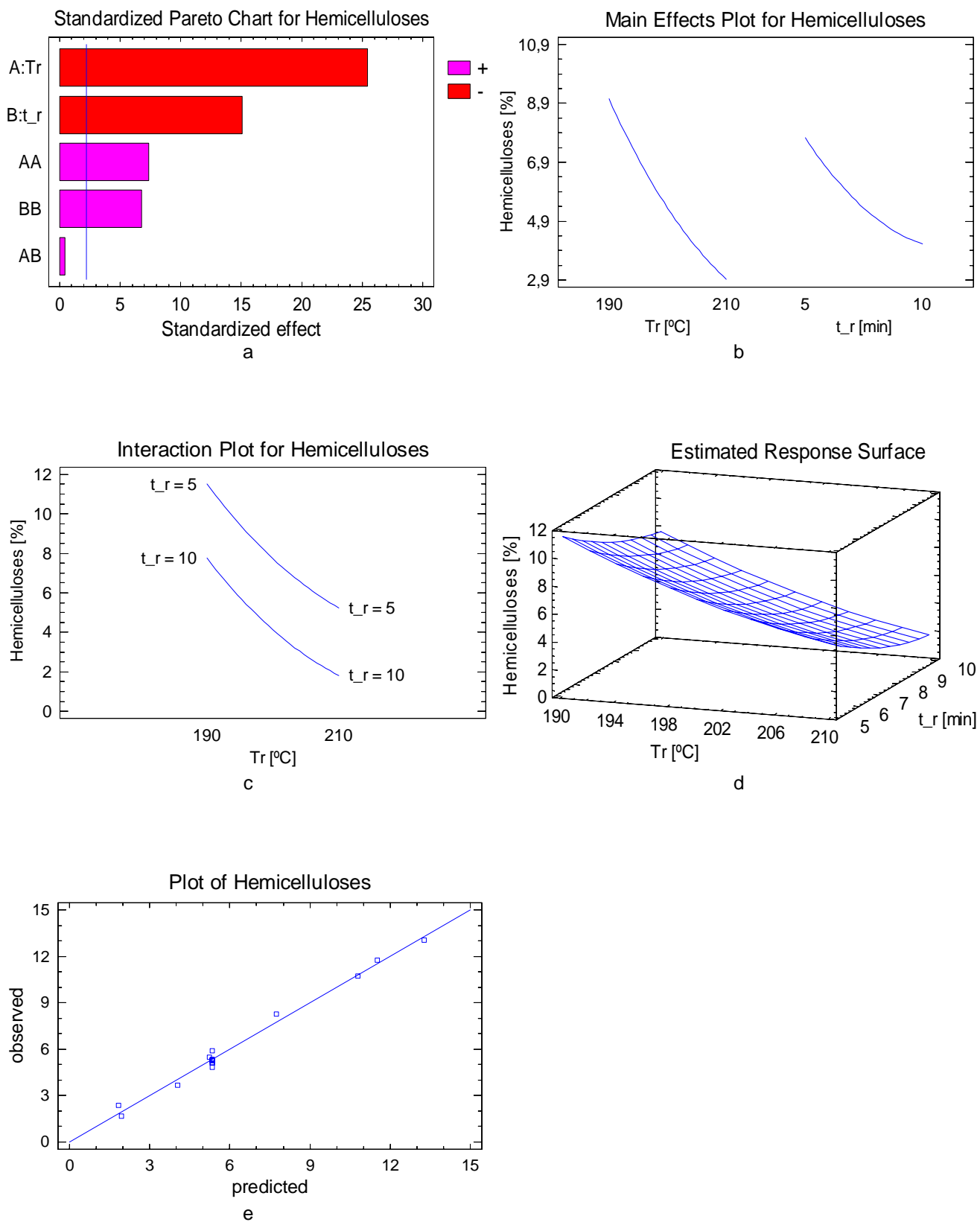


**Figure 5.12.** Statistical Plots for Hemicelluloses Analysis  
 a. Pareto chart, b. Main effects plot, c. Interaction plot, d. Response surface, e. Diagnostic plot

### 5.3 RESPONSE VARIABLES RELATIONSHIP

In this section some relations between response variables are investigated. We should be very careful analyzing these relations because the pressing conditions were changed and this evidently affects in a different way the physical and mechanical properties of boards.

#### 5.3.1 Density relations with mechanical and physical properties

Several authors (Sekino 1999; Suchsland, Woodson et al. 1983; Wilcox 1953) have stated the relationship between density and physicomechanical properties of the fiberboards. In this study, the fiberboards were produced using the same quantity of pretreated material, dry basis, so the variations in density are produced by changes in the pretreatment and pressing conditions rather than intentional changes to study the density impact over the physicomechanical properties of the fiberboards. Because of that, density does not vary a lot among the fiberboards produced, from 1259 to 1363 kg/m<sup>3</sup>, and the relationship between density and the physicomechanical properties can not be established properly from this data.

Figure 5.13 shows the correlation plots between density and physicomechanical properties. The results of fitting a linear model to describe the relationship between the variables and density are the following:

Variables	R-Squared	SDR	P-Value
MOR	0.037	3.6	0.3118
MOE	0.097	480.1	0.0939
IB	0.014	0.1	0.5333
WA	0.048	8.5	0.2441
TS	0.000	5.7	0.9706

P-values only show that there is a statistically significant relationship between MOE and density at a confidence of 90%. For all the other variables not statistically significant relationships with density were found. Although, the P-values suggest the existence of a relationship between density and MOE, the R-squared statistics show that these relations are very weak.

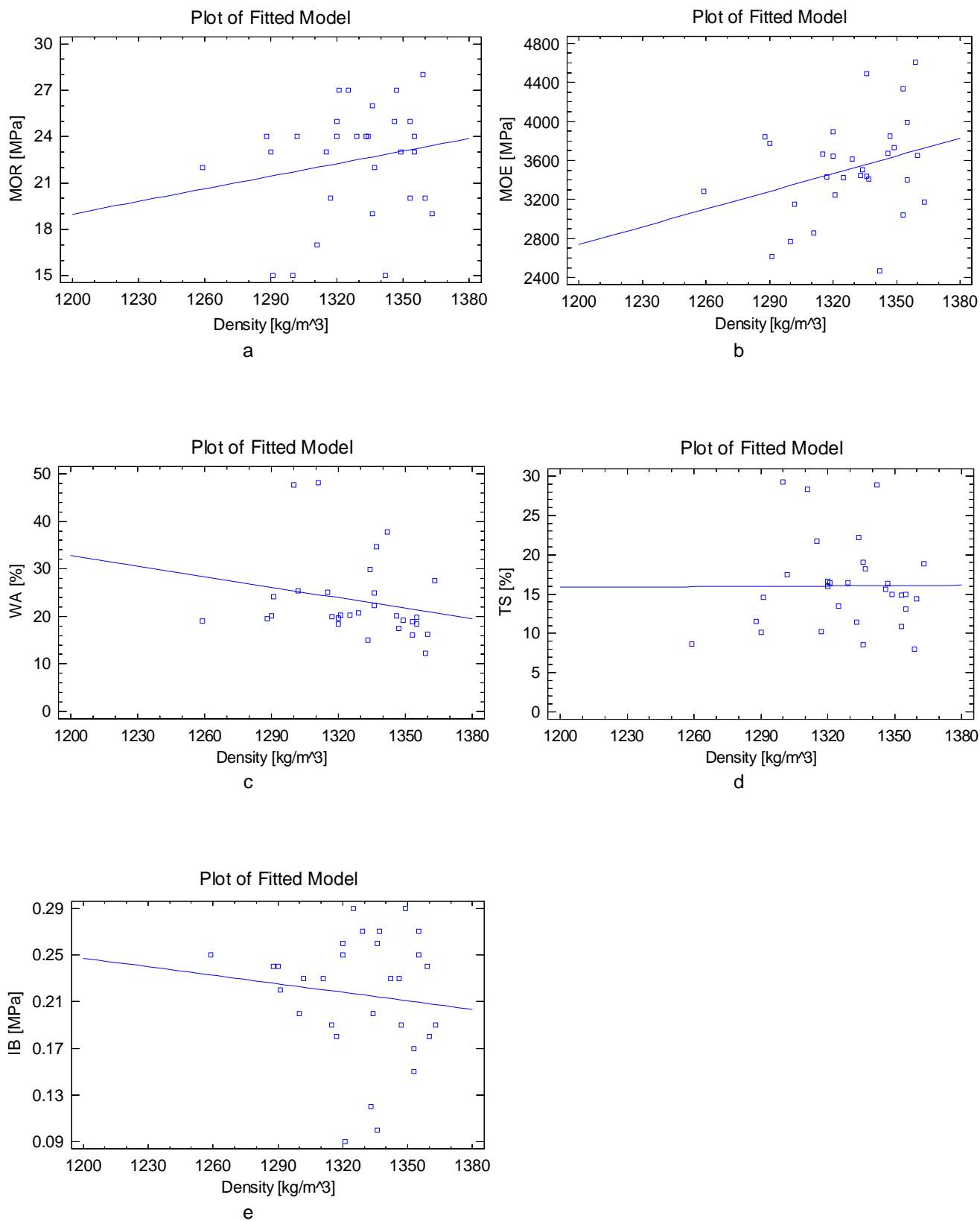


**Figure 5.13.** Correlation Plots between Physico-mechanical properties and Density  
a. MOR, b. MOE, c. WA, d. TS, e. IB

### 5.3.2 Chemical composition relations with mechanical and physical properties

It is well known that the dimensional stability of the fiberboards is related to partial hemicelluloses hydrolysis because hemicelluloses are very hydrophilic. In figure 5.14a we can see that, as expected, WA decreased as the hemicelluloses content decreased. The same was true for TS (figure 5.14b). Some authors (Hsu, W. et al. 1988; Jianying, Ragil et al. 2006; Suchsland, Woodson et al. 1987; Velásquez, Ferrando et al. 2003) have obtained similar results with other materials. The relationship between WA and TS with hemicelluloses is supported by the good R-squared statistics: 0.784 for WA and 0.676 for TS. The SDR were 4.50% for WA and 3.65% for TS.

It has been said also that the mechanical properties of the boards are related to cellulose and lignin content of the material. From figures 5.14c and d we can see that an increment of cellulose content enhances both MOR and MOE, thus confirming the structural function of cellulose in the boards. The relationships between MOR and MOE with lignin are supported by the good R-squared statistics obtained: 0.647 for MOR and 0.76 for MOE. The SDR's were: 2.28 MPa for IB and 262.93 MPa for MOE.

The relationships between IB, MOR and MOE with lignin are not very clear because the lignin from *Vitis vinifera* seems to be very stable with the pretreatment used. In addition to this fact, the changing pressing conditions also affect negatively every analysis that we could do regarding the interaction between lignin and any other variable. The relations between lignin and the physicomechanical properties will be analyzed in more detail in the section of addition of exogenous lignin, chapter 7.

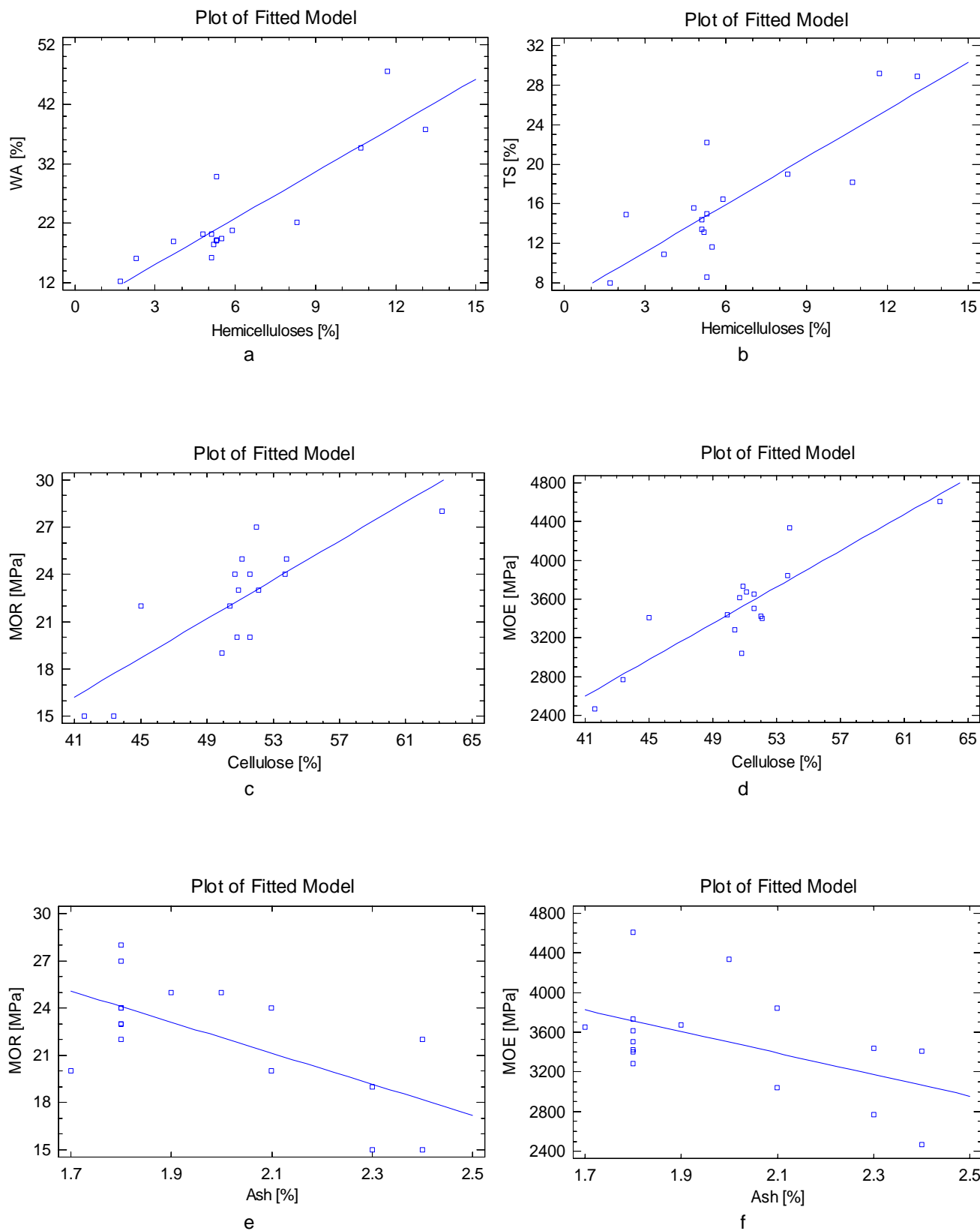


**Figure 5.14.** Relationships between chemical composition and physico-mechanical properties  
 a., b. WA, TS vs Hemicelluloses, c., d. MOR, MOE vs Cellulose, e., f. MOR, MOE vs Ash

## 5.4 MULTIPLE RESPONSE OPTIMIZATION

Multiple response optimization determines the combination of levels for the experimental factors that simultaneously optimize several response variables. The procedure consists of building a desirability function based on the fitted models of each factor to be optimized. The goals for each of the responses were set as follows: MOR, MOE and IB to be maximized and WA and TS to be maintained as close to zero as possible. Figure 5.15 shows the statistical plots for multiple response optimization. The optimum value of desirability was 0.902 over 1 for the following factor levels:

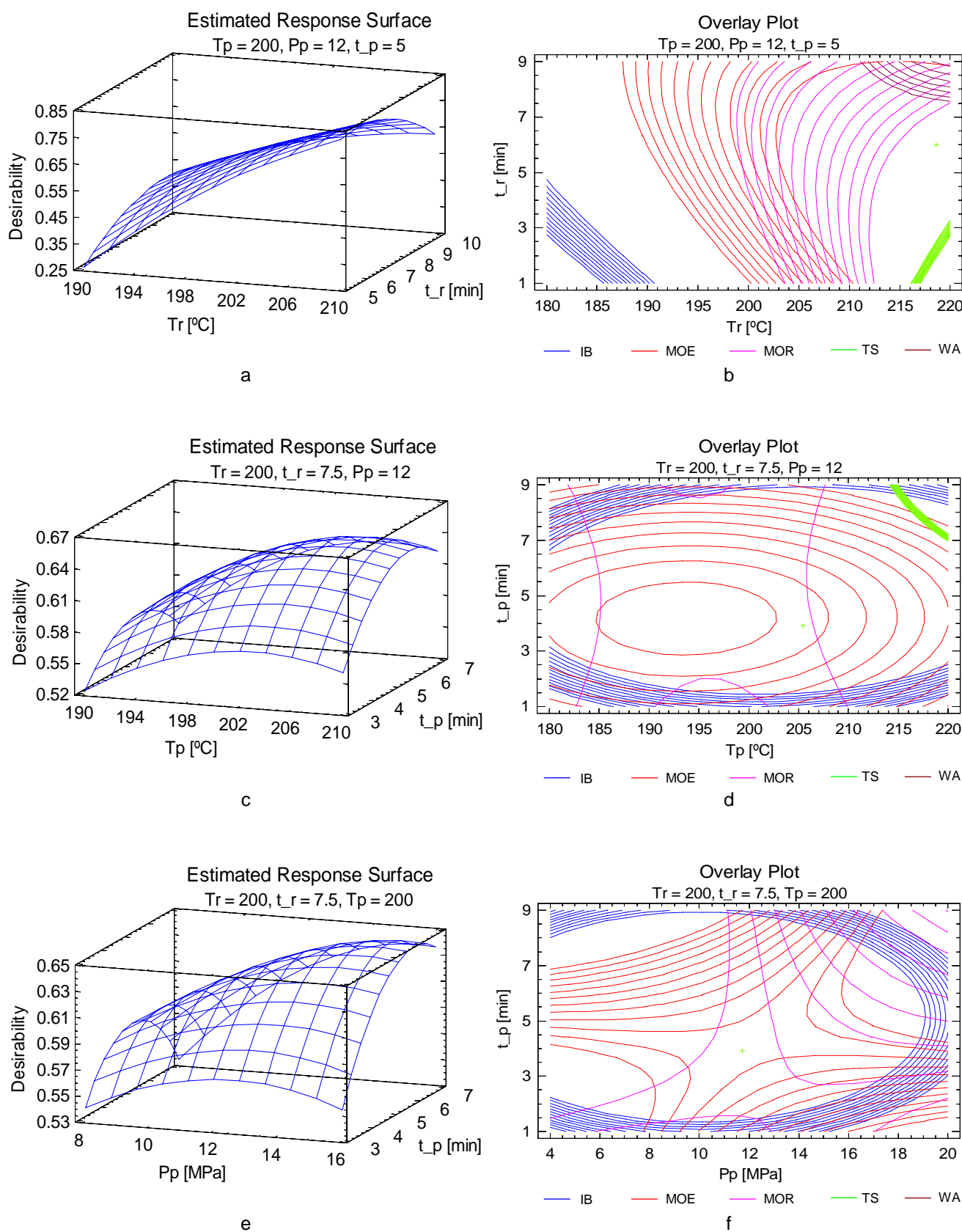
Tr	t_r	Tp	Pp	t_p
[°C]	[min.]	[°C]	[MPa]	[min.]
218	6	205	12	4

Figure 5.15a shows that high pretreatment temperatures and intermediate times are the best choice for simultaneously preserving the fiber structure and encouraging hemicelluloses hydrolysis and lignin release. A set of fiberboards were prepared using the combination of factors provided by the multiple response optimization. These fiberboards fully satisfy the European standards, except for MOR and IB. The mean values for the board properties were:

Density	MOR	MOE	IB	WA	TS
[kg/m <sup>3</sup> ]	[MPa]	[MPa]	[MPa]	[%]	[%]
1382	25	4135	0.14	12.5	9

Figures 5.15 b, d and f show that the factor levels provided by the multiple response optimization are in the region of the values that optimize IB and MOR which are the properties that did not accomplished the standard.

The multiple response optimization model studied suggests that the best physicomechanical properties for the boards are found at high pretreatment temperatures and intermediate pretreatment times. The model also suggests using intermediate pressing temperatures in combination with mid to short pressing times and intermediate pressing pressures in the first pressing step. In the first pressing stage, the humidity is vaporized and the lignin is redistributed over the fibers where the chemical bonds are developed, after the relaxation step, in the third pressing step, the internal defects generated during relaxation are corrected and the moisture remaining on the board is vaporized.



**Figure 5.15.** Multiple Response Optimization  
 a, c, e. Estimated responses surfaces, b, d, f. Overlay plots

## 5.5 CONCLUSIONS

It was possible to produce binderless fiberboards from *Vitis vinifera* that meet the European standards for fiberboards of internal use, except for MOR and IB properties. However, authors believe that *Vitis vinifera* is a good starting material to produce binderless fiberboards and further research efforts should be carried out to find appropriate methods or natural additives to improve those properties that did not fulfill the standards. Strategies such as exogenous lignin addition will be proved.

Both, steam explosion pretreatment and hot pressing, had great influence on the final physicochemical properties of the fiberboards obtained. The optimum value of pretreatment temperature found by multiple response optimization was at the higher limit of the experimental design, further experimentation was performed going beyond this value but mechanical properties diminished due to fiber structure deterioration.

Increasing the severity of the pretreatment improves the physical properties (WA and TS) of the boards. Similarly, hemicelluloses and ash contents of the pretreated fibers clearly decrease as the severity increases, which lead to lower hygroscopicity and to avoid the presence of abrasive materials that is undesirable for the fabrication of fiberboards. Pretreated vine prunings generally have higher cellulose and lignin net contents than original material due to diminishing of the hemicelluloses content.

The multiple response optimization model has been useful for finding the best levels of the process factors for producing the best fiberboards, particularly for the difference found between the optimization trends for physical and mechanical properties.



## REFERENCES

- Anglès, M. N., J. Reguant, *et al.* Binderless Composites from Pretreated Residual Softwood. *Journal of Applied Polymer Science* 73: 2485-2491. 1999.
- FAOSTAT. Database results. 2008
- Hague, J., A. McLauchlin, *et al.* Agri-materials for panel products: a technical assessment of their viability. in: Proceeding of the 32nd international particleboard composite materials symposium: 151-159. 1998.
- Hsu, W. E., S. W., *et al.* Chemical and physical changes required for producing dimensionally stable wood-based composites. Part1: Steam pretreatment. *Wood Science and Technology* 22. 1988.
- Jianying, X., W. Ragil, *et al.* Development of binderless fiberboard from kenaf core. *Journal of Wood Science* 52(3): 236-243. 2006.
- Jiménez, L., V. Angulo, *et al.* Comparison of various pulping processes for producing pulp from vine shoots. *Industrial Crops and Products* 23: 122-130. 2006.
- Ntalos, G. A. and A. H. Grigoriou. Characterization and utilisation of vine prunings as a wood substitute for particleboard production. *Industrial Crops and Products* 16: 59-68. 2002.
- Overend, R. P. and E. Chornet. Fractionation of lignocellulosics by steam-aqueous pretreatments. *Phil. Trans. R. Soc. Lond. A* 321: 523-536. 1987.
- Roffael, E. Raw materials for panel products. in: First European Panel Products Symposium: 113. 1997.
- Schultz, H. The development of wood utilization in the 19th, 20th, and 21st centuries. *Forestry chronicle* 69(4): 413-418. 1993.
- Seber, D. H. and E. H. Lloyd. Bast fiber applications for composites. in: Proceedings of the thirtieth international particleboard/composite materials symposium: 215-235. 1996.

Sekino, N., Inoue M., Irle M., Adcock T. The Mechanisms Behind the Improved Dimensional Stability of Particleboards Made from Steam-Pretreated Particles. *Holzforschung* 53: 435-440. 1999.

Suchsland, O., G. E. Woodson, *et al.* Effect of hardboard process variables on fiberbonding. *Forest Products Journal* 33(4): 58-64. 1983.

Suchsland, O., G. E. Woodson, *et al.* Effect on cooking conditions on fiber bonding in dry-formed binderless hardboard. *Forest Products Journal* 37: 65-69. 1987.

Velásquez, J. A., F. Ferrando, *et al.* Binderless fiberboard from steam exploded *Miscanthus sinensis*. *wood science and technology* 37: 269-278. 2003.

Wilcox, h. Interrelationships of Temperature, Pressure, and Pressing Time in the Production of Hardboard from Douglas-Fir Fiber. *Tappi Journal* 36(2): 89-94. 1953.

Youngquist, J. A. and T. E. Hamilton. Wood products utilization. A call for reflection and innovation. *Forest Products Journal* 49(11-12): 18-27. 1999.

## **6. KRAFT LIGNIN BEHAVIOR DURING REACTION IN AN ALKALINE MEDIUM**

UNIVERSITAT ROVIRA I VIRGILI  
BINDERLESS FIBERBOARD PRODUCTION FROM CYNARA CARDUNCULUS AND VITIS VINIFERA  
Camilo Mancera Arias  
ISBN:978-84-692-1537-1/DL:T-300-2009

## CHAPTER 6

### Kraft lignin behavior during reaction in an alkaline medium

In this chapter the results obtained from the reaction of Kraft lignin in an alkaline medium are presented. I also described how the different process factors affect the lignin structure and its properties.

#### 6.1 INTRODUCTION

With the exception of cellulose, no other lignocellulosic renewable resource is more abundant than lignin. Lignin is an amorphous, polyphenolic material arising from the copolymerization of three phenylpropanoid monomers: coniferyl, sinapyl, and p-coumaryl alcohol. These structures are linked by a multitude of interunit bonds that include several types of ether ( $\alpha$ -O-4,  $\beta$ -O-4, 4-O-5) and carbon-carbon linkages. Lignin is a highly branched, three-dimensional polymer with a wide variety of functional groups providing active centers for chemical and biological interactions. In wood, the lignin content generally ranges from 19 to 35% (*Dence and Lin 1992*). It is extracted by several pulping techniques and as a by-product of the ethanol production process. It is inexpensively and available in large quantities.

Technical lignins are divided into two categories (*Gosselink, de Jong et al. 2004*). The first comprises sulfur-containing lignins, including lignosulfonates and Kraft lignins, which are produced in huge quantities. Lignosulfonates are found in large quantities (around 1 million tonnes of solids per year), and Kraft lignins are found in more moderate quantities (around 100,000 tonnes of solids per year) (*Gosselink, de Jong et al. 2004*). Conventional lignins that are used industrially are mainly obtained from softwoods. The second category comprises sulphur-free lignins obtained from many different processes. Most of these –soda lignins, organosolv lignins, steam-explosion lignins, bioethanol lignins, and oxygen-delignification lignins– are not yet used commercially. Of these, only the soda lignins have the short-term potential for industrial availability. Hydrolysis lignins offer important new opportunities, such as the production of bioethanol to replace fossil fuels for transportation. They may come from woods or

non-woods. Almost all of the lignins extracted from lignocellulosic materials in the pulp and paper (P&P) industry are burned to generate energy and recover chemicals. Only 1–2% of the lignins produced in the P&P industry are used commercially. Lignins can be used in a wide range of products, including materials for automotive brakes, wood-panel products, phenolic resins, biodispersants, polyurethane foams, epoxy resins for printed circuit boards, and surfactants (Gargulak and Lebo 2000; Glasser and Lora 2002; Gosselink, de Jong et al. 2004). In our laboratory, Kraft lignin has successfully been converted into activated carbon (Fierro, Torné et al. 2003) and used in the production of fiberboard (Velásquez, Ferrando et al. 2003). Derivatives of other technical lignins such as adhesives –especially lignin–phenol–formaldehyde resins– are also being developed.

Kraft lignins are clearly underutilized, as nearly all lignins produced in the P&P industry are burned to generate energy and recover chemicals. However, industrial applications are only possible if lignin's added value is enhanced and its quality and properties are standardized. Researchers currently face several problems that could be overcome, such as the low purity, heterogeneity, odour and colour of lignin-based products and the absence of reliable analytical methods for characterizing lignin (Gosselink, de Jong et al. 2004). Lignins must have acceptable purity and the desired chemical and physical properties if they are to be used for any industrial applications. One attractive area for commercial lignin applications is wood adhesives, for instance phenolic resins.

Lignin is more readily available, less toxic and less expensive than phenol. Using lignin to replace phenol in phenol–formaldehyde resin, where the price is subjected to fluctuations in oil prices and supply is generally lower than demand, is considered a potentially attractive application from the economic and environmental points of view. Moreover, this polymer is obtained from renewable resources, can be used without previous treatment and has a similar chemical structure to that of phenol–formaldehyde resins (Nimz 1983).

There is a considerable mass of literature on partially replacing the phenol in phenolic resins with lignin (Alonso, Rodríguez et al. 2001; El Mansouri and Salvadó 2006; Fernández, Oliet et al. 2004). Because of their low phenolic-hydroxyl content, high ring substitution and steric hindrance, the reactivity of industrial lignins is much lower than that of phenolic resins (Fredheim, Braaten et al. 2003). Only a limited amount of industrial lignin can therefore be used as a direct replacement for phenol in the formulation of phenolic adhesives without losing adhesive properties (El Mansouri and Salvadó 2006; Gonçalves and Benar 2001). However, a higher level of

replacement can be achieved if modified lignins are used. Modification enhances the reactivity of lignins by increasing their functionality via demethylation, phenolation and methylolation. These modification techniques have been widely studied (Gilarranz, Rodríguez et al. 2000; Gosselink, de Jong et al. 2004; Lin 1992; McDonough 1993). Several studies have focused on producing high-functionality (i.e., high-reactivity) lignin in the pulping process, which is desirable for most applications, by optimizing the operation conditions to produce both a good pulp and a high-reactivity lignin (Fredheim, Braaten et al. 2003; Miller, Evans et al. 1999). These studies have confirmed that although very severe conditions produce high-functionality lignin, they also lead to a loss in pulp quality. These conditions therefore cannot be used because pulp is the main product of the process. Alkaline depolymerization of lignin has recently been proposed as an easier process that obtains lignin with properties suitable for use in adhesives for particleboards production (El Mansouri, Farriol et al. 2006).

The hydrolysis of lignin in an alkaline medium degrades lignin molecules so that new phenolic-hydroxyl groups can be generated. Under proper conditions, this technique yields reactive degradation products that can be used in the condensation reaction that forms phenolic resins. Another advantage of this technique is that the hydrolyzed products can be used directly in the synthesis of phenolic resins.

A lignin's suitability for manufacturing of lignin-phenol-formaldehyde resins depends on the sources of wood and on the intensity of the delignification process, which determines whether it has enough free phenolic-hydroxyl groups and whether the ortho and para positions of its phenyl rings are blocked by methoxyl groups or aliphatic side chains (Vázquez, González et al. 1997).

In this study, the behaviour of Kraft lignin was observed during reaction in an alkaline medium. The optimum reaction conditions for producing lignin with an acceptable purity and properties suitable for adhesives production were determined. The structural changes and purity of all Kraft lignins were studied using FTIR spectroscopy, proton nuclear magnetic resonance ( $^1\text{H-NMR}$ ) spectroscopy, ultraviolet (UV) spectroscopy and gel permeation chromatography (GPC).

## 6.2 RESULTS AND DISCUSSION

The experimental factors and their levels were chosen based on the literature review and previous experiences on structural modification of technical lignins inside the investigation group, they are:

- A: Reaction temperature (Tr): 116 – 180 °C.
- B: Reaction time (t\_r): 18 – 103 min.

In this section, I will discuss the structural and chemical modifications endure by Kraft lignin during the reaction. Each of the response variables will be analyzed separately using the tools of the experimental design and afterwards the interactions between the experimental factors will be analyzed, if there is any.

The results obtained are shown in table 6.1 and table 6.2. For each response variable a variance analysis was performed at a confidence level of 95%.

### 6.2.1 Alkaline hydrolysis

Within the range of NaOH usage studied, the workable concentration of the aqueous Kraft lignin solution was about 10%. Table 6.1 shows the changes in the pH of the lignin solutions subjected to various reaction conditions. The pH of all reacted lignins decreased as the treatment severity increased. The decrease in the pH was due to the formation of acidic components. These acidic components reacted with the sodium hydroxide and led to a loss of pH.

**Table 6.1.** Chemical composition of Kraft lignins at different reaction conditions

Samples	Tr [°C]	t_r [min]	pH	Solid yield [%]	Ash [%]	Klason Lignin [%]	ASL [%]	Sugars [%]
Lk 0	-	-	13.7		51.49	69.44	0.95	1.37
Lk 1	125	30	12.89	64.44	1.07	95.99	0.61	0.79
Lk 2	125	90	12.8	61.28	0.93	92.66	0.74	0.87
Lk 3	170	30	12.75	62.6	0.76	94.89	0.62	0.6
Lk 4	170	90	12.43	60.88	1.04	95.95	0.6	0.63
Lk 5	147.5	60	12.58	63.2	0.9	93.89	0.62	0.84
Lk 6	147.5	60	12.51	63.24	2	93.51	0.63	0.88
Lk 7	147.5	60	12.56	63.18	1.21	94.79	0.61	0.89
Lk 8	180	60	12.38	60.01	1.4	93.66	0.64	0.25
Lk 9	116	60	12.72	63.26	0.85	92.06	0.59	0.97
Lk 10	147.5	103	12.32	64.04	0.9	93.75	0.66	0.87
Lk 11	147.5	18	12.85	63.1	0.93	94.54	0.61	0.8



**Table 6.2.** Results of the response surface experiment

Muestra	Tr [°C]	t_r [min]	OCH3 [%]	OHph [%]	OHALif [%]	OHTotal [%]	Mw	Mn	Mw/Mn	Increment of active sites [%]
Lk 0			0.158	0.051	0.158	0.208	1135	537	2.12	
Lk 1	125	30	0.325	0.114	0.218	0.332	1255	606	2.07	29
Lk 2	125	90	0.379	0.121	0.326	0.447	1357	615	2.21	30
Lk 3	170	30	0.462	0.143	0.254	0.397	1279	588	2.18	32
Lk 4	170	90	0.401	0.168	0.236	0.405	1239	582	2.13	43
Lk 5	147.5	60	0.321	0.151	0.199	0.350	1355	627	2.16	36
Lk 6	147.5	60	0.297	0.146	0.196	0.342	1296	596	2.17	36
Lk 7	147.5	60	0.317	0.155	0.190	0.346	1368	624	2.19	36
Lk 8	180	60	0.325	0.159	0.192	0.351	1258	596	2.11	40
Lk 9	116	60	0.315	0.142	0.211	0.353	1412	644	2.19	20
Lk 10	147.5	103	0.347	0.139	0.229	0.368	1344	613	2.19	42
Lk 11	147.5	18	0.332	0.126	0.212	0.339	1348	604	2.23	27

### 6.2.2 FTIR-spectroscopy

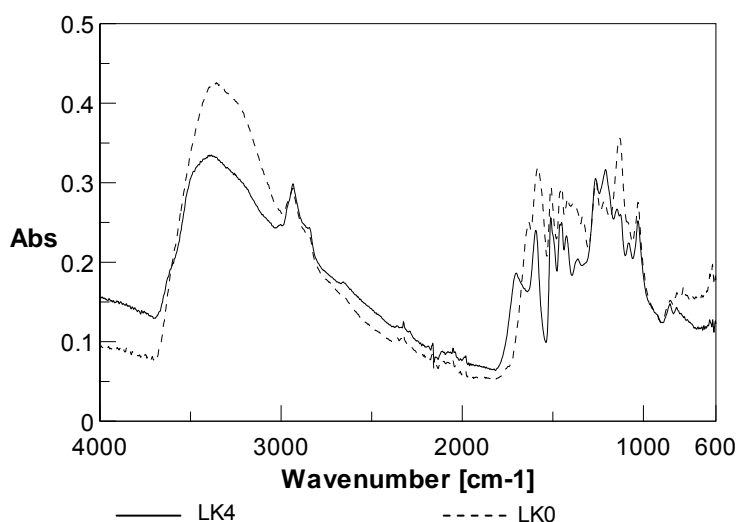
Figure 6.1 shows the FTIR spectrums for raw Kraft lignin (sample LK0) and Kraft lignin reacted at 170°C for 90 min in an alkaline medium (sample LK4); FTIR spectrums for the rest of the samples can be found at the annex C. The absorption intensities for each band were normalized based on the vibration of the aromatic ring appearing at a wavenumber of 1600 cm<sup>-1</sup> (see Table 6.3). This table shows that the mean value of the relative absorbance of OH bands in LK4 is higher than in LK0. This is due to the alkaline treatment under the reaction conditions, which causes the degradation of β-O-4 ether linkages and helps increase the amount of phenolic O-H groups. This is confirmed by the increase in the relative absorbance of the phenolic O-H groups at 1,375 cm<sup>-1</sup> with the alkaline reaction and, consequently, the lower relative absorbance of the ether-bond band at 1,120 cm<sup>-1</sup>.

Table 6.3 also shows that the mean value of the methoxyl group's relative absorptions increases with the alkaline reaction. This can be also attributed to the degradation of the lignin polymer and the aliphatic chain of phenyl-propane units of the lignin molecules. This degradation increases the ratio of the methoxyl group to the

other functional groups, which either are oxidized or disappear with the alkaline treatment.

The mean value of the relative absorbance of the aromatic ring's C–H vibration bands at 1,600 and 1,500  $\text{cm}^{-1}$  also increased with the alkaline reaction. The greater the absorption intensity of this bond, the greater the possibility of the formaldehyde reacting and being incorporated into the aromatic ring in later hydroxymethylation reactions or in resin formulations.

Alkaline treatment also promotes the formation of carbonyl groups. The degradation of  $\beta$ -O-4 bond and the aliphatic chains are the main explanations for the increase in the number of carbonyl groups during alkaline hydrolysis. Carbonyl groups different from those found in natural lignin may appear in the  $\alpha$  or  $\beta$  position if the propane chain is cleaved. All the results of the semi-quantitative FTIR analysis agreed with those obtained using  $^1\text{H-NMR}$ .



**Figure 6.1.** FTIR spectrums for LK4 and LK0

**Table 6.3.** Relative absorbance of different group bands of LK0 and LK4 samples

Group	Band	Relative Absorption	
		LK0	LK4
<b>OH</b>	3411	1.295	1.382
<b>Phenolic OH</b>	1375	0.831	0.851
	1325	0.799	0.821
<b>2nd OH</b>	1220	0.872	1.319
<b>1ry OH</b>	1044	0.868	1.051
	Mean Value	0.933	1.085
<b>Ether-O-</b>	1120	1.122	1.084
<b>Methoxy-OCH<sub>3</sub></b>	2935	0.924	1.244
	2830	0.724	1.000
	1460	0.907	1.031
	1425	0.885	0.972
	Mean Value	0.860	1.062
<b>C-H vibration of</b>	1600	1.000	1.000
<b>Aromatic Ring</b>	1500	0.928	1.065
	Mean Value	0.964	1.033
<b>Carbonyl C=O</b>	1720	0.344	0.776

### 6.2.3 Response surface experiment

Figure 6.2 and figure 6.3 show the <sup>1</sup>H-NMR spectra for raw Kraft lignin (sample LK0) and Kraft lignin reacted at 170°C for 90 min in an alkaline medium (sample LK4) respectively. <sup>1</sup>H-NMR spectrums for the rest of the samples can be found at the annex C. The results of the response surface experiment, including the phenolic hydroxyl, aliphatic hydroxyl and total hydroxyl content, solid yield percentage, Mw, Mn and polydispersity are shown in Table 2. For each response variable, a variance analysis was carried out. All the hypothesis tests were carried out at a 95% confidence level.

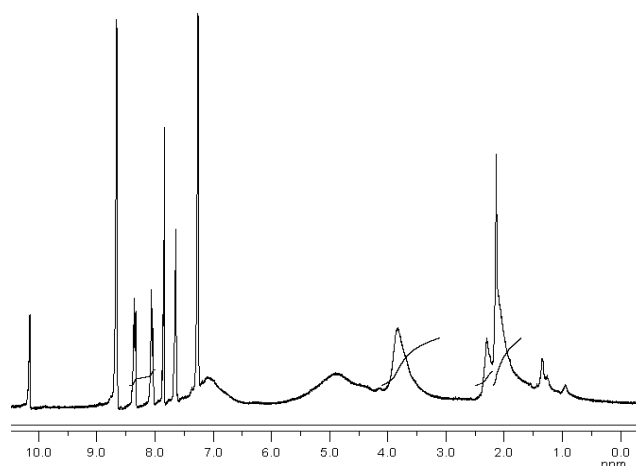


Figure 6.2.  $^1\text{H-NMR}$  spectra of raw Kraft lignin (LK0 sample).

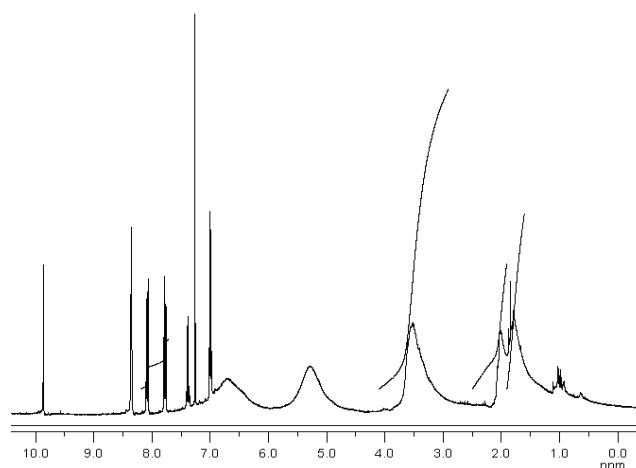


Figure 6.3.  $^1\text{H-NMR}$  spectra of highly reacted Kraft lignin at 170 °C and 90 min (LK4 sample).

### 6.2.3.1 Solid yield

ANOVA table for solid yield is shown in table 6.4 and the statistical plots for solid yield are shown in figure 6.4. The fitted model in this case gave an R-squared value of 0.699 and a standard deviation of residuals (SDR) of 1.06%. The two factors (reaction temperature and reaction time) did not appear to have significant influence over solid yield content at a confidence level of 95%; and only one factor, reaction temperature was found to be statistically significant at a confidence level of 90%.

The model surface (Fig. 6.4d) indicates that an increase in treatment severity led to a decrease in recovered Kraft lignin. The same trend was observed by Miller et al.

(Miller, Evans et al. 1999) in a study of lignin depolymerization by bases in an alcohol solvents in a batch microreactor. This is due to evaporation, during the lignin recovery, of volatile compounds generated under high-severity conditions in the reaction.

Pareto chart (figure 6.4a) and ANOVA table (table 6.4) show that the combined effect of reaction temperature and reaction time was not statistically significant, this is confirmed by the interaction plot (figure 6.4c), which shows that the trends of the variables do not crossed between them in the range studied, indicating that there is not interaction between these variables. Figure 6.4b shows that reaction temperature has a higher effect over solid yield than reaction temperature.

There is a very good correlation between the observed values and the values predicted by the model as shown in figure 6.4e.

### 6.2.3.2 Phenolic hydroxyl content

ANOVA table for phenolic hydroxyl content is shown in table 6.5 and the statistical plots for phenolic hydroxyl content are shown in figure 6.5. In this case, the fitted model gave an R-squared value of 0.84 and an SDR of 0.01%. Only one factor (reaction temperature) was found by an F-test to be significant at a value of  $P > 0.05$ .

The model surface (Fig. 6.5d) indicates that an increase in treatment severity led to an increase in the phenolic-hydroxyl content. The increase in the number of phenolic-hydroxyl groups can be attributed to the cleavage of  $\alpha$ - and  $\beta$ -ether linkages. In fact, the cleavage of these linkages leads to the appearance of phenolic-hydroxyl groups in the aryl substituent removed from the  $\beta$  position (McDonough 1993; Sarkanen 1990). The same trend was observed by Gilarranz (Gilarranz, Rodríguez et al. 2000) in a study of lignin behavior during the autocatalyzed methanol pulping of *Eucalyptus globulus*.

The phenolic-hydroxyl content of the reacted lignin (0.114–0.168%) was lower than that reported in the literature for Kraft and other soda lignins. The highest values were found for samples LK4 and LK8 (0.168% and 0.159%, respectively).

Pareto chart (figure 6.5a) and ANOVA table (table 6.5) show that the combined effect of the reaction temperature and reaction time was not statistically significant, as well as for solid yield the interaction plot (figure 6.5c) show that the trends of the variables do not crossed between them in the range studied, indicating that there is not interaction between these variables, which means that both reaction temperature and reaction time affect the phenolic hydroxyl content separately in the range studied, irrespective the level of the other factor. The main effects plot (figure 6.5b) show that the effect of the reaction temperature over phenolic OH is rather linear compared to the effect of reaction time, which appears to be more quadratic.

Figure 6.5e shows that there is a good correlation between the observed values and the values predicted by the model.

### 6.2.3.3 Aliphatic hydroxyl content

ANOVA table for aliphatic hydroxyl content is shown in table 6.6 and the statistical plots for aliphatic hydroxyl content are shown in figure 6.6. The fitted model gave an R-squared of 0.657 and an SDR of 0.032%. The two factors (reaction temperature and reaction time) did not appear to have significant influence over aliphatic-hydroxyl content at a confidence level of 95%, nor at 90%. The modeled surface (Fig. 6.6d) shows that an increase in treatment severity leads to an increase in aliphatic-hydroxyl content; mainly a reaction time increase favors aliphatic-hydroxyl content increase. Figure 6.6d also shows that reaction time has greater influence than temperature on aliphatic-hydroxyls content, but these behaviors can not be completely explained by the model.

The increased number of aliphatic-hydroxyl groups can also be attributed to the hydrolysis of  $\beta$ -ether linkages that takes place after  $\alpha$ -ether linkages are split. Hydrolysis implies the addition of the elements of water under the formation of one aliphatic-hydroxyl group and one phenolic-hydroxyl group per bond hydrolyzed (*Forss and Fremer 2003*).

Pareto chart (figure 6.6a) and ANOVA table (table 6.6) show that there is not any combined effect statistically significant. The main effects plot show that the effect of reaction time is higher than the effect of reaction temperature over the aliphatic hydroxyl content; this figure also show that both effects have a quadratic effect over the aliphatic OH content but in a reverse direction. However, this behavior is different compared to the behavior of the phenolic-hydroxyl content. An increase in the reaction temperature affects positively the phenolic-hydroxyl content, while it affects adversely the aliphatic-hydroxyl content.

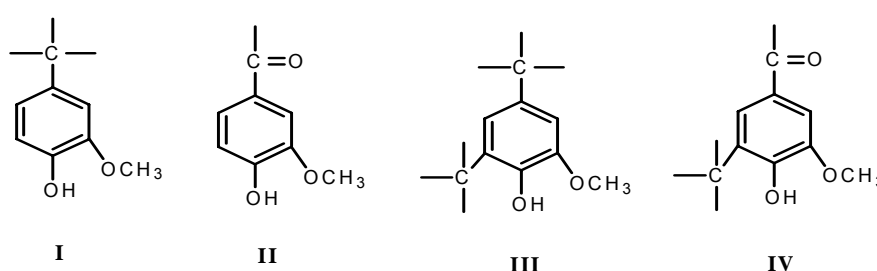
### 6.2.3.4 Total hydroxyl content

ANOVA table for total hydroxyl content is shown in table 6.7 and the statistical plots for aliphatic hydroxyl content are shown in figure 6.7. The fitted model gave an R-squared of 0.626 and an SDR of 0.03%. Neither of the experimental factors (reaction temperature and reaction time) appeared to be significant at a confidence level of 95%, nor at 90%. Figure 6.7d shows that an increase in treatment severity increases the total amount of hydroxyl in the treated lignin. As with aliphatic-hydroxyl content, the reaction time had greater influence than temperature on the total amount of hydroxyls. Total hydroxyl content comprises for phenolic- and aliphatic-hydroxyl groups.

### 6.2.3.5 Active sites increment

ANOVA table for active sites increment is shown in table 6.8 and the statistical plots for active sites increment are shown in figure 6.8. The fitted model gave an R-squared of 0.929 and an SDR of 2.61%. The two factor (reaction temperature and reaction time) were found by an F-test to be significant at a value of  $P > 0.05$ .

The model surface (figure 6.8d) indicates that an increase in treatment severity led to an increase in the active sites increment. The highest increment of active sites – phenolic structures of the type I and II – were found for samples LK4 and LK8 (43% and 40%, respectively) compared to the raw lignin, see Table 6.2. The different types of phenolic structure in the lignin samples are shown in the figure below.



This behavior is in accordance to the behavior of the phenolic-hydroxyl content, where LK4 and LK8 samples were found to have the higher phenolic-hydroxyl content.

Main effects plot (figure 6.8b) show that reaction temperature has a bigger effect over the active sites increment than reaction time. The interaction between reaction temperature and time presents the same characteristics that presented for phenolic-hydroxyl content as shown in Pareto chart (figure 6.8a), ANOVA table (table 6.8) and interaction plot (figure 6.8c) for this variable.

Figure 6.8e shows that there is a good correlation between the observed values and the values predicted by the model.

### 6.2.3.6 Weight-average molecular weight (Mw)

ANOVA table for Mw is shown in table 6.9 and the statistical plots for Mw are shown in figure 6.9. The fitted model in this case gave an R-squared of 0.615 and an SDR of 49 g/mol. Neither reaction temperature nor reaction time was found to be significant by an F-test at an  $\alpha$  value of  $P > 0.05$ , but reaction temperature became significant at an  $\alpha$  value of  $P > 0.10$ . The modeled surface (Fig. 6.9d) shows that an increase in treatment severity led to a decrease in the weight-average molecular weight and, consequently, a more extensive depolymerization of lignin molecules. Figure 6.9d also shows that the influence of reaction temperature is greater than the influence of

reaction time. The decrease in the weight-average molecular weight is confirmed by the increase in the number of phenolic-hydroxyl groups and is caused by the cleavage of  $\alpha$ - and  $\beta$ -ether linkages. The molecular weights measured ranged from 1,239 to 1,412 g/mol.

#### 6.2.3.7 Number-average molecular weight (Mn)

ANOVA table for Mn is shown in table 6.10 and the statistical plots for Mn are shown in figure 6.10. The fitted model gave an R-squared of 0.647 and an SDR of 15 g/mol. Only reaction temperature was found to be significant at a confidence level of 95%. The modeled surface (Fig. 6.10d) shows that an increase in the treatment severity led to a decrease in number-average molecular weight. As with weight-average molecular weight, the number-average molecular weight of all modified lignins was greater than that of original lignin, probably due to condensation reactions. Intermediate reaction times led to larger molecular weights throughout the temperature range, but temperature proved to have more influence than reaction time on lignin molecular weight. This decrease in number-average molecular weight is explained by the same causes as the decrease in weight-average molecular weight with increased severity. For all treated lignins, Mn ranged from 582 to 644 g/mol.

Both effects molar mass and the reactivity on the adhesive performance, have a favorable effect on the quality of adhesive performance. High molecular weight lignins, due to its high level of crosslinking act like active extenders compare to low molecular weight lignins that act like inactive fillers (Pranda, Brezny et al. 1991).

#### 6.2.3.8 Polydispersity

ANOVA table for polydispersity is shown in table 6.11 and the statistical plots of polydispersity are shown in figure 6.11. The fitted model in this case gave an R-squared of 0.641 and an SDR of 0.04. The polydispersities of the treated lignins (Mw/Mn) were rather constant. No significant differences were found between original and treated lignins for this response variable. Neither temperature nor time was found significant at a confidence level of either 95% or 90%. The values found for this parameter ranged from 2.07 to 2.21. The modeled response surface (Fig. 6.11d) shows a slight increase in polydispersity when low reaction temperatures are combined with long reaction times, but these changes cannot be confirmed by the statistical analysis.



**Table 6.4.** Variance Analysis for Solid yield

Source	Sum of Squares	Df	Mean Square	F-Ratio	P-Value
A:Tr	5.58E+00	1	5.58E+00	4.97	0.0762
B:t_r	1.58E+00	1	1.58E+00	1.41	0.2887
AA	4.15E+00	1	4.15E+00	3.7	0.1126
AB	5.18E-01	1	5.18E-01	0.46	0.5269
BB	8.20E-02	1	8.20E-02	0.07	0.7978
Total error	5.61E+00	5	1.12E+00		
Total (corr.)	1.86E+01	10			

**Table 6.5.** Variance Analysis for Phenolic OH

Source	Sum of Squares	Df	Mean Square	F-Ratio	P-Value
A:Tr	1.26E-03	1	1.26E-03	14.13	0.0132
B:t_r	3.36E-04	1	3.36E-04	3.78	0.1096
AA	1.49E-05	1	1.49E-05	0.17	0.6988
AB	8.10E-05	1	8.10E-05	0.91	0.3836
BB	6.13E-04	1	6.13E-04	6.9	0.0467
Total error	4.44E-04	5	8.89E-05		
Total (corr.)	2.72E-03	10			

**Table 6.6.** Variance Analysis for Aliphatic OH

Source	Sum of Squares	Df	Mean Square	F-Ratio	P-Value
A:Tr	8.92E-04	1	8.92E-04	0.84	0.4002
B:t_r	1.51E-03	1	1.51E-03	1.43	0.2853
AA	1.29E-03	1	1.29E-03	1.22	0.3201
AB	3.97E-03	1	3.97E-03	3.76	0.1103
BB	3.32E-03	1	3.32E-03	3.14	0.1364
Total error	5.28E-03	5	1.06E-03		
Total (corr.)	1.54E-02	10			

**Table 6.7.** Variance Analysis for Total OH

Source	Sum of Squares	Df	Mean Square	F-Ratio	P-Value
A:Tr	3.52E-05	1	3.52E-05	0.04	0.8541
B:t_r	3.25E-03	1	3.25E-03	3.47	0.1217
AA	9.97E-04	1	9.97E-04	1.06	0.3499
AB	2.86E-03	1	2.86E-03	3.05	0.1412
BB	1.09E-03	1	1.09E-03	1.16	0.3303
Total error	4.69E-03	5	9.39E-04		
Total (corr.)	1.26E-02	10			

**Table 6.8.** Variance Analysis for Active sites increment

Source	Sum of Squares	Df	Mean Square	F-Ratio	P-Value
A:Tr	2.50E+02	1	2.50E+02	36.7	0.0018
B:t_r	1.38E+02	1	1.38E+02	20.26	0.0064
AA	4.04E+01	1	4.04E+01	5.92	0.0591
AB	2.50E+01	1	2.50E+01	3.67	0.1137
BB	9.80E-01	1	9.80E-01	0.14	0.7201
Total error	3.41E+01	5	6.82E+00		
Total (corr.)	4.82E+02	10			

**Table 6.9.** Variance Analysis for Mw

Source	Sum of Squares	Df	Mean Square	F-Ratio	P-Value
A:Tr	1.18E+04	1	1.18E+04	4.87	0.0785
B:t_r	4.32E+02	1	4.32E+02	0.18	0.6908
AA	1.59E+03	1	1.59E+03	0.65	0.4555
AB	5.04E+03	1	5.04E+03	2.07	0.2095
BB	7.75E+02	1	7.75E+02	0.32	0.5967
Total error	1.22E+04	5	2.43E+03		
Total (corr.)	3.16E+04	10			

**Table 6.10.** Variance analysis for Mn

Source	Sum of Squares	Df	Mean Square	F-Ratio	P-Value
A:Tr	1.75E+03	1	1.75E+03	7.34	0.0423
B:t_r	3.63E+01	1	3.63E+01	0.15	0.7122
AA	1.87E+01	1	1.87E+01	0.08	0.7905
AB	5.63E+01	1	5.63E+01	0.24	0.6473
BB	3.36E+02	1	3.36E+02	1.41	0.2883
Total error	1.19E+03	5	2.38E+02		
Total (corr.)	3.37E+03	10			

**Table 6.11.** Variance analysis for Polydispersity

Source	Sum of Squares	Df	Mean Square	F-Ratio	P-Value
A:Tr	7.83E-04	1	7.83E-04	0.5	0.5096
B:t_r	1.33E-04	1	1.33E-04	0.09	0.782
AA	2.31E-03	1	2.31E-03	1.48	0.2774
AB	9.03E-03	1	9.03E-03	5.8	0.061
BB	5.17E-04	1	5.17E-04	0.33	0.5891
Total error	7.78E-03	5	1.56E-03		
Total (corr.)	2.17E-02	10			

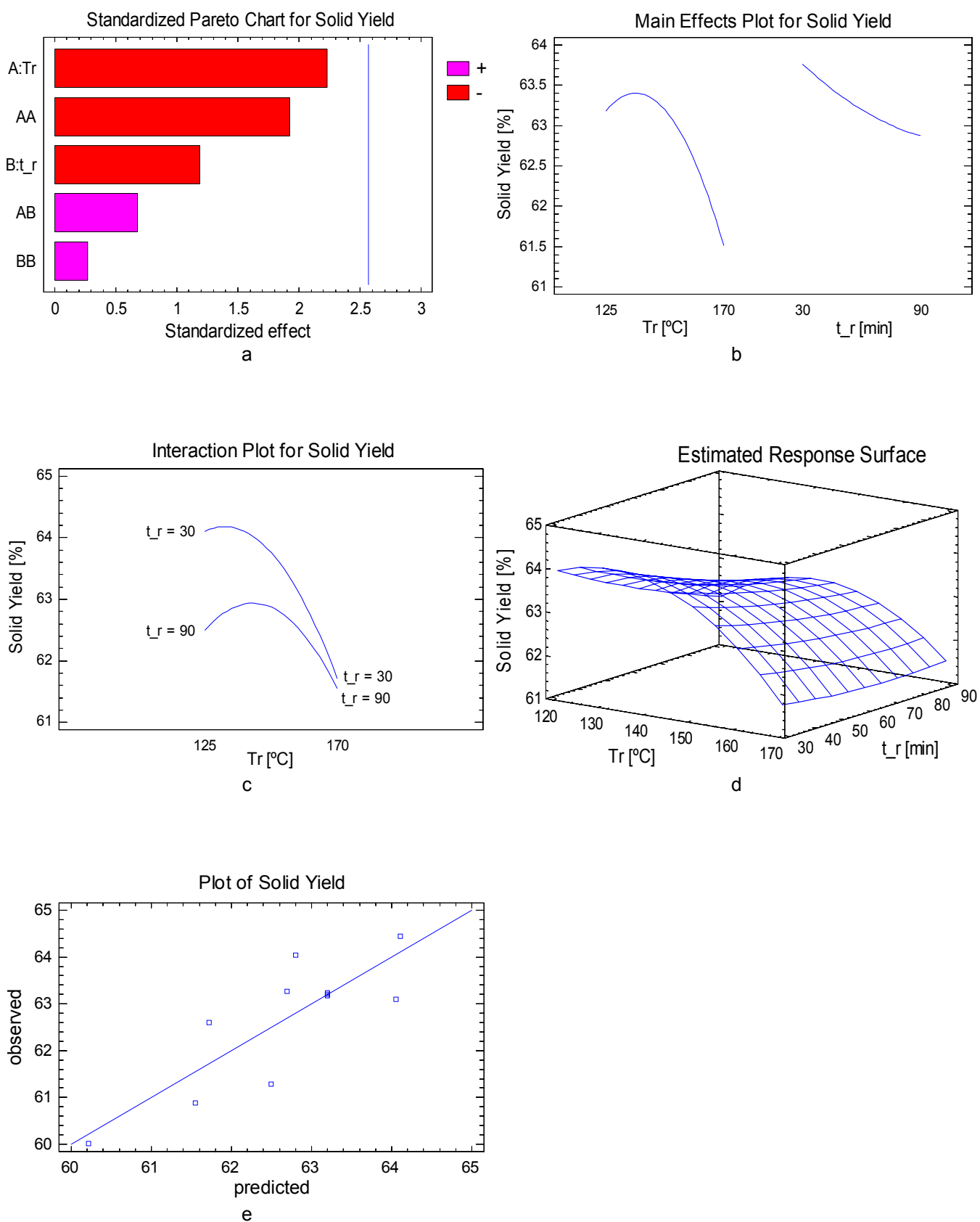


**Figure 6.4.** Statistical Plots for Solid Yield Analysis  
 a. Pareto chart, b. Main effects plot, c. Interaction plot, d. Response Surface, e. Diagnostic plot

Binderless Fiberboard Production from *Cynara cardunculus* and *Vitis vinifera*

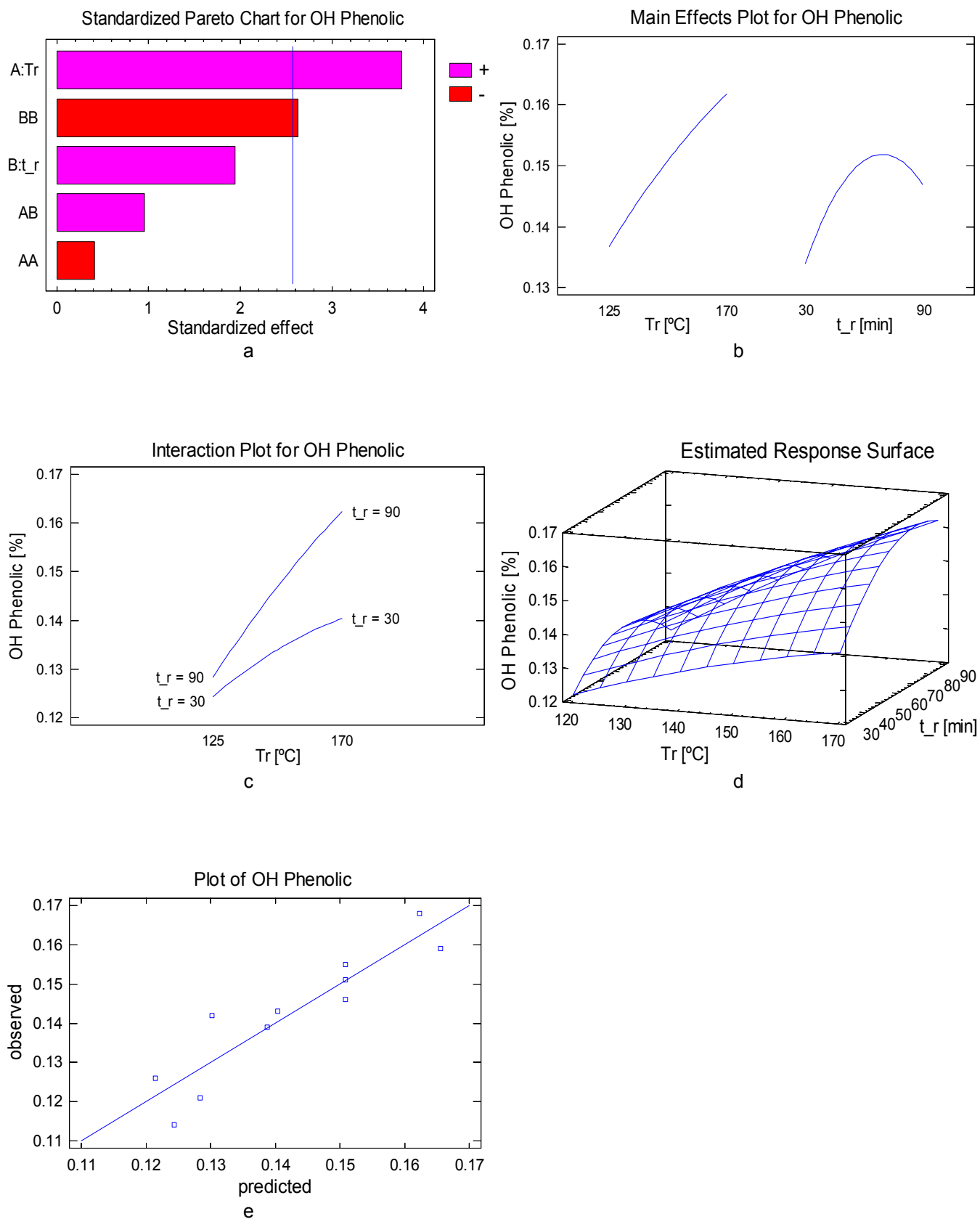


**Figure 6.5.** Statistical Plots for Phenolic OH Analysis  
 a. Pareto chart, b. Main effects plot, c. Interaction plot, d. Response Surface, e. Diagnostic plot

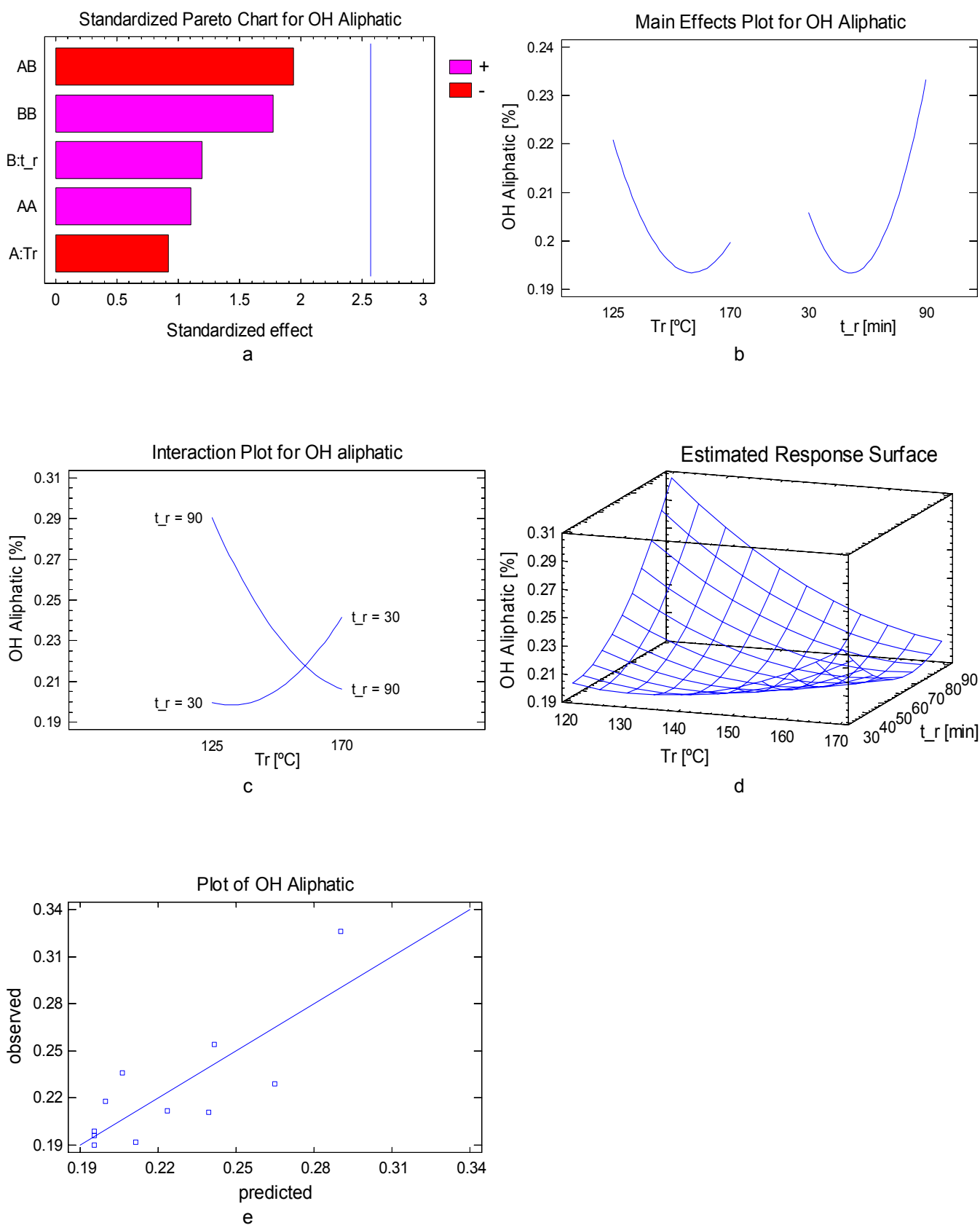


**Figure 6.6.** Statistical Plots for Aliphatic OH Analysis  
 a. Pareto chart, b. Main effects plot, c. Interaction plot, d. Response Surface, e. Diagnostic plot

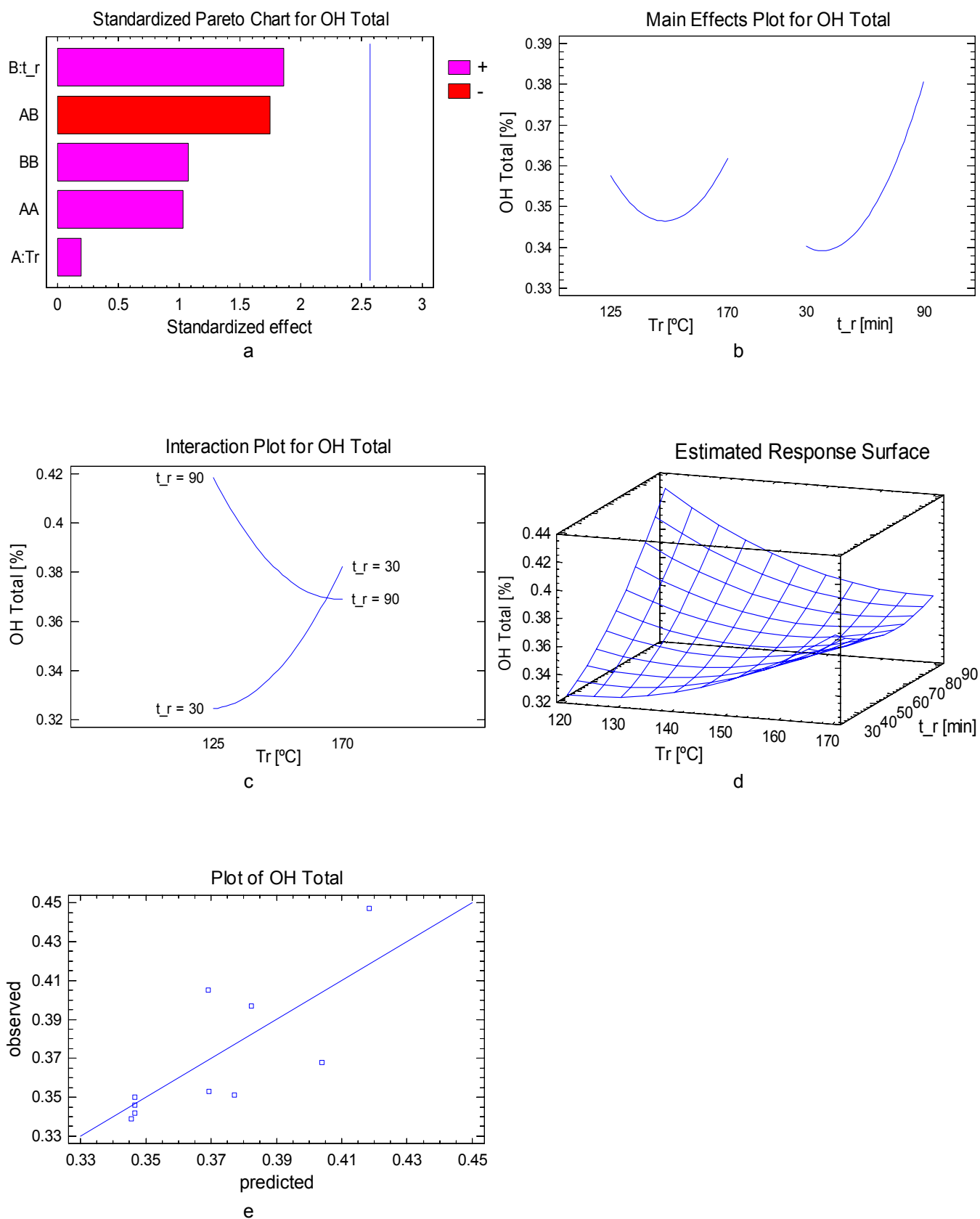


**Figure 6.7.** Statistical Plots for OH Total Analysis  
 a. Pareto chart, b. Main effects plot, c. Interaction plot, d. Response Surface, e. Diagnostic plot

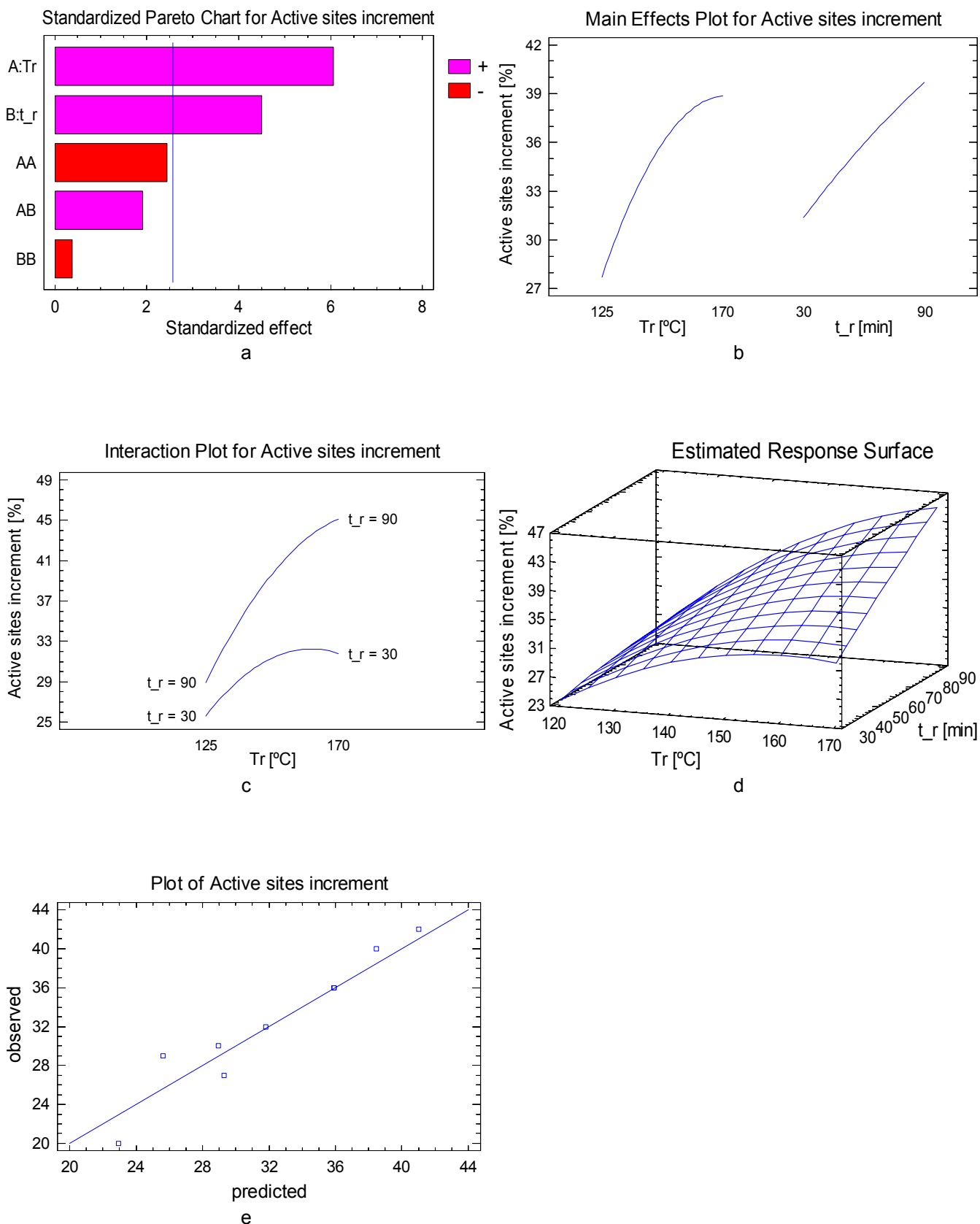


**Figure 6.8.** Statistical Plots for Active Sites Increment Analysis  
 a. Pareto chart, b. Main effects plot, c. Interaction plot, d. Response Surface, e. Diagnostic plot

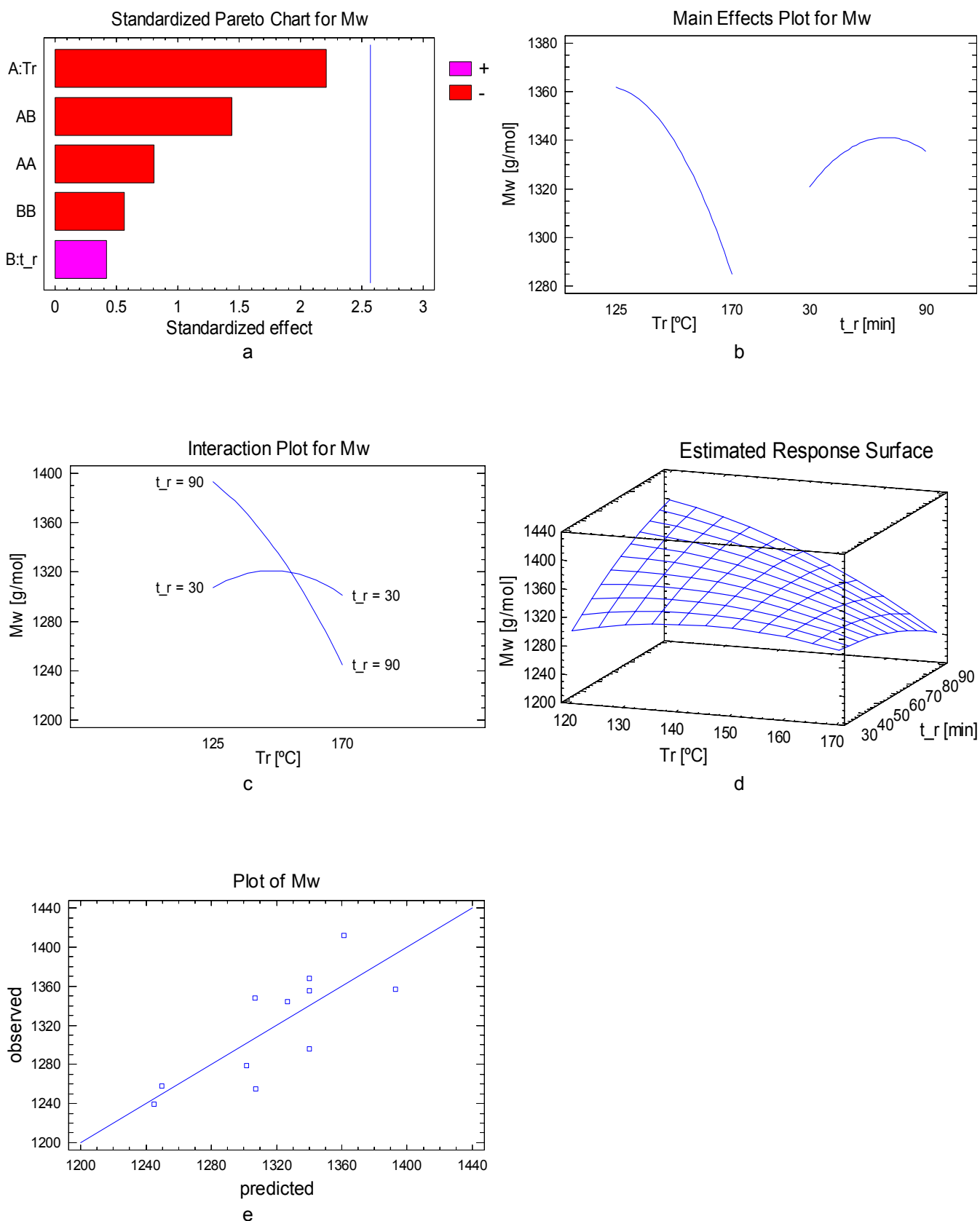


**Figure 6.9.** Statistical Plots for Mw Analysis  
 a. Pareto chart, b. Main effects plot, c. Interaction plot, d. Response Surface, e. Diagnostic plot



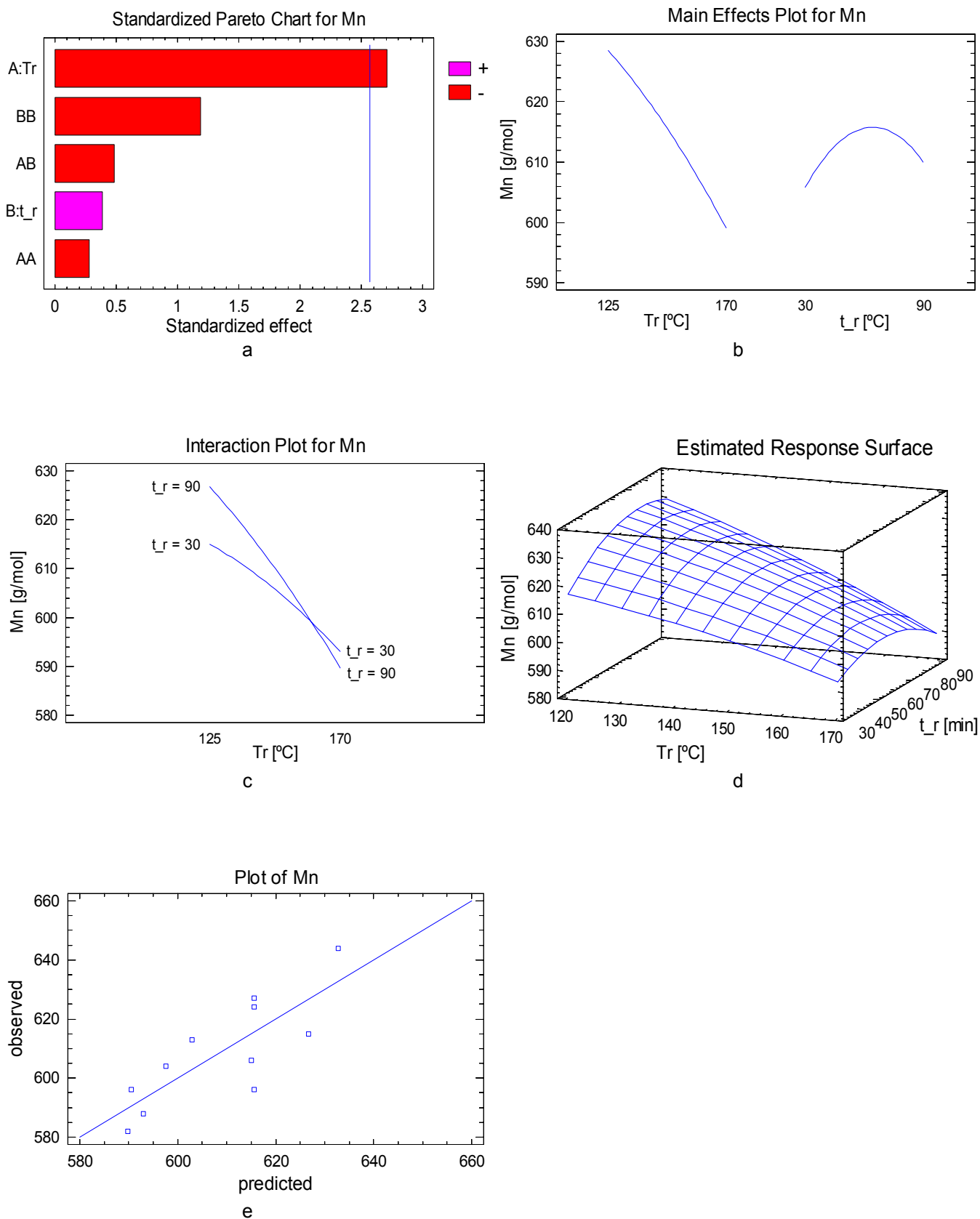


**Figure 6.10.** Statistical Plots for Mn Analysis  
 a. Pareto chart, b. Main effects plot, c. Interaction plot, d. Response Surface, e. Diagnostic plot

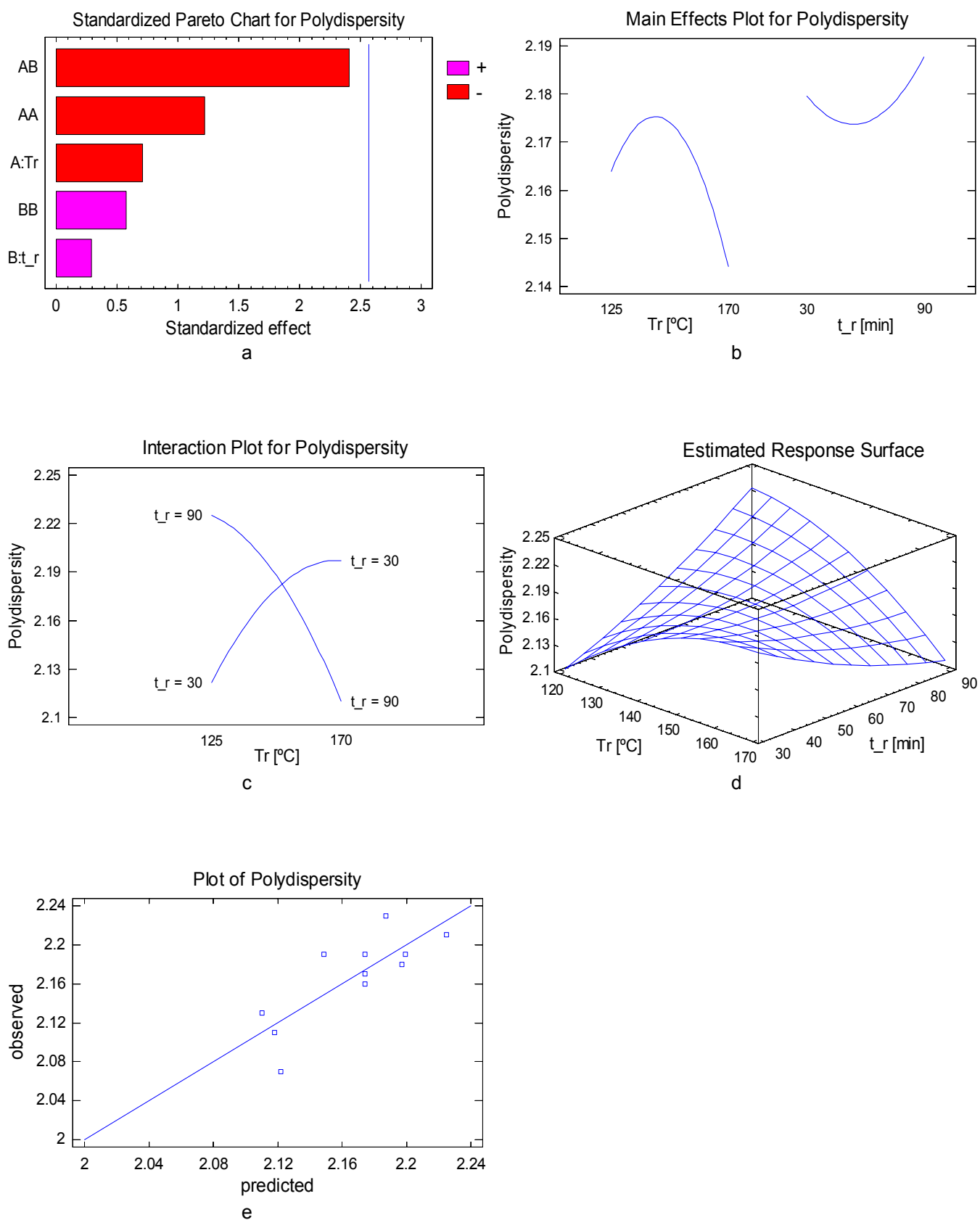


**Figure 6.11.** Statistical Plots for Polydispersity Analysis  
 a. Pareto chart, b. Main effects plot, c. Interaction plot, d. Response Surface, e. Diagnostic plot

### **6.3 CONCLUSIONS**

Kraft lignin behavior during reaction in an alkaline medium was modeled. The empirical models predict content of the various functional groups and the molecular weight of isolated lignin as a function of the treatment parameters. These models show that alkaline treatment of highly condensed lignins causes an increase in the content of the various functional groups, such as phenolic hydroxyl and aliphatic hydroxyl, and a decrease in impurities, such as sugars and extractives, as shown by the decreased ash content of the treated lignins. The alkaline treatment also caused an increase in the molecular weight of treated lignins compared to raw lignin; this increase in molecular weight combined with the increase in reactivity, make alkaline-treated lignins more suitable for formulating phenolic resins or for direct use in wood panels.

Modified Kraft lignin produced at 170°C for 90min (sample LK4) showed the best characteristics for formulating phenolic resins or for directly use in wood panels due to its high content of phenolic and aliphatic hydroxyls groups and active sites.

## REFERENCES

- Alonso. M. V.. J. J. Rodríguez. *et al.* Characterization and structural modification of ammoniac lignosulfonate by methylation. *Journal of applied polymer science* 82: 2661-2668. 2001.
- Dence. C. W. and S. Y. Lin. Introduction. in: *Methods in lignin chemistry*. C. W. Dence and S. Y. Lin. Berlin. Springer-Verlag. 1992
- El Mansouri. N.-E.. X. Farriol. *et al.* Structural Modification and Characterization of Lignosulfonate by a Reaction in an Alkaline Medium for Its Incorporation into Phenolic Resins. *Journal of applied Polymer Science* 102: 3286-3292. 2006.
- El Mansouri. N. E. and J. Salvadó. Structural Characterization of technical lignins for the production of adhesives: Application to lignosulfonate. Kraft. soda-anthraquinone. organosolv and ethanol process lignins. *Industrial crops and products* 24: 8-16. 2006.
- Fernández. A.. M. Oliet. *et al.* Caracterización de Ligninas Organosolv procedentes de Kenaf (*hibiscus Cannabinus* L). in: Congreso Ibero Americano de Celulosa y papel. 2004.
- Fierro. V.. V. Torné. *et al.* Activated carbons prepared from Kraft lignin by phosphoric acid impregnation. in: *Carbon'03 an international conference on carbon*. 2003.
- Forss. K. G. and K. E. Fremer. *The nature and reactions of lignin - A new paradigm*. Helsinki. Forss. K. G.; Fremer. K. E. 2003.
- Fredheim. G. E.. S. M. Braaten. *et al.* Comparison of Molecular Weight and Molecular Weight Distributions of Softwood and Hardwood Lignosulfonates. *Journal of wood and technology* 23(2): 197-215. 2003.
- Gargulak. J. G. and S. E. Lebo. Commercial use of lignin-based materials. in: *Lignin: Historical. Biological. and Materials Perspectives*. American Chemical Society. ACS Symposium series 742: 304-320. 2000.

- Gilarranz, M. A., F. Rodríguez. *et al.* Lignin Behavior During the autocatalyzed methanol pulping of Eucalyptus Globulus: Changes in molecular weight and functionality. *Holzforschung* 54: 373-380. 2000.
- Glasser, W. G. and J. H. Lora. Recent Industrial Applications of Lignin: A Sustainable Alternative to Nonrenewable Materials. *journal of polymers and the environment* 10(1-2): 39-47. 2002.
- Gonçalves, A. R. and P. Benar. Hydroxymethylation and oxidation of organosolv lignins and utilization of the products. *Bioresource technology* 79: 103-111. 2001.
- Gosselink, R. J. A., E. de Jong. *et al.* Co-ordination network for lignin—standardisation, production and applications adapted to market requirements (EUROLIGNIN). *Industrial crops and products* 20: 121-129. 2004.
- Lin, S. Y. Ultraviolet spectrophotometry. in: *Methods in lignin chemistry*. S. Y. Lin and C. W. Dence. Berlin. Springer-Verlag: 215-232. 1992
- McDonough, T. J. The chemistry of organosolv delignification. *Tappi Journal* 76(8): 186-193. 1993.
- Miller, J. E., L. Evans. *et al.* Batch microreactor studies of lignin and lignin model compound depolymerization by bases in alcohol solvents. *Fuel* 78: 1363–1366. 1999.
- Nimz, H. H. Lignin-based wood adhesives. in: *Wood adhesives : chemistry and technology*. A. Pizzi. New York. Marcel Dekker: 247-288. 1983
- Pranda, J., R. Brezny. *et al.* Structure and performance of Kraft lignin fractions as components in resole adhesives. *Tappi Journal* 74(8): 176-182. 1991.
- Sarkanen, K. V. Chemistry of solvent pulping. *Tappi Journal* 73(10): 215-219. 1990.
- Vázquez, G., J. González. *et al.* Effect of chemical modification of lignin on the gluebond performance or lignin-phenolic resins. *Bioresource technology* 60: 191-198. 1997.

Velásquez. J. A.. F. Ferrando. *et al.* Effects of kraft lignin addition in the production of binderless fiberboard from steam exploded *Miscanthus sinensis*. *Industrial crops and products* 18: 17-23. 2003.

## **7. EXOGENOUS LIGNIN ADDITION FOR THE PRODUCTION OF BINDERLESS FIBERBOARDS**

UNIVERSITAT ROVIRA I VIRGILI  
BINDERLESS FIBERBOARD PRODUCTION FROM CYNARA CARDUNCULUS AND VITIS VINIFERA  
Camilo Mancera Arias  
ISBN:978-84-692-1537-1/DL:T-300-2009



## CHAPTER 7

### Exogenous lignin addition for the production of binderless fiberboards

In this chapter, results of the exogenous addition of two different kinds of Kraft lignin for the production of fiberboards are shown. Different amounts of raw Kraft lignin and alkali treated lignin were used to the production of binderless fiberboards from *Vitis vinifera* prunings based on the optimum operational conditions found for this material, see chapter 5.

#### 7.1 INTRODUCTION

Byproducts of the forest products industry are potentially primary sources of natural resource-based adhesives. This industry is both a producer of huge tonnage of residues (pulp and paper industry) and a major consumer of adhesives (wood composites industry); because of this, research has been focused on adhesive from renewable resources derived from trees (*Hemingway and Conner 1989*).

Adhesives based on renewable resources had been successfully used in the wood products industry for long time before the expansion of the petrochemical industry provided compounds for synthetic resin adhesives at very low costs, thus displacing natural adhesives. The woodworking industry, converted completely to synthetics, grew and prospered until the worldwide crude oil crisis abruptly interrupted the access to low cost and seemingly endless raw materials supplies for synthetic resin adhesives. Wood product manufacturers reacted with an intermediate and partial return to natural adhesives but as oil's availability improved and prices became more competitive, synthetic resins adhesives became the industrial standard again. Even though oil crisis is long gone it remains in the memory of the woodworking industry, and current events in the Middle East increased the fears of another oil embargo or sudden regional war. Even if none of this occurs, the question of what is going to happen as world oil reserves become increasingly limited in the nor-too-distant future still remains (*Lambuth 1989*).

In a restrictive situation where petrochemicals are no longer freely available, the wood industry priorities would be:

1. To maintain the performances of any given wood product as near normal as possible and adequate for the public use.
2. To obtain adhesives which permit the manufacture of on-grade products at normal production rates and costs.
3. To exhaust all reasonable alternatives before changing plant process or reducing plant capacity, that could be caused by longer press times, more complex or limited assembly procedures, or restrictive handling requirements dictated by the operating features of the adhesives available. Loss of productive capacity for any of these reasons translates to higher unit costs, profit margins decrease and finally shutdown (*Lambuth 1989*).

Woodworking industry strongly endorses research dealing with the production of adhesives based on renewable resources, particularly due to its vulnerability to interruption in petrochemical raw material supplies for adhesive production and the fact that adhesives based on renewable resources may not be fully competitive in price or performance with currently synthetic adhesives should not be deterrent to their development and optimization. Moreover, the failure by industry to implement an adhesive based on renewable resources is not due to its performance or value but rather to the person's resistance to change not matter how small the real or perceived change might be. Nevertheless, adhesives based on renewable resources represent vital reserve technology for the woodworking industry that will be implemented as circumstances require (*Lambuth 1989*).

One of the primary objectives of lignin utilization research has been focused on the use of industrial lignins as binders or to incorporate them into phenolic wood adhesives for panel products. A thorough discussion of the development of lignin-based wood adhesives was done by Nimz (*Nimz 1983*).

Several studies have been carried out to assess fiber replacement by lignin during the production of fiberboards. Anglés et al. (*Anglés, Ferrando et al. 2001*) have tried the addition of different types of technical lignins and found that a fiber replacement up to 20% by Kraft lignin improved board's physical stability towards water as well as mechanical properties without affecting significantly the density of the boards. Subsequently, Velasquez et al. (*Velásquez, Ferrando et al. 2003*) studied the addition of Kraft lignin to steam exploded *Miscanthus sinensis* finding that increasing quantities of lignin improved fiberboard properties but also the presence of internal bubbles was increased, this problem was somehow reduced mixing the *Miscanthus* fibers with the Kraft lignin before the steam explosion, thus reducing the amount of low molecular

weight substances present in commercial Kraft lignins (i.e. carbohydrates, inorganic and organic extractives) and improving the mixing between fibers and exogenous lignin.

In the present study, an attempt was made to use different amounts of alkali treated Kraft lignin and compared to the addition of same amounts of raw Kraft lignin in the production of binderless fiberboards from steam exploded *Vitis vinifera* and to explore whether Kraft lignin can be used as a natural adhesive to enhance the fiberboard properties.

## 7.2 RESULTS AND DISCUSSIONS

In this part of the research, we only used one experimental factor, lignin addition percentage, with four levels, which were chosen based on the literature review and previous experiences on production of binderless boards with exogenous lignin addition inside the investigation group. Lignin addition percentage levels chosen were: 5%, 10%, 15% and 20%. The figures and tables shown in the results also include the 0% level, which corresponds to *Vitis vinifera* binderless fiberboard produced at the optimum conditions found in the analysis reported in chapter 5. Addition of alkali treated Kraft lignin and crude acid washed Kraft lignin will be analyzed separately and afterwards comparison between them will be done based on SEM microphotographs analysis and on the individual analysis based on the experimental design.

Characteristics of the experimental design employed and descriptions of the statistical plots employed during the analysis can be found in chapter 3.

### 7.2.1 Alkali treated Kraft lignin exogenous addition

In this section, I will discuss the physical and mechanical properties variations found as a consequence of the substitution of varying amounts of steam exploded *Vitis vinifera* fibers by alkali treated Kraft lignin. Table 1 shows the results obtained. Each of the response variables will be analyzed separately using the tools of the experimental design. For each response variable a variance analysis was performed at a confidence level of 95%.

**Table 1.** Alkali treated Kraft lignin exogenous addition

	% Lignin Added	Density [Kg/m <sup>3</sup> ]	MOR [Mpa]	MOE [Mpa]	IB [Mpa]	WA [%]	TS [%]
	0	1376	24	4331	0.14	12.6	8.8
	0	1386	25	3876	0.12	13.1	9.1
	0	1384	26	4198	0.15	11.8	9.0
Alkali treated Kraft Lignin	5	1347	39	5234	0.26	8.9	3.9
	5	1330	39	5552	0.29	8.6	4.1
	5	1348	40	5329	0.24	9.3	3.8
	10	1376	28	4994	0.33	10.8	8.6
	10	1358	34	4748	0.33	10.1	9.3
	10	1362	28	4578	0.32	10.7	8.5
	15	1291	27	4261	0.27	12.0	7.1
	15	1304	28	4382	0.30	11.5	6.0
	15	1302	31	4106	0.26	12.1	6.2
	20	1147	24	3211	0.23	7.0	5.2
	20	1152	24	2883	0.18	6.8	5.4
20	1150	22	3116	0.20	5.7	5.1	

### 7.2.1.1 Density

ANOVA table for density is shown in table 7.2 and the statistical plots for density are shown in figure 7.1. Since the P-value of the F-test is less than 0.05 (see table 7.2), there is a statistically significant difference between the mean density from one level of alkali treated Kraft lignin addition to another at a 95% confidence level. Figure 7.1b shows that the means for all the intervals of lignin addition are significantly different between each other. Scatter plot, figure 7.1a, shows that there is a pattern indicating that increasing quantities of alkali treated Kraft lignin decrease the density of the boards; this is caused by the formation of internal bubbles into the boards that could be caused, in turn, by the accumulation of lignin in located points inside the boards and the subsequent formation of polymerized lignin networks. Formation of these lignin networks are desired if they are distributed and attached properly to the fibers but undesirable if they are formations involving only lignin molecules that could cause the appearance of voids inside the boards.

Figure 7.1d shows that a replacement of 20% of the fibers by alkali treated Kraft lignin decrease drastically the density of the fiberboards and that the mean of the interval is well beyond the decision limits of the grand mean. This is caused by a generalization of the effect commented above.

**Table 7.2.** Variance Analysis for Density

Source	Sum of Squares	Df	Mean Square	F-Ratio	P-Value
Between groups	1.05E+05	4	2.63E+04	477.9	0
Within groups	5.50E+02	10	5.50E+01		
Total (Corr.)	1.06E+05	14			

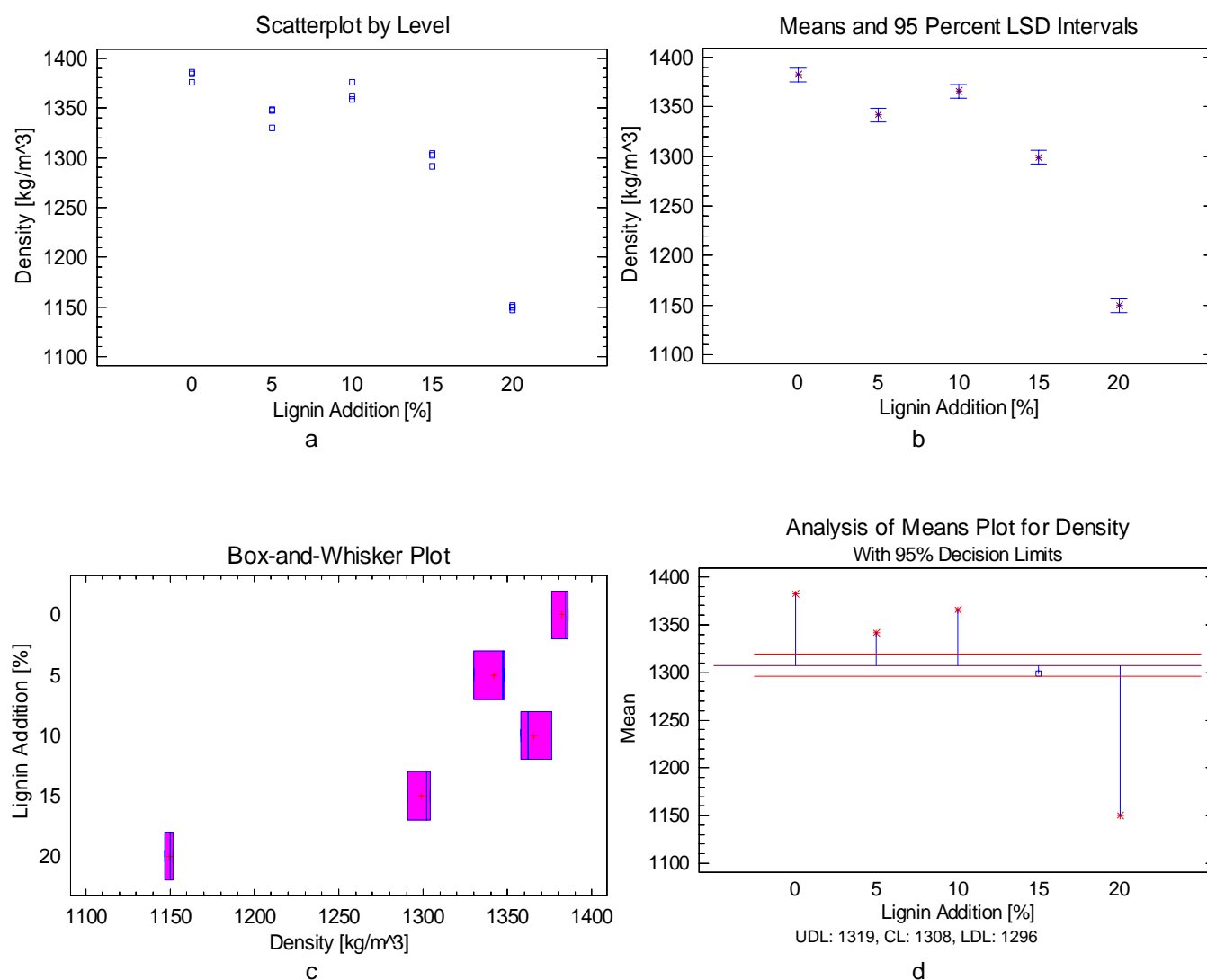


**Figure 7.1** Statistical plots for Density analysis

a. Scatter plot, b. Means and 95% LSD intervals plot, c. Box and Whisker plot, d. Analysis of mean plot

### 7.2.1.2 Mechanical properties (MOR, MOE, IB)

The modulus of rupture (MOR) and modulus of elasticity (MOE) were analyzed together because they came from the same bending assay. ANOVA tables for MOR and MOE are shown in tables 7.3 and 7.4, respectively. The statistical plots for MOR and MOE are shown in figures 7.2 and 7.3, respectively. Since the P-value of the F-test is less than 0.05 for both MOR and MOE (see table 7.3 and 7.4), there is a statistically significant difference between the means of MOR and MOE from one level of alkali treated Kraft lignin addition to another at a 95% confidence level. To determine which means are significantly different from which others, we must focus our attention in figure 7.2b and 7.3b.

Figure 7.2b shows that there is a statistically significant difference between the means of all the intervals except for the means of 0%-20% and 10%-15%. The scatter plot, figure 7.2a, shows that a 5% of fiber replacement by alkali treated Kraft lignin improves the MOR but increasing amounts of lignin are adverse; even returning to the initial values at 20% of replacement.

Figure 7.2d shows that the mean of the interval of 5% of lignin addition is beyond the decision limits of the grand mean, this indicates that part of the lignin added develops lignin networks connecting fiber between them, but when the lignin quantity is increased internal defects arise where lignin molecules gather together.

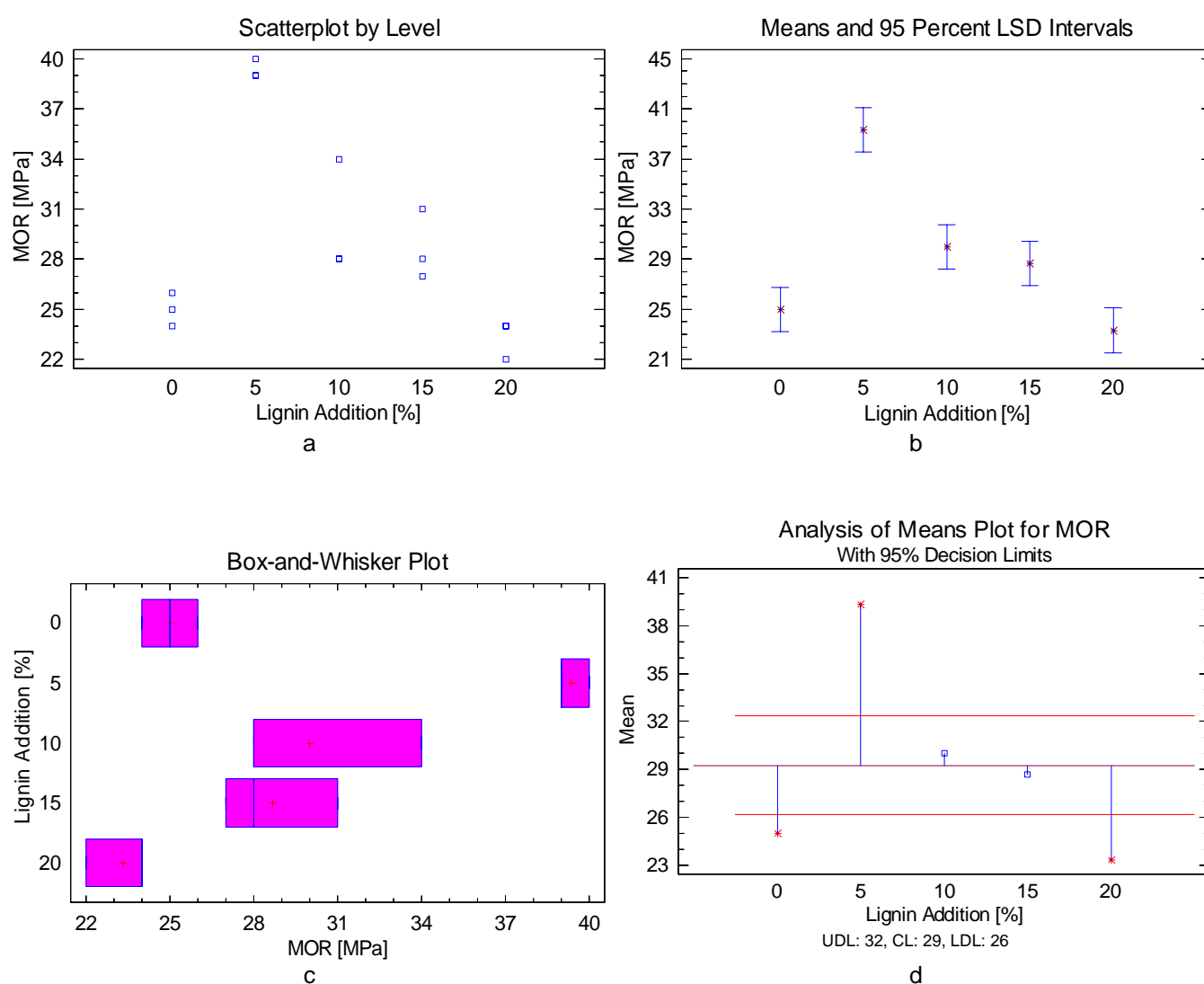
Figure 7.3b shows that there is a statistically significant difference between the means of all the intervals except for the mean of 0%-15%. The scatter plot, figure 7.3a, shows that, as well as for MOR, a 5% of fiber replacement by alkali treated Kraft lignin improves the MOE but increasing quantities of lignin are adverse; going even to lower values than the material without exogenous lignin addition at 20% of replacement.

Figure 7.3d shows that the mean value of the interval 5% of lignin addition, as well as for MOR, is beyond the decision limits of the grand mean; supporting the theory that alkali treated lignin partially accomplish the desired function but it is not able to develop its full potential to increase the stiffness and interfiber bond strength.

MOR and MOE present a similar behavior compared to density. High amounts of fiber replacement by alkali treated Kraft lignin are adverse to fiberboard conformation. Increased reactivity of lignin could cause that lignin prefers to react with itself rather than to attach to *Vitis vinifera* fibers and act like a matrix, this cause internal defects and ineffective distribution of efforts inside the fiberboard.

**Table 7.3.** Variance analysis for MOR

Source	Sum of Squares	Df	Mean Square	F-Ratio	P-Value
Between groups	4,67E+02	4	1,17E+02	30.72	0
Within groups	3,80E+01	10	3,80E+00		
Total (Corr.)	5,05E+02	14			



**Figure 7.2** Statistical plots for MOR analysis

a. Scatter plot, b. Means and 95% LSD intervals plot, c. Box and Whisker plot, d. Analysis of mean plot

**Table 7.4.** Variance analysis for MOE

Source	Sum of Squares	Df	Mean Square	F-Ratio	P-Value
Between groups	8.74E+06	4	2.18E+06	63.24	0
Within groups	3.45E+05	10	3.45E+04		
Total (Corr.)	9.09E+06	14			

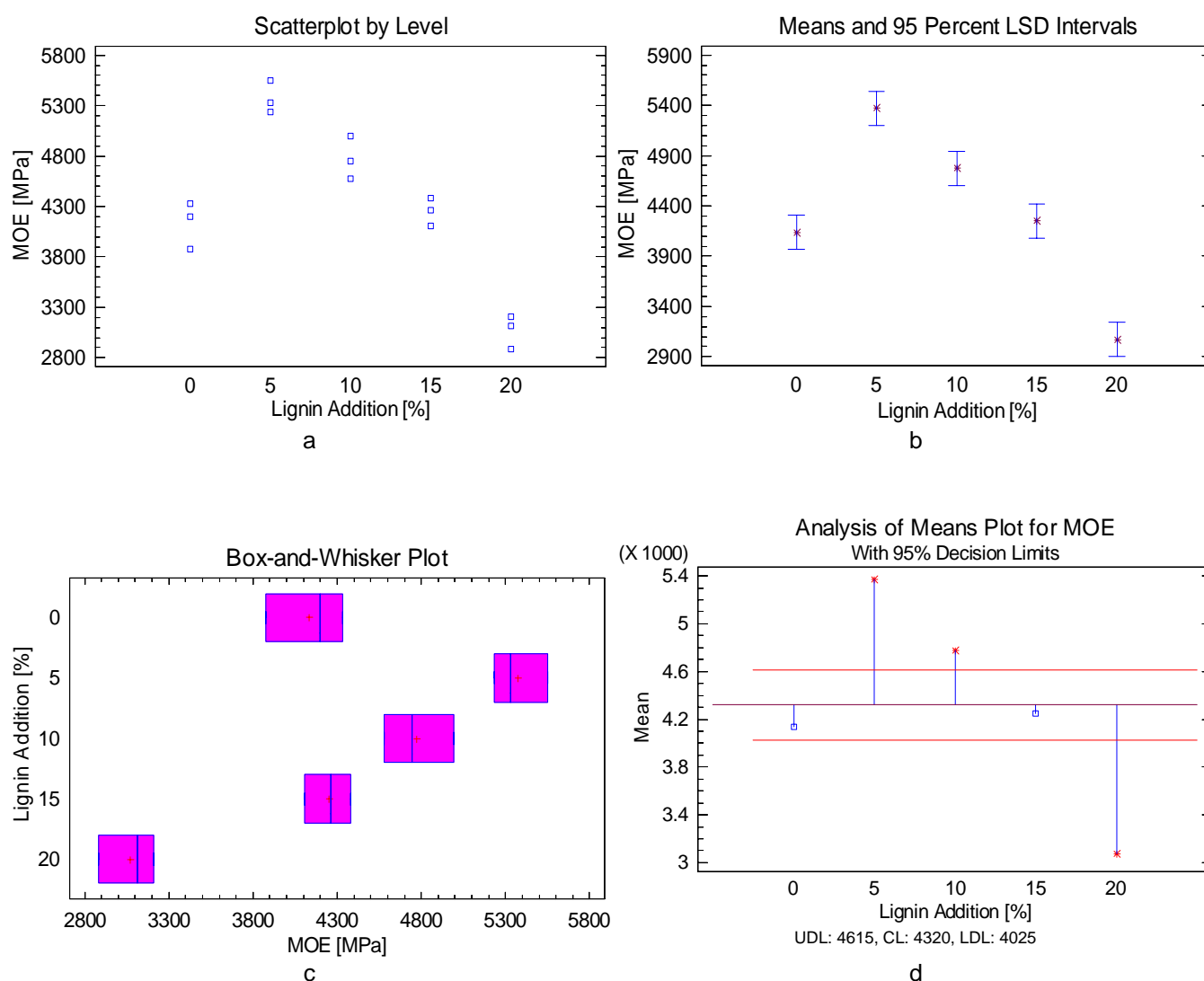


**Figure 7.3** Statistical plots for MOE analysis

a. Scatter plot, b. Means and 95% LSD intervals plot, c. Box and Whisker plot, d. Analysis of mean plot



As mentioned before in previous chapters, internal bond (IB) is the mechanical property that accounts for the strength of the bonds between the fibers; because the fibers are mainly oriented in the board plane the IB measures the tension perpendicular to the faces of the board. It is particularly in this property in which the addition of exogenous lignin is expected to improve the performance of fiberboards, because lignin is the main responsible of interfiber bond strength. ANOVA table for IB is shown in table 7.5 and the statistical plots are shown in figure 7.4. Since the P-value of the F-test is less than 0.05 for IB (see table 7.5), there is a statistically significant difference between the means of IB from one level of alkali treated Kraft lignin addition to another at a confidence level of 95%. Figure 7.4b shows that there is a statistically significant difference between the means of all the intervals except for the means of 5%-15%. The scatter plot, figure 7.4a, shows that an increase of fiber replacement by alkali treated Kraft lignin improves IB, but increasing quantities of lignin addition beyond 10% is detrimental, even though fiberboards with 15% and 20% of fiber replacement by lignin present better performance in IB than *Vitis vinifera* fiberboards without any addition of exogenous lignin.

Figure 7.4d shows that the mean of the interval of 10% of lignin addition is beyond the decision limits of the grand mean, indicating that part of the lignin added is actually performing the desired function of developing adhesive networks which connect fibers between them and improve the strength of parallel planes inside the board, but we should improve the technique used to mix the exogenous lignin with the fibers and also improve the affinity of alkali treated Kraft lignin towards fiber surface to avoid the appearance of localized high concentrations of polymerized lignin where there is not any fiber.

**Table 7.5.** Variance analysis for IB

Source	Sum of Squares	Df	Mean Square	F-Ratio	P-Value
Between groups	6.42E-02	4	1.61E-02	40.83	0
Within groups	3.93E-02	10	3.93E-02		
Total (Corr.)	6.82E-02	14			

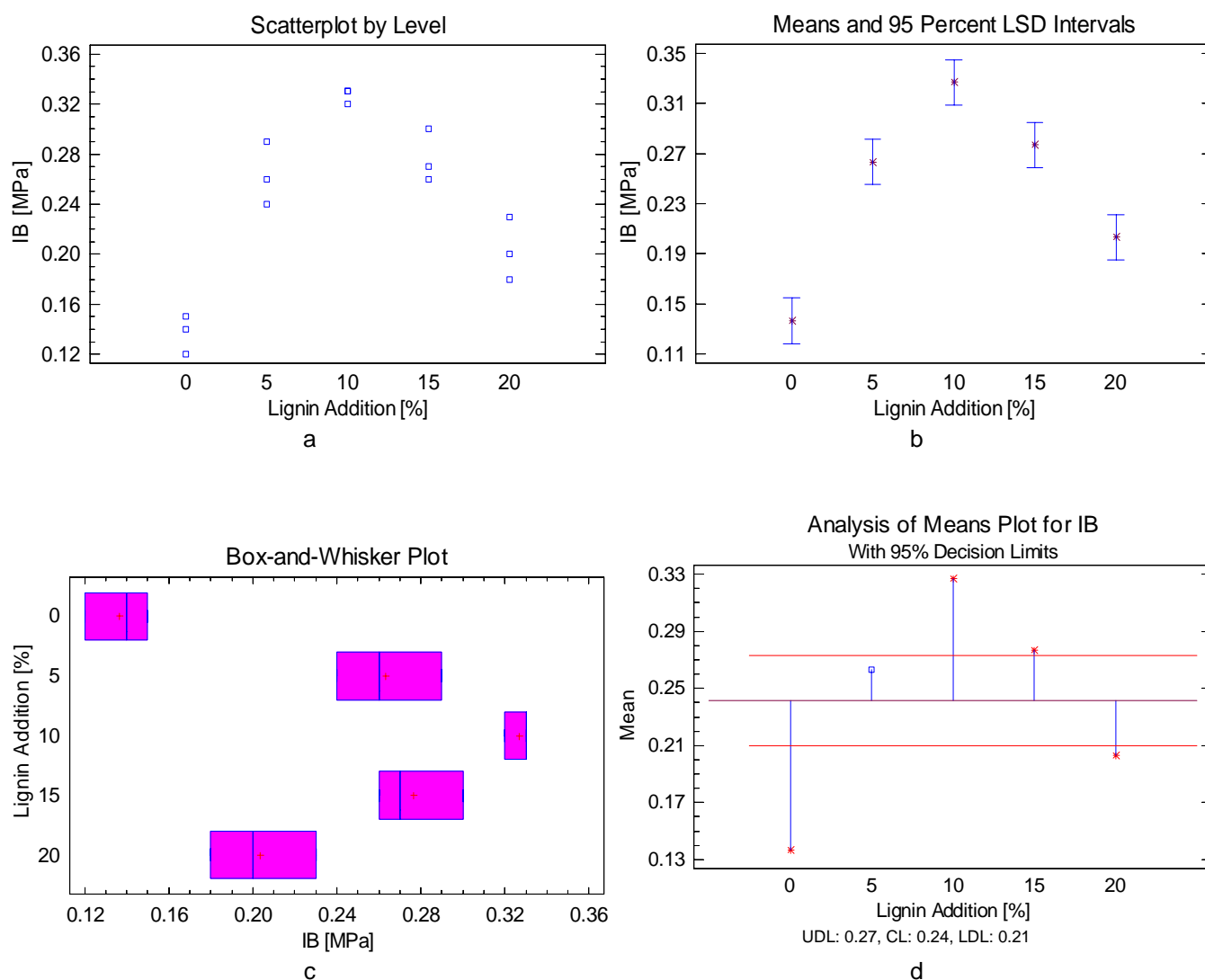


**Figure 7.4** Statistical plots for IB analysis

a. Scatter plot, b. Means and 95% LSD intervals plot, c. Box and Whisker plot, d. Analysis of mean plot

### 7.2.1.3 Physical properties (WA, TS)

Water absorption (WA) and Thickness swelling (TS) are the physical properties related with the dimensional stability of the boards. These properties give us an idea of how the boards will behave when used under conditions of severe humidity, they are especially important to boards for external use. WA and TS were analyzed together because came from the same assay. ANOVA tables for WA and TS are shown in tables 7.6 and 7.7, respectively. The statistical plots for WA and TS are shown in figures 7.5 and 7.6, respectively. Since the P-value of the F-test is less than 0.05 for both WA and TS (see table 7.6 and 7.7), there is a statistically significant difference between the means of WA and TS from one level of alkali treated Kraft lignin addition to another at a 95% confidence level. To determine which means are significantly different from which others, we must focus our attention in figure 7.5b and 7.6b.

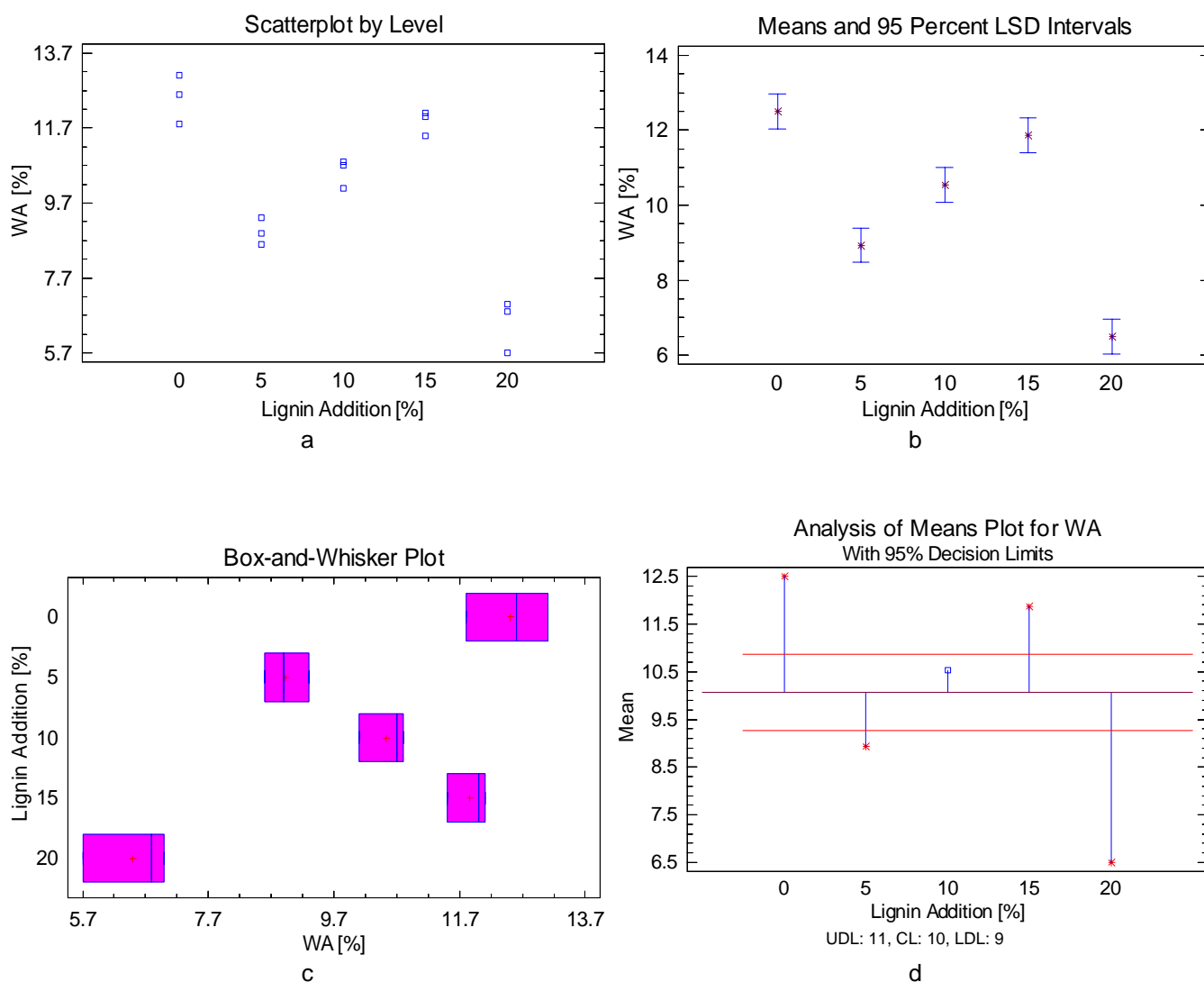
Figure 7.5b shows that there is a statistically significant difference between the means of all the intervals except for the means of 0%-15%. The scatter plot, figure 7.5a, shows that all the intervals involving lignin addition present lower WA than the interval of 0% of lignin addition, even though the interval of 15% of lignin addition seems to present lower WA values than 0% interval, this can not be confirmed by the statistical analysis based on the Fisher least significant difference at a 95% confidence level. Figure 7.5a also shows that 20% of fiber replacement by alkali treated lignin presents the lowest values of WA, as low as 6.5%.

Figure 7.5d shows that a replacement of 20% of fibrous material by alkali treated Kraft lignin diminished drastically the WA of the fiberboards. The characteristics of lignin as a plastic can easily explain this performance. After the vapor pretreatment of *Vitis vinifera* prunings, part of the cellulose and the remaining hemicelluloses have been replaced by exogenous lignin, providing a higher resistance to water permeation.

Figure 7.6b shows that there is a statistically significant difference between the means of all the intervals studied except for the means of 0%-10%. The scatter plot, figure 7.6a, shows that all the intervals involving lignin addition present lower TS than the interval of 0% of lignin addition. However, it should be notice that the tools of experimental design analysis can not confirmed a significant difference between 10% lignin addition interval and 0% lignin addition interval. Figure 7.6a also shows that 5% and 20% fiber replacement by lignin present the lowest values of TS, as low as 3.9% and 5.2%, respectively. Lignin confers impermeability toward water intake to the *Vitis vinifera* fibers, but it should be properly distributed over the fibers to be a positive influence on the water stability of the boards; same problems arise here when lignin accumulates in localized points inside the fiberboards creating voids where water could be accumulated.

**Table 7.6.** Variance analysis for WA

Source	Sum of Squares	Df	Mean Square	F-Ratio	P-Value
Between groups	7.02E+01	4	1.75E+01	67.98	0
Within groups	2.58E+00	10	2.58E-01		
Total (Corr.)	7.27E+01	14			



**Figure 7.5** Statistical plots for WA analysis

a. Scatter plot, b. Means and 95% LSD intervals plot, c. Box and Whisker plot, d. Analysis of mean plot

**Table 7.7.** Variance analysis for TS

Source	Sum of Squares	Df	Mean Square	F-Ratio	P-Value
Between groups	5.83E+01	4	1.46E+01	120.71	0
Within groups	1.21E+00	10	1.21E-01		
Total (Corr.)	5.95E+01	14			

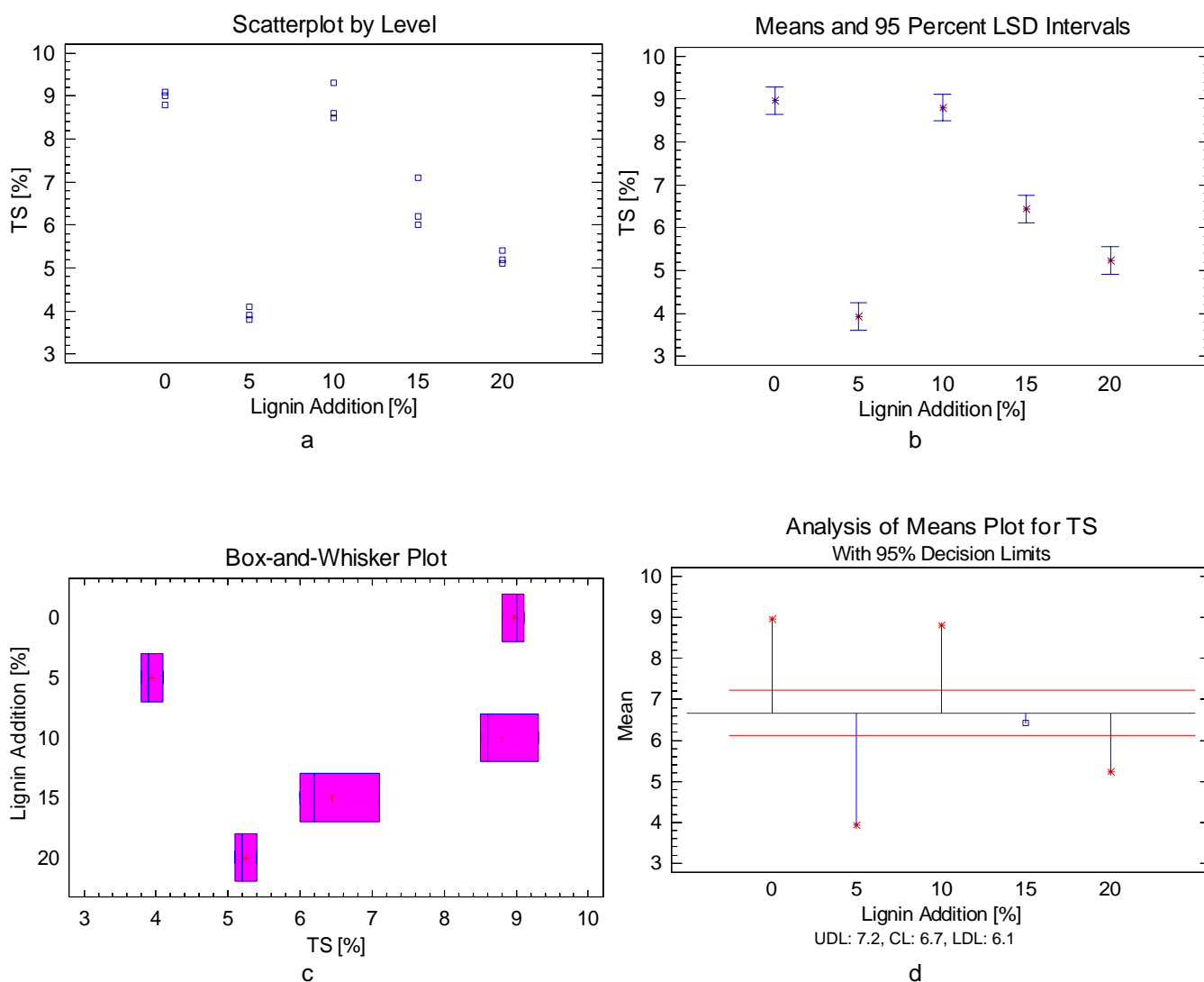


**Figure 7.6** Statistical plots for TS analysis

a. Scatter plot, b. Means and 95% LSD intervals plot, c. Box and Whisker plot, d. Analysis of mean plot

## 7.2.2 Crude acid washed Kraft lignin exogenous addition

In this section, I will discuss the physical and mechanical properties variations found as a consequence of the substitution of varying amounts of steam exploded *Vitis vinifera* fibers by crude acid washed Kraft lignin. Table 7.8 shows the results obtained. Each of the response variables will be analyzed separately using the tools of the experimental design described in chapter 3. For each response variable a variance analysis was performed at a confidence level of 95%.

**Table 7.8.** Crude acid washed Kraft lignin exogenous addition

	% Lignin Added	Density [Kg/m <sup>3</sup> ]	MOR [Mpa]	MOE [Mpa]	IB [Mpa]	WA [%]	TS [%]
	0	1376	24	4331	0.14	12.6	8.8
	0	1386	25	3876	0.12	13.1	9.1
	0	1384	26	4198	0.15	11.8	9.0
Crude Acid Washed Kraft Lignin	5	1362	40	5073	0.33	12.2	9.1
	5	1365	41	4940	0.24	12.3	9.3
	5	1367	43	5135	0.27	11.6	8.5
	10	1369	42	5671	0.53	9.0	7.1
	10	1366	43	5334	0.49	8.8	7.4
	10	1368	44	5436	0.53	9.5	6.8
	15	1378	48	6014	0.70	9.0	4.0
	15	1368	45	6481	0.67	9.5	4.2
	15	1374	46	6219	0.62	10.3	4.3
	20	1362	50	5665	1.09	3.9	2.1
	20	1380	52	5610	1.12	3.3	1.6
	20	1382	55	5592	1.06	4.2	1.7

### 7.2.2.1 Density

ANOVA table for density is shown in table 7.9 and the statistical plots for density are shown in figure 7.7. Since the P-value of the F-test is less than 0.05 (see table 7.9), there is a statistically significant difference between the mean density from one level of crude Kraft lignin addition to another at a 95% confidence level. Figure 7.7b shows that there are only two means (0%-5% and 0%-10%) of intervals which are significantly different from each other. Scatter plot, figure 7.7a, shows that there is not a great difference between the densities of the fiberboards produced with exogenous lignin and those without any addition of lignin. This is confirmed by the analysis of means plot, figure 7.7d, where we can see that none of the means is significantly different from the grand mean.

**Table 7.9.** Variance analysis for Density

Source	Sum of Squares	Df	Mean Square	F-Ratio	P-Value
Between groups	5.41E+02	4	1.35E+02	3.69	0.0428
Within groups	3.67E+02	10	3.67E+01		
Total (Corr.)	9.08E+02	14			

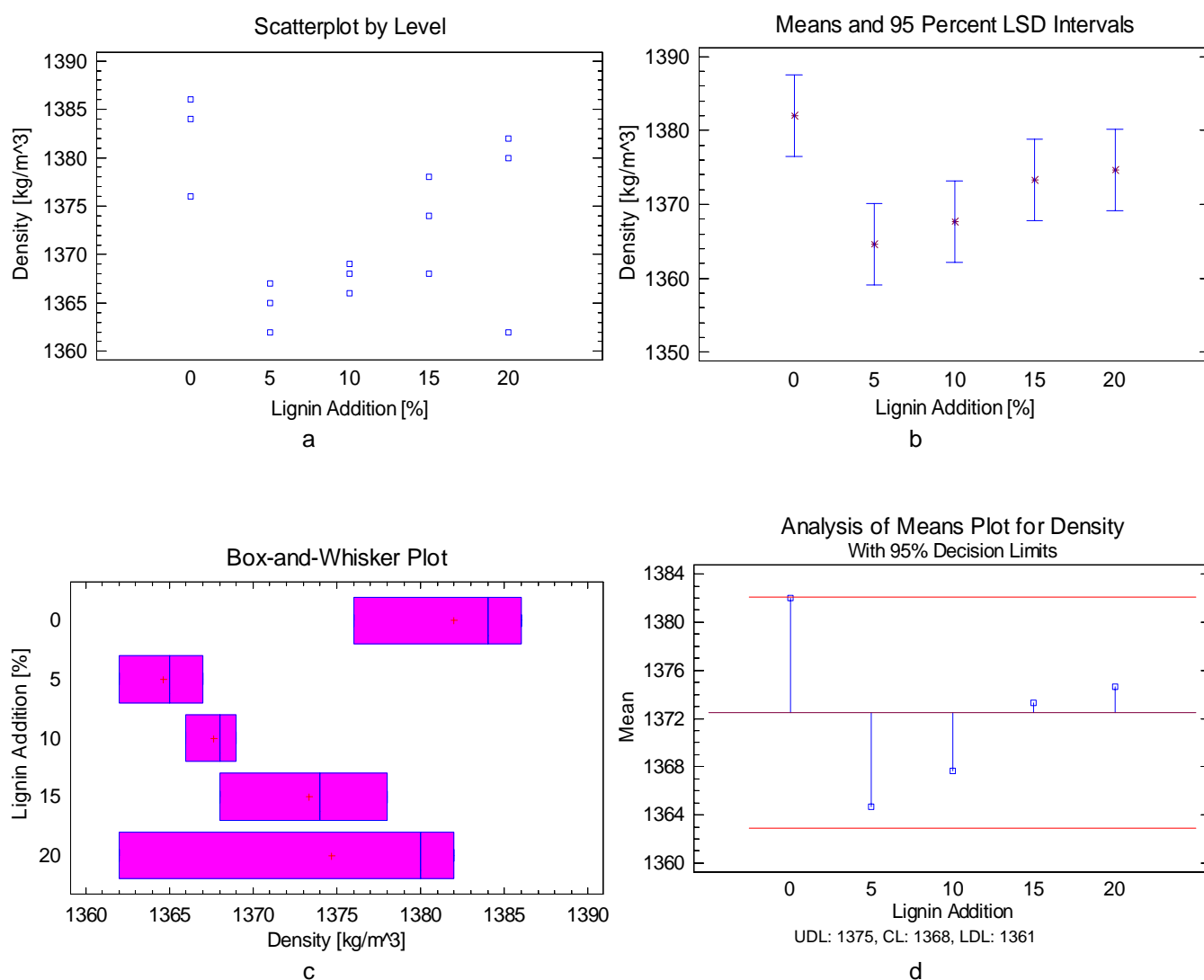


**Figure 7.7** Statistical plots for Density analysis

a. Scatter plot, b. Means and 95% LSD intervals plot, c. Box and Whisker plot, d. Analysis of mean plot

### 7.2.2.2 Mechanical properties (MOR, MOE, IB)

The modulus of rupture (MOR) and modulus of elasticity (MOE) were analyzed together because they came from the same bending assay. ANOVA tables for MOR and MOE are shown in tables 7.10 and 7.11, respectively. The statistical plots for MOR and MOE are shown in figures 7.8 and 7.9, respectively. Since the P-value of the F-test is less than 0.05 for both MOR and MOE (see table 7.8 and 7.9), there is a statistically significant difference between the means of MOR and MOE from one level of crude Kraft lignin addition to another at a 95% confidence level. To determine which means are significantly different from which others, we must focus our attention in figure 7.8b and 7.9b.

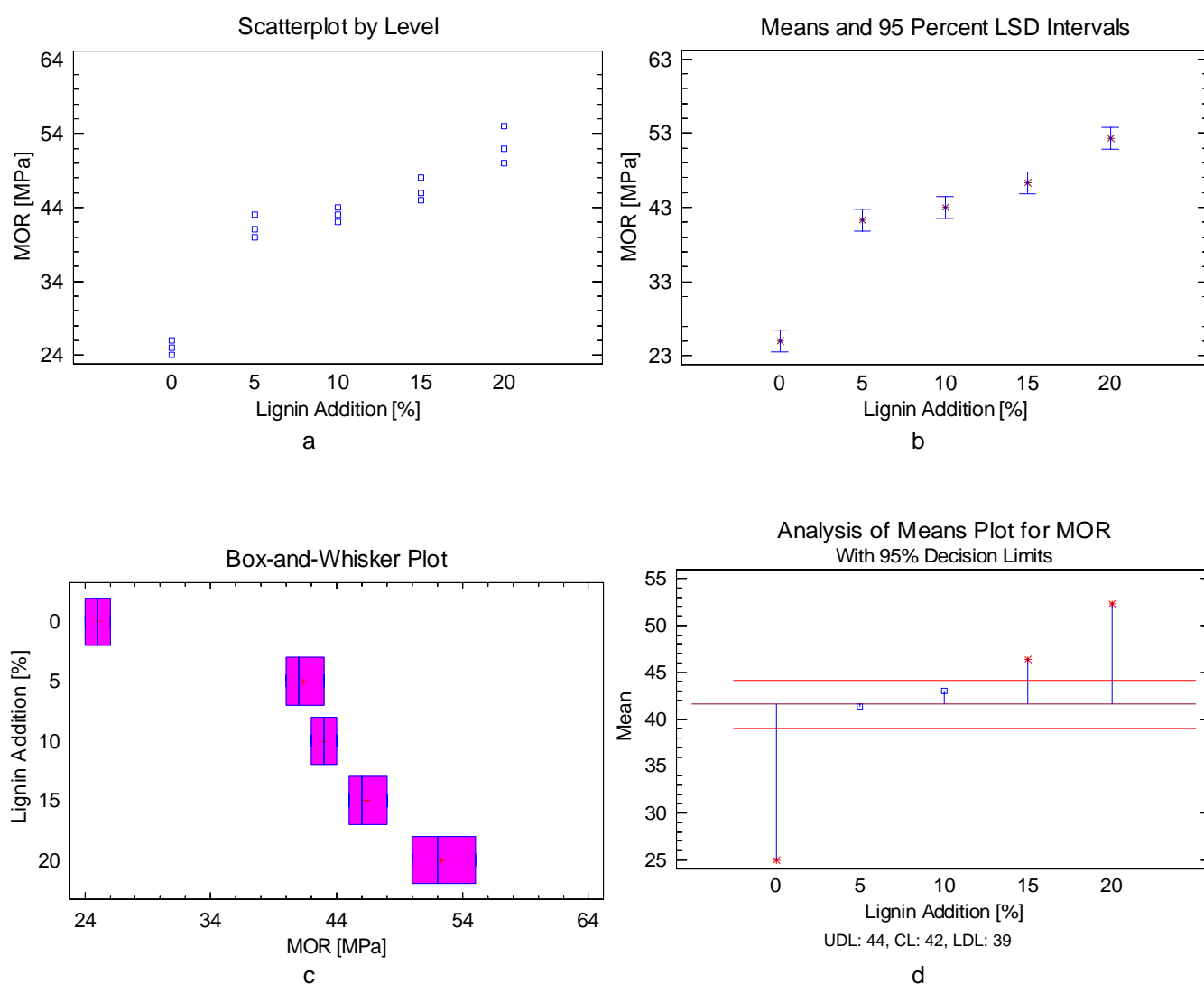
Figure 7.8b shows that there is a statistically significant difference between the means of all the intervals except for the means of 5%-10%. The scatter plot, figure 7.8a, shows that increasing amounts of crude Kraft lignin addition have a beneficial effect on the MOR, obtaining results as high as twice the results obtained without any addition of lignin when adding 20% of crude Kraft lignin. MOR values for 0% interval were around 25 MPa while MOR values for 20% interval were around 52 MPa. These results are confirmed by figure 7.8d, in which significant difference between 0%, 15% and 20% of crude lignin addition can be found, compared to the grand mean.

Figure 7.9b shows that there is a statistically significant difference between the means of all the intervals except for the mean of 10%-20%. The scatter plot, figure 7.9a, shows that there is a pattern in which increasing quantities of crude Kraft lignin improve MOE, similar to the MOR behavior, but for MOE the best values are found at 15% crude Kraft lignin addition. MOE values for the interval 0% were around 4135 MPa while MOE values for the interval of 15% of lignin addition were around 6238 MPa. Likewise than for MOR, figure 7.9d confirm these results. Acid washing of crude Kraft lignin was done with the intention of hydrolyzing organic compounds that could cause bubbles during hot pressing of the boards and to improve physical stability of boards towards water intake. Differences between MOR and MOE behaviors can be explained by the impossibility of completely remove hemicelluloses and organic volatile compounds with the acid washing treatment of commercial Kraft lignin. These compounds could cause internal defect in the boards during hot pressing, limiting the practical amount of crude Kraft lignin addition that can be used to improve fiberboard properties.



**Table 7.10.** Variance analysis for MOR

Source	Sum of Squares	Df	Mean Square	F-Ratio	P-Value
Between groups	1.25E+03	4	3.11E+02	119.77	0
Within groups	2.60E+01	10	2.60E+00		
Total (Corr.)	1.27E+03	14			



**Figure 7.8** Statistical plots for MOR analysis  
 a. Scatter plot, b. Means and 95% LSD intervals plot, c. Box and Whisker plot, d. Analysis of mean plot

**Table 7.11.** Variance analysis for MOE

Source	Sum of Squares	Df	Mean Square	F-Ratio	P-Value
Between groups	7.31E+06	4	1.83E+06	60.6	0
Within groups	3.02E+05	10	3.02E+04		
Total (Corr.)	7.61E+06	14			

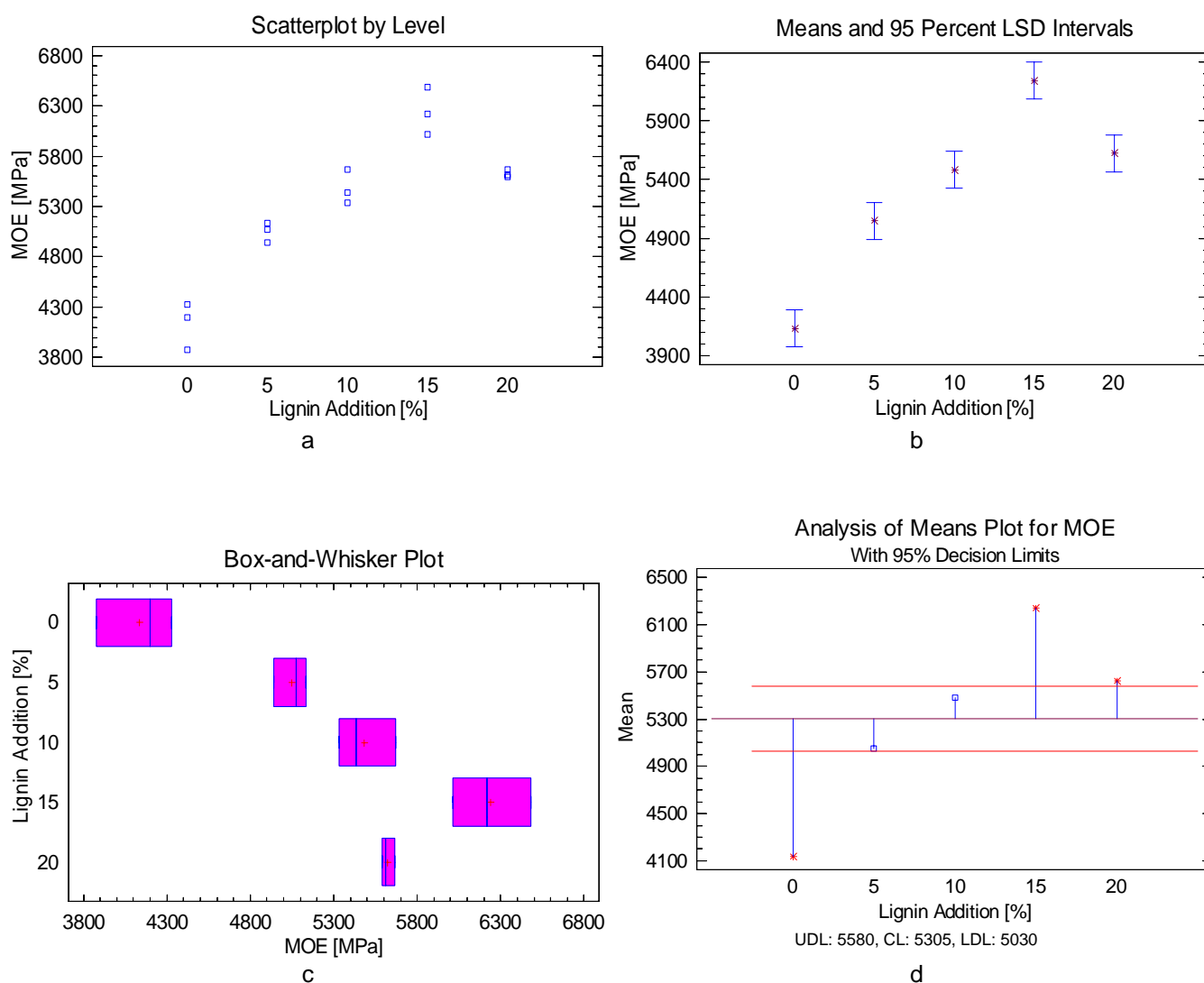


**Figure 7.9** Statistical plots for MOE analysis

a. Scatter plot, b. Means and 95% LSD intervals plot, c. Box and Whisker plot, d. Analysis of mean plot

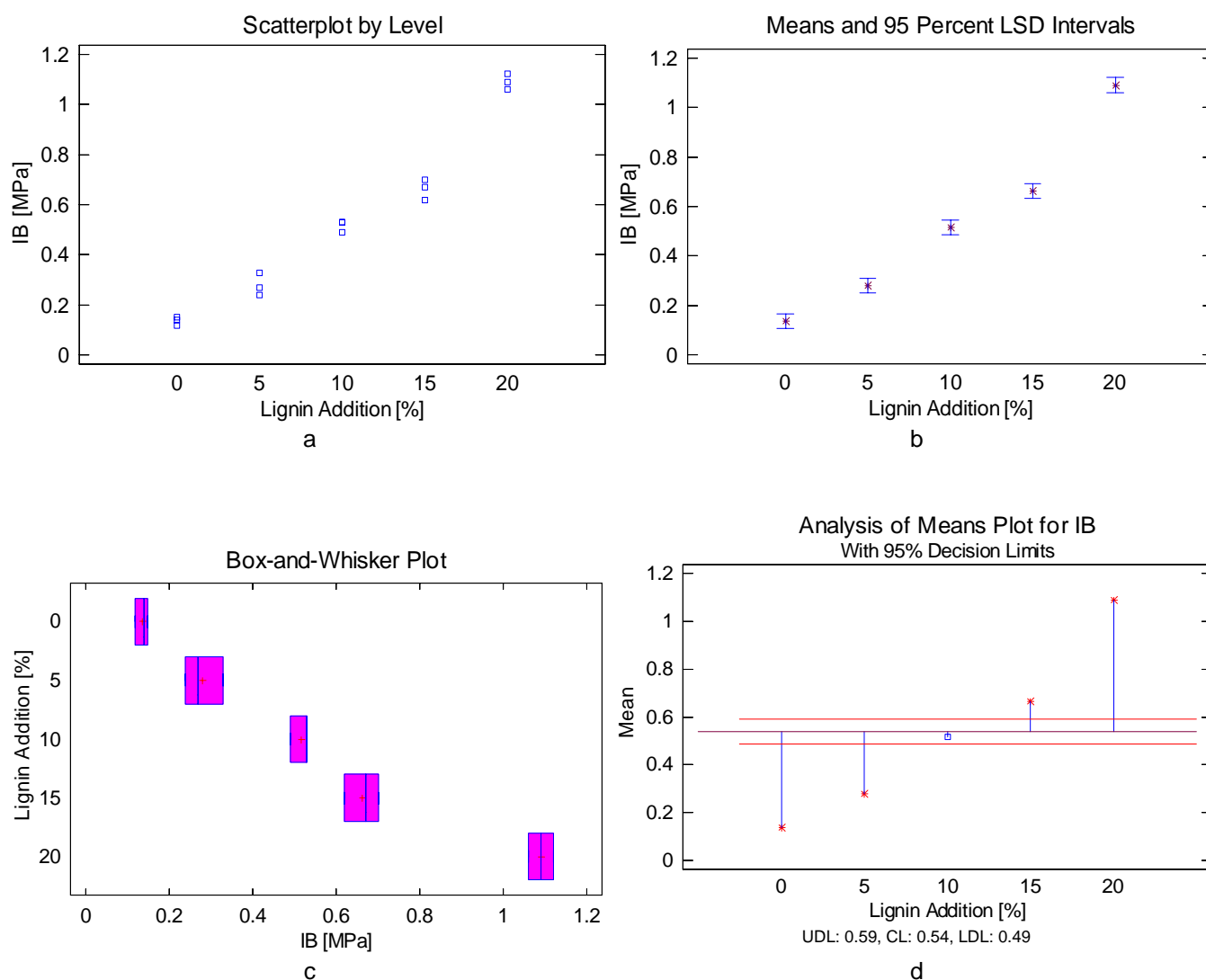
ANOVA table for IB is shown in table 7.12 and the statistical plots are shown in figure 7.10. Since the P-value of the F-test is less than 0.05 for IB (see table 7.12), there is a statistically significant difference between the means of IB from one level of crude Kraft lignin addition to another at a confidence level of 95%.

Figure 7.12b shows that there is a statistically significant difference between the means of all the intervals. The scatter plot, figure 7.12a, shows that an increase of fiber replacement by crude Kraft lignin improves IB developing a pattern pretty similar to the behaviors of MOR and MOE. This is also confirmed by the analysis of means show in the figure 7.12d, where 0%, 5%, 15% and 20% are beyond the decision limits of the grand mean. All the intervals involving exogenous lignin addition presented a significant improvement over the production of *Vitis vinifera* binderless fiberboards without exogenous lignin addition.

Acid washed Kraft lignin develops three dimensional adhesive networks that improve all the mechanical properties of the boards, but proper distribution of this exogenous material between fibers should be improved to extend the beneficial effects of lignin addition throughout the whole board and to avoid localized high concentrations of lignin. Lignin matrix inside the wood composite materials has the function of communicate the stress suffer by the composite to the fibers, and to correctly do this the fiber-matrix interface adhesion is crucial (Saheb and Jog 1999). As we can see from the results obtained with the addition of alkali treated Kraft lignin; even though the lignin has more active sites and it is more reactive, which could allow us to foresee an improved performance related to developing of three-dimensional adhesive networks, it is not a guarantee that composites will perform better if affinity of the fibers surface to the alkali treated Kraft lignin does not fit the needs. In this sense, acid washed Kraft lignin, even though less reactive and with less active sites, have proved to perform better due to its affinity towards fibers surface.

**Table 7.12.** Variance analysis for IB

Source	Sum of Squares	Df	Mean Square	F-Ratio	P-Value
Between groups	1.65E+00	4	4.11E-01	380.9	0
Within groups	1.08E-02	10	1.08E-03		
Total (Corr.)	1.66E+00	14			



**Figure 7.10** Statistical plots for IB analysis

a. Scatter plot, b. Means and 95% LSD intervals plot, c. Box and Whisker plot, d. Analysis of mean plot

### 7.2.2.3 Physical properties (WA, TS)

Water absorption (WA) and Thickness swelling (TS) are the physical properties related with the dimensional stability of the boards. These properties give us an idea of how the boards will behave when used under conditions of severe humidity, they are especially important to boards for external use. WA and TS were analyzed together because came from the same assay. ANOVA tables for WA and TS are shown in tables 7.13 and 7.14, respectively. The statistical plots for WA and TS are shown in figures 7.11 and 7.12, respectively. Since the P-value of the F-test is less than 0.05 for both WA and TS (see table 7.13 and 7.14), there is a statistically significant difference between the means of WA and TS from one level of alkali treated Kraft lignin addition to another at a 95% confidence level.

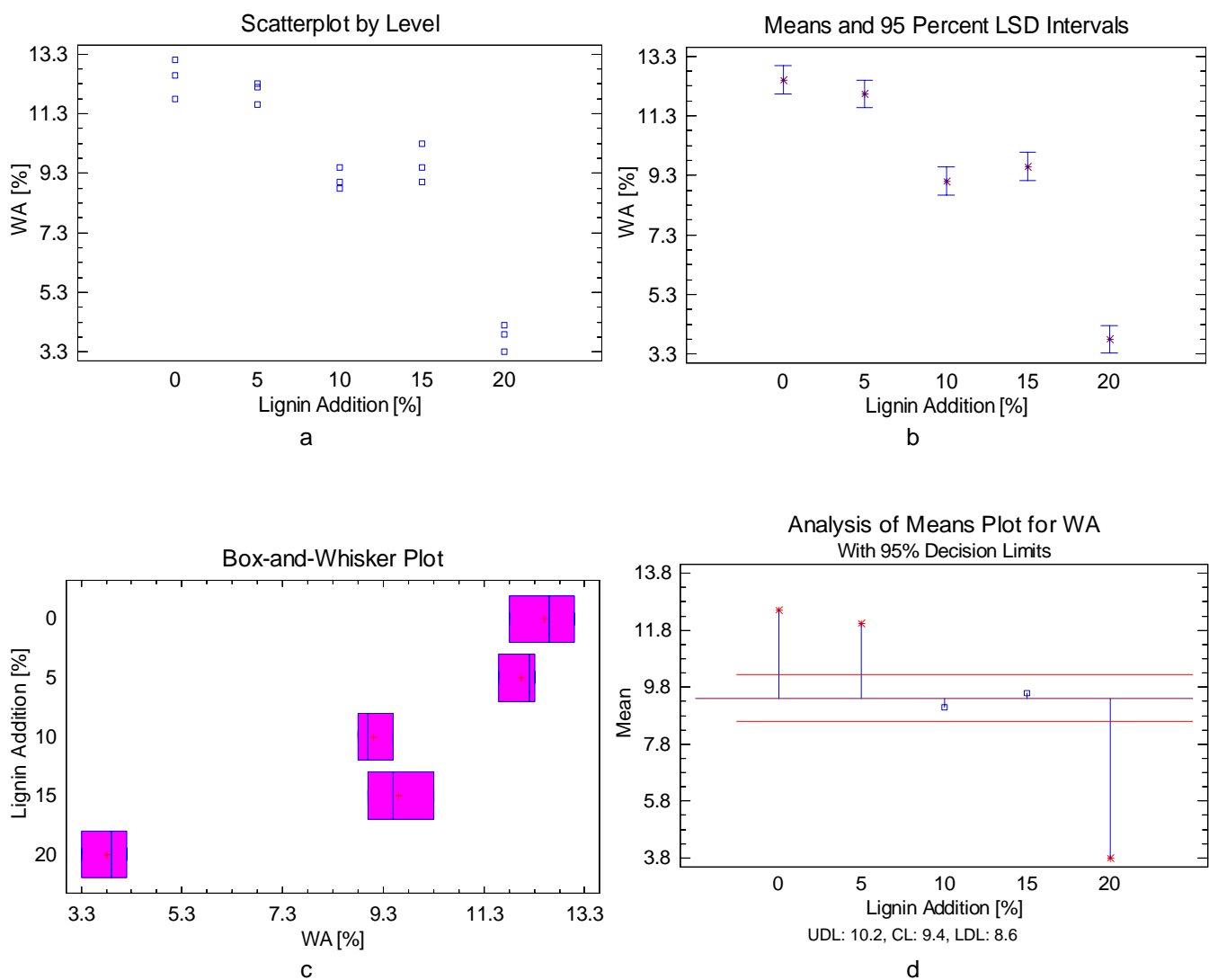
Figure 7.11b shows that all the intervals exhibit a statistically significant difference between each other, except for the intervals 0%-5% and 10%-15%. The scatter plot, figure 7.11a, shows that increasing quantities of crude Kraft lignin addition improve the WA of fiberboards, diminishing it. Figure 11a also shows that 20% fiber replacement by crude Kraft lignin present the fiberboards with the lowest values of WA; values as low as 3.8%. This value is lower than the obtained with the addition of same amount of alkali treated Kraft lignin. This can be explained by the permeation of water into the cavities formed where alkali treated lignin develops adhesive networks in absence of fibers. Figure 7.11d confirmed that a 20% replacement of fibers by crude Kraft lignin drastically diminished the WA of fiberboards

Figure 7.12b shows that all the intervals exhibit a statistically significant difference between each other, except for the intervals 0%-5%. The scatter plot, figure 7.12a, shows that TS present a similar behavior than WA, in which increasing amounts of acid washed crude Kraft lignin enhance the physical stability of the fiberboards towards water intake. We can see that 20% of fiber replacement by crude Kraft lignin presents the lowest value of TS; values around 1.8% were found in this interval. Comparisons between fiberboards produced based on alkali treated and crude Kraft lignins show that, as well as for WA, although both types of lignin additions enhance the fiberboard performance; crude Kraft lignin addition presents more consistent improvement and better results than alkali treated Kraft lignin addition.

Differences between values of WA and TS are cause by the quantities each of these values account for. WA takes into account the water taken by the fibers as well as the water located into the cavities or internal defects presented in the boards, while TS only takes into account the absorption of water by the fibers and its consequent swelling.

**Table 7.13.** Variance analysis for WA

Source	Sum of Squares	Df	Mean Square	F-Ratio	P-Value
Between groups	1.44E+02	4	3.60E+01	134.09	0
Within groups	2.69E+00	10	2.69E-01		
Total (Corr.)	1.47E+02	14			



**Figure 7.11** Statistical plots for WA analysis

a. Scatter plot, b. Means and 95% LSD intervals plot, c. Box and Whisker plot, d. Analysis of mean plot

**Table 7.14.** Variance analysis for TS

Source	Sum of Squares	Df	Mean Square	F-Ratio	P-Value
Between groups	1.19E+02	4	2.97E+01	390.92	0
Within groups	7.60E-01	10	7.60E-02		
Total (Corr.)	1.20E+02	14			

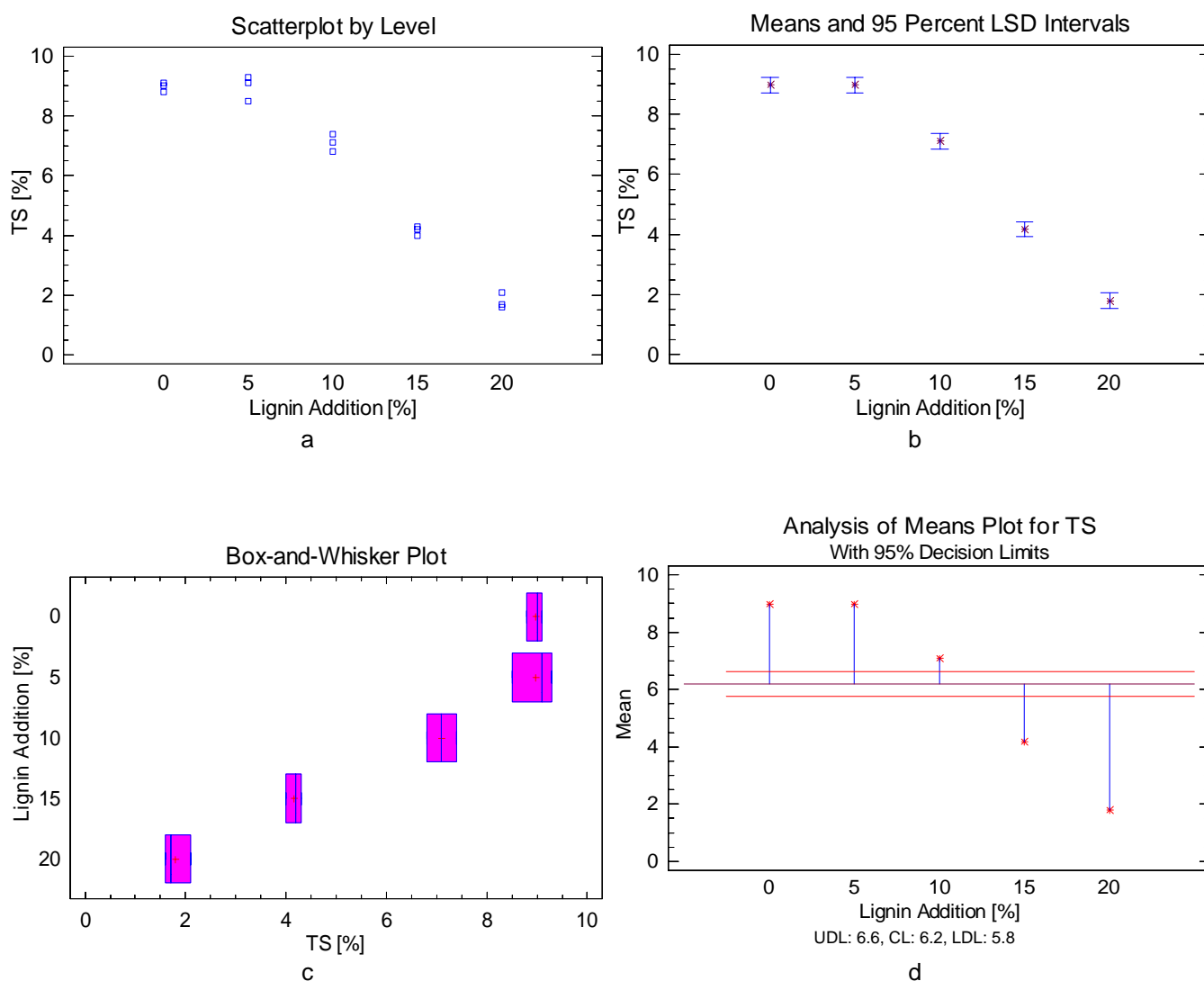


**Figure 7.12** Statistical plots for TS analysis

a. Scatter plot, b. Means and 95% LSD intervals plot, c. Box and Whisker plot, d. Analysis of mean plot

### 7.2.3 Observations by scanning electron microscope (SEM)

The internal bond (IB) test was performed in order to study the internal adhesion between the lignin matrix and the fibers and to assess the suitability of alkali treated Kraft lignin and crude Kraft lignin exogenous addition for the production of binderless fiberboards. The test consists in separating the major parallel planes one from the other inside the boards until it breaks. The measure of the strength needed to do so give us a value of IB. We can imagine that what is looked for is the linkage strength between the different parallel planes of fibers. By performing the test this way, we are measuring the weakest union between the parallel planes in the board.

Statistical analysis of IB values obtained with different amounts of alkali treated and crude Kraft lignins was already done and reported above. Some comparisons between those values were also mentioned during the analysis of the statistical information. SEM microphotographs just pretend to support the results found in previous sections and to show graphically the differences presented by the rupture surfaces of fiberboards when the two different types of exogenous lignin studied were employed.

Figure 7.13 a, c, e. show IB test rupture surfaces of fiberboards produced with 5%, 10% and 20% of fibrous material replacement by alkali treated Kraft lignin, respectively. Corresponding pictures of crude Kraft lignin are shown in figure 7.13 b, d and f. As we can see, the rupture surfaces of fiberboards with alkali treated lignin addition presented three-dimensional networks of lignin with the formation of cavities due to the absence of fibers; this behavior is more or less extended over the rupture surface of the fiberboards directly depending on the quantity of alkali treated lignin added. On the other hand, the rupture surfaces of fiberboards with crude Kraft lignin addition presented developed three-dimensional networks of lignin but fully integrated with the fibers, obtaining in this way the best combination of properties from the lignin matrix and the fibers reinforcement acting like a whole. Main differences found during the statistical analysis of boards produced using these two types of Kraft lignin are principally due to the lack of adhesion or affinity between alkali treated Kraft lignin and fibers surface. Thus the treatment of fibers or the chemical modification of alkali treated Kraft lignin became a critical step to improve adhesion and subsequently produced binderless fiberboards with enhanced properties.



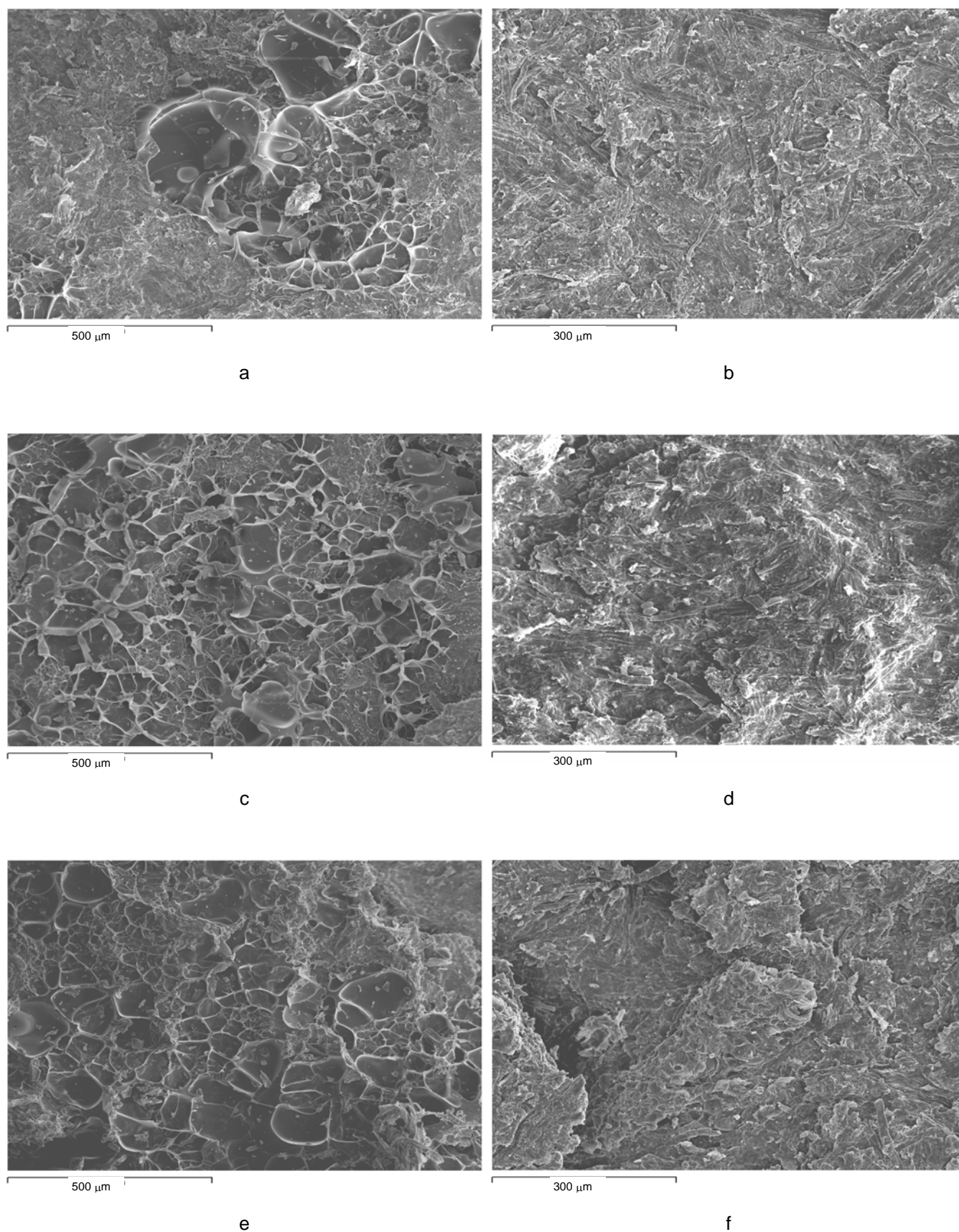


**Figure 7.13.** SEM Microphotographs of IB tested fiberboards  
a, c, e. 5%, 10%, 20% Alkali treated Kraft lignin addition; b, d, f. 5%, 10%, 20% Crude Kraft lignin addition

### 7.3 CONCLUSIONS

Exogenous lignin addition has proved to enhance mechanical and physical properties of binderless fiberboards from *Vitis vinifera* prunings. As any other composite, reconstituted wood composites should present good surface adhesion or affinity between matrix and fibers and good dispersion of the fibers in the matrix to perform properly during use. When any of these elements fail, poor behavior of composites emerges. It is in this sense that, although promising, alkali treated Kraft lignin do not performed as good as crude Kraft lignin.

Alkali treated Kraft lignin has proved to have the ability to develop three-dimensional networks at the conditions tested to produced the fiberboards but more efforts should be employed to enhance its affinity towards fibers an be able to exploit its full adhesive potential.

The addition of crude Kraft lignin in different amounts has helped to improve all the parameters tested. Further work has to be developed to determine the maximum allowable addition of this type of lignin without losing mechanical properties.

## REFERENCES

Anglès, M. N., F. Ferrando, *et al.* Suitability of steam exploded residual softwood for the production of binderless panels. Effect of the pretreatment severity and lignin addition. *Biomass & Bioenergy* 21(3): 211-224. 2001.

Hemingway, R. W. and A. H. Conner. Opportunities for future development of adhesives from renewable resources. in: Adhesives from renewable resources. R. W. Hemingway and A. H. Conner, Ed. ACS symposium series, 385. 1989

Lambuth, A. L. Adhesives from renewable resources - Historical perspective and wood industry needs. in: Adhesives from renewable resources. R. W. Hemingway and A. H. Conner, Ed. ACS symposium series, 385: 1-10. 1989

Nimz, H. H. Lignin-based wood adhesives. in: Wood adhesives - Chemistry and technology. A. Pizzi, Ed. New york: 247-288. 1983

Saheb, D. N. and J. P. Jog. Natural fiber polymer composites: A review. *Advances in polymer technology* 18(4): 351-363. 1999.

Velásquez, J. A., F. Ferrando, *et al.* Effects of Kraft lignin addition in the production of binderless fiberboard from steam exploded *Miscnathus sinensis*. *Industrial crops and products* 18: 17-23. 2003.

UNIVERSITAT ROVIRA I VIRGILI  
BINDERLESS FIBERBOARD PRODUCTION FROM CYNARA CARDUNCULUS AND VITIS VINIFERA  
Camilo Mancera Arias  
ISBN:978-84-692-1537-1/DL:T-300-2009

## **GENERAL CONCLUSIONS, SYNTHESIS AND FUTURE WORK**

UNIVERSITAT ROVIRA I VIRGILI  
BINDERLESS FIBERBOARD PRODUCTION FROM CYNARA CARDUNCULUS AND VITIS VINIFERA  
Camilo Mancera Arias  
ISBN:978-84-692-1537-1/DL:T-300-2009

## General Conclusions, Synthesis and Future Work

We shall not cease from exploration  
And the end of all our exploring  
Will be to arrive where we started  
And know the place for the first time.

Thomas Stearns Eliot

In this last chapter are detailed the general conclusions from each of the objectives established at the beginning of the research based on the results obtained and their respective discussions. Subsequently, suggestions about future research work are mentioned.

### Steam explosion pretreatment

Pretreatment of lignocellulosic material is essential for the production of binderless fiberboards because of the various physical and chemical barriers that greatly restrain its use directly in its natural form.

The best pretreatment options are those which combine elements of both physical and chemical methods. In this regards, high pressure steaming, with flash expansion is one of the most successfully used options for fractionating wood into its three major component, cellulose, lignin and hemicelluloses; causing structural and chemical changes in the lignocellulosic material.

The steam pretreatment in a batch reactor involves heating lignocellulosic material chips at high temperatures and pressures, followed by a mechanical disruption of the material by a violent discharge into a collecting tank. The high pressure steam modifies the plant cell structure, producing a dark brown material together with a liquid of a lighter color. Solid fraction is mainly composed of cellulose and residual hemicelluloses and chemically modified lignin. The liquid fraction is composed mainly of hydrolyzed hemicelluloses and other minor mineral and organic extractives.

The more drastic the conditions used for the pretreatment (higher severities), the greater the relative amount of Klason lignin present in the pretreated material. At lower pretreatment severities, there is a partial conversion of acid-instable polysaccharides into water soluble sugars but in the mid-range of pretreatment severities, these soluble

sugars are partially lost as dehydration by-products (i.e. furfural and hydroxymethylfurfural), causing a further increase in the relative amount of lignin, at this conditions, some of the lignin may also undergo partial hydrolysis. At last, at extremely high pretreatment temperatures (220-240°C) and residence times into the steam explosion reactor, condensation reactions involving lignin, cellulose and hemicelluloses derived by-products take place, leading to the production of acid-insoluble extraneous-polymeric materials.

Physically, increasing severities cause diminishing fibers length, with two recognizable effects: shorter fibers could cause poorer mechanical properties but at the same time shorter fibers translate to higher contact surface, which in turn could cause better adhesion between fibers and improved mechanical properties.

Physical properties of binderless fiberboards are also affected by pretreatment severity. As mentioned above, increasing pretreatment severities diminish the hemicelluloses content in the pretreated material and due to their high hygroscopicity the final fiberboards are much more stable in presence of water.

Therefore, pretreatment optimization results from a compromise between all the consequences mentioned above caused by two opposite trends, increasing pretreatment severities or decreasing ones.

Other important factor influencing pretreatment efficiency is the permeability of the lignocellulosic tissue to the penetrating steam. Based on its morphological characteristics and structural properties one lignocellulosic material can be more porous and generally more permeable to steam than another, affecting directly the ease of steam pretreatment and its subsequent fractionation.

Particularly for the two lignocellulosic materials studied, the optimal conditions found for the steam explosion pretreatment were very similar, namely, high temperatures, around 218 °C and intermediate reaction times, around 5-6 min.

### **Hot pressing conditions**

Wood based composites manufacturing by means of heat and mechanical pressure is a very common and well known process. The hot pressing operation is one of the most important and is often the bottle neck of the production process. This is why studies in this area are focus on improving board performance, reduce pressing time, minimize energy consumption and maximize wood utilization.

Hot pressing functions are to consolidate the fiber mat to a desirable panel density and thickness, to cure or polymerized the adhesive, and to heat stabilize the panel so it remains at the desired thickness and density.



Heating is not only necessary to shorten the polymerization time of the adhesive (lignin for binderless fiberboards), but also to soften lignocellulosic material, allowing to achieve a high degree of board densification using minimum board pressure. The density of the boards obtained is no uniform, presenting higher density in the surface layers and lower density in the core. This density profile is the result of spatial and temporal interaction between board pressure and heat and mass transfer during the hot pressing.

Heat and mass transfer during the hot pressing involves two mechanisms of transport, conduction and convection. Heat is transferred from the press platens to the material by conduction. The water contained in the lignocellulosic-material surface layers vaporizes due to the fast heating of board surfaces in direct contact with the press at the beginning of the process. Water vapor movement is induced towards decreasing vapor pressure in the board core. The vapor carries its latent heat of vaporization and sensible heat, which allows heating of the board core. During relaxation step, vapor moves out of the board. Vapor flow has major implications on the heating of the board core and the relief of internal pressure.

During the hot pressing process the relationship between pressure and board density is govern by a very complex strain-stress compression process, at the same time the board temperature and moisture content flow is a coupled heat and mass transfer process and finally both, the mechanical deformation process and the heat and mass transfer process interact with each other as follows: while heat and moisture soften the material facilitating board densification, the change in board density significantly affects the heat conduction and moisture flow. The heat transfer causes the flow of moisture or vice versa. Additionally, polymerization of the lignin can result in the release or absorption of heat and water, which in turn may affect the heat and mass transfer process. The bonds formed between the lignin and the fibers have an important effect over the board deformation behavior particularly spring-back during and after pressing. This coupling and interactive nature of the hot pressing process makes it very difficult to predict the fiberboard properties based on the controllable process factors.

Board conditions during pressing such as temperature, moisture content, and gas pressure (air plus water vapor) are closely related to basic board properties including thermal conductivity and permeability. Permeability controls the convective heat and mass transfer from surfaces to core, and the ease with which internal vapor evaporates from board center to its edges during pressing and from core to surfaces during press opening (relaxation step and final opening of the press). Thus, the former controls the

rate of core temperature rise and consequently the lignin polymerization and the final controls the minimization of blows and blisters in finished boards and pressing time.

Particularly for the two lignocellulosic materials studied, we found some differences between *Cynara cardunculus* and *Vitis vinifera* during the pressing process. The optimal conditions found were somehow different but the process factors were compensated between them. For instance, optimal pressing temperature for *Cynara* was higher but optimal pressing pressure was lower than *Vitis* optimal pressing temperature and optimal pressing pressure, respectively. These differences can be explained based on the different basic properties existing between the two materials (i.e. compressibility, conductivity, porosity) and their differences in chemical composition.

Pressing temperature must be at least 200 °C for plasticize the lignin and promoting its proper distribution between fibers and its subsequent polymerization, developing adhesive three-dimensional networks. Furthermore, this temperature allows dehydration and even polymerization of the remaining hemicelluloses, producing more suitable compounds for board hot pressing.

Optimal pressing times for both *Cynara* and *Vitis*, were located in the lower part of the range studied. This is environmentally and economically encouraging for an eventual commercialization of binderless panels from any of these two materials.

### **Exogenous lignin addition**

Lignin is one of the most valuable and abundant renewable resources found on Earth. In Nature, lignin forms the matrix sheath around the fibers that holds the plants structure together.

When manufacturing reconstituted wood composites, compatibility of the matrix and the fibers and proper distribution of lignin matrix between fibers are critical to ensure a good behavior of the composite during use.

Generally, the addition of lignin has a synergic effect over increasing water stability of the fiberboards. Lignin, behaves as in nature covering remaining hemicelluloses and cellulosic fibers, thus avoiding water absorption by these hydrophilic compounds. Particularly, crude acid-washed Kraft lignin have proved to be more effective than alkali treated Kraft lignin, this is because acid-washed Kraft lignin was found to have better compatibility with *Vitis vinifera* fibers than alkali treated lignin, thus covering fibers to a higher extent. However, fiberboards with increasing quantities of both alkali-treated and acid-washed Kraft lignins behave better in presence of water than the control boards without exogenous lignin addition.

Mechanical properties were also improved with the addition of exogenous lignin. Particularly, crude acid-washed Kraft lignin due to its higher affinity towards *Vitis* fibers and its capacity to develop three-dimensional adhesive networks. Although, alkali treated Kraft lignin failed to consolidate fiberboards as a composite acting like a whole, its adhesive properties were developed and three dimensional adhesive networks were formed.

### **Comparison between lignocellulosic materials**

*Cynara cardunculus* by itself and *Vitis vinifera* with crude acid-washed lignin addition have been successfully used for manufacturing binderless fiberboards that fulfill the European standards. *Cynara cardunculus* stalks are a more suitable material for binderless fiberboards production than *Vitis vinifera* prunings, due to their structural, morphological and chemical differences.

The stalks of *C. cardunculus* are about 1.5–1.9 m tall branching in the upper half. In cross-section the stalks are circular with a slightly grooved surface and longitudinally they are homogeneous, without nodes.

*Vitis vinifera* is a perennial, woody climbing plant that, when left to grow freely can reach more than 30 m long, but in cultivation usually reduced by annual pruning to 1 to 3 m bush. Its trunk twisted and tortuous, presents a thick and rugged crust that comes off in longitudinal strips. Young branches are flexible and thickened in the nodes.

Principal reasons for the poor behavior of *V. vinifera* compared to *C. cardunculus* in the production of binderless fiberboards are mainly: The presence of nodes in branches, their short length and short growing time (poor lignification), joint to the fact that during its natural growing process *Vitis vinifera* branches withstand no weight at all, that otherwise could make it to develop stronger branches.

Better results were obtained in previous studies conducted by the research group with other lignocellulosic materials (i.e. *Miscanthus sinensis* and mixtures of softwood sawdust, *Abies alba* and *Pinus insignis*).

*M. sinensis* is a non-woody, herbaceous perennial plant, structurally similar to bamboo-cane that could grow up to 0.8-2 m (rarely 4 m) tall. Mechanical properties of binderless fiberboards produced from this material were superior to those found for binderless fiberboards from *V. vinifera* and *C. cardunculus*. This is probably due to the natural differences between these materials; *M. sinensis*, as well as most of the cane type plants presents stronger structures than cardoon and vine prunings which can be translated to stronger fibers, which in turn are more suitable for developing composite materials with good mechanical properties. Physical properties, related mainly to

physical stability towards water, revealed no significant differences between fiberboards produced using these materials.

Binderless fiberboards from softwood sawdust were generally superior in their mechanical properties to *V. vinifera* fiberboards, particularly in IB values. This is caused by the structural differences between the lignocellulosic materials employed, but also by the poor lignification developed in young vine prunings compared to the lignification process undergo by older softwoods. Physical stabilities of binderless fiberboards from *V. vinifera* were superior to those of softwood sawdust binderless fiberboards; this can be due to natural chemical differences between lignocellulosic materials and to different pretreatment conditions and how these materials undergo the pretreatment.

### **Future work**

Based on the results obtained in the present study and focusing in the different possibilities that could be explored, the following suggestions are highlighted:

Most of the lignocellulosic agricultural residues can be used to produce binderless fiberboards, but the more suitable material for obtaining boards that fulfill European standards, guarantying its good performance in use, are the ones that a priori seem to present strong structures and fibers, and high aspect ratios; that is the case of cane type plants (i.e. sugarcane, Kenaf and Hemp). Nevertheless, other agricultural residues could be used in combination with those structurally stronger to obtain good products at the same time that agricultural residues are valorized.

It is important to clarify the adhesion mechanisms that occur between the different lignocellulosic polymers and between themselves, particularly the polymerization reactions of lignin and hemicelluloses and how the polymerization products interact between them and with cellulose fibers. Studies with model compounds alone and mixtures of them can be used to perform common adhesive analysis in addition to thermal behavior tests to elucidate its adhesive properties and its possible effects on developing fiberboards properties.

Alkali treated Kraft lignin is a powerful tool to enhance lignin adhesive potential, but further work should be done to increase compatibility between fibers and modified lignin. This can be done submitting the fibers surface to chemical treatments. Other possibility is to use alkali treated Kraft lignin to produce an adhesive resin, without using phenol, carrying out condensation reaction with glyoxal.

## **ANNEX**

UNIVERSITAT ROVIRA I VIRGILI  
BINDERLESS FIBERBOARD PRODUCTION FROM CYNARA CARDUNCULUS AND VITIS VINIFERA  
Camilo Mancera Arias  
ISBN:978-84-692-1537-1/DL:T-300-2009

## ANNEX A

### Experimental design

The use of experimental design in developing products can substantially reduce development lead-time and cost, leading to products that perform better and with high reliability on the field.

Statistically designed experiments offer to investigators a valid basis for developing an empirical model of the system being investigated. This empirical model can then be manipulated through response surfaces, contour plots or mathematically for obtaining optimal operation points.

However, it is important to remember that statistical methods does not prove that a factor  $x$  have a specific effect. They just make possible conclude, with a certain level of confidence, over the system performance.

#### *Objectives for Designing the Experiments*

The main objective is to develop a model that interrelate the response variables, in this case mechanical, physical or chemical properties of the fiber boards, with the controllable factors that will be investigated, and use this model to optimize the responses.

#### *Particular Objectives*

- Determine which factors have more influence on the different response variables.
- Find out the optimal region of the influence parameters to obtain the desirable properties on the fiber boards.
- Identify the factors that have more influence in the variability of the response variables and where to set those factors to reduce this variability.

At the end, the results and conclusions of any experiment will depend on the way the data were taken.

Statistical methods were used to analyze the data, thus guarantying that the results and conclusions are objective rather than judgmental. Simple graphical methods were used to facilitate data analysis and interpretation under a hypothesis-testing framework

together with confidence interval estimations. Part of the results were also presented in terms of empirical models, that is, an equation derived from the data that expresses the relationship between the response and the important design factors.

Each response variable studied in the different parts of the research was analyzed based on the variability of the data obtained. Analysis of variance (ANOVA) was used for this purpose. The ANOVA table shows which of the factors are statistically significant and if there are relevant interactions between them.

### Analysis of variance

In this type of analysis, the variability of the response been analyzed is separated in different parts which correspond to each of the effects studied. Subsequently, statistically significant effects are identified comparing their average quadratic mean to the estimated experimental error. During the analysis of the data of this study a confidence level of 95% was used. Any area under the curve lower than 0.05 in the ANOVA table indicates that the effect analyzed is statistically significant at a confidence level of 95%.  $R^2$  statistic (determination coefficient) indicates the percentage of the variability explained by the fitted model, the closer to 1 or 100% it is the better. The SDR statistic (standard deviation of residues) indicates the dispersion of the data related to the fitted model, the smallest it is the better.

Estimated effects of each factor and the interactions between them were also calculated, these calculations were finally used to fit first and second order models, like these ones:

First order model: 
$$y = \beta_0 + \sum_{i=1}^k \beta_i x_i + \epsilon$$

Second order model: 
$$y = \beta_0 + \sum_{i=1}^k \beta_i x_i + \sum_{i=1}^k \beta_{ii} x_{ii}^2 + \sum_{i < j} \beta_{ij} x_i x_j + \epsilon$$

More detail information about experimental design planning and analysis can be found in Montgomery (*Montgomery 2000*)



## ANNEX B

### Detail description of the test equipments and characterization methods

#### B.1. EQUIPMENTS

##### Steam explosion reactor

It is a batch reactor with a nominal volume of 8 liters, built in stainless steel AISI 304 L, was designed to work at a pressure of 40 bar and 250 °C. There is a 1.5 inches valve at the top of the reactor used to feed the lignocellulosic material to be treated.

The steam can be fed both at the bottom and at the top of the reactor, as needed. Steam comes from a steam boiler SADEC SDE-75 fitted with a diesel burner EL-02-9-1D. The boiler can provide 75 kg / h of saturated steam at 40 bar (250 ° C) with a diesel consumption of between 5 and 9 kg / h. Fuel is supplied from a 25 liter tank which feeds the pump of the burner. Deionized water is fed to the boiler from a 100 L tank which in turn is fed from a reverse osmosis equipment plugged in to the net.

The whole set up has an autonomous control system outfitted with alarms on failure of the water pump, burner's engine failure, damage in the burner, high temperature of combustion gases and high steam temperature. It also has a pressure control and a pressure relief valve. There is a supporting security system that allows switching off the boiler from another room in case of malfunctioning.

Reactor is also outfitted with a jacket plugged in to the steam net, which allows a better control of the reaction temperature during the reaction time.

The steam explosion reactor is connected to a depressurization tank of 100 L of volume through a 1 inch pneumatic valve; it was built in stainless steel AISI 304 L and was designed to withstand pressures up to 4 bar. Depressurization tank has a lid of about 75 cm in diameter which allows an easy discharge of the reaction products after the flash expansion. It has a purge valve at the bottom that allows the removal of fluids generated during the reaction. At the top, it has a valve that allows the removal of vapor to reduce pressure inside the tank.

## **Mechanical characterization equipment**

Mechanical characterization equipment has a supporting frame outfitted with an actuation and mechanical reduction system; required to perform the mechanical characterization tests.

### *Actuation and mechanical reduction system*

It presents a mobile surface connected to a screw which confers movement to the surface. The screw is actuated by a crown of jagged teeth with 100 teeth and interior thread. The crown is geared into another endless screw that produces a reduction of 100:1. Endless screw entry has attached a jagged pulley of 32 teeth with a step of  $T = 2.5$  mm. The pulley is driven by an electric motor with a jagged pulley of 11 teeth. This mechanical actuation system delivers 1500 rpm of the electric motor which in turn entails a velocity of 30 mm/min of the mobile surface. Additionally, it is possible to attach different pulleys, thus changing the gear ratio so that the obtained speed range can be changed by changing the speed of the electric motor.

### *Speed regulation*

It uses an electric motor of 12V (nominal). The system is powered by two 12V batteries in series that provide a steady stream of 24V with very little electromagnetic noise.

Engine speed regulation was accomplished building a circuit that inhibits the electric flow during a percentage of the time, which can be varied at will with a potentiometer. The regulation system was prepared with a bi-stable circuit with an integrated IC555 chip that feeds a power transistor MJ11011 Darlington. It also includes an aluminum heat sink and a fan to enhance cooling of the transistor.

### *Sensors*

To measure the applied forces it was used an extensometric load cell (EPPEL) with a full scale of 226.8 kgf for flexion assays and 1512 kgf for tensile strength perpendicular to the faces assays. The load cells were calibrated. The reading of the displacements was made by a potentiometric displacement transducer (TR-75 mm Novotechnik) which linearity output exceeds 0.075%.

### **10 L Batch reactor**

Alkali treatment of commercial Kraft lignin at optimum conditions found from the response surface assays done in a microreactor set was done in the 10 L batch reactor. This reactor was design by the university staff to perform fractionations of lignocellulosic materials. It has a maximum capacity of 10 L and can stand pressures of up to 40 kg/cm<sup>2</sup> and temperatures of up to 250°C. The reactor was built with stainless steel AISI 304 L. The agitation system consists of a triphasic engine of 0.37kw which delivers agitation speeds in the range of 0-1360 rpm. Internal agitation devices were refrigerated with compressed air from the net.

Direct vapor circulation throughout an internal coil was used to heat the reaction mixture; the tube of the coil has a diameter of ¼ of inch and the average coil diameter is of 13 cm. Steam comes from the same steam boiler that feeds the steam explosion reactor. Fresh water can also be fed to the coil to cool down the reaction mixture at the end of the process or at any other time.

A more detailed description can be found in Anglès (*Anglès Llauradó 1999*)

## B.2 Fiberboard characterization methods

### Physical properties

#### *Density*

To determine the relation between the mass of a testing piece and its volume, the testing pieces were first conditioned at 20°C and 65% of relative humidity until they reach equilibrium humidity.

After being conditioned, the test piece is weighed with a precision of 0.1 g. Thickness of the test piece is measured at the interception of the diagonals and subsequently, length and width are measured at the center of the test piece. With these measurements the volume of the test piece can be calculated with an accuracy of 0.1 cm<sup>3</sup>.

Summarizing, the density of the test pieces are calculated with the following formula:

$$\rho = \left( \frac{m}{v} \right) \times 1000$$

Where:

$\rho$ : Density [kg/m<sup>3</sup>]

m: Test piece mass [g]

v: Test piece volume [cm<sup>3</sup>]

Results are expressed with an error of 10 kg/m<sup>3</sup>

#### *Water absorption and thickness swelling*

The method is based on the determination of the water absorbed by the board by calculating the increase in mass and thickness swelling of the test board after a total immersion in water for 24 h ± 15 min.

Test pieces are squared with a length of 50 mm. They are weighed with an accuracy of 0.01 g and their width is measured with an accuracy of 0.01 mm. Afterwards, the test pieces are placed vertically and separated from each other in a container filled with distilled water with a neutral pH and a temperature of 20 °C. The test boards must be submerged about 20 mm below the water surface for 24 h ± 15 min.

Test pieces are then taken out of the water and leave over cellulose sheets to withdraw the excess of water. During the following 10 min. the test boards are weighed and their thickness is measure just like at the beginning of the test.

Water absorption percentage is calculated with the following formula:

$$WA = \frac{(M_1 - M_0)}{M_0} \times 100$$

Where:

WA: Water absorption percentage

M<sub>1</sub>: Mass of the test piece after water immersion

M<sub>0</sub>: Mass of the test piece before water immersion

Results are expressed with an error of 0.1%

Thickness swelling percentage is calculated with the following formula:

$$TS = \frac{(L_1 - L_0)}{L_0} \times 100$$

Where:

TS: Thickness swelling percentage

L<sub>1</sub>: Thickness of the test piece after water immersion

L<sub>0</sub>: Thickness of the test piece before water immersion

Results are expressed with an error of 0.1%

## **Mechanical properties**

### *Modulus of elasticity and bending strength*

Bending strength and modulus of elasticity determination were done through a flexibility-traction test. During this test a load is applied in the middle of a rectangular test piece that is supported by its ends. Figure B1 shows a diagram of the testing device.

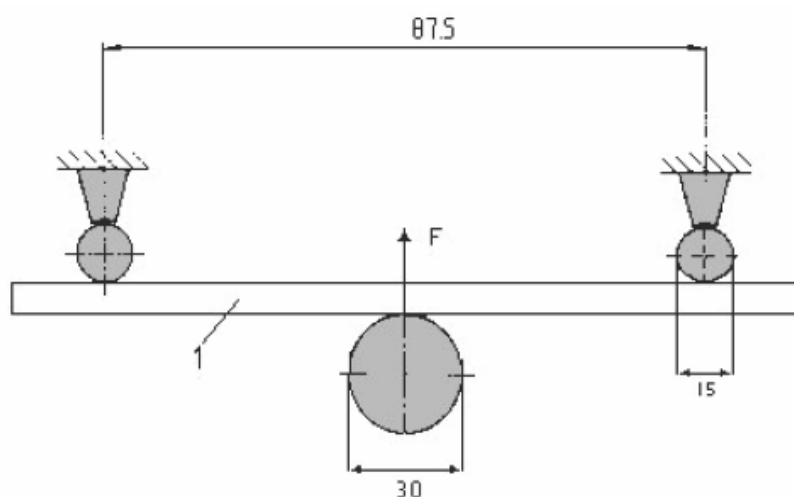


**Figure B1.** Flexion apparatus description

Measures in mm

1 test piece

Modulus of elasticity is calculated using the secant of the curve load-deformation in the first third, since within this zone boards have a linear behavior. The estimated value could be called apparent module, because this test method includes both the influence of shear and bending and not strictly meet the assumptions previously enunciated.

Rupture strength is affected by the same constraints, especially the lack of linearity observed at the end of the assay.

Modulus of elasticity and modulus of rupture are calculated based on the basic theory of beams, as indicate below.

The testing device consists of a support with two parallel cylinders that provide support to the test piece. These cylinders have a length greater than the width of the test piece and a diameter of  $15 \pm 0.5$  mm. The distance between the two supporting points can be adjusted depending on the size of the test piece. Additionally, the testing device has a cylindrical loading head with the same length of the supporting cylinders and with a diameter of  $30 \pm 0.5$  mm, placed parallel and equidistant from them.

The instruments used to measure the deformation endure by the test pieces have an accuracy of 0.1 mm. The system for measuring the load applied in the test pieces has an accuracy of 1% of reading.

Test pieces were rectangular Of 50 mm x 150 mm conditioned as required by the European standard. Before being tested, width and thickness of the test pieces were measured. Thickness of the test piece determines the distance between the two supporting cylinders, which is 20 times the nominal thickness of the board  $\pm 1$  mm.

The test pieces are supported with its longitudinal axis perpendicular to the axis of the supporting cylinders. The load is applied in the center of the test piece. The strain

rate must be constant during the assay and should reach the maximum load at  $60 \pm 30$  s.

Modulus of elasticity is calculated with the following equation:

$$MOE = \frac{(l_1^3 (F_2 - F_1))}{(4bt^3 (a_2 - a_1))}$$

Where:

MOE: Modulus of elasticity

$l_1$ : Distance between support cylinder axis, in mm

b: Test piece width, in mm

t: test piece thickness, in mm

$F_2$ : 40% of the maximum load, in N

$F_1$ : 10% of the maximum load, in N

$a_2$ : Strain obtained at  $F_2$ , in mm

$a_1$ : Strain obtained at  $F_1$ , in mm

Modulus of rupture is calculated with the following equation:

$$MOR = \frac{3F_{\max} l_1}{2bt^2}$$

Where

MOR: Modulus of rupture

$F_{\max}$ : Maximum load, in N

$l_1$ , b and t: The same than the equation above.

#### *Tensile strength perpendicular to the faces*

The tensile strength perpendicular to the faces determines the strength of the link (internal cohesion) between the fibers of the board. Basically, this assay determines the resistance of a test piece submitted to a traction effort evenly distributed over the test piece surface, until it breaks. This resistance is expressed as the maximum load perpendicular to the faces that endures the board related to the surface over which the load is applied.

It is then needed a device that is able to apply a force of traction perpendicular to the faces of the test piece, by clamping metallic-square grip devices and measuring the

force applied with an accuracy of 1%. Additionally, the metallic grip pieces must incorporate a self-aligning device with kneecap joints at each side of the testing piece.

The dimensions of the testing pieces are  $50 \times 50 \text{ mm}^2$  and must to be cut with precision, with the angles of 90 degrees and the edges straight and clean. Subsequently thickness and length of the test piece are determined.

The testing pieces are stick to the metallic grip devices as describe in the European standard. After the adhesive has cured the test pieces are conditioned.

The whole metallic grip device-testing piece is placed in the clamping devices of the testing machine and the force needed to breaking it is applied. The load should be applied at a steady speed during the assay. Speed should also be tune up to reach the maximum load at  $60 \pm 30 \text{ s}$ . The maximum load endure by the testing piece is recorded with a precision of 1%. Figure B2 shows a diagram of the testing device.

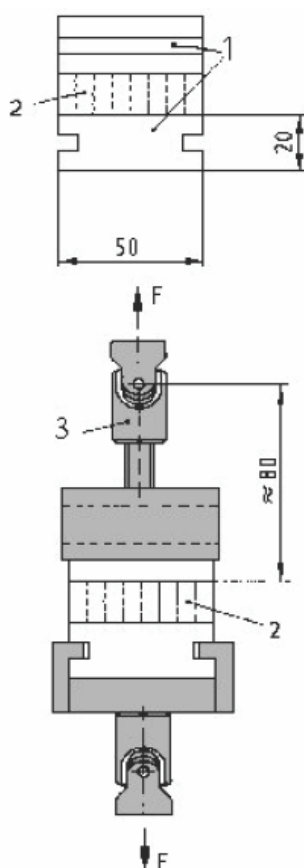


**Figure B2.** Internal bond testing device

Measures in mm

1 Metallic-square grips

2 Testing piece

3 Self-aligning device with kneecap joint



Internal bond is calculated with the following equation:

$$IB = \frac{F_{\max}}{(a \times b)}$$

Where

IB: Tensile strength perpendicular to the faces (Internal bond), in MPa

$F_{\max}$ : Breaking load, in N

a, b: Test piece dimensions, length and width, in mm

### **B3. Chemical characterization of lignocellulosic material and Lignin**

#### *Humidity*

Moisture determination is critical to refer the results to a dry basis. Initially, lignocellulosic material is weighed, around 2 g., the sample is subsequently oven dried at 105°C for 24 h. Afterwards, the sample is left to cool down in a desiccator and weighed to determine its dry mass. The procedure is then repeated every hour until the dry mass of the sample is stable.

Humidity, moisture content, of the sample is calculated with the following equation:

$$\%H = \frac{(M_2 - M_3)}{(M_2 - M_1)} \times 100$$

Where:

%H: Humidity percentage

$M_1$ : Crucible weight, in g

$M_2$ : Crucible plus humid sample weight, in g

$M_3$ : Crucible plus dry sample weight, in g

#### *Ash content*

Ashes are the remaining solid after the combustion of lignocellulosic material at 575 °C for 3 h or more. This method measure the amount of inorganic compounds present in the lignocellulosic material. Crucibles are first treated without sample at 575 °C for 1h to remove any organic residue, and then A sample of 2 to 5 g of lignocellulosic material is placed in the crucible and left in the oven for the combustion

at  $575 \pm 25^\circ\text{C}$  for at least 3 h. Crucibles are retrieved from the furnace when the temperature is around  $200^\circ\text{C}$  and left to cool down in a dessecator under vacuum. The whole, crucible plus ashes, is weighed after reaching environmental temperature until mass measure is stable.

Ash content of the sample is referred to its dry basis and is calculated using the following equation:

$$\% \text{ Ash} = \frac{(M_3 - M_1)}{(M_2 - M_1) \cdot \left(\frac{1-H}{100}\right)} \times 100$$

Where:

$M_1$ : Crucible weight, in g

$M_2$ : Crucible plus humid sample weight, in g

$M_3$ : Crucible plus ashes weight, in g

#### *Klason lignin*

Lignin represents about 30% of lignocellulosic material. The total content of lignin is the addition of the residual amount of lignin, called Klason lignin and the lignin soluble in acid. Klason lignin is quantified as the residual lignin or the lignin insoluble in acidic medium. The method consists in treating lignin with a concentrated acidic medium at room temperature, and subsequently with diluted acid at moderated temperature. After these two stages of hydrolysis, polysaccharides are hydrolyzed into their respective monomers and remaining residual solid is identified as Klason lignin.

Initially, in the first hydrolysis, 0.3 g of lignocellulosic material, dry basis, are treated with concentrated sulfuric acid (24.1 N, 3ml) in a thermostatic bath at  $30^\circ\text{C}$ . Lignocellulosic material is stirred constantly for 1h. In this first hydrolysis, polysaccharides are degraded to short chain oligomers, soluble in water. In the second hydrolysis, the resulting solution from the first hydrolysis stage is diluted with 84 ml of distilled water, obtaining a suspension with an acidic concentration of 0.82N. This suspension is left to react in an autoclave at  $120^\circ\text{C}$  for 30 min.; after this time the suspension is left to cool down at room temperature and subsequently it is filtrated with a filter crucible previously weighed and using vacuum. The remaining solid is then rinsed with distilled water until the filtrated reach a neutral pH. The whole filter crucible plus Klason lignin is then dried at  $105^\circ\text{C}$  until constant mass.

The filtrate is recovered in a flask for volume quantification, in a 100 ml graduated tube and for its posterior used in the quantification of acid soluble lignin and elemental sugars.

Klason lignin is calculated with the following equation:

$$\% \text{ Klason Lignin} = \frac{(M_3 - M_2)}{M_1} \times 100$$

Where:

%Klason lignin: Percentage of Klason lignin, dry basis

M<sub>3</sub>: Weight of the filtrating crucible plus dried solid residue, in g.

M<sub>2</sub>: Weight of the filtrating crucible, in g.

M<sub>1</sub>: Weight of dried lignocellulosic material, in g.

#### *Acid soluble lignin (ASL)*

The absorbance of the filtrated, obtained after the two hydrolysis stages describe above, is measured with a UV spectrophotometer at a wave length of 205 nm. Sulfuric acid solution 0.82N is used as a blank; it is prepared diluting 3 ml of concentrated sulfuric acid 24.1 N with 84 ml of distilled water. If absorbance of the sample exceeds 0.7, the sample must be diluted to obtain an absorbance in the range of 0.2-0.7. Sulfuric acid 0.82 N used as a blank must be diluted in the same way than samples to be used as reference.

Acid soluble lignin is calculated with the following equation:

$$\% \text{ ASL} = \frac{A \times V \times df}{b \times a \times W} \times 100$$

Where:

%ASL: Percentage of acid soluble lignin

A: Absorbance at 205 nm

V: Filtrate volume

df: Dilution factor

b: Bucket width in cm

a: Absorption coefficient, 110 L/g/cm. This is mean value of different woods and pulps

W: Dry sample weight.

### *Sugars*

The monomeric sugars content of the filtrated, obtained after the two hydrolysis stages describe above, is measured with a HPLC Beckman System Gold, outfitted with Beckman126 pumps. The column used was Biorad aminex HPX-87H (300x7.5mm). Ionic exchange precolumn from Biorad was also used. Refraction index detector Beckman 156 was employed to measure sugars concentration in the sample. The mobile phase used was sulfuric acid with a concentration of 0.005M.

Initially, the system is purged and the column is heated to the desired temperature, around 30 °C. Mobile phase flow is set to 0.1 ml/min and the equipment is left to reach stable state. Once equipment reaches stability the samples are injected, 30 µl per sample.

Sugars content determination is done based on calibration curves obtained with patrons of known concentrations. Once the chromatograph has been obtained, the signals are related to a specific sugar monomer comparing the retention times obtained in the chromatograph with the retention times of the patrons; the integration areas of the identified signals allow finding the concentration of the sugars in the sample. Sugars content is then calculated with the following equation:

$$\%Elemental\ Sugar = \frac{C \times V}{W} \times 100$$

Where:

%Elemental sugar: Percentage of the elemental sugar

C: Concentration of each elemental sugar, in mg/ml

V: Filtrate volume

W: Dry weight of the sample.

### **Functional group in lignin determination**

#### *Hydroxyls: Phenolic and aliphatic*

Phenolic hydroxyl groups in lignin were determined using to analytical techniques, UV differential spectrophotometry and proton nuclear magnetic resonance. NMR allows us to determine both phenolic hydroxyl groups and aliphatic hydroxyl groups.

### UV differential spectrophotometry

Phenolic hydroxyl content determination provides crucial information relating to the lignin structure, its reactivity, the mechanism and extent of its degradation. This method is based on measuring the difference in absorbance at 300 and 360nm between lignin compounds and their respective models in two solutions with different pH, one neutral and the other basic.

$\Delta\epsilon$ -spectrum is obtained by subtracting the absorbance of the studied compound obtained in alkaline medium from the one obtained in neutral medium. Ionized phenolic hydroxyl content was evaluated comparing  $\Delta\epsilon$  values of lignins at determine wave lengths with  $\Delta\epsilon$  values of its respective model compounds, phenolic structure I, II, II, IV (see figure B3)

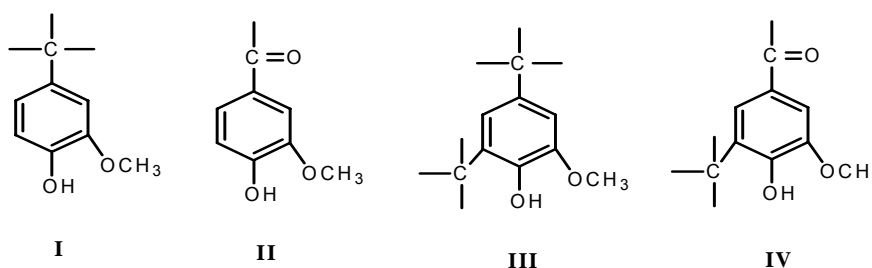


**Figure B3.** Phenolic structures determined in lignin

10 to 15 mg of lignin are diluted in 10 ml dioxane chemically pure. 2 ml of this solution are transferred to 3 beakers of 50 ml. In the first beaker, a plug solution of pH 6 is added until complete 50 ml. In the second, a plug solution of pH 12 is added until complete 50 ml and finally, in the third beaker, a solution of NaOH (0.2N) is added until complete 50 ml. After stirring the solutions, the absorbances of the alkaline solutions are measured against the neutral solution at 300 nm and 360 nm.

Solution of pH 6 is prepared as follows: 495 ml of dihydrogen potassium phosphate  $\text{KH}_2\text{PO}_4$  0.2N are mixed with 113 ml of NaOH 0.1N and the solution is completed with deionized water until 2L. Solution of pH 12 is prepared as follows: 40 ml of anhydride disodic tetraborate  $\text{Na}_2\text{B}_4\text{O}_7$  are mixed with 60 ml of NaOH 0.1N.

The procedure for calculating the phenolic hydroxyl content is as follows:  $\Delta a$ , difference in the absorbance coefficient is calculated for every absorbance measured with the following equation:

$$\Delta a = \frac{D}{C \times b}$$

Where:

$\Delta a$ : Absorbance coefficient difference

D: Absorbance difference between alkaline solution and neutral solution

C: Lignin solution concentration, in mg/ml

b: Bucket width, in cm

Codification used for the difference in absorbance and absorbance coefficients between alkaline and neutral solutions is written below:

Wave length, [nm]	NaOH 0.2N	Plug solution, pH 12
300	$D'_1; \Delta a'_1$	$D'_2; \Delta a'_2$
360	$D''_1; \Delta a''_1$	$D''_2; \Delta a''_2$

The percentage in the sample of each phenolic structure from figure B3 is calculated with the following equations:

$$[OH_{I+III}] = \frac{(\Delta a'_1 + 0.238 \cdot \Delta a''_1) \times 1700}{4000} = 0.425 \cdot \Delta a'_1 + 0.101 \cdot \Delta a''_1$$

$$[OH_{II+IV}] = \frac{\Delta a''_1 \cdot 1700}{21000} = 0.081 \cdot \Delta a''_1$$

$$[OH_{I+II+III+IV}] = 0.425 \cdot \Delta a'_1 + 0.182 \cdot \Delta a''_1$$

$$[OH_I] = \frac{\Delta a'_2 \cdot 1700}{4000} = 0.425 \cdot \Delta a'_2$$

$$[OH_{II}] = \frac{\Delta a''_2 \cdot 1700}{21000} = 0.081 \cdot \Delta a''_2$$

$$[OH_{III}] = [OH_{I+III}] - [OH_I]$$

$$[OH_{IV}] = [OH_{II+IV}] - [OH_{II}]$$

#### Proton nuclear magnetic resonance

Acetylated lignins were analyzed with <sup>1</sup>H-NMR using a Varian Gemini 300 MHz. This technique quantitatively determined the relative amount of methoxyl, aromatic and aliphatic-acetoxyl groups with reference to the internal standard, p-nitrobenzaldehyde,

as suggested by Kubo et al.<sup>28</sup>. The measurement conditions were as follows: 5  $\mu$ s pulse width, 45° pulse angle, 2 s acquisition time, 2 s pulse delay time, 256 accumulations.

The procedure was to dissolve 30 mg of a sample in 0.70 ml of CDCl<sub>3</sub> and add about 1.5 mg of p-nitrobenzaldehyde as an internal standard.

The signals appearing around 1.70-2.17, 2.17-2.50 and 3.10-4.10 were assigned to aliphatic acetoxy, aromatic acetoxy and methoxyl protons, respectively. The amount of each functional group in the hydrolyzed Kraft lignins was estimated based on the integral intensity of corresponding signals by applying the following equation:

$$\text{Relative amount} = \frac{\left( \frac{I_a}{W_{ta}} \right)}{\left( \frac{I_{is}}{W_{tis}} \right)}$$

Where:

I<sub>a</sub>: Area of the functional group in Kraft lignin.

I<sub>is</sub>: Area of the internal standard

W<sub>ta</sub>: Weight of the lignin sample

W<sub>tis</sub>: Weight of the internal standard.

The <sup>1</sup>H-NMR spectrum signals were assigned as follows:

**Table B1.** <sup>1</sup>H-NMR spectrum signals assignment (Lundquist 1992)

Chemical displacement, $\delta$ (ppm)	
2.04	Aliphatic hydroxyl groups
2.31	Phenolic hydroxyl groups
3.82	Methoxyls
6.62	Aromatic protons (S units)
6.91	Aromatic protons (G units)
7.26	Chloroform
7.42	Aromatic protons in benzaldehyde units

#### Fourier transform infrared spectroscopy (FTIR)

FTIR determines semi-quantitatively chemical structure of lignins due to its capacity to detect vibrational absorptions characteristics of specific functional groups and

structures. The FTIR spectra of the unacetylated lignin samples were obtained, by pressing the fine powder on the diamond surface of an ATR probe, with a JASCO FTIR-680 plus spectrometer. Thirty-two co-addition scans were made in a frequency range of 400 to 4600  $\text{cm}^{-1}$  at resolution of 2  $\text{cm}^{-1}$ . The spectra were analyzed using MestRe-C software to compare the absorbance of each functional group. The absorption bands were assigned as follows:

**Table B2.** Characteristic bands assigned to lignin in FTIR spectra (Faix 1992)

Wave number [ $\text{cm}^{-1}$ ]	Band origin
3412-3460	O–H stretch
3000-2842	C–H stretch in methyl and methylene groups
1738-1709	C=O stretch in unconjugated ketones, carbonyls and in ester groups (frequently of carbohydrate origin); conjugated aldehydes and carboxyl acids absorb around and below 1700 $\text{cm}^{-1}$
1655-1675	C=O stretch in conjugated p subst. aryl ketones
1593-1605	Aromatic skeletal vibrations plus C=O stretch; S > G; G condensed > G etherified
1505-1515	Aromatic skeletal vibrations, G > S
1460-1470	C – H deformation, asym. in $-\text{CH}_3$ and $-\text{CH}_2-$
1422-1430	Aromatic skeletal vibrations combined with C–H in-plane deform.
1365-1370	Aliphatic C–H stretch in $\text{CH}_3$ ; not in OMe; phen. OH
1325-1330	S ring plus G ring condensed
1266-1270	G-ring plus C=O stretch
1221-1230	C–C plus C–O plus C=O stretch; G condensed > G etherified
1140	Aromatic C–H in-plane deformation; typical for G units; whereby G condensed > G etherified
1086	C–O deformation in secondary alcohols and aliphatic ethers.
1030-1035	Aromatic C–H in-plane deformation, G > S; plus C–O deform. in primary alcohols; plus C=O stretch (unconj.)
915-925	C–H out of plane, aromatic
853-858	C–H out of plane in position 2, 5 and 6 of G units

#### *Molecular weight distribution*

The molecular weight of acetylated lignins was determined by GPC. Aqueous medium should be used for unacetylated lignins and organic medium for acetylated ones.



Acetylated lignin was diluted in tetrahydrofuran (THF) HPLC grade. The samples were dissolved in THF at a concentration of 1 mg/ml and stored for 24 h at 5°C to avoid variations in molecular weight. Three styrene–divinylbenzene copolymer gel columns were used, columns size were of 50, 500, and 10<sup>4</sup> Å from Polymer Laboratories. The effluent was monitored at 254 nm with a Beckman UV detector. The columns were calibrated using polystyrene standards in the 92–66,000 g/mol range. The flux of THF was 1 ml/min. The detected signal was digitized at a frequency of 2 Hz. The molecular weight distribution was calculated from the recorded signal using normal GPC calculation procedures. The equations are as follows:

$$M_w = \frac{\sum_{i=1}^N h_i \cdot M_i}{\sum_{i=1}^N h_i}$$

Where:

M<sub>w</sub>: Weight average molecular weight, in g/mol

h<sub>i</sub>: Pick height in a given moment, in mm

M<sub>i</sub>: Molecular weight in a given moment, in g/mol.

N: Number of integrations

$$M_n = \frac{\sum_{i=1}^N h_i}{\sum_{i=1}^N \frac{h_i}{M_i}}$$

Where:

M<sub>n</sub>: Number average molecular weight, in g/mol

h<sub>i</sub>: Pick height in a given moment, in mm

M<sub>i</sub>: Molecular weight in a given moment, in g/mol.

N: Number of integrations

$$Polydispersity = \frac{M_w}{M_n}$$

#### *Active sites increment*

Active sites determination or reactive structures was done by UV spectroscopy. It consists in determining the amount of structure type I and II present in lignin, during

phenolic hydroxyls content determination. These structures have one C-3 position free in the aromatic ring. The equation used for its calculation is as follows:

$$[\%OH]_{I+II} = \frac{(0.425 \times A_{300} + 0.081 \times A_{360})}{C \times b}$$

Where:

%OH<sub>I+II</sub>: Percentage of active sites

C: concentration of the lignin solution, in mg/ml

B: Bucket width, in cm

A<sub>300</sub> and A<sub>360</sub>: Absorbance of lignin solution in plug solution of pH 12.

Active sites increment due to alkali treatment is calculated based on the active sites content of the raw or crude lignin.

$$\text{Active Sites Increment} = \frac{[OH]_{I+II(\text{Alkali Treated Lignin})} - [OH]_{I+II(\text{Crude Lignin})}}{[OH]_{I+II(\text{Crude Lignin})}}$$

## ANNEX C

### <sup>1</sup>H-NMR and FTIR spectrums of alkali treated lignin at different reaction conditions

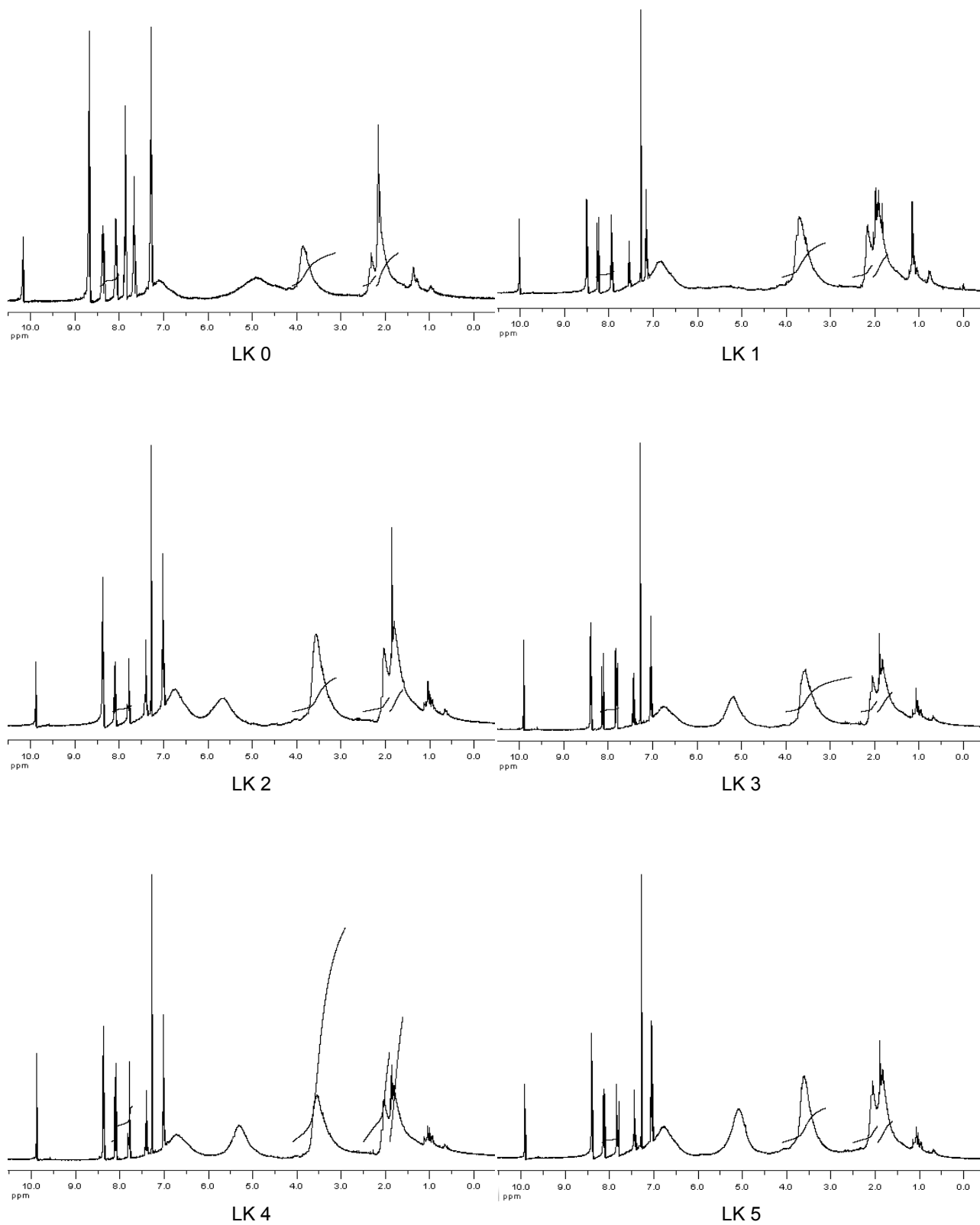


**Figure C1.** <sup>1</sup>H-NMR spectrums of alkali treated Kraft lignin

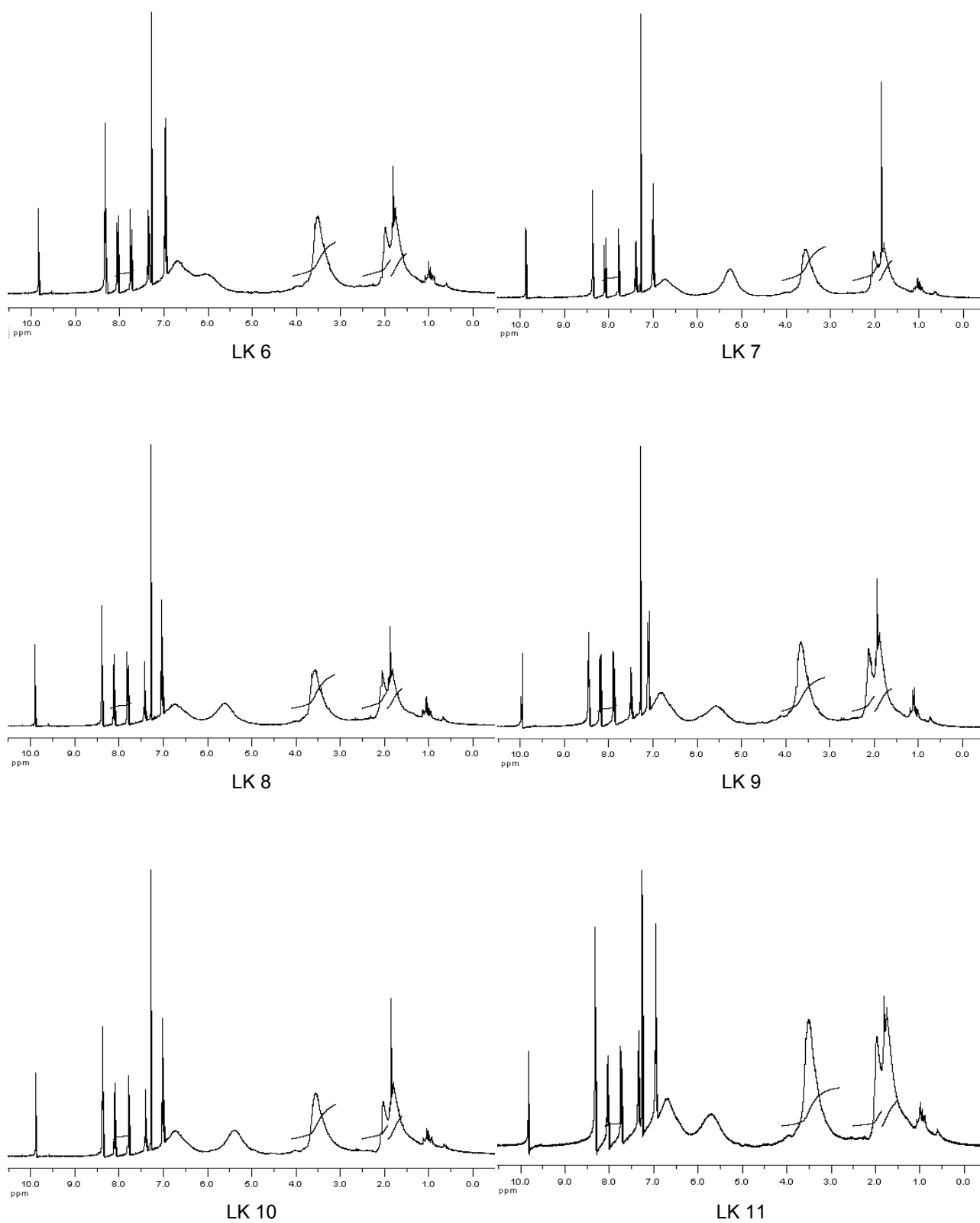
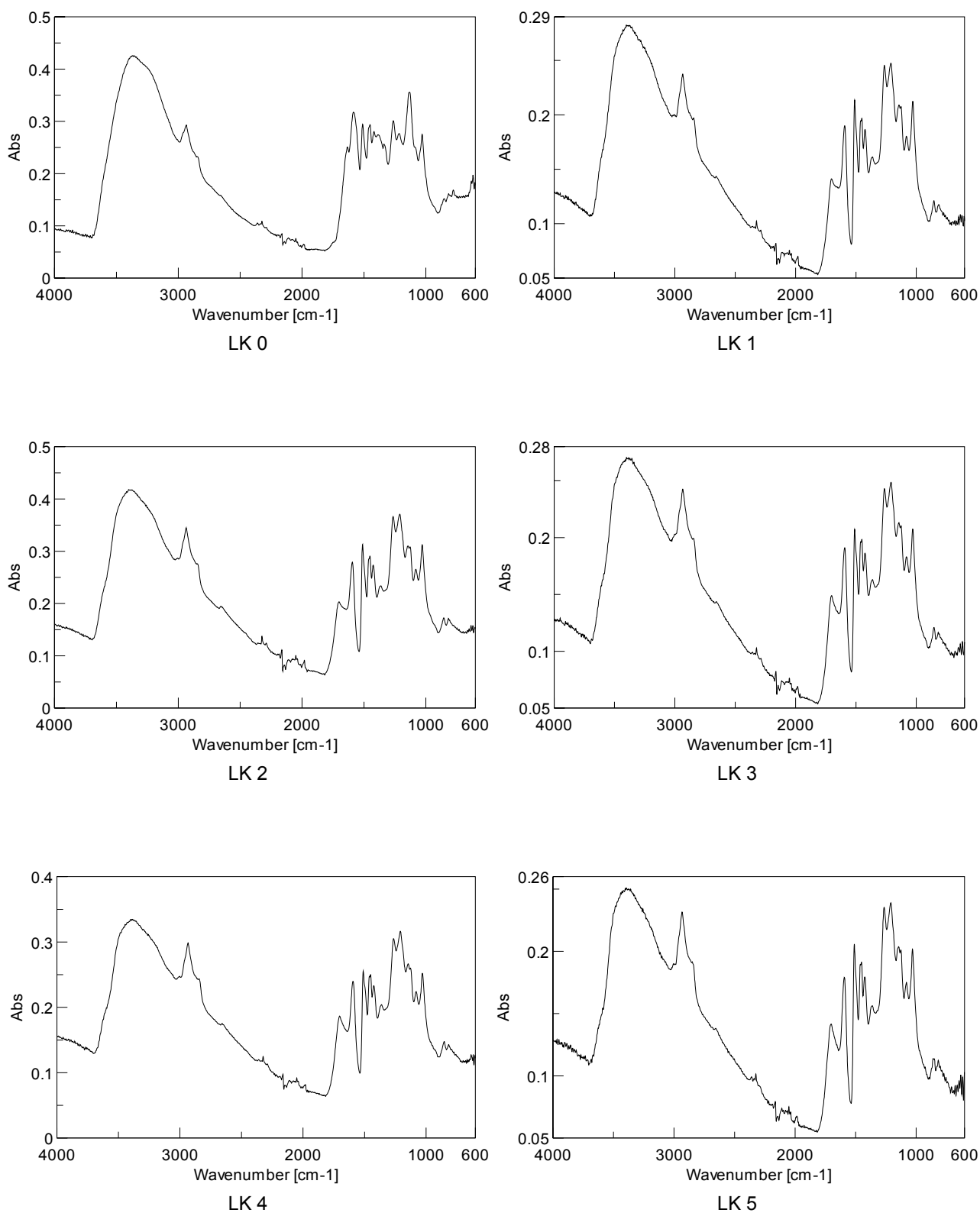


Figure C1. <sup>1</sup>H-NMR spectrums of alkali treated Kraft lignin (continuation)



**Figure C2.** FTIR spectrums of alkali treated Kraft lignin

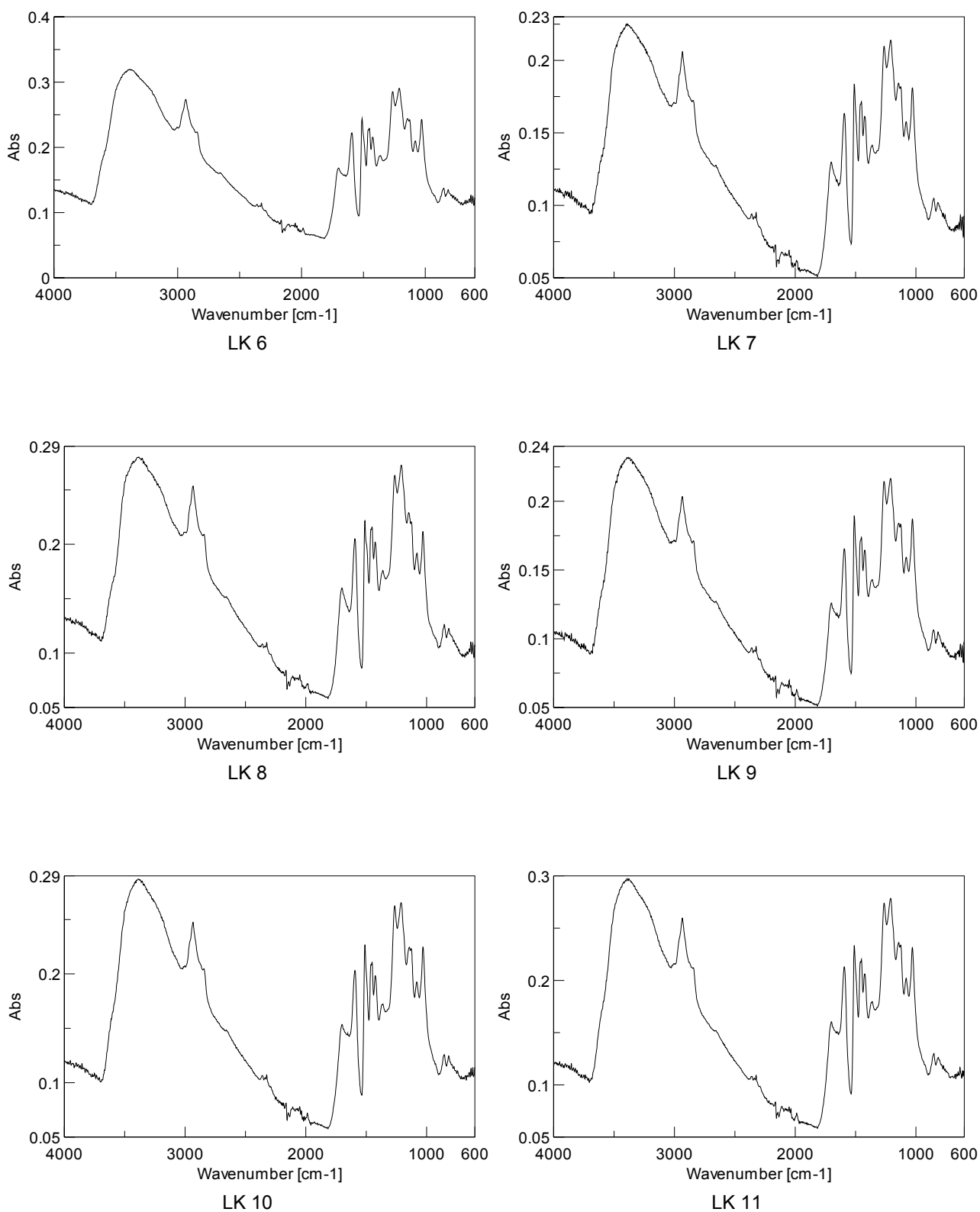


Figure C2. FTIR spectrums of alkali treated Kraft lignin (continuation)

## REFERENCES

Anglès Llauradó, M. N. Producció de taulers amb material lignocel·lulòsic residual sense addició d'adhesius sintètics. Tarragona, Universitat Rovira i Virgili. 1999.

Faix, O. Fourier transform infrared spectroscopy. in: Methods in lignin chemistry. S. Y. Lin and C. W. Dence, Ed. Berlin: 83-109. 1992

Lundquist, K. Proton (<sup>1</sup>H) NMR spectroscopy. in: Methods in Lignin Chemistry. S. Y. Lin and C. W. Dence, Ed. Berlin. Springer series in wood science: 242-247. 1992

Montgomery, D. C. Design and Analysis of Experiments, Wiley. 2000.